Aircraft Wing Rock Dynamics And Control

by

Tiauw Hiong Go

Ir., Institut Teknologi Bandung, Indonesia (1990)

S.M., Massachusetts Institute of Technology (1994)

Submitted to the Department of Aeronautics and Astronautics
in partial fulfillment of the requirements for the degree of

Doctor of Science in Aeronautics and Astronautics

at the

MASSACHUSETTS INSTITUTE OF TECHNOLOGY

September 1999

Author .....
Department of Aeronautics and Astronautics
September 3, 1999

Certified by .....
Rudrapatna V. Ramnath
Senior Lecturer of Aeronautics and Astronautics
Committee Chairman, Thesis Supervisor

Certified by .....
Richard H. Battin
Senior Lecturer of Aeronautics and Astronautics
Committee Member

Certified by .....
Wallace Vander Velde
Professor of Aeronautics and Astronautics
Committee Member

Certified by .....
John Dugundji
Professor of Aeronautics and Astronautics, Emeritus
Committee Member

Accepted by .....
Nesbitt Hagood
Chairman, Department Committee on Graduate Students

Aircraft Wing Rock Dynamics And Control

by

Tiauw Hiong Go

Submitted to the Department of Aeronautics and Astronautics
on September 3, 1999, in partial fulfillment of the
requirements for the degree of
Doctor of Science in Aeronautics and Astronautics

Abstract

The dynamics of wing rock on rigid aircraft having single, two, and three rotational degrees-of-freedom are analyzed. For the purpose of the analysis, nonlinear mathematical models of the aircraft are developed. The aerodynamic expressions contained in the models can be built by fitting the appropriate aerodynamic data into the model. The dynamic analysis is performed analytically using a technique combining the Multiple Time Scales method, Center Manifold Reduction principle, and bifurcation theory. The technique yields solutions in parameteric forms and leads to the separation of fast and slow dynamics, and a great insight into the system behavior. Further, a unified framework for the investigation of wing rock dynamics and control of aircraft is developed. Good agreement between the analytical results and the numerical simulations is demonstrated.

Based on the results of the dynamic analysis, appropriate control strategies for the wing rock alleviation are developed. The control power limitation of the conventional aerodynamics control surfaces is considered and its effects on the alleviation of wing rock are investigated. Finally, the potential use of advanced controls to overcome the conventional controls limitation is discussed.

Committee Chairman, Thesis Supervisor: Rudrapatna V. Ramnath
Title: Senior Lecturer of Aeronautics and Astronautics

Committee Member: Richard H. Battin
Title: Senior Lecturer of Aeronautics and Astronautics

Committee Member: Wallace Vander Velde
Title: Professor of Aeronautics and Astronautics

Committee Member: John Dugundji
Title: Professor of Aeronautics and Astronautics, Emeritus

dedicated to
Jusvin *and* **Jason**
who have been my inspiration

Simplicity is the glory of expression
-Walt Whitman

Acknowledgments

First and foremost, I would like to express my deepest gratitude to Professor Ramnath for his guidance throughout this research and throughout my years at MIT. His enthusiasm to solve challenging problems encountered in the research has been enlightening and encouraging. Our countless hours of discussion have really broadened my perspective on life in general and on engineering science in particular. His meticulous effort to perfect the thesis is greatly appreciated.

I would like to express my special thanks to other members of my doctoral committee: Professor Battin, Professor Vander Velde, and Professor Dugundji. Their discerning comments and suggestions have been invaluable for the successful completion of the thesis.

I also wish to express my deep appreciation to my wife, Lyenny, for her patience and unconditional support. The precious help from my mother and mother-in-law, and the blessing from my father, have really helped me in going through the busy time of writing the thesis. My twin sons, Jusvin and Jason, are too young to understand all this, but I just want them to know that their cheerful smiles at the end of a busy day always keep my spirit up.

Finally, I would like to thank the following people at the Volpe Center for their concerns and support on my thesis: Bob DiSario, Judith Burki-Cohen, and Young Jin Jo. And a very special thanks to Bob for proofreading several chapters of the thesis and for helping me in preparing for my presentation.

Contents

Chapter 1

Introduction

1.1 Background

Most modern aircraft, especially of the fighter type, are required to have enhanced performance capabilities in order to expand their flight envelopes for superiority. Such requirements necessitate an aircraft to operate in nonlinear flight regimes in which the dynamics are highly complex. One example is flight at high angles-of-attack, where many interesting but often undesirable phenomena can occur. Examples of such phenomena include jump responses, yaw departure, pitching oscillations, and wing rock. These phenomena often limit the potential maneuver performance of the aircraft and could even lead to catastrophic consequences.

Understanding the nonlinear phenomena in aircraft dynamics is the key to alleviating many such problems. Research on many of these phenomena have been reported in the technical literature [1-21]. However, due to the complexity of the problems, there is, as yet, no complete and satisfactory treatment. More research is still needed to gain a better insight into the flight dynamics phenomena.

1.2 Wing Rock Phenomenon

An important manifestation of the effect of nonlinearities is the phenomenon of *wing rock*. This phenomenon occurs at moderate to high angles-of-attack and involves sustained lateral oscillation dominated by roll motion oscillating with a constant amplitude and definite frequency. An example of this phenomenon is given in Figure 1-1,

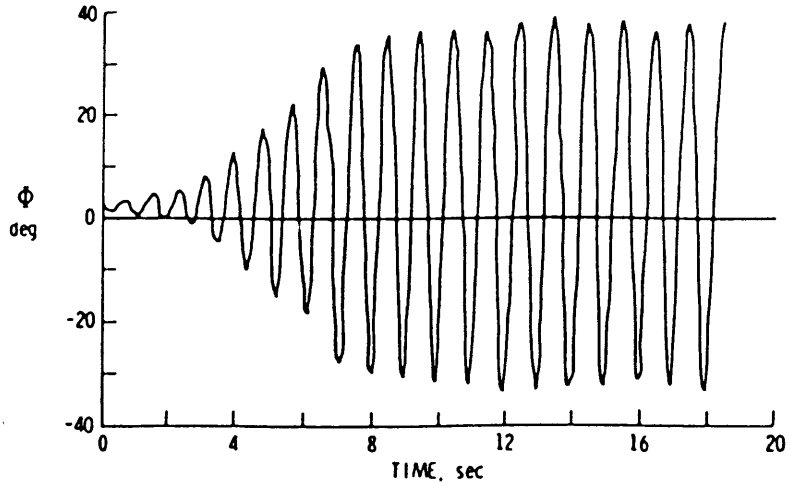

Figure 1-1: Wing rock build-up of an 80^o delta wing at $\alpha = 27^o$ [15]

where the wing rock build-up of an 80^o delta wing at an angle-of-attack of 27^o is depicted. Another example is given in Figure 1-2, where the wing rock motion on the F-4 aircraft is shown. The degree of severity of wing rock is determined mainly by the amplitude of the motion and to a lesser extent by the period of the oscillation.

Wing rock is a concern for current and future aircraft because it proves to be a major maneuver limitation. The capability of modern combat aircraft to perform enhanced agility maneuvers at high angles-of-attack, such as point-and-shoot maneuver and positioning (Figure 1-3), will suffer if wing rock comes into play, since it impairs the tracking and tactical effectiveness. In addition, it also poses a safety problem in some critical flight conditions, such as landing. In this situation, wing rock might cause loss of aircraft controllability and might prove to be catastrophic.

Because wing rock has potentially severe adverse effects on maneuver capability and safety, the alleviation or control of this undesirable motion is of great interest in the operation of modern aircraft. A good control strategy has to be devised in order to successfully alleviate the wing rock motion. The development of such strategy requires a thorough understanding of wing rock dynamics. Several work in the area as an attempt to gain a better understanding of wing rock motion has been reported, although none is comprehensive, especially in the multiple degrees-of-freedom cases. A brief review of the literature in the area will be presented next.

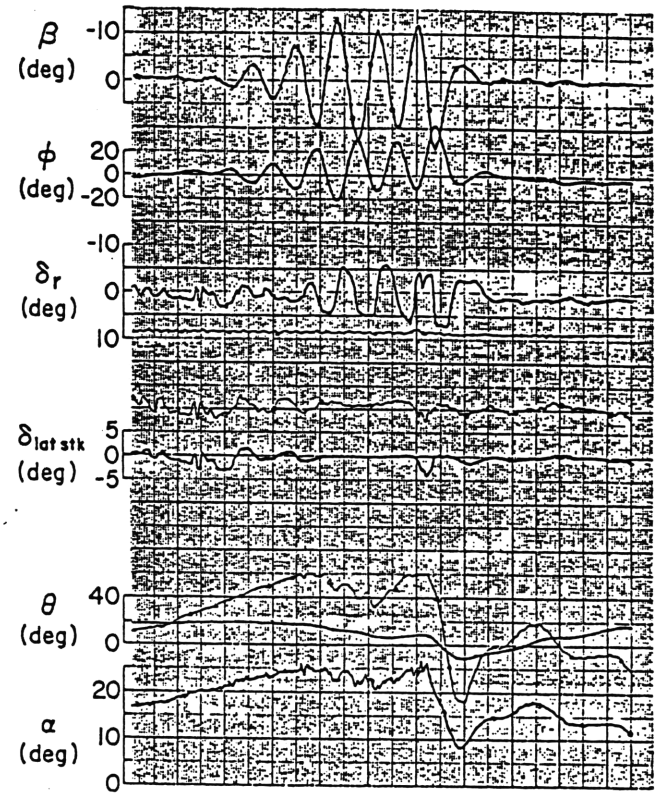

Figure 1-2: Wing rock motion as observed on the F-4 aircraft [4]

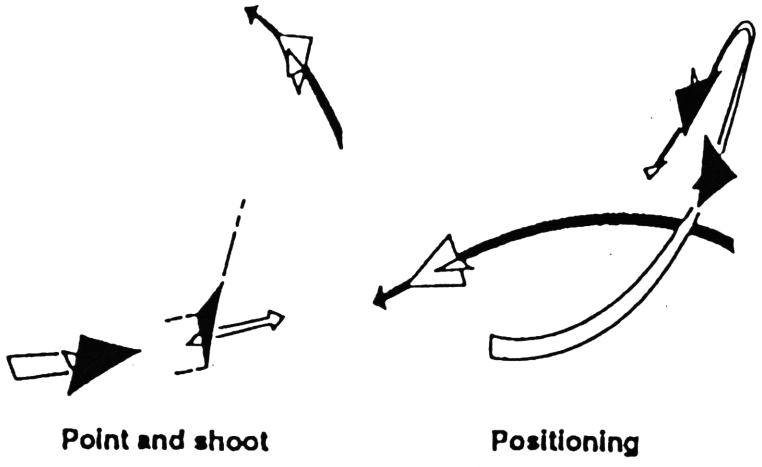

Figure 1-3: Point-and-shoot and positioning maneuvers

1.2.1 Previous Work

While there is a considerable body of work on conventional flight dynamics, the situations involving nonautonomous or nonlinear flight regimes are infrequently investigated. This is mainly because of the fundamental mathematical difficulties in dealing with such systems. Ramnath [30] analyzed the time-varying dynamics of a VTOL vehicle during a transition from hover to forward flight, by the Generalized Multiple Scales (GMS) method. Ramnath [34] also analyzed the re-entry dynamics of the space shuttle by the GMS method and developed a separation of the fast and slow aspects of the aircraft through variable flight conditions.

In particular, research on wing rock in the literature can be divided into three major groups. The division is based on whether the emphasis of the work is about the aerodynamic causes of wing rock, wing rock dynamics, or wing rock control.

On the subject of aerodynamic sources of wing rock, the most notably is the work done by Ericsson [12, 13, 14]. He investigates the fluid flow mechanisms causing wing rock. For aircraft with highly swept wing leading edges, wing rock is caused by asymmetric vortex shedding. For aircraft with straight or moderately swept leading edges, the causative mechanism of wing rock is usually the asymmetric airfoil stall. If the aircraft has a slender forebody, wing rock can also be generated by asymmetric body vortices from the nose. By representing the aerodynamic time history effect with a lumped time lag and by using the experimental static data, the amplitude of the wing rock can be predicted. However, in this method, the frequency of the wing rock must be known in advance for the amplitude prediction.

Several work emphasizing the dynamics of wing rock motion will now be described. A study of the aerodynamic factors which cause the low speed wing rock of a free-to-roll flat plate delta wing with 80^o leading edge sweep is conducted by Nguyen *et al.* [15]. Static force tests and dynamic wind tunnel experiments are utilized in their investigation. Their results indicate that the wing rock phenomenon is caused by a dependence of aerodynamic damping in roll on sideslip such that negative (unstable) roll damping is obtained at smaller sideslip angles and positive (stable) roll damping is obtained at the larger angles. A mathematical model of this effect is also developed and shown to agree closely with the experimental results.

Based on the test data in [15], Hsu and Lan [16] develop a mathematical model to calculate the wing rock characteristics. The amplitude and frequency of the wing rock motion are obtained analytically by solving the resulting dynamic equations using the Beecham-Titchener asymptotic method. They extend their analysis to also

include the case involving additional lateral degrees-of-freedom (sideslip and yaw). The result is a set of coupled nonlinear algebraic equations which can be solved through numerical iterations to get the amplitude and the frequency of the wing rock.

In a series of papers [17-20], Nayfeh *et al.* present some numerical simulations and analytical study of wing rock phenomenon on slender delta wings. In the numerical simulation of free-to-roll delta wings in [17], the governing dynamic equation of rolling motion is coupled with the unsteady vortex-lattice method, which is then integrated using a predictor-corrector technique. The simulation and the experimental results are shown to be in agreement. Based on the numerical simulation results, some analytical models of single degree-of-freedom wing rock are developed and analysis of the models are done using Multiple Time Scales Method [18, 19]. In [20], the influence of the second degree-of-freedom in pitch on wing rock motion is simulated numerically. The results suggest that the motion of the two degree-of-freedom case can differ significantly compared to the single degree-of-freedom one. However, no analysis is given to explain the phenomenon.

Wing rock phenomenon on Gnat aircraft is considered by Ross [21]. Effects of cubic nonlinearities in roll rate and sideslip are considered and analytical approximations of the solution using the Beecham-Titchener method were obtained. The analysis is performed by considering only the lateral degrees-of-freedom of the aircraft. As in [16], a set of nonlinear algebraic equations has to be solved numerically to get the amplitude and frequency of the resulting wing rock motion. It is shown that such nonlinearities can cause wing rock on the aircraft.

In [9, 10], Planeaux *etal.* examines the high angle-of-attack solution structure of an eight-state nonlinear equations of motion representative of a high performance fighter aircraft. A numerical approach using bifurcation theory and continuation method is used to trace the branches of both equilibria and periodic solutions. Their analysis shows that for some parameter combinations, wing rock can appear in the system. Since the focus of their work is mainly on obtaining the structure of the solutions at high angles-of-attack and on interpreting the results, no attempts are made to extract the parameters causing certain phenomena. In a similar fashion, Jahnke [11] performs a similar numerical analysis on various nonlinear aircraft equations of motion representing the F-15 aircraft. Wing rock is also shown to occur in the system for some parameter combinations.

Some work on wing rock control has also been reported. An example is the work of Luo and Lan [22], where the theoretical analysis of the optimal control input for wing

rock suppression is conducted. The one degree-of-freedom wing rock model in [16] is used in their analysis. Although the control law obtained in their analysis is quite complicated (a nonlinear function of roll angle and roll rate), after observing some simulations, they conclude that controlling roll rate is an effective way to suppress the wing rock. Other work involving the application of other nonlinear control methods, such as adaptive control and neural network, to the one degree-of-freedom model is given in [24, 25].

Most of the earlier work concerns wing rock on aircraft with only one degree-of-freedom in roll, although some attempts to extend the investigation to include more degrees-of-freedom have been made. Most of the work involving multiple degrees-of-freedom, however, is numerical in nature, hence the results apply only to specific cases considered.

1.3 Contributions of the Dissertation

This dissertation extends the previous work on wing rock in an attempt to gain a better understanding of the nonlinear aircraft dynamics. The extension includes the use of a more general nonlinear aircraft model in the analysis, the development of an analysis technique in the treatment of multiple rotational degrees-of-freedom wing rock cases, and the derivations of analytical solutions to the problem. The technique utilizes the powerful Multiple Time Scales (MTS) method in conjunction with the center manifold reduction principle and bifurcation theory. As we shall see later, this technique offers a systematic approach to uncover the important dynamics of the system and enables us to separate the rapid and slow aspects of the complex nonlinear dynamics. Moreover, the application of the above technique leads us to solutions in a parametric form, which enables us to see how each parameter influences the resulting system dynamics. The technique also leads to the development of a unified framework for the single and multiple degrees-of-freedom wing rock dynamics, the results of which can easily be utilized for control design.

The development of strategies for wing rock alleviation is also considered in the dissertation. The strategies are based on the results of the dynamics analysis. Unlike most of the previous work in the area, the control power issue is emphasized, as it is a main limiting factor for an aircraft flying at high angles-of-attack. Several control strategies are described and the advantages and disadvantages of each strategy are discussed.

1.4 Outline of the Dissertation

The discussion in this dissertation is arranged in the following order.

- Chapter 1 provides an introduction to the wing rock problem, discusses the previous work in the area, and describes the general contributions of the dissertation.
- Chapter 2 describes in brief the theories and methods which are used in the analysis.
- Chapter 3 treats the simplest case of wing rock motion, where the aircraft is assumed to have only a single rotational degree-of-freedom in roll. This case is useful in building our understanding of the basic wing rock dynamics.
- Chapter 4 discusses the wing rock motion on an aircraft having two rotational degrees-of-freedom, in roll and pitch. It is shown that the additional degree-of-freedom increases the complexity of the analysis. Some interesting phenomena not found in the single degree-of-freedom case are noted and discussed.
- Chapter 5 considers an aircraft having the complete rotational degrees-of-freedom: roll, pitch, and yaw. A significant increase in the complexity of the analysis can be observed for this case as compared to the previous simpler cases. More interesting phenomena are also uncovered by the analysis.
- Chapter 6 describes the possible control strategies for the alleviation of wing rock motion. The effects of the limitation in controls are also discussed. Possible use of nonconventional control techniques to satisfy control power requirement to alleviate wing rock is also addressed.
- Chapter 7 provides the conclusions of the work described in the dissertation and also the recommendations for future work.

Chapter 2

Theories and Methods

2.1 Introduction

In the following sections, the main theories and methods directly used in the analysis of the wing rock problem are discussed. The interested reader may refer to the cited literature for a more detailed discussion of the subjects.

In general, the analysis is based on the *Multiple Time Scales* (MTS) method in conjunction with techniques derived from dynamical systems theory, such as *Center Manifold Reduction* techniques and *bifurcation analysis*. As we shall see later, these tools are very useful in uncovering the complex dynamics of the system.

2.2 The Multiple Time Scales Method

2.2.1 Concept

The concept of the Multiple Time Scales (MTS) Method described here is based on the work of Ramnath [27, 28, 29]. The interested reader may consult those references for a complete treatment of the method.

The motion of many dynamic systems consists of a mixture of fast and slow behaviors. Some parameters of a system may mainly affect the fast behavior, while some others may mainly affect the slow behavior of the system. In most dynamic systems, this is not easy to detect. Knowledge of how a certain parameter affects the system behavior would be very valuable, as this would provide a clue on what to

do if we are to alter the system behavior. For this reason, it would be advantageous to separate the fast and the slow behaviors of a system. The Multiple Time Scales (MTS) approach is a technique based exactly on this idea.

The MTS method belongs to a larger body of knowledge called *Perturbation Methods*. As with other perturbation methods, the MTS method enables us to obtain approximate solutions to a problem in *limiting cases*. This kind of problem is usually recognized by the existence of a very small or very large parameter in a system. In dynamic systems the existence of such parameters generally implies the existence of fast or slow behaviors. Since many physical systems of interest contain such parameters, the MTS method can find a wide range of applications. One example of such a system is a rigid body in orbit around the earth (see [31]). For this system, the small parameter is the ratio of the orbital frequency to the nutational frequency.

The main concept of the MTS approach is selecting the appropriate *scales* to observe the behavior of a system. For a dynamic system, in most cases *time* is the independent variable, hence the words *time scales* or *clocks* are often used instead of *scales*. In general, one can employ as many scales as one wishes to represent the dynamics of a system, depending on the level of accuracy to be achieved. In many applications, however, the use of only two scales is adequate to capture the important dynamics of the system. It is worth noting that the choice of scales determines the quality of the solution. The inappropriateness of the scales used will show up as an incompatibility with the assumptions previously made or as a nonuniformity in the solution.

The time scales used in the MTS method are generally real and linear. Ramnath [27, 29] generalized the method to the Generalized Multiple Scales (GMS) method by including nonlinear and complex scales. In general, the GMS method introduces additional degrees-of-freedom to the problem, which can be used to determine the appropriate time scales for the problem. Because of this reason, this approach normally generates better results than the regular MTS approach. Several applications of the GMS method in science and engineering can be found in [29, 33, 34, 35].

2.2.2 Mathematical Concept of the MTS Approach

The following is based on the development of Ramnath and Sandri [27]. The MTS approach relies on the concept of extension. The fundamental idea of the concept of extension is to enlarge the domain of the independent variable to a space of higher dimension. Since our main interest is on dynamic systems, we will think of *time* as

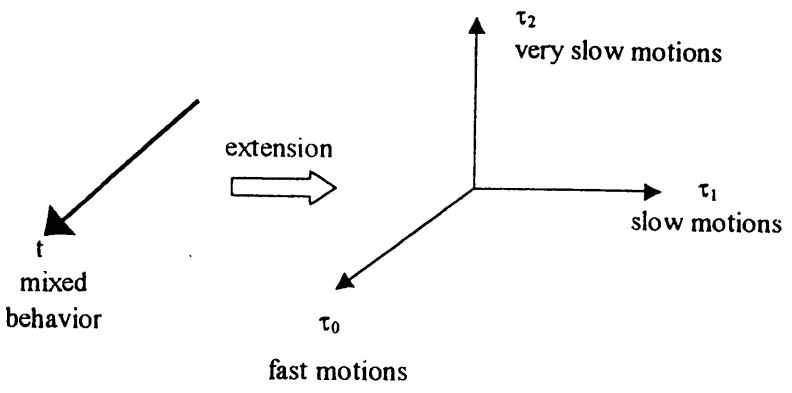

Figure 2-1: The concept of extension

our independent variable. *Time* as the independent variable is extended to a set of new independent timelike-variables which are called *time scales* or *clocks*. Each clock captures a certain behavior of the system. For example, the fast clock captures only the fast behavior of the system. The extension of time t is symbolized as follows :

$$t \longrightarrow \{\tau_0, \tau_1, \ldots, \tau_n\} \tag{2.1}$$

where $\tau_0, \tau_1, \ldots, \tau_n$ are the time scales or the clocks, which are normally functions of t and the small or large parameter in the system ϵ, that is

$$\tau_i = t_i(t, \epsilon) \tag{2.2}$$

How τ_i relates to t determine the nature of the time scale. In GMS approach, this relation is determined in the course of analysis and not determined a priori. The relation of τ_i to ϵ in this case determines whether the clock is fast or slow. Figure 2-1 shows a schematic illustration of the concept.

Suppose now that $y(t, \epsilon)$ is the dependent variable in a dynamic equation and restrict the discussion to a dynamic equation in the form of an ordinary differential equation. Then, since t is extended, $y(t, \epsilon)$ is also extended as

$$y(t, \epsilon) \longrightarrow Y(\tau_0, \tau_1, \ldots, \tau_n; \epsilon) \tag{2.3}$$

It is understood from the discussion above that due to the extension of the independent variable, an ordinary differential equation will become a partial differential equation. This is not a limitation, however, since the resulting partial differential

equation is usually simpler than the initial ordinary differential equation.

From the definition of extension, when Equation (2.2) is inserted into extended function Y we have

$$Y(\tau_0(t,\epsilon),\tau_1(t,\epsilon),\ldots,\tau_n(t,\epsilon);\epsilon) = y(t,\epsilon) \tag{2.4}$$

The result of substituting the trajectory in the extended function Y is called the *restriction* of Y.

2.2.3 Principle of Minimal and Subminimal Simplification

The following treatment is based on the development by Ramnath [32]. The purpose of all approximation methods, including the MTS method, is to make a difficult problem become more tractable. In essence, by employing these methods, one wishes to have a simpler problem. One subtle question is; how far can one simplify a problem. Of course, what one wants is to capture all the important behaviors of the system. In other words, the simplification should be as minimal as possible so as to retain all the important information of the system. This is called the *principle of minimal simplification.* This facilitates a derivation of the correct and optimal ordering of the terms in the mathematical model which then leads to accurate asymptotic solutions in a systematic manner.

There are some cases where the principle of minimal simplification needs to be extended in order to develop meaningful solutions. This refinement, i.e. the *principle of subminimal simplification* was developed by Ramnath [27, 33] and has been applied succesfully in several cases (see [33] and [35]).

2.3 Dynamical Systems Theory

Some main points of dynamical systems theory that are used in the later analysis are discussed briefly in the following subsections. The interested reader may refer to the literature [36, 38, 39] for a more detailed development of the subjects.

A dynamical system is a set of ordinary differential equations of the form

$$\dot{\mathbf{x}} = \mathbf{f}(\mathbf{x}, t; \mu) \tag{2.5}$$

where $\mathbf{x} \in \mathbf{R}^n$, $\mathbf{f}$ is an n-dimensional vector field, t is time, and $\mu \in \mathbf{R}^m$. $\dot{(\cdot)}$ represents differentiation of $(\cdot)$ with respect to time t. n is referred to as the dimension of the system. The representation (2.5) shows explicit dependence on time, t. A dynamical system with this property is called *nonautonomous.*

Many physical systems can be represented by dynamical systems, including aircraft equations of motion. Although in general, the aircraft motion is nonautonomous, work in this dissertation will be focused on the situations where the aircraft equations of motion can be validly assumed to be time independent. Dynamical systems of this type are called *autonomous* and have the form

$$\dot{\mathbf{x}} = \mathbf{f}(\mathbf{x}; \mu) \tag{2.6}$$

The discussion in the next subsections is limited to the autonomous type of system.

Another assumption made in the following discussion is that all vector fields considered are smooth. This means that the vector field and all of its derivatives are continuous. This assumption allows us to ignore the questions about the degree of differentiability of the vector field for the theorems introduced in the subsequent subsections.

The solution history of a dynamical system for some initial condition is usually referred to as a *trajectory.* The solution trajectories are smooth for smooth vector fields. For many systems, including aircraft, it is impossible to determine the solution trajectories exactly. Therefore, some approximation techniques have to be employed to find the approximation of the solutions.

The families of solution trajectories of a system can be expressed graphically in the *phase space*, that is the Euclidean space of the dependent variables. The shortcoming of phase space representations is that for systems of dimension four or higher, it is not possible to show the entire phase space in one plot. In this situation, the phase space has to be projected onto two or three dimensional space, and this makes the interpretation of the system behavior more difficult. For low dimensional systems, phase space representations can be very useful and can provide clear pictures of the system behavior.

2.3.1 Equilibrium Points and Their Stability

Equilibrium points or fixed points are points in phase space where all time derivatives are zero. As its name implies, these points describe the equilibrium states of

the system but provide no information about the transient response of the system. Equilibrium points of the system (2.6) are determined by solving the equation

$$\mathbf{f}(\mathbf{x};\mu) = \mathbf{0} \tag{2.7}$$

It is equivalent to finding the zeros of a set of algebraic equations, which are in general nonlinear. In many problems, finding zeros may not be an easy task, however there have been many techniques developed to overcome this difficulty (for example, see [40]). Note also that one can always apply a transformation to (2.7) such that it has an equilibrium point at the origin. Such an equilibrium point is also referred to as *zero solution.* Often in a physical system, the zero solution represents the nominal or equilibrium condition of interest.

The stability of an equilibrium point provides an important information in a dynamical system. It determines whether the states of the system are attracted or repelled from the equilibrium point. In general, one can differentiate two types of stability : *global stability* and *local stability.* Global stability characterizes the stability of an equilibrium point for any initial condition in the phase space, while local stability determines the stability of an equilibrium point in a small region around the point. Global stability information, while useful, is very difficult to obtain in most situations. Fortunately, in many cases, local stability information, which is easier to obtain, is enough to uncover the important dynamics of a system.

The local stability of an equilibrium point of a nonlinear dynamical system can be derived using the Poincare-Liapunov's linearization method. The great value of this method lies in the fact that under certain conditions, the local stability properties of a nonlinear system can be inferred by studying the behavior of a linear system, which is obtained by linearizing the nonlinear system around an equilibrium point of interest. Then the stability can be determined by calculating the eigenvalues of the linearized system. An equilibrium point is asymptotically stable if the real parts of all eigenvalues are negative and unstable if any eigenvalue has a positive real part. If one or more eigenvalues have zero real parts, then the stability of the nonlinear system cannot be deduced from the linearized system. In this case, one has to use other means to determine stability, such as the Center Manifold theorem, which will be discussed in the next subsection.

The linearization of the system (2.6) at an equilibrium point $(\mathbf{x}^*;\mu^*)$ is

$$\dot{\mathbf{u}} = \nabla_{\mathbf{f}}(\mathbf{x}^*;\mu^*)\mathbf{u} \tag{2.8}$$

where $\mathbf{u} = \mathbf{x} - \mathbf{x}^*$ and $\nabla_{\mathbf{f}}(\mathbf{x}^*; \mu^*)$ is the Jacobian matrix of $\mathbf{f}$ evaluated at $(\mathbf{x}^*; \mu^*)$, or symbolically

$$\nabla_{\mathbf{f}}(\mathbf{x}^*; \mu^*) = \frac{\partial \mathbf{f}}{\partial \mathbf{x}}|_{\mathbf{x}=\mathbf{x}^*, \mu=\mu^*} \tag{2.9}$$

The eigenvalues of $\nabla_{\mathbf{f}}(\mathbf{x}^*; \mu^*)$ determine the stability of the equilibrium point $(\mathbf{x}^*; \mu^*)$ as discussed in the above.

2.3.2 Center Manifold Theory

An *invariant manifold* of a dynamical system is a curve in phase space such that a solution trajectory starting from a point on that curve will remain on the curve for all time. Based on this definition, any equilibrium point is also an invariant manifold because if a system starts at an equilibrium point, it will stay there forever. We will specifically look at the invariant manifolds of an equilibrium point, that is the invariant manifolds that contain the equilibrium point. The stable manifold of an equilibrium point is an invariant manifold containing the equilibrium point such that if the system starts on the invariant manifold, it will asymptotically approach the equilibrium point as time goes to infinity. The unstable manifold can be defined in the same manner, only reversely, that is the system starting on the invariant manifold will asymptotically approach the equilibrium point as time goes to negative infinity. Mathematically, these can be expressed as

$$\begin{aligned} \mathbf{W}^s &= \{\mathbf{x} \to \mathbf{x}^* \; as \; t \to \infty\} \\ \mathbf{W}^u &= \{\mathbf{x} \to \mathbf{x}^* \; as \; t \to -\infty\} \end{aligned} \tag{2.10}$$

where $\mathbf{W}^s$ and $\mathbf{W}^u$ symbolized the stable and unstable manifolds respectively.

For a linear system, such manifolds are called stable and unstable *eigenspaces* and defined respectively as follows

$$\begin{aligned} \mathbf{E}^s &= span\{\mathbf{v}_i | \Re(\lambda_i) < 0\} \\ \mathbf{E}^u &= span\{\mathbf{v}_i | \Re(\lambda_i) > 0\} \end{aligned} \tag{2.11}$$

where $\mathbf{v}_i$ is the eigenvector and λ_i is the corresponding eigenvalue. The notation $\Re(\cdot)$ denotes the real part of the term in the parenthesis. We note without proof that $\mathbf{W}^s$ and $\mathbf{W}^u$ of a nonlinear system are tangent to $\mathbf{E}^s$ and $\mathbf{E}^u$ of the corresponding linearized system [38]. This makes sense intuitively as the behavior of a nonlinear system in the neighborhood of an equilibrium point can be approximated by the

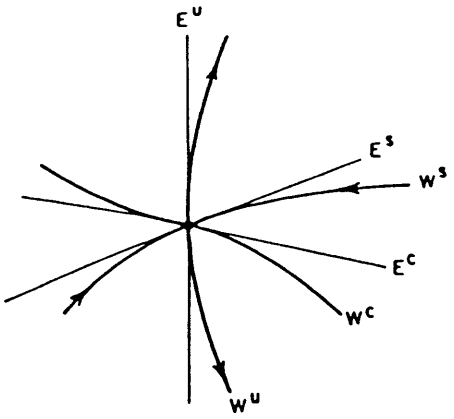

Figure 2-2: Illustration of stable, unstable and center manifolds

behavior of the linearized system about the equilibrium point in the absence of pure imaginary eigenvalues (zero real part).

In the case where eigenvalues with zero real part are present, one can define center eigenspace as follows

$$\mathbf{E}^c = span\{\mathbf{v}_i | \Re(\lambda_i) = 0\} \tag{2.12}$$

In a way similar to the stable and unstable manifolds, a *center manifold* ($\mathbf{W}^c$ can also be defined for a nonlinear system. The center manifold of an equilibrium point is an invariant manifold that contains the equilibrium point and is tangent to the center eigenspace of the linearized system. Note that no evolution information is given by the definition. This is because one cannot draw conclusions about the behavior of the nonlinear system around an equilibrium point from the corresponding linearized system having a center eigenspace. The behavior of the system on the center manifold has to be examined in the nonlinear context. An illustration of the nonlinear and linear manifolds is given in Figure 2-2. Several theorems on center manifolds which will be useful for later analysis are discussed next.

We consider the system of the following form

$$\begin{aligned} \dot{\mathbf{x}} &= \mathbf{A}\mathbf{x} + \mathbf{p}(\mathbf{x}, \mathbf{y}) \\ \dot{\mathbf{y}} &= \mathbf{B}\mathbf{y} + \mathbf{q}(\mathbf{x}, \mathbf{y}) \end{aligned} \tag{2.13}$$

where $\mathbf{x} \in \mathbf{R}^l$, $\mathbf{y} \in \mathbf{R}^m$, $\mathbf{A}$ and $\mathbf{B}$ are constant matrices such that $\Re(\lambda_i[\mathbf{A}]) = 0$; $i = 1, \ldots, l$ and $\Re(\lambda_i[\mathbf{B}]) < 0$; $i = 1, \ldots, m$. The functions $\mathbf{p}$ and $\mathbf{q}$ along with their Jacobians vanish at the origin, which is the equilibrium point of interest. In other words, $\mathbf{p}(\mathbf{0}, \mathbf{0}) = \nabla_{\mathbf{p}}(\mathbf{0}, \mathbf{0}) = \mathbf{0}$ and $\mathbf{q}(\mathbf{0}, \mathbf{0}) = \nabla_{\mathbf{q}}(\mathbf{0}, \mathbf{0}) = \mathbf{0}$.

The linearized equation around the origin in this case takes the form

$$\begin{aligned} \dot{\mathbf{x}} &= \mathbf{A}\mathbf{x} \\ \dot{\mathbf{y}} &= \mathbf{B}\mathbf{y} \end{aligned} \tag{2.14}$$

This system has two obvious eigenspaces, namely $\mathbf{x} = \mathbf{0}$ and $\mathbf{y} = \mathbf{0}$ which represent stable and center eigenspaces, respectively. As $t \to \infty$ all solutions of Equation (2.14) tend to go exponentially to the solutions of

$$\dot{\mathbf{x}} = \mathbf{A}\mathbf{x} \tag{2.15}$$

That is, the equation on the center eigenspace determines the asymptotic behavior of the solutions of the system (2.14) modulo exponentially decaying terms. Analogous results can be expected for the nonlinear system.

First, it is a well-known result that the system (2.13) possesses a center manifold, as stated in the following theorem.

Theorem 1 **[39]** Equation (2.13) has a local center manifold $\mathbf{y} = \mathbf{h}(\mathbf{x})$ for $|\mathbf{x}| < \delta$, $0 < \delta \ll 1$, where $\mathbf{h}(\mathbf{0}) = \nabla_{\mathbf{h}}(\mathbf{0}) = \mathbf{0}$

The flow on the center manifold is then governed by the l-dimensional system

$$\dot{\mathbf{z}} = \mathbf{A}\mathbf{z} + \mathbf{p}(\mathbf{z}, \mathbf{h}(\mathbf{z})) \tag{2.16}$$

which generalizes the corresponding problem (2.15) for the linearized case. The conditions $\mathbf{h}(\mathbf{0}) = \nabla_{\mathbf{h}}(\mathbf{0}) = \mathbf{0}$ reflect the tangency of the center manifold to the center eigenspace at the origin. The dynamics of the system will converge to the dynamics of the center manifold after some transients as stated in the following lemma.

Lemma 1 **[39]** Let $(\mathbf{x}(t), \mathbf{y}(t))$ be a solution of Equation (2.13) with $|(\mathbf{x}(0), \mathbf{y}(0))|$ sufficiently small. Then there exist positive constants K and ν such that

$$|\mathbf{y}(t) - \mathbf{h}(\mathbf{x}(t))| \leq K \exp(-\nu t) |\mathbf{y}(0) - \mathbf{h}(\mathbf{x}(0))| \tag{2.17}$$

for all $t \geq 0$.

Therefore it can be understood that Equation (2.16) contains all the necessary information to determine the asymptotic behavior of the solutions of Equation (2.13), as stated in the following theorem.

Theorem 2 **[39]** (a) The zero solution of Equation (2.16) has the same stability property as the zero solution of Equation (2.13).

(b) Suppose the zero solution of Equation (2.16) is stable. Let $(\mathbf{x}(t), \mathbf{y}(t))$ be a solution of Equation (2.13) with $(\mathbf{x}(0), \mathbf{y}(0))$ sufficiently small. Then there exists a solution $\mathbf{z}(t)$ of Equation (2.16) such that as $t \to \infty$

$$\begin{aligned} \mathbf{x}(t) &= \mathbf{z}(t) + O(\exp(-\gamma t)) \\ \mathbf{y}(t) &= \mathbf{h}(\mathbf{z}(t)) + O(\exp(-\gamma t)) \end{aligned} \tag{2.18}$$

where $\gamma > 0$ is a constant depending only on $\mathbf{B}$.

This result enables one to deal only with an l-dimensional equation, which is the dimension of the center manifold, to obtain the asymptotic behavior of the $(l+m)$-dimensional system. This systematic order reduction method is called *center manifold reduction.*

Now we will discuss on how to compute the center manifold. The substitution of $\mathbf{y} = \mathbf{h}(\mathbf{x})$ into the second equation in (2.13) and the use of chain rule yield

$$\nabla_{\mathbf{h}}(\mathbf{x})\left[\mathbf{A}\mathbf{x} + \mathbf{p}(\mathbf{x}, \mathbf{h}(\mathbf{x}))\right] = \mathbf{B}\mathbf{h}(\mathbf{x}) + \mathbf{q}(\mathbf{x}, \mathbf{h}(\mathbf{x})) \tag{2.19}$$

or

$$\mathbf{N}(\mathbf{h}(\mathbf{x})) \equiv \nabla_{\mathbf{h}}(\mathbf{x})\left[\mathbf{A}\mathbf{x} + \mathbf{p}(\mathbf{x}, \mathbf{h}(\mathbf{x}))\right] - \mathbf{B}\mathbf{h}(\mathbf{x}) - \mathbf{q}(\mathbf{x}, \mathbf{h}(\mathbf{x})) = 0 \tag{2.20}$$

This equation together with the conditions $\mathbf{h}(\mathbf{0}) = \nabla_{\mathbf{h}}(\mathbf{0}) = \mathbf{0}$ is the system to be solved for finding the center manifold. Unfortunately, this equation for $\mathbf{h}(\mathbf{x})$ in general cannot be solved exactly, since to do so would imply that a solution of the original equation had been found. The next theorem, however, shows that in principle, its solution can be approximated arbitrarily closely.

Theorem 3 **[39]** If a function $\vartheta(\mathbf{x})$, with $\vartheta(\mathbf{0}) = \nabla_{\vartheta}(\mathbf{0}) = \mathbf{0}$, can be found such that $\mathbf{N}(\vartheta(\mathbf{x})) = O(|\mathbf{x}|^r)$ for some $r > 1$ as $|\mathbf{x}| \to 0$ then it follows that as $\mathbf{x} \to 0$,

$$\mathbf{h}(\mathbf{x}) = \vartheta(\mathbf{x}) + O(|\mathbf{x}|^r) \tag{2.21}$$

In case the center manifold is analytic, we can approximate $\mathbf{h}(\mathbf{x})$ to any degree of accuracy by seeking series solutions of (2.19).

2.3.3 Bifurcation Analysis

The term *bifurcation* was originally used to describe the branching of equilibrium solutions in a family of differential equations as certain parameters are varied. Bifurcations of equilibria are normally accompanied by changes in the topological properties of the solutions. For system (2.5), $\mu = \mu_0$ is called a *bifurcation point* if the qualitative nature of the solutions of (2.5) changes at $\mu = \mu_0$. That means that in any neighborhood of $\mu = \mu_0$, there exist μ_1 and μ_2 such that the topological behavior of the solutions of (2.5) for $\mu = \mu_1$ and $\mu = \mu_2$ are not equivalent.

In this section, only one parameter bifurcation (also called *codimension one* bifurcation) is discussed. Such bifurcation normally occurs in one or two dimensional systems. As we shall see, although the dimension of the aircraft equations of motion in general is greater than two, the application of the center manifold technique described above could reduce the representation of the important dynamics of the system into one or two dimensional equations. The bifurcation analysis can then be done on this reduced system. Several prototypical one parameter bifurcations are discussed next.

Consider the first order system

$$\dot{x} = \mu + x^2 \equiv f(x) \tag{2.22}$$

where μ is a parameter, which maybe positive, negative, or zero. The Jacobian of the system in this case is

$$\nabla_f(x) = 2x \tag{2.23}$$

When μ is negative, there are two equilibrium points at $x^* = \pm\sqrt{|\mu|}$ with $\nabla_f(x^*) = \pm 2\sqrt{|\mu|}$. The linearized system around each of the equilibrium points is

$$\dot{u} = \nabla_f(x^*)u \tag{2.24}$$

Here, the Jacobian is the same as the eigenvalue of the linearized system. Based on the stability theory discussed earlier, the equilibrium point at $x^* = -\sqrt{|\mu|}$ is stable and the one at $x^* = \sqrt{|\mu|}$ is unstable (see Figure 2-3). As μ approaches zero from below, the parabola moves up and the two equilibrium points move toward each other. When $\mu = 0$, the two equilibrium points coalesce into the so-called half-stable equilibrium point at $x^* = 0$ (see Figure 2-3). Such an equlibrium point is very delicate, it vanishes as soon as μ moves away from zero. There are no equilibrium points when $\mu > 0$ (see Figure 2-3). In this example, $\mu = 0$ is the bifurcation point of the system, since the

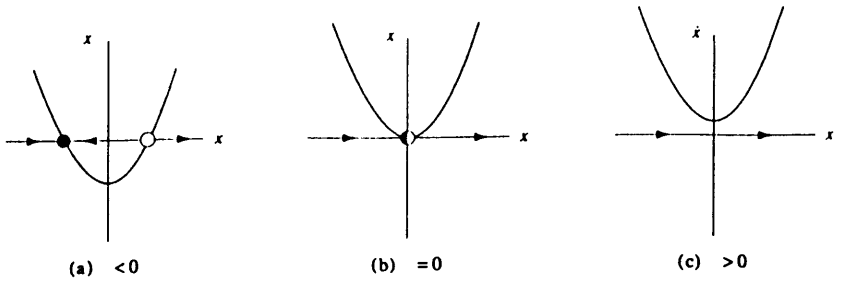

Figure 2-3: The plots of $\dot{x} = \mu + x^2$ as μ varies

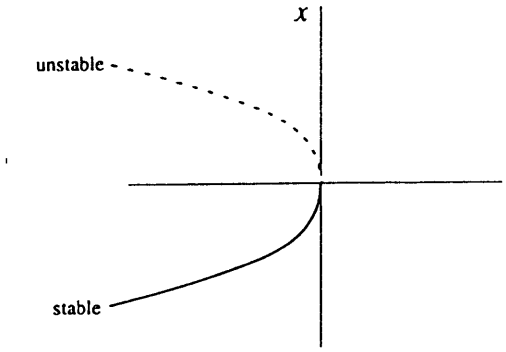

Figure 2-4: The bifurcation diagram of $\dot{x} = \mu + x^2$

system is qualitatively different for $\mu < 0$ and for $\mu > 0$.

Bifurcation is often represented in a diagram the showing the values of the equilibrium points and their stability as a parameter varies. Such diagram is called a *bifurcation diagram.* The bifurcation diagram for the example above is given in Figure 2-4. In the diagram, the solid line indicates the locus of the stable equilibrium points, while the dotted line indicates the locus of the unstable equilibrium points. Bifurcation of this type is called *saddle-node* bifurcation.

Other types of bifurcation, which typically occur in a one dimensional system, are *transcritical* and *pitch fork* bifurcations. The prototypical first order equations for the occurence of these types of bifurcation and their bifurcation diagrams are shown in Figure 2-5. The transcritical bifurcation is characterized by the exchange of stabilities between the equilibrium points. In the example, the two equilibrium points do not dissappear after the bifurcation (as in the saddle-node case), they merely switch their stability. Pitchfork bifurcation is common in physical problems that have a symmetry, where the equilibrium points tend to appear and dissappear in symmetrical pairs.

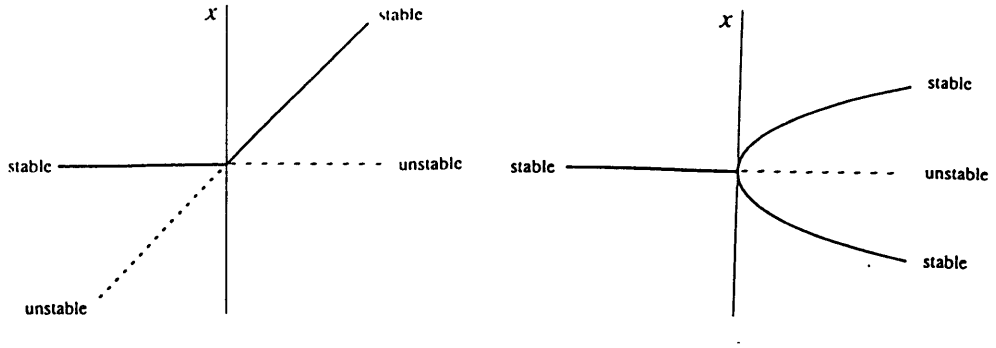

Figure 2-5: Transcritical and pitchfork bifurcations

The term 'pitchfork' becomes clear from the shape of the bifurcation diagram for this type of bifurcation. There are two different types of pitchfork bifurcation and they are categorized as *supercritical* and *subcritical* (see Figure 2-5). Note that in the subcritical case, the only stable equilibrium is $x^* = 0$ when $\mu < 0$.

In systems of dimension two or greater, more than one eigenvalue could be zero at the bifurcation point and this gives rise to a very involved situation. Such a situation, however, occurs very rarely, and hence it will not be discussed further here. A more important case occurs when the system posseses a pair of pure imaginary eigenvalues at certain parameter value. In this situation, if the stability type of the equilibrium changes when subjected to perturbations, then this change is usually accompanied with either the appearance or dissappearance of a periodic orbit encircling the equilibrium point. This type of bifurcation is called *Hopf bifurcation* and is often encountered in physical systems. The following theorem formulates this type of bifurcation formally.

Theorem 4 [37, 38] Let $\dot{\mathbf{x}} = \mathbf{f}(\mathbf{x}, \mu)$ be a dynamical system of dimension two depending on a scalar parameter μ with $\mathbf{f}(\mathbf{0}, \mu) = \mathbf{0}$. Assume that the linearized system at the origin $\dot{\mathbf{u}} = \nabla_{\mathbf{f}}(\mathbf{0}, \mu)$ has the complex conjugate eigenvalues $\lambda(\mu)$ with $\Re(\lambda(0)) = 0$ and $\Im(\lambda(0)) \neq 0$. Furthermore, suppose that the eigenvalues cross the imaginary axis with nonzero speed, that is

$$\frac{d\Re(\lambda)}{d\mu}(0) \neq 0 \tag{2.25}$$

Then, in any neighborhood N of the origin and any given $\mu_0 > 0$ there is a $\bar{\mu}$ with $|\bar{\mu}| < \mu_0$ such that the differential equation $\dot{\mathbf{x}} = \mathbf{f}(\mathbf{x}, \bar{\mu})$ has a nontrivial periodic orbit in N.

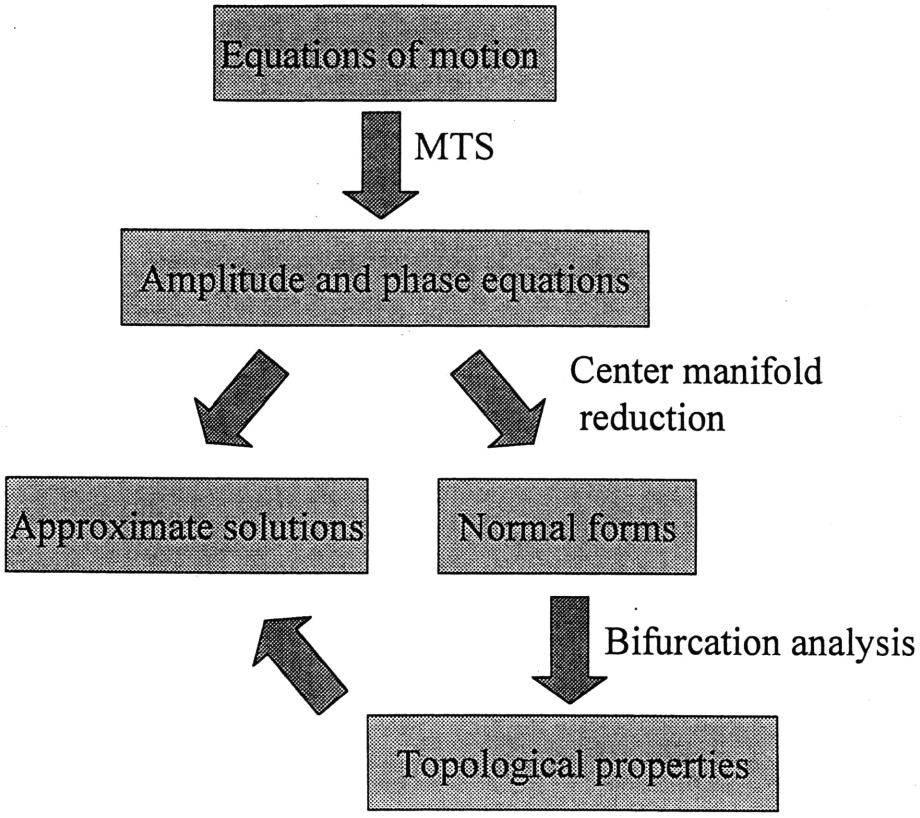

Figure 2-6: The analysis technique utilizing the MTS method, center manifold reduction principle, and bifurcation theory

It is interesting to note that the above theorem allows us to detect the occurence of a periodic orbit in a nonlinear system by examining the properties of the eigenvalues of the corresponding linearized system. However, to learn more about the properties of the resulting periodic orbit, such as its stability, one has to do further analysis by including the nonlinear terms.

2.4 Methodology

By virtue of the methods discussed so far, Figure 2-6 shows schematically the logical flow of their application in the analysis.

Starting with the equations of motion, which are parameterized by introducing

a small parameter, ϵ, the MTS method is then applied. The time scales used in the analysis are selected based on the Principle of Minimal Simplification and its extensions. As we shall see later, the systems of interest are oscillatory in nature and the application of the MTS method usually leads to the amplitude and phase-correction equations in the slower time scales. These equations may or may not be solvable, depending on the system. In the single degree-of-freedom wing rock case, the amplitude and phase-correction equations are solvable analytically. However, in the multiple degrees-of-freedom cases, these equations are coupled and hence are very difficult to be solved exactly. As we can see later, in all cases we consider in the dissertation, the amplitude equations can be solved independently from the phase-correction equations. The phase-correction equations can usually be solved once the solution of the amplitude equations are found. This fact simplifies the problems. However, it should be remembered that in the multiple degrees-of-freedom cases, the amplitude equations are also multi dimensional and coupled.

As we have mentioned, the exact solutions of the amplitude equations are very difficult or may be imposible to obtain. Approximate solutions can be derived with some information of the system dynamics, such as its topological properties. To obtain such properties, we first simplify the problem by reducing its dimension using the center manifold reduction principle. Bifurcation analysis can then be performed on the reduced dimensional system to get the topological picture of the system around the equilibrium point of interest. As we can see from Figure 2-6, the information on the topological properties of the system will be used to obtain the analytical approximation of the solution.

The above paragraphs describe the technique of analysis in general. The technique provides a systematic approach to obtain approximate solutions to the problems. Moreover, the application of the technique leads to considerable insight into the complex phenomenon, as will be demonstrated in the next three chapters.

Chapter 3

Single Degree-of-Freedom Wing Rock

3.1 Introduction

In this chapter, a simplified treatment of the problem is considered, where it is assumed that the aircraft has only one rotational degree-of-freedom in roll. This simplification is based on the fact that the wing rock motion in most situations is dominated by oscillations in roll. Most published work on wing rock deals with such simplified case [12-18]. The largely available data of wind tunnel experiment on wing rock motion for a one degree-of-freedom aircraft or wing model also explains why much work is focused on this very special case.

Although relatively less difficult, a great deal of insight can be gained by studying the single degree-of-freedom wing rock problem. Note however, that because of the model limitation, some important physical effects, such as aerodynamic cross-coupling, are not included.

This chapter revisits and extends the previous work on single degree-of-freedom wing rock dynamics. It serves as a basis for later work on multiple degrees-of-freedom cases, which require more complex analysis.

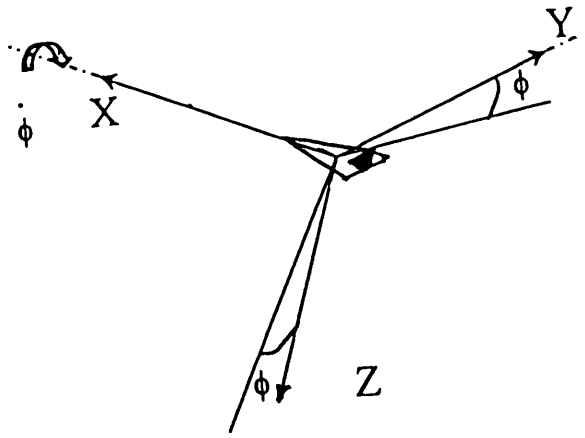

Figure 3-1: The aircraft axis systems

3.2 Equation of Motion

In this and subsequent chapters, the Lagrangian approach is used in deriving the equations of motion of the aircraft. This approach reduces the formulation of problems in dynamics to that of the variation of a scalar integral irrespective of the coordinate systems used. Note that for the simple case of single rotational degree-of-freedom motion, the equation of motion can be derived easily using any available methods. However, the Lagrangian approach will be used in this derivation to provide uniformity with the derivations in subsequent chapters, which deal with multiple degrees-of-freedom problems.

The axis systems needed in deriving the equations of motion are established next. The first axis system is denoted as $X_oY_oZ_o$ and referred to as the stability axis system. Its origin is at the center of mass of the aircraft and the orientation of the axes describes the nominal or unperturbed attitude of the aircraft. The X_o axis is oriented towards the nominal nose direction of the aircraft, the Z_o axis is on the nominal vertical plane of the aircraft pointing down and perperdicular to the X_o axis, while the Y_o axis completes the righthanded axis system. The second axis system ($X_bY_bZ_b$) is called the body-fixed axis system. As the name implies, this axis system has its origin on the center of mass of the aircraft and it is fixed to the aircraft body. The X_b axis points towards the nose of the aircraft, the Z_b axis is on the aircraft vertical plane and perpendicular to X_b, while Y_b completes the righthanded axis system. In nominal flight condition, these two axis systems coincide with each other. See Figure 3-1.

The aircraft is assumed to be rigid and has only a single rotational degree-of-

freedom in roll. Hence, in this case, X_b and X_o axes coincide. Perturbations in the system will only make the aircraft rotate about this axis. In perturbed situation, the Y axis of the body and stability axis systems makes an angle ϕ with respect to each other. Similarly for the Z axis. This angle is called roll angle. Because of the assumption, the angular rate of the aircraft can simply be expressed as follows.

$$\begin{aligned} \boldsymbol{\omega} &= p\,\mathbf{i}_{\mathbf{x_b}} \\ &= \dot{\phi}\,\mathbf{i}_{\mathbf{x_o}} \end{aligned} \tag{3.1}$$

where the notation $\mathbf{i}$ denotes the unity vector along the axis described in its subscript. Following the usual convention, p denotes the roll rate of the aircraft. For this special case, $p = \dot{\phi}$.

As the aircraft has only the degree-of-freedom to roll, the rotational kinetic energy of the aircraft is given by

$$T = \frac{1}{2} I_{xx} \dot{\phi}^2 \tag{3.2}$$

where I_{xx} is the moment of inertia of the aircraft about the X_b-axis. By substituting the above expression of kinetic energy into the Lagrange's equation

$$\frac{d}{dt}\left(\frac{\partial T}{\partial \dot{\phi}}\right) - \frac{\partial T}{\partial \phi} = Q \tag{3.3}$$

we get

$$I_{xx}\ddot{\phi} = Q \tag{3.4}$$

where Q is the generalized force, which is assumed to be contributed solely by the aerodynamics. The generalized force in this case is just the aerodynamic rolling moment of the aircraft. The generalized force, Q, can be found using

$$Q = \frac{\delta W}{\delta \phi} \tag{3.5}$$

which is basically the variation of the work done by the generalized forces due to the variation of the generalized displacement. The influences of gravity and propulsive forces are neglected in current analysis. Also, since we are interested in the free motion of the aircraft, we assume that no controls have been applied to the aircraft system. We will now discuss the aerodynamic moment acting on the aircraft.

3.3 Aerodynamic Moment

In this section, the aerodynamic moment on the aircraft is derived. The purpose of this section is to find the appropriate nonlinear form of aerodynamic moment to be used in the analysis. The details of the aerodynamic coefficients appearing in the final moment expression are of no importance at this point. These coefficients can be calculated by interpolating a polynomial of a certain order to the aerodynamics data of the aircraft found by using various techniques : analytical, computational, or experimental. This point will be further clarified as we proceed with the derivation.

The aerodynamic moment is derived under the assumption that the air flow around the aircraft is incompressible and quasi-steady. Simple modified strip theory aerodynamics is utilized in the derivation, since, as we have stated before, we only need to obtain an appropriate expression of the aerodynamic moment. In the usual strip theory, the local aerodynamic force is determined solely by the aerodynamic properties of each aircraft segment (c_L vs. α, c_D vs. α) and the gross angle-of-attack of the aircraft, with no consideration of three dimensional flow effects. Here, to keep the generality of the aerodynamic moment developed, the three-dimensional effect of the flow is taken into account. Because of this effect, each segment of the aircraft may see a different effective angle-of-attack. Nominally, it is assumed that the aircraft flies a horizontal straight path at specific angle-of-attack. It is also assumed that only the wings and the horizontal tail of the aircraft are effective in generating the aerodynamic forces.

We consider the derivation of aerodynamic forces on the wing in detail. The derivation for the horizontal tail will then follow in a similar fashion. Consider a streamwise segment of the wing of width dy. The incremental lift and drag forces produced by this segment are

$$\begin{aligned} dL(y) &= \bar{q}c(y)c_L(y)dy \\ dD(y) &= \bar{q}c(y)c_D(y)dy \end{aligned} \tag{3.6}$$

where $\bar{q} = \frac{1}{2}\rho V^2$ is the dynamic pressure, $c(y)$ is the airfoil chord at location y along the Y_b axis, $c_L(y)$ and $c_D(y)$ are the local lift and drag coefficients, respectively. The relationship of the local lift and drag coefficients ($c_L(y)$ and $c_D(y)$) on the local effective angle-of-attack ($\alpha_e(y)$) is represented by a cubic polynomial as follows.

$$\begin{aligned} c_L &= c_{L_0} + c_{L_1}\alpha_e + c_{L_2}\alpha_e^2 + c_{L_3}\alpha_e^3 \\ c_D &= c_{D_0} + c_{D_1}\alpha_e + c_{D_2}\alpha_e^2 + c_{D_3}\alpha_e^3 \end{aligned} \tag{3.7}$$

As we will point out later, the inclusion of the cubic terms in the above relations is necessary for the generation of wing rock motion. In Equation (3.7), the dependence of the coefficients and α on the spanwise location, y, has been omitted for simplicity.

The effective angle-of-attack distribution along the wing span consists of several contributions. For the one degree-of-freedom case, in general, this distribution depends on the nominal angle-of-attack, roll rate, sideslip angle and sideslip rate. Since we only consider small deviations from the nominal condition, then the contributions of the above factors on the effective angle-of-attack distribution can be expressed using a linear relation as follows.

$$\alpha_e(y) = \alpha_1(y) + \frac{\partial \alpha(y)}{\partial p} p + \frac{\partial \alpha(y)}{\partial \beta} \beta + \frac{\partial \alpha(y)}{\partial \dot{\beta}} \dot{\beta} \tag{3.8}$$

or alternatively,

$$\alpha_e(y) = \alpha_1(y) + \alpha_2(y) + \alpha_3(y) + \alpha_4(y) \tag{3.9}$$

where $\alpha_1(y)$, $\alpha_2(y)$, $\alpha_3(y)$, and $\alpha_4(y)$ indicate the component of the effective angle-of-attack distribution contributed by the nominal angle-of-attack, roll rate, angle-of-sideslip, and sideslip rate, respectively. The following itemization describes each of the above components briefly.

- Nominal angle-of-attack (α_0).
  Since the aircraft in the nominal condition is assumed to fly symmetrically, then the resulting effective angle-of-attack distribution due to α_0 is symmetric. This distribution generates aerodynamic forces necessary to keep the aircraft in equilibrium. For a wing in three dimensional flow,

  $$\alpha_1(y) = \alpha_g(y) - \alpha_i(y) \tag{3.10}$$

  where $\alpha_e(y)$ denotes the local true angle-of-attack seen by the local wing section, α_g denotes the local angle-of-attack in case the flow is two dimensional, and $\alpha_i(y)$ denotes the induced angle-of-attack, which is basically a three-dimensional effect. Equation (3.10) can be expressed as

  $$\alpha_1(y) = \sin^{-1}(\sin\alpha_0 \cos\Gamma \cos\phi) - \alpha_i(y) \tag{3.11}$$

  where Γ is the dihedral angle of the wing.

- Roll rate (p).
  By convention, positive roll rate tends to move the right wing tip down and

the left wing tip up. It is clear therefore that positive roll rate increases the effective angle-of-attack seen by the right wing and decreases the one seen by the left wing. In this work, it is assumed that the angle-of-attack distribution due to roll rate is perfectly antisymmetric and can be generally expressed using

$$\alpha_2(y) = f_2(y)p \tag{3.12}$$

where $f_2(y)$ is an odd function of y, which may take into account the three dimensional nature of the flow. In a simple case where the three-dimensional aerodynamic effects are absent, α_2 is given by

$$\alpha_2(y) = \frac{yp}{U} \tag{3.13}$$

where U is the component of the aircraft speed on the X_b-axis.

- Angle-of-sideslip (β).
  Nonzero angle-of-sideslip indicates the presence of cross flow, and such a cross flow destroys the symmetry of the flow and induces changes in the angle-of-attack seen by each streamwise segment of the wing. For an aircraft flying at high angles-of-attack, the angle-of-sideslip can be induced by the deviation of the aircraft from the wing level position. At low angles-of-attack, the induced angle-of-sidelip is negligible. The magnitude of the incremental angle-of-attack due to sideslip is dependent on several factors such as wing dihedral angle, wing position on the fuselage (high, low or mid), fuselage shape and wing sweep angle. The angle-of-attack distribution generated by this effect is assumed to be antisymmetric and can be expressed as

$$\alpha_3(y) = f_3(y)\beta \tag{3.14}$$

  $f_3(y)$ is an odd function of y, whose values and sign depend on the factors mentioned above.

- Sideslip rate ($\dot{\beta}$)
  The $\dot{\beta}$ effect is mostly due to the lag effect of the flow between the right and left wings. The component of the effective angle-of-attack distribution due to this effect is assumed to be antisymmetric and is expressed as

$$\alpha_4(y) = f_4(y)\dot{\beta} \tag{3.15}$$

  where $f_4(y)$ is an odd function of y. There is no known simple expression for

$f_4(y)$.

The effective angle-of-attack seen by each streamwise segment of the wing can then be calculated by summing up the components discussed above, that is

$$\alpha_e(y) = \alpha_1(y) + f_2(y)p + f_3(y)\beta + f_4(y)\dot{\beta} \tag{3.16}$$

In a similar fashion, we can obtain the local effective angle-of-attack for each streamwise segment of the horizontal tail. By substituting Equation (3.16) into Equation (3.7), we get c_L and c_D expressions in terms of α_1, p, β, and $\dot{\beta}$. From Equation (3.6), the incremental lift and drag forces generated by each streamwise segment can also be expressed in terms of the above variables. The work done by the aerodynamic forces through a displacement $\delta\phi$ can then be calculated using

$$\delta W = -\int_{a/c} (dL\cos\alpha_0 + dD\sin\alpha_0)\, y\, \delta\phi \tag{3.17}$$

where a/c underneath the integration sign means that the integration is performed along the wings and the horizontal tail, which are the only effective aerodynamic surfaces of the aircraft (by assumption).

The integrands in the above expression can be expanded in terms of variables α_1, p, β, and $\dot{\beta}$. Term-by-term integration can then be performed. The integration process is not difficult, however it is quite lengthy and is described in more detail in Appendix A. Several important aspects of the integration which lead us to the integration result below are discussed next. In general, the integrands can be divided into two groups of terms. The first group contains even terms (even functions of y), and the other contains odd terms (odd functions of y). It can be understood that the odd integrands are integrated to zero and hence the final integration result is the contribution of the even integrands only. Then, by using Equation (3.5), the resulting aerodynamic moment, which is rolling moment for this single degree-of-freedom model, is given by

$$\begin{aligned}\bar{Q} \;=\; & \bar{c}_1\beta + \bar{c}_2 p + \bar{c}_3\dot{\beta} + \bar{c}_4\beta^3 + \bar{c}_5\beta^2 p + \bar{c}_6\beta^2\dot{\beta} + \bar{c}_7\beta p^2 + \bar{c}_8\beta\dot{\beta}^2 + \bar{c}_9\dot{\beta}^3 + \\ & \bar{c}_{10}p^3 + \bar{c}_{11}\beta\dot{\beta}p\end{aligned} \tag{3.18}$$

where $\bar{Q} \equiv \dfrac{Q}{I_{xx}}$. The above equation can be expressed in terms of aircraft stability derivatives as follows.

$$\bar{Q} = \frac{L}{I_{xx}} = L_p p + L_\beta\beta + L_{\dot{\beta}}\dot{\beta} \tag{3.19}$$

where L_p, L_β, and $L_{\dot{\beta}}$ are the rolling moment derivatives with respect to roll rate, angle-of-sideslip, and rate of sideslip, respectively. It should be noted, that in the above equation, the stability derivatives L_p, L_β, and $L_{\dot{\beta}}$ are not constant in general, as in the linear treatment of aircraft dynamics. They may be functions of the variables β, p, $\dot{\beta}$, α, and in general, can be nonlinear. For example, by comparing Equations (3.19) and (3.18), L_p can be written as follows.

$$L_p = \bar{c}_2 + \bar{c}_5\beta^2 + \bar{c}_7\beta p + \bar{c}_{10}p^2 + \bar{c}_{11}\beta\dot{\beta} \tag{3.20}$$

In practice, numerical or experimental techniques are usually used to get the values of the aerodynamic moment. Various aerodynamic moment values for various combination of α_0, p, β, and $\dot{\beta}$ can be computed. One can then utilize curve-fitting techniques to the numerical or experimental results to obtain the values of the coefficients in Equation (3.18). Note that curve-fitting can be applied only to the range of angle-of-attack of interest. It can be understood, that for some cases, some of the coefficients are not important or significant. For these cases, the terms associated with these coefficients can be dropped and this will simplify the rolling moment expression (3.18). For the sake of generality, however, all the terms in Equation (3.18) will be carried over to the subsequent analysis.

3.4 Motion Analysis

Before doing further analysis, we will first express the equation of motion in terms of roll angle, ϕ, only, by using the following kinematic relations :

$$\begin{aligned} p &= \dot{\phi} \\ \beta &= \phi \sin\alpha_0 \\ \dot{\beta} &= \dot{\phi} \sin\alpha_0 \end{aligned} \tag{3.21}$$

The equation of motion of the aircraft (Equations (3.4) and (3.18) then becomes

$$\ddot{\phi} = \hat{c}_1\dot{\phi} + \hat{c}_2\phi + \hat{c}_3\phi^3 + \hat{c}_4\phi^2\dot{\phi} + \hat{c}_5\phi\dot{\phi}^2 + \hat{c}_6\dot{\phi}^3 \tag{3.22}$$

where

$$\hat{c}_1 = \bar{c}_2 + \bar{c}_3 \sin\alpha_0$$

$$
\begin{aligned}
\hat{c}_2 &= \bar{c}_1 \sin\alpha_0 \\
\hat{c}_3 &= \bar{c}_4 \sin^3\alpha_0 \\
\hat{c}_4 &= \bar{c}_5 \sin^2\alpha_0 + \bar{c}_6 \sin^3\alpha_0 \\
\hat{c}_5 &= \bar{c}_7 \sin\alpha_0 + \bar{c}_8 \sin^3\alpha_0 + \bar{c}_{11} \sin^2\alpha_0 \\
\hat{c}_6 &= \bar{c}_9 \sin^3\alpha_0 + \bar{c}_{10}
\end{aligned} \tag{3.23}
$$

In the above relations, there are some coefficients which are equivalent to the linear stability derivatives, that is the constant stability derivatives used for linear aircraft dynamics analysis. They are summarized below.

$$
[\bar{c}_1 \quad \bar{c}_2 \quad \bar{c}_3] \equiv [L_{\beta_0} \quad L_{p_0} \quad L_{\dot{\beta}_0}] \tag{3.24}
$$

Here, the subscript *0* is used to indicate the linear stability derivatives.

As can be seen from Equation (3.23), the sign of the coefficient $\hat{c}_2$ depends on the static lateral stability derivative $L_{\beta_0} \equiv \bar{q}SbC_{l_{\beta_0}}$. Typical variation of the static lateral stability derivative with angle-of-attack is shown in Figure 3-2. For the range of angles-of-attack of interest here (0^o to 90^o), $C_{l_{\beta_0}}$, and hence L_{β_0} is negative. It is possible that L_{β_0} becomes positive on some range of angles-of-attack. This case, however is not typical and results in a divergent motion due to loss of static stability and of no interest here. The analysis in this work is based on the case where L_{β_0} is negative. To signify this, we define

$$
\omega^2 \equiv -\hat{c}_2 = -L_{\beta_0} \sin\alpha_0 \tag{3.25}
$$

The damping term $\hat{c}_1\dot{\phi}$ plays an important role in the dynamics of the aircraft and we define the following.

$$
\tilde{\mu} \equiv \hat{c}_1 \tag{3.26}
$$

Then, by also defining

$$
[\tilde{c}_1 \quad \tilde{c}_2 \quad \tilde{c}_3 \quad \tilde{c}_4] \equiv [\hat{c}_3 \quad \hat{c}_4 \quad \hat{c}_5 \quad \hat{c}_6] \tag{3.27}
$$

the equation of motion (3.22) becomes

$$
\ddot{\phi} + \omega^2\phi = \tilde{\mu}\dot{\phi} + \tilde{c}_1\phi^3 + \tilde{c}_2\phi^2\dot{\phi} + \tilde{c}_3\phi\dot{\phi}^2 + \tilde{c}_4\dot{\phi}^3 \tag{3.28}
$$

It should be noted that when the nonlinear aerodynamic effects are insignificant and

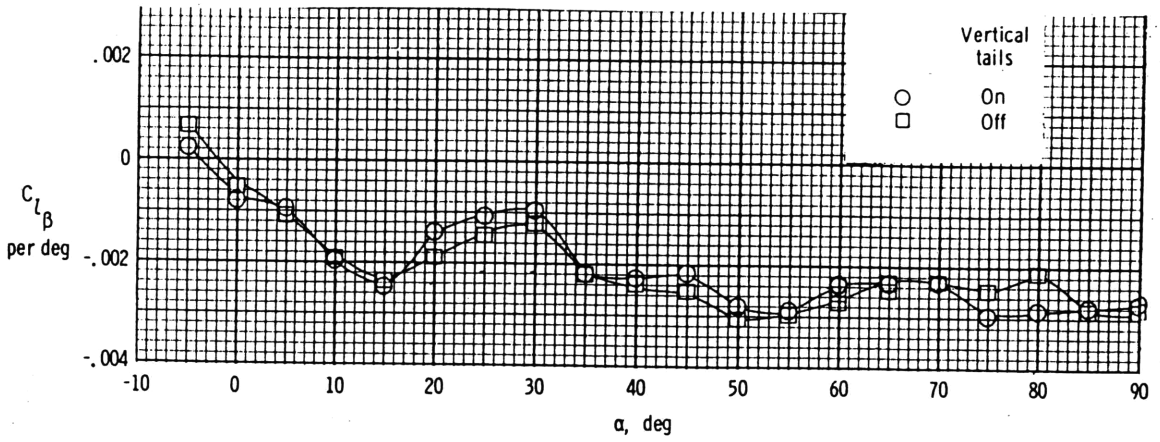

Figure 3-2: Static lateral stability derivative vs angle-of-attack for a fighter configuration with wing sweep angle of 22^o [44]

the aircraft flies at low angles-of-attack, the equation of motion is represented by

$$\ddot{\phi} = \tilde{\mu}\dot{\phi} \tag{3.29}$$

In this case, roll motion is not oscillatory and is usually called *roll subsidence* mode. Aerodynamic nonlinearity and high angle-of-attack change the nature of the roll motion to become oscillatory.

We focus on the small motions of the aircraft about an equilibrium condition near wing rock situation. In this case, we have

$$\lim_{\mathbf{x}\to\bar{\mathbf{0}}} \frac{|N(\mathbf{x})|}{|\mathbf{x}|} = 0 \tag{3.30}$$

where $\mathbf{x} = \{\phi\ \dot{\phi}\}^{\mathrm{T}}$ and $N(\mathbf{x})$ contains all the nonlinear terms in the equation. This is equivalent to saying that $N(\mathbf{x}) = \mathbf{O}(\epsilon)$, where $0 < \epsilon \ll 1$. Also, as previously mentioned, the roll damping parameter $\tilde{\mu}$ plays an important role in the aircraft dynamics. We shall see later that wing rock situation is associated with the loss of such damping. Therefore, because our analysis focuses on the dynamics of the system in the vicinity of wing rock, it is reasonable to assume that the damping term is small. By virtue of experience with numerical solutions for the wing rock problems, the following parameterization in terms of a small parameter, ϵ, is found to be convenient and constructive. Thus, we parameterize the equation of motion as

$$\ddot{\phi} + \omega^2\phi = \epsilon(\mu\dot{\phi} + c_1\phi^3 + c_2\phi^2\dot{\phi} + c_3\phi\dot{\phi}^2 + c_4\dot{\phi}^3) \tag{3.31}$$

It is possible to do a more refined parameterization based on each individual value of the coefficients of the nonlinear terms. However, to keep the generality of the analysis, we do not do such a refinement.

Before doing further analysis based on the nonlinear parameterized equation of motion (3.31), we first look at some properties of the linearized equation around the equilibrium conditions of the system. We first write Equation (3.31) in terms of a system of first order differential equations as follows

$$\begin{aligned} \dot{x}_1 &= x_2 \\ \dot{x}_2 &= -\omega^2 x_1 + \epsilon(\mu x_2 + c_1 x_1^3 + c_2 x_1^2 x_2 + c_3 x_1 x_2^2 + c_4 x_2^3) \end{aligned} \tag{3.32}$$

where $x_1 \equiv \phi$ and $x_2 \equiv \dot{\phi}$. The equlibrium points of the system can be found be setting $\dot{x}_1 = \dot{x}_2 = 0$ and then solving the resulting equation. Doing so, we get

$$\begin{aligned} x_2 &= 0 \\ \epsilon c_1 \phi^3 - \omega^2 \phi &= 0 \end{aligned} \tag{3.33}$$

The solutions of this algebraic equation are $(x_1, x_2) = (0, 0)$ and $(x_1, x_2) = (\pm\sqrt{\frac{\omega^2}{\epsilon c_1}}, 0)$. Note that the second set of equilibrium points may not be real, depending on the value of c_1. If $c_1 > 0$, the second set of equilibrium points are real, while if $c_1 < 0$, they are imaginary.

Now the properties of linear system around these equilibrium points are examined. The linearized system around the equilibrium at $(0, 0)$ is given by

$$\begin{Bmatrix} \dot{x}_1 \\ \dot{x}_2 \end{Bmatrix} = \begin{bmatrix} 0 & 1 \\ -\omega^2 & \epsilon\mu \end{bmatrix} \begin{Bmatrix} x_1 \\ x_2 \end{Bmatrix} \tag{3.34}$$

The eigenvalues of the system are

$$\lambda_{1,2} = \frac{\epsilon\mu}{2} \pm \frac{1}{2}\sqrt{\epsilon^2\omega^2 - 4\omega^2} \tag{3.35}$$

The stability of the linear system is determined by the real part of the eigenvalues, which is $\frac{\epsilon\mu}{2}$. Based on the stability theory (see Chapter 2), the equilibrium $(0, 0)$ is asymptotically stable for $\mu < 0$ and unstable for $\mu > 0$. We will focus now on the equilibrium points at $(x_1, x_2) = (\pm\sqrt{\frac{\omega^2}{\epsilon c_1}}, 0)$. The linearized equation of motion

around these equilibria is

$$\begin{Bmatrix} \dot{x}_1 \\ \dot{x}_2 \end{Bmatrix} = \begin{bmatrix} 0 & 1 \\ \omega^2 & \epsilon\mu + \frac{c_2\omega^2}{c_1} \end{bmatrix} \begin{Bmatrix} x_1 \\ x_2 \end{Bmatrix} \tag{3.36}$$

and the eigenvalues for the system are

$$\lambda_{1,2} = \frac{1}{2}\left(\epsilon\mu + \frac{c_2\omega^2}{c_1}\right) \pm \frac{1}{2}\sqrt{\left(\epsilon\mu + \frac{c_2\omega^2}{c_1}\right)^2 + 4\omega^2} \tag{3.37}$$

Note that in the above expression $\frac{1}{2}\sqrt{\left(\epsilon\mu + \frac{c_2\omega^2}{c_1}\right)^2 + 4\omega^2} > \frac{1}{2}\left(\epsilon\mu + \frac{c_2\omega^2}{c_1}\right)$. Therefore, the eigenvalues of the system are real and have opposite signs. This implies that the equilibrium points at $(x_1, x_2) = (\pm\sqrt{\frac{\omega^2}{\epsilon c_1}}, 0)$ are unstable and of the saddle-point type.

The rest of the analysis developed in this chapter will be focused on the dynamics of the system around the equilibrium at $(x_1, x_2) = (0, 0)$, which is physically the nominal condition of the aircraft. Because of the nature of the analysis, the results will not be accurate for the situations which are close to the other equilbrium points. In essence, the knowledge about the locations of the other equilibrium points of the system is crucial in that it gives us an information about possible limitation in the region of validity of the analysis developed. It should be noted that the nonzero equilibrium roll angle are proportional to $\frac{1}{\sqrt{\epsilon}}$. Since ϵ is small, these roll equilibrium usually occurs at large angles. Hence, their effects on the system dynamics around the nominal condition may not be noticable in the region of validity of the analysis.

The MTS method is invoked and applied to Equation (3.31). Two time scales approach is used in the analysis. Using this approach, the independent and dependent variables are extended as follows.

$$\begin{aligned} t \;&\rightarrow\; \{\tau_0, \tau_1\} \;\;;\;\; \tau_0 = t \\ &\qquad\qquad\;\; \tau_1 = \epsilon t \\ \phi(t) \;&\rightarrow\; \phi_0(\tau_0, \tau_1) + \epsilon\phi_1(\tau_0, \tau_1) + \ldots \end{aligned} \tag{3.38}$$

In this formulation, τ_0 is the fast time scale, while τ_1 is the slow one. By this extension, the equation of motion (3.31), which is an ordinary differential equation, becomes a partial differential equation. Grouping the terms in the resulting partial differential

equation according to the order of ϵ, we get

$$\frac{\partial^2\phi_0}{\partial\tau_0^2} + \omega^2\phi_0 + \epsilon\left[\frac{\partial^2\phi_1}{\partial\tau_0^2} + \omega^2\phi_1 + 2\frac{\partial^2\phi_0}{\partial\tau_0\partial\tau_1}\right] = \epsilon\left[\mu\frac{\partial\phi_0}{\partial\tau_0} + c_1\phi_0^3 + c_2\phi_0^2\frac{\partial\phi_0}{\partial\tau_0} + c_3\phi_0\left(\frac{\partial\phi_0}{\partial\tau_0}\right)^2 + c_4\left(\frac{\partial\phi_0}{\partial\tau_0}\right)^3\right] + \ldots \quad (3.39)$$

where the dependence of ϕ on τ_0 and τ_1 has been suppressed for notational simplicity. Only terms up to $O(\epsilon)$ are shown in the above equation. As we shall see later, only terms up to this order are needed to obtain the zeroth order approximation of the solution. The approximate solution is built by equating groups of the same order on the left and the righthand side of Equation (3.39), beginning from the leading order one (dominant group of terms).

The dominant terms from the above equation are of $O(1)$ and equating these terms to zero yields

$$O(1) \; : \; \frac{\partial^2\phi_0}{\partial\tau_0^2} + \omega^2\phi_0 = 0 \quad (3.40)$$

The solution of this equation is

$$\phi_0 = A(\tau_1)\sin\Psi \quad ; \quad \Psi \equiv \omega\tau_0 + B(\tau_1) \quad (3.41)$$

Note that the amplitude and the phase of the solution vary with the slow time scale τ_1. Once these variations are known, the zeroth order approximation to the motion dynamics is complete. The variation of the amplitude and phase with τ_1 is found from the next order analysis of Equation (3.39), which is

$$O(\epsilon) \; : \; \frac{\partial^2\phi_1}{\partial\tau_0^2} + \omega^2\phi_1 = -2\frac{\partial^2\phi_0}{\partial\tau_0\partial\tau_1} + \mu\frac{\partial\phi_0}{\partial\tau_0} + c_1\phi_0^3 + c_2\phi_0^2\frac{\partial\phi_0}{\partial\tau_0} + c_3\phi_0\left(\frac{\partial\phi_0}{\partial\tau_0}\right)^2 + c_4\left(\frac{\partial\phi_0}{\partial\tau_0}\right)^3 \quad (3.42)$$

By substituting Equation (3.41) into the above equation, we get

$$\frac{\partial^2\phi_1}{\partial\tau_0^2} + \omega^2\phi_1 = -\left[2\omega\frac{dA}{d\tau_1} - \mu\omega A - \frac{1}{4}\omega(c_2 + 3c_4\omega^2)A^3\right]\cos\Psi + \left[2\omega A\frac{dB}{d\tau_1} + \frac{1}{4}(3c_1 + c_3\omega^2)A^3\right]\sin\Psi - \frac{1}{4}\omega\left(c_2 - c_4\omega^2\right)A^3\cos 3\Psi - \frac{1}{4}\left(c_1 - c_3\omega^2\right)A^3\sin 3\Psi \quad (3.43)$$

If the $\cos\Psi$ and $\sin\Psi$ terms on the righthand side of the equation are nonzero, secular terms of the form $\tau_0\cos\Psi$ and $\tau_0\sin\Psi$ appear in the solution for ϕ_1. These secular terms destroy the uniformity of the approximation. Therefore, to keep the approximation uniform, the coefficients of the $\cos\Psi$ and $\sin\Psi$ terms are set to zero. This obtains

$$\begin{aligned} \frac{dA}{d\tau_1} &= \frac{1}{2}\mu A + p_1 A^3 \\ \frac{dB}{d\tau_1} &= p_2 A^2 \end{aligned} \tag{3.44}$$

where

$$\begin{aligned} p_1 &= \frac{1}{8}\left(c_2 + 3c_4\omega^2\right) \\ p_2 &= -\frac{1}{8}\left(\frac{3c_1}{\omega} + c_3\omega\right) \end{aligned} \tag{3.45}$$

The sign of p_1 and p_2 depends on the nonlinearities involved. Equation (3.44) are the governing equations for the slowly varying amplitude and phase corrections. The amplitude equation determines whether the solution increases or decreases with time, hence the stability of the motion. Note that the amplitude equation can be solved independently. Once this amplitude solution is found, the solution of the phase-correction equation can be obtained, since the phase-correction equation depends only on A. For this simple one degree-of-freedom case, the exact solution of the amplitude equation can be obtained analytically. Before doing so, we will first look at the properties of the solution in the framework of bifurcation as μ varies.

3.4.1 Bifurcation Analysis

The equilibria of the amplitude equation are $A_1 = 0$ and $A_1 = \sqrt{-\frac{\mu}{2p_1}}$. Plotted in $A_1 - \mu$ diagram, the equilibria consist of the μ-axis and the parabola $\mu = -2p_1A_1^2$. The stability of these equilibria for any $\mu = constant \neq 0$ can be determined by examining the eigenvalues of the linearized systems around the equilibria of interest. As has been discussed in Chapter 2, an equilibrium point is stable if all the eigenvalues of the corresponding linearized system about this point have negative real parts, and an equilibrium point is unstable if one of the eigenvalues of the linearized system has positive real part.

The linearization around the equilibria at μ-axis ($A_1 = 0$) yields

$$\frac{dA}{d\tau_1} = \frac{1}{2}\mu A \tag{3.46}$$

The eigenvalue of this simple equation is $\frac{1}{2}\mu$. Therefore, it is clear that the equilibria are stable for $\mu < 0$ and unstable for $\mu > 0$. Physically, this means that the nominal flight condition at angles-of-attack where $\mu < 0$ is stable, but becomes unstable at angles-of-attack where $\mu > 0$. The linearized system around the equilibria at $\mu = -2p_1 A_1^2$ is

$$\frac{dA}{d\tau_1} = -\mu A \tag{3.47}$$

The eigenvalue of this linearized system is $-\mu$. It is obviously stable for $\mu > 0$ and unstable for $\mu < 0$.

The previous discussion is only valid for $\mu \neq 0$. When $\mu = 0$, we cannot conclude about the stability based on the linearized system. The stability of the system has to be determined by including the nonlinear term in the equation. For $\mu = 0$, the amplitude equation becomes

$$\frac{dA}{d\tau_1} = p_1 A^3 \tag{3.48}$$

which is a first order nonlinear ordinary differential equation, whose properties are quite well known. Basically, the solution of this equation ($A(\tau_1)$) decays to zero when $\frac{dA}{d\tau_1} < 0$ and increases when $\frac{dA}{d\tau_1} > 0$. In other words, the system is stable if $p_1 < 0$ and unstable if $p_1 > 0$.

The above discussion clearly shows that the properties of the solution changes as μ varies from negative to positive. For example, the number of the equilibrium points changes across $\mu = 0$. Consider the case when $p_1 < 0$. For this situation, the system only has one equilibrium point when $\mu < 0$, but it has three equilibria when $\mu > 0$. In mathematical terms, the system undergoes topological changes as μ varies from negative to positive. Hence, $\mu = 0$ is the bifurcation point of the system. The bifurcation diagrams of the system for $p_1 > 0$ and $p_1 < 0$ are given in Figure 3-3. These diagrams imply that there is a finite amplitude oscillation (limit cycle) appearing or dissapearing in the system as μ is varied across $\mu = 0$. Thus, this is a Hopf type bifurcation. For $p_1 > 0$, the Hopf bifurcation is subcritical, since the new branch of equilibria appear for the values of μ below the onset of bifurcation. For $p_1 < 0$, the Hopf bifurcation is supercritical, as the new branch of equilibria exist only for values of μ larger than the onset of bifurcation. It can also be seen from the diagram, that the stable limit cycle is only possible when $p_1 < 0$. This implies

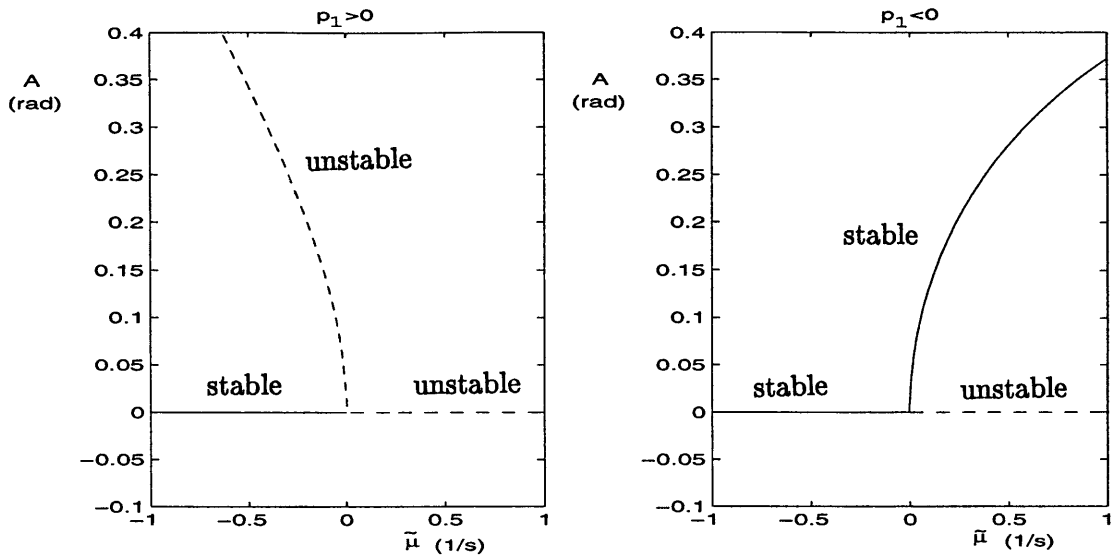

Figure 3-3: Bifurcation diagrams for (a) $p_1 > 0$ and (b) $p_1 < 0$

that sustained wing rock motion can only occur in this situation and the wing rock amplitude is given by $A_1 = \sqrt{-\frac{\mu}{2p_1}}$.

3.4.2 Analytical Approximation of the Solution

In this subsection, the zeroth order solution of the MTS expansion will be completed. We have already had the form of the solution in (3.41) and the governing differential equations for the amplitude and phase-correction variations. To complete the zeroth order solution, we need to derive the analytical solutions of these equations.

We first focus on the amplitude equation and we discuss specifically the case where wing rock is possible, that is $p_1 < 0$. By separating the variables and integrating Equation (3.44), and after some manipulations, A can be explicitly expressed as

$$A = \frac{\sqrt{K\frac{\mu}{2}}\exp(\frac{\mu}{2}\tau_1)}{\sqrt{1 - Kp_1\exp(\mu\tau_1)}} \tag{3.49}$$

The constant K in the above equation is determined from the initial condition.

Some properties of Equation (3.49) are now examined. If $\mu < 0$, then the numerator of Equation (3.49) goes to zero as τ_1 goes to infinity, because $\exp(\frac{\mu}{2}\tau_1)$ decays monotonically with time. Hence, $A \to 0$ as $\tau_1 \to \infty$. In other words, the amplitude of the motion decays with time, and so the system is stable. If $\mu > 0$, the exponentials

in the numerator and the denominator are dominant, and for sufficiently large τ_1,

$$A \to \frac{\sqrt{K\frac{\mu}{2}}\exp(\frac{\mu}{2}\tau_1)}{\sqrt{Kp_1\exp(\mu\tau_1)}} = \sqrt{-\frac{\mu}{2p_1}} \tag{3.50}$$

As has been previously stated, $p_1 < 0$, so A is real in this case. This fact is consistent with the previous analysis using bifurcation theory, where it is found that the nominal condition is stable for $\mu < 0$ and unstable for $\mu > 0$. The aircraft undergoes limit cycle oscillations for $\mu > 0$ (wing rock). Note also that the steady state amplitude of the limit cycle obtained in this analysis is consistent with the one obtained from the bifurcation theory. This analytical development, however, has an advantage, that is it also captures the transient part of the solution.

The substitution of the analytical solution for A into the phase-correction equation (3.44) yields

$$\frac{dB}{d\tau_1} = p_2\frac{K\frac{\mu}{2}\exp(\mu\tau_1)}{1 - Kp_1\exp(\mu\tau_1)} \tag{3.51}$$

Integrating this equation, we get

$$\begin{aligned} B(\tau_1) &= Kp_2\frac{\mu}{2}\int\frac{\exp(\mu\tau_1)}{1 - Kp_1\exp(\mu\tau_1)}d\tau_1 \\ &= \frac{1}{2}Kp_2\int\frac{d\exp(\mu\tau_1)}{1 - Kp_1\exp(\mu\tau_1)} \\ &= -\frac{1}{2}\frac{p_2}{p_1}\ln K_1\left(1 - Kp_1\exp(\mu\tau_1)\right) \end{aligned} \tag{3.52}$$

where K_1 is a constant depending on the initial condition. For $\mu < 0$, as $\tau_1 \to \infty$, $\exp(\mu\tau_1) \to 0$ and so $B \to -\frac{1}{2}\frac{p_2}{p_1}\ln K_1$ (a constant). This means that after some transients, the frequency of the system is described very well by ω and no correction is necessary. For $\mu > 0$, $B \to -\frac{1}{2}\frac{p_2}{p_1}\mu\tau_1 - \frac{1}{2}\frac{p_2}{p_1}\ln(-KK_1p_1)$. This shows that in steady state, the phase correction vary linearly with the slow time scale τ_1. Since $\tau_1 = \epsilon t$, this also implies that in steady state, the frequency of the system is constant and is given by $\omega - \frac{1}{2}\frac{p_2}{p_1}\mu$.

With these results, we can write the zeroth order approximation of the aircraft rolling motion in terms of t as follows.

$$\phi_0(t) = \frac{\sqrt{K\frac{\mu}{2}}\exp(\epsilon\frac{\mu}{2}t)}{\sqrt{1 - Kp_1\exp(\epsilon\mu t)}}\sin\left(\omega t - \frac{1}{2}\frac{p_2}{p_1}\ln K_1\left(1 - Kp_1\exp(\mu\tau_1)\right)\right) \tag{3.53}$$

The above result subsume the result of the linear analysis, that is the analysis without the inclusion of all the nonlinear terms. For the linear case, the solution we get is

$$\phi_0(t) = K_2 \exp(\frac{\epsilon\mu}{2}t) \sin(\omega t - K_3) \tag{3.54}$$

where K_2 and K_3 are constants depending upon the initial conditions. The linear analysis only leads to an asymptotically stable solution when $\mu < 0$ and an unstable solution (divergent) when $\mu > 0$. Limit cycle oscillations cannot be captured by the linear analysis.

3.5 Comparison with Numerical Results

To examine the accuracy of the analytical approximation obtained, dynamics of a generic fighter aircraft model in the vicinity of wing rock is looked at. The model includes nonlinearities in most of its aerodynamic parameters, as can be seen from Table 3.1. Note that this model is only valid for angles-of-attack in the range 20^o to 40^o, which is the range where transition from stable to wing rock motion occurs.

$I_{xx} = 36610\ kg\ m^2$ $\quad$ $b = 12\ m$
$I_{yy} = 162700\ kg\ m^2$ $\quad$ $c = 4.8\ m$
$I_{zz} = 183000\ kg\ m^2$ $\quad$ $S = 164.6\ m^2$
$I_{xz} = 6780\ kg\ m^2$
$\rho = 1.225\ kg/m^3$
$V = 100\ m/s$

$$C_l = (-0.295\alpha_0 + 0.1975\alpha_0^2)\beta + (0.22 + 0.63\alpha_0 - 0.797\alpha_0^2 + 0.975\alpha_0^3)\frac{bp}{2V} + 5.2\beta^3 - 0.075(\frac{bp}{2V})^3 - 1.42\beta^2\frac{bp}{2V} - 0.6\beta(\frac{bp}{2V})^2 - 0.011\dot{\beta} - 0.5\beta^2\dot{\beta}$$

Table 3.1: Generic fighter aircraft parameters for $10^o \leq \alpha_0 \leq 50^o$

For this aircraft the variations of the parameters $\tilde{\mu}$ and $\tilde{p}_1 \equiv \epsilon p_1$ with angle-of-attack are given in Figure 3-5. We can see that $\tilde{\mu}$, and hence μ, changes sign from negative to positive at $\alpha_0 = 27.34^o$. This specific angle-of-attack is the onset of wing rock. Below this angle-of-attack, the nominal flight condition is stable with no wing rock motion. Above this angle-of-attack, the free response of the aircraft begins to exhibit a wing rock motion. The variation of the eigenvalues of the linearized system about the nominal condition as a function of the angle-of-attack is shown on the complex plane in Figure 3-4. The points where the eigenvalues cross the imaginary

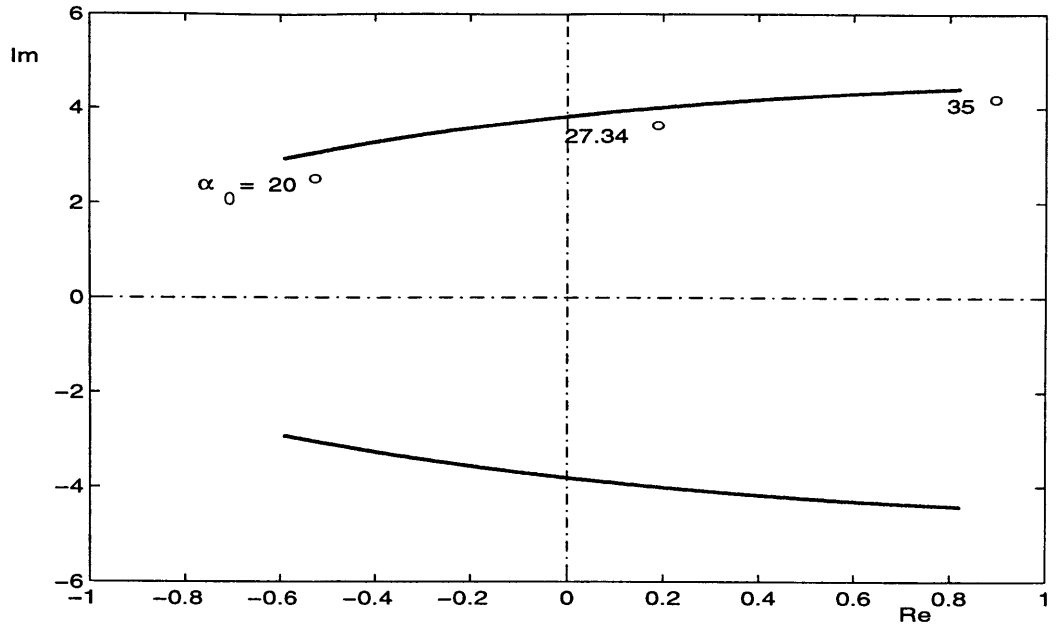

Figure 3-4: The variation of the eigenvalues of the system as the angle-of-attack increases

axis correspond to $\alpha_0 = 27.34^o$ ($\mu = 0$), which is the onset of bifurcation. This illustrates the Hopf bifurcation theorem discussed in Chapter 2.

In order to examine the accuracy of the prediction on the onset of wing rock, the aircraft responses slightly below ($\alpha_0 = 27.2^o$) and slightly above the onset angle-of-attack ($\alpha_0 = 27.6^o$) are simulated. The results are depicted in Figure 3-6. As can be seen from the figure, the amplitude of the aircraft oscillations below the onset decreases, while above the onset, the amplitude increases initially until limit cycle amplitude is attained. Thus, the analytical wing rock onset is very accurate.

Comparison of the aircraft response obtained from the analytical result to the exact one obtained using numerical integration is given in Figure 3-7 for $\alpha_0 = 29^o$. At this angle-of-attack, μ is positive and so the aircraft exhibits wing rock motion. The figure shows that the analytical approximation is in excellent agreement with the numerical integration result. The amplitude and phase history of the response are very well predicted by the analytical result.

The phase plane of the system is now examined. As an example, the phase plane of the system at the nominal angle-of-attack of 30^o is depicted in Figure 3-8. Based on Equation (3.33), this particular aircraft model at nominal angle-of-attack of 30^o possesses saddle-type equilibrium points at $(\phi, \dot{\phi}) = (\pm 0.71, 0)$ rad. These two saddle points and the limit cycles of the system can be observed from the figure. As can be

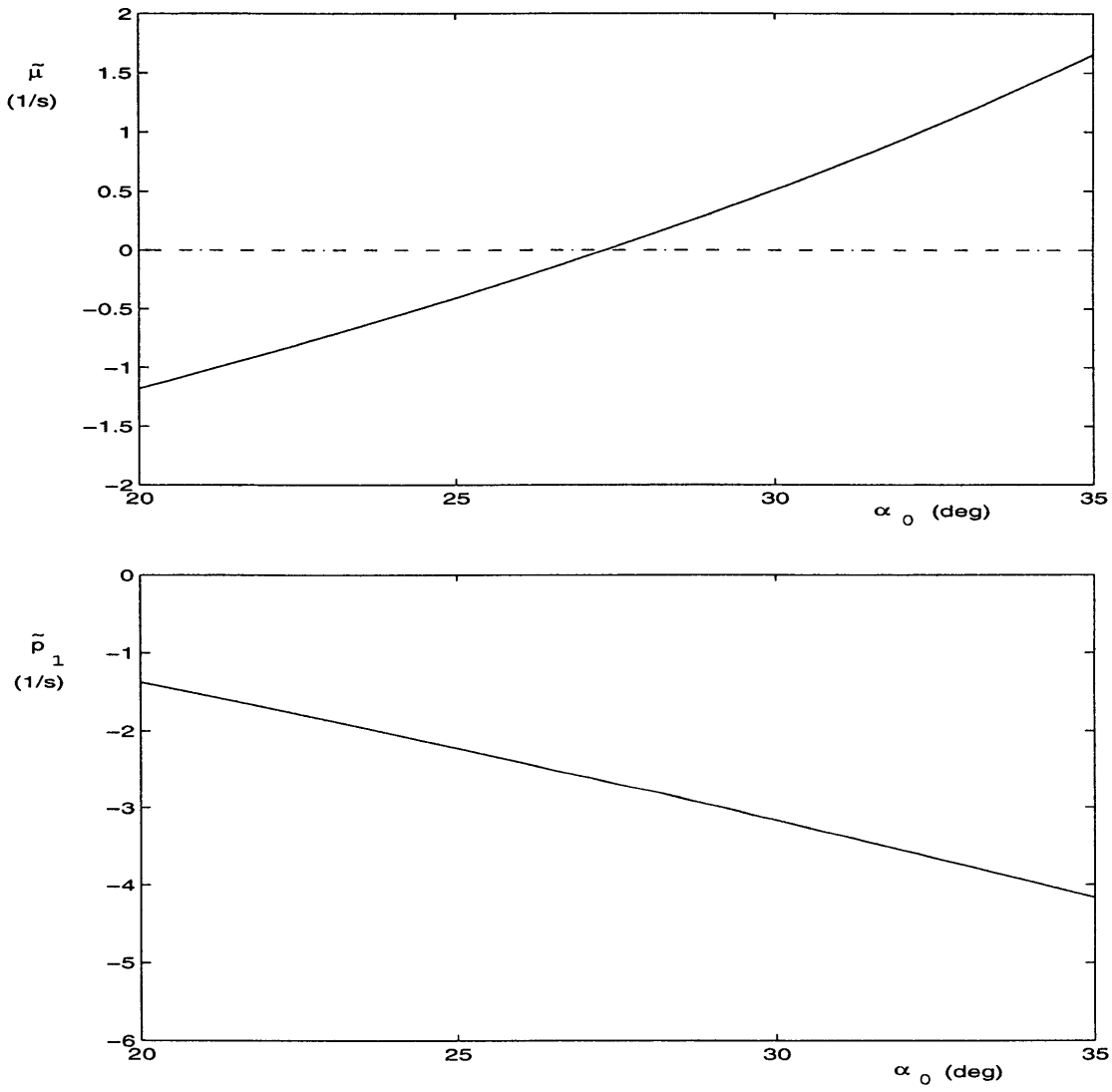

Figure 3-5: $\tilde{\mu}$ and $\tilde{p}_1$ variations with nominal angle-of-attack α_0

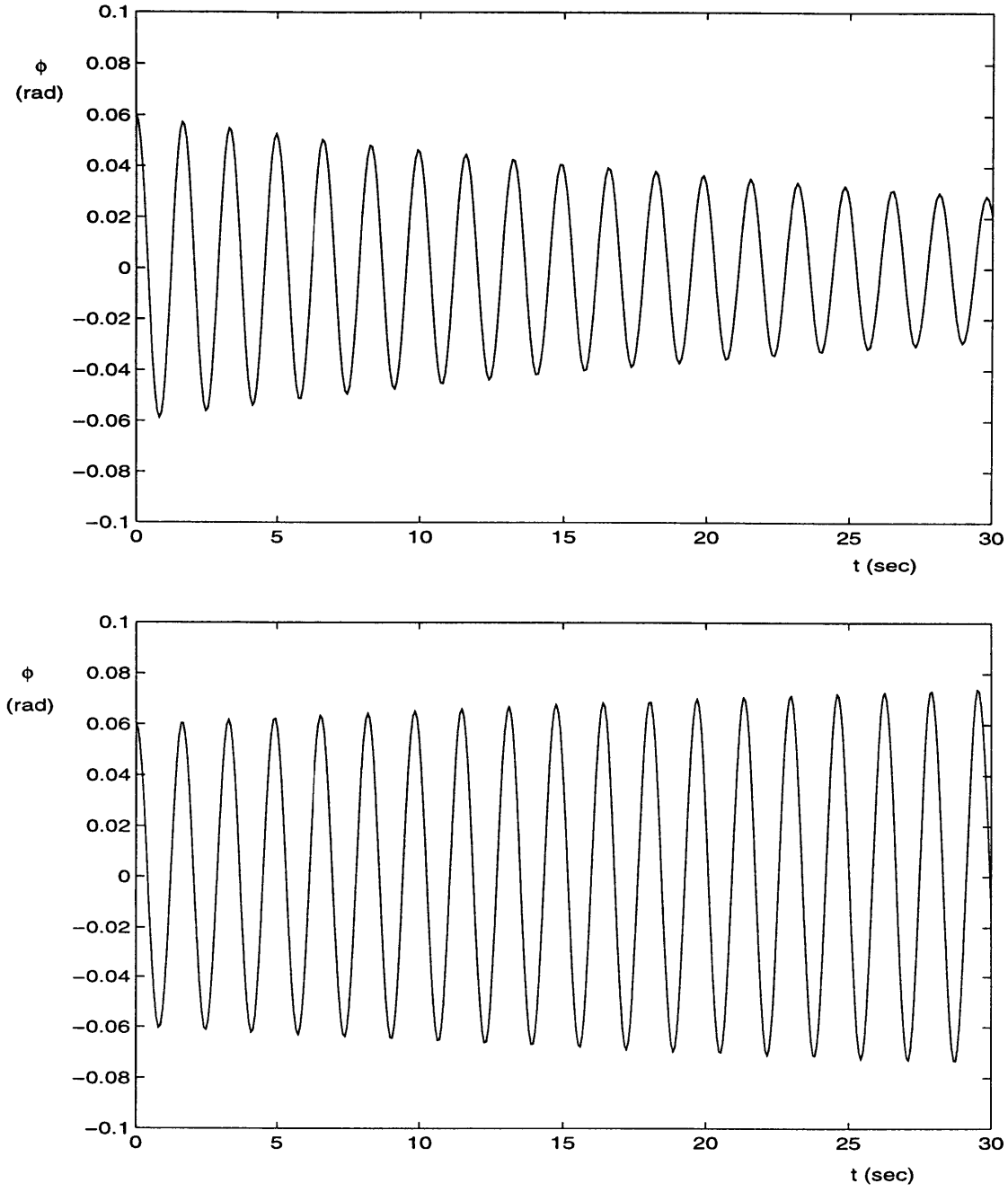

Figure 3-6: Aircraft response for $\alpha_0 = 27.2^o$ (upper) and $\alpha_0 = 27.6^o$ (below)

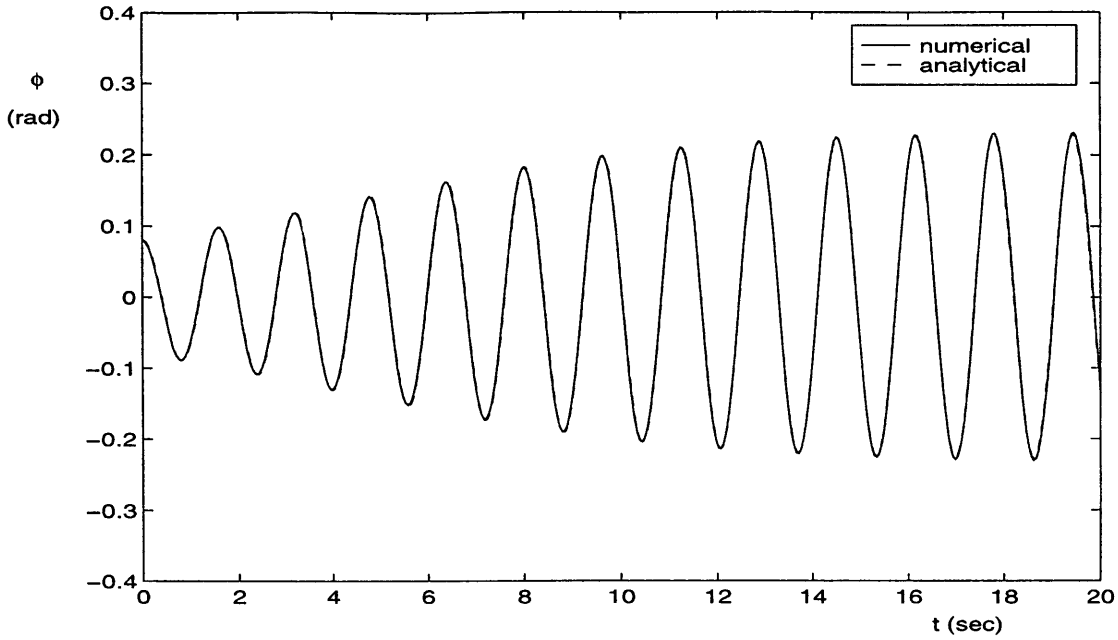

Figure 3-7: Roll angle response for $\alpha_0 = 29^o$ and initial condition $\phi(0) = 0.08$ rad

seen, the locations of the saddle points match very well with the analytical prediction.

3.5.1 Energy Exchange Concept

A useful tool to gain physical insight on the motion dynamics is the concept of energy exchange. Since no control action is assumed during the motion, the change in aerodynamic energy during a certain time interval is given by

$$\Delta E = \int_{t_1}^{t_2} \bar{q} S b C_l(t) \dot{\phi}(t) dt \tag{3.55}$$

Through a change in integration variable, the above expression can be written as a line integral as follows

$$\Delta E = \int_{C_\phi} \bar{q} S b C_l(\phi) d\phi \tag{3.56}$$

where C_ϕ is the curve of C_l versus ϕ for $t_1 \leq t \leq t_2$. Such curve is usually called histogram. In a wing rock situation, C_ϕ is a closed curve over one oscillation cycle. The net energy change over a cycle is given by

$$\Delta E = \oint_{C_\phi} \bar{q} S b C_l(\phi) d\phi \tag{3.57}$$

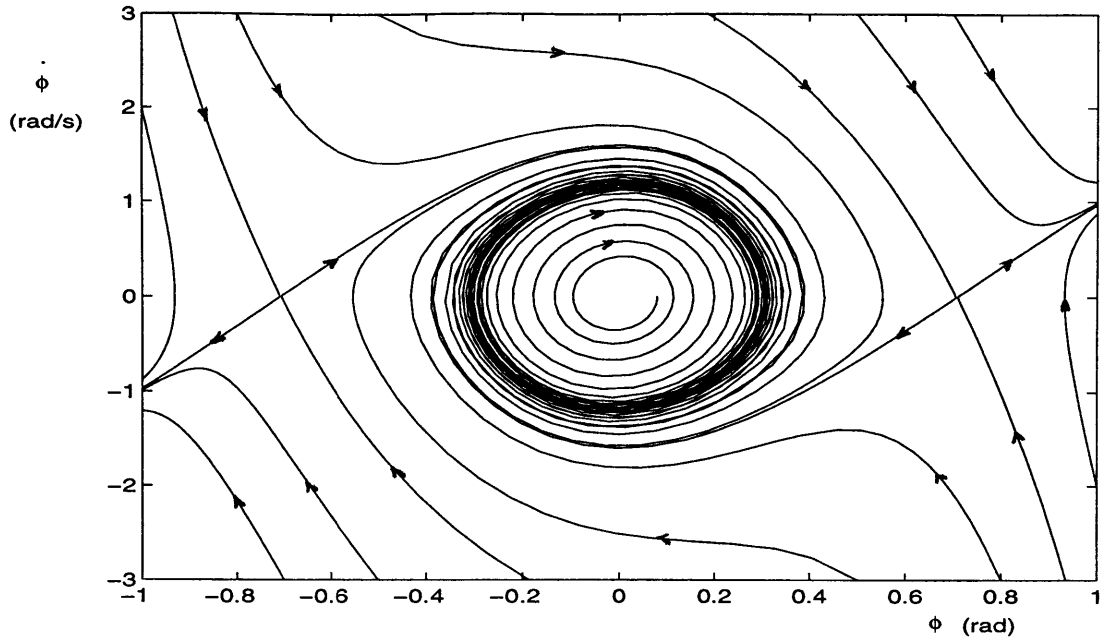

Figure 3-8: Phase plane for $\alpha_0 = 30^o$

It is clear that the net aerodynamic energy exchange in a cycle is directly proportional to the areas contained within the histogram loops. For a clockwise loop, $\Delta E > 0$ or, in other words, energy is added to the system (destabilizing). Conversely, for a counter-clockwise loop, $\Delta E < 0$, which means that energy is extracted from the system (stabilizing).

In a sustained free wing rock motion, it is obvious that the system is in energy balance and so no energy is added or extracted from the system. In this situation, we will find that $\Delta E = 0$, which implies that the area within the clockwise loop must be the same as the area within the counter-clockwise loop. How the area is distributed within the clockwise and the counter-clockwise loops in a cycle can help us to gain some insights about the wing rock mechanism.

The histogram for the aircraft model considered at $\alpha_0 = 30^o$ is shown in Figure 3-9 for one wing rock cycle. A relatively large destabilizing loop (clockwise, $\Delta E > 0$) is observed around the origin for roll angle magnitudes less than about 8^o (0.14 rad). Smaller stabilizing loops (counter-clockwise, $\Delta E < 0$) are observed for roll angle magnitudes greater than 8^o. The net area within these loops has to be zero from the energy exchange concept. This diagram also implies that the rolling moment in the system is destabilizing when the roll angle is small and becomes stabilizing when the roll angle is large. The magnitude of the roll angle continues to increase up to a point and then decreases such that the stabilizing moment has enough energy to balance

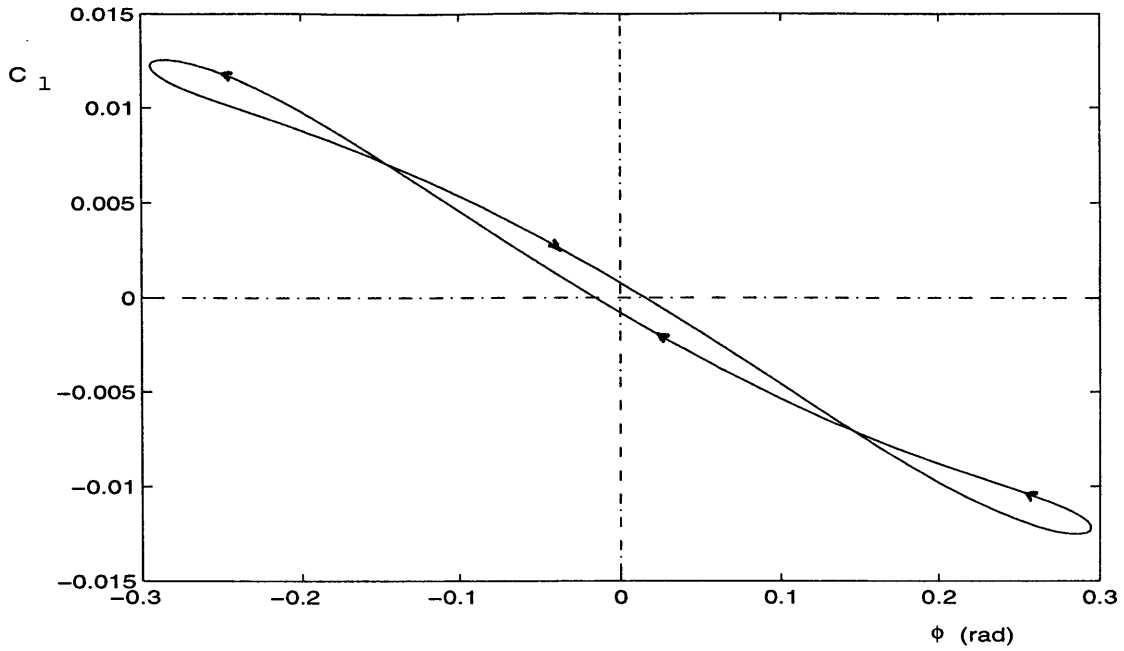

Figure 3-9: C_l vs ϕ for one cycle of wing rock at $\alpha_0 = 30^o$

the destabilizing energy generated by the destabilizing rolling moment. When such an energy balance is achieved, a wing rock limit cycle is sustained in the system.

3.6 Effects of Specific Types of Aerodynamic Nonlinearity

3.6.1 Effects of Nonlinearity in Roll Damping Parameter With Sideslip and Roll Rate

Evidence on the nonlinear variation of damping in roll with respect to angle-of-sideslip and roll rate has been reported in literature (see [1, 15]). To examine this specific type of nonlinearity, a simplified single rotational degree-of-freedom aircraft model which includes only this type of aerodynamic nonlinearity is studied. The other aerodynamic characteristics of the aircraft are assumed to be linear. To be more specific, we consider an aircraft with the following rolling moment.

$$L = L_p p + L_{\beta_0}\beta + L_{\dot{\beta}_0}\dot{\beta} \tag{3.58}$$

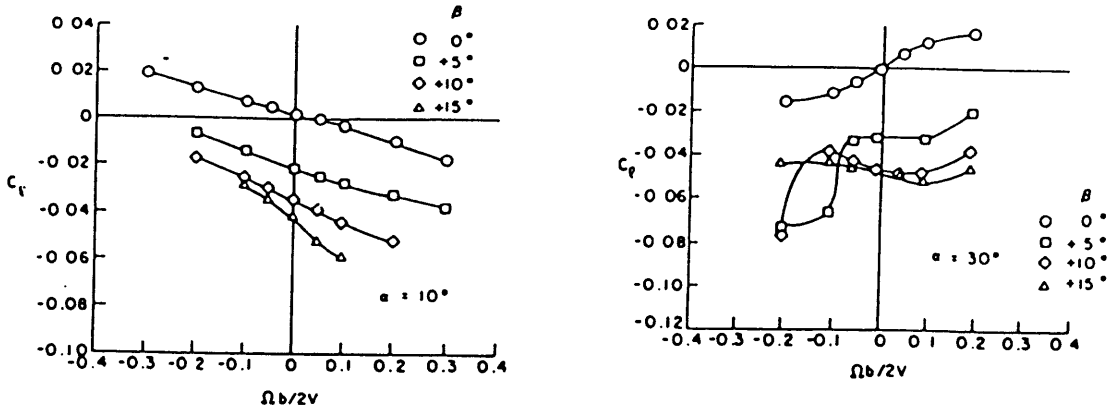

Figure 3-10: Roll damping variation with sideslip and roll rate for 80^o delta wing [15]

The stability derivatives L_{β_0} and $L_{\dot{\beta}_0}$ are constant and usually used in the linear treatment of aircraft dynamics. Here they are taken to be constant In Equation (3.58), only L_p is not constant and will be modeled as

$$L_p = L_{p_a}(p) + L_{p_b}(\beta) \tag{3.59}$$

In the above model, L_{p_a} reflects how L_p varies with roll rate and L_{p_b} reflects how L_p varies with sideslip angle. Note that for simplicity, nonlinear interaction between p and β is not included in the above model. The forms of the function $L_{p_a}(p)$ and $L_{p_b}(\beta)$ in the current analysis are based on available data found in the literature [15].

Figure 3-10 shows the variation of rolling moment coefficient C_l with sideslip and roll rate as obtained from an 80^o delta wing experiment. From the figure, we can see that C_l is an odd function of roll rate p. This fact can also be inferred from the aerodynamics of the aircraft. Based on this fact, the simplest approximation for L vs p is a cubic polynomial in p with no p^2-term, that is

$$L = k_1 p + k_2 p^3 \tag{3.60}$$

In other words, L_{p_a} is a quadratic function of p as follows

$$L_{p_a} = L_{p_0} + L_{p_1} p^2 \tag{3.61}$$

The C_{l_p} variation with respect to sideslip angle β on the other hand is typically

symmetric, as can be seen from Figure 3-10. The model we employ here is the simplest model that still reflects the symmetrical variation with respect to β, namely a simple quadratic β function, as follows.

$$L_{p_b} = L_{p_2}\beta^2 \tag{3.62}$$

Based on this development, the nonlinear L_p model used here is

$$L_p = L_{p_0} + L_{p_1}p^2 + L_{p_2}\beta^2 \tag{3.63}$$

Inserting this L_p model into Equation (3.58) and comparing the result with Equation (3.18), the following correspondence is observed.

$$[\bar{c}_1\ \bar{c}_2\ \bar{c}_3\ \bar{c}_5\ \bar{c}_{10}] \equiv [L_{\beta_0}\ L_{p_0}\ L_{\dot{\beta}_0}\ L_{p_2}\ L_{p_1}] \tag{3.64}$$

Hence, for this case, the equation of motion becomes

$$\ddot{\phi} + \omega^2\phi = \epsilon(\mu\dot{\phi} + c_2\phi^2\dot{\phi} + c_4\dot{\phi}^3) \tag{3.65}$$

which is much simpler than its complete form (Equation (3.31)). Following the procedure in Section 3.4, the following amplitude and phase-correction differential equations are obtained.

$$\begin{aligned} \frac{dA}{d\tau_1} &= \frac{1}{2}\mu A + p_1 A^3 \\ \frac{dB}{d\tau_1} &= p_2 A^2 \end{aligned} \tag{3.66}$$

where

$$\begin{aligned} p_1 &= \frac{1}{8}[c_2 + 3c_4\omega^2] \\ p_2 &= -\frac{1}{8\omega}[3c_1 + c_3\omega^2] \end{aligned} \tag{3.67}$$

Notice that the form of the amplitude and phase equations in this case is the same as the complete version, so the analytical solution obtained for this case is the same as before.

For a more detailed analysis of wing rock amplitude, we express μ and p_1 in terms

of stability derivatives as follows.

$$\begin{aligned}\tilde{\mu} &\equiv \epsilon\mu = (L_{p_0} + L_{\dot{\beta}_0}\sin\alpha_0) \\ \tilde{p}_1 &\equiv \epsilon p_1 = \frac{I_{xx}}{8}\left[L_{p_0} + L_{\dot{\beta}_0}\sin\alpha_0 + 3L_{p_1}L_{\beta_0}\sin\alpha_0 + L_{p_2}\sin^2\alpha_0\right] \end{aligned} \quad (3.68)$$

It is clear from this detailed parameter representation that the coefficients L_{p_1} and L_{p_2} affect the resulting steady state wing rock amplitude. Note also that the μ expression here is the same as in general case, which implies that the onset on wing rock for this specific case is the same as in the general case considered in this chapter. The wing rock onset is determined by the linear roll damping parameter $(L_{p_0} + L_{\dot{\beta}_0}\sin\alpha_0)$. The loss of this linear roll damping (μ becomes zero and positive) causes the aircraft to encounter the wing rock oscillation.

A physical explanation on how the wing rock motion develops in this situation is discussed using the energy concept. The aircraft model in the previous section is used again here with all nonlinearities removed, except the ones contributed by L_{p_1} and L_{p_2}. The histogram for this system at $\alpha_0 = 30^o$ with $C_{l_{p_1}} = \dfrac{L_{p_1}}{qSb} = -0.011$ and $C_{l_{p_2}} = \dfrac{L_{p_2}}{qSb} = -2.84$ are shown in Figure 3-11. The histogram shows similarity with the example in the previous section. It has a destabilizing loop for roll angle magnitudes less than 8^o (0.14 rad) and stabilizing loops for roll angle magnitudes greater than 8^o.

When $C_{l_{p_1}}$ is sufficiently large, a counter intuitive situation can arise. Figure 3-12 shows the histogram of one wing rock cycle for $C_{l_{p_1}} = -0.043$ and $C_{l_{p_2}} = -0.426$. In this case, a stabilizing loop exists when the roll angle magnitudes are small and a pair of destabilizing loops exist when the roll angle magnitudes are relatively large. This situation might suggest that if the initial roll angle is small and in the range of the stabilizing loop, wing rock would not occur. This is not true, however, as Figure 3-13 shows. To explain this phenomenon, histograms for several oscillation cycles of Figure 3-13 are plotted in Figure 3-14. The histogram of cycle 1 shows that initially the rolling moment in the system is destabilizing, as indicated by the single clockwise loop. This destabilizing loop still appears in histogram for cycle 2, which indicates that at this point aerodynamic energy is still added to the system, hence the amplitudes of oscillations continue to increase. At the time when the wing rock amplitude is approached, the stabilizing loop starts to appear, as can be seen from the histogram for cycle 3. At this point, however, the amount of the energy extracted from the system is still less than the amount of energy added, and therefore, the amplitude of motion still increases. When the balance of energy is achieved, wing

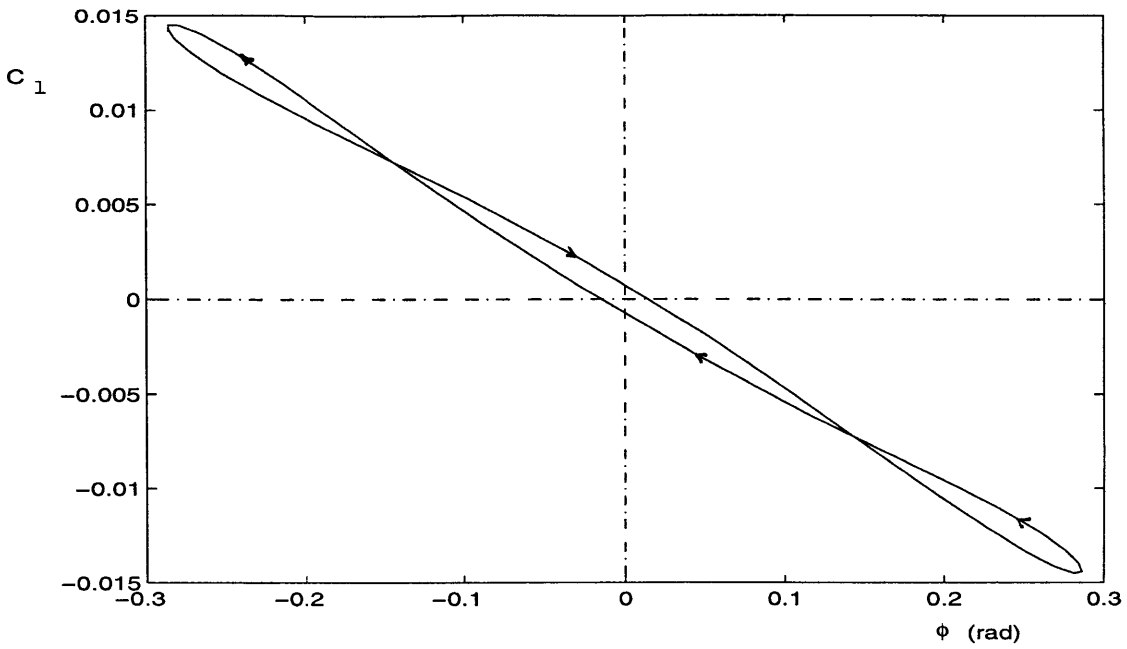

Figure 3-11: Histogram for $\alpha_0 = 30^o$ ($C_{l_{p_1}} = -0.011$, $C_{l_{p_2}} = -2.84$)

rock motion is sustained.

We will now examine how the wing rock amplitude variation with the the variations of L_{p_1} and L_{p_2}. We start by assuming that wing rock occurs in the system, which means that all the requirements for the wing rock occurence are satisfied. The derivatives of the amplitude A_1 with respect to L_{p_1} and L_{p_2} are

$$\begin{aligned} \frac{dA_1}{dL_{p_1}} &= \frac{dA_1}{dp_1}\frac{dp_1}{dL_{p_1}} = \frac{1}{2}\left(-\frac{\mu}{2p_1}\right)^{\frac{3}{2}}\left(\frac{\mu}{2p_1^2}\right)(-L_{\beta_0}\sin\alpha_0) \\ \frac{dA_1}{dL_{p_2}} &= \frac{dA_1}{dp_1}\frac{dp_1}{dL_{p_2}} = \frac{1}{2}\left(-\frac{\mu}{2p_1}\right)^{\frac{3}{2}}\left(\frac{\mu}{2p_1^2}\right)\sin^2\alpha_0 \end{aligned} \tag{3.69}$$

In the above expressions, the factor in the first parenthesis is the square of steady-state wing rock amplitude, hence it is of positive value. For the factor in the second parenthesis, the denominator is always positive because of the square and the numerator (μ) is also positive in wing rock situation. Hence this factor is also positive. Therefore the sign of the last factor in each of the expressions determines whether the derivatives are positive or negative. The last factor in the $\frac{dA_1}{dL_{p_1}}$ expression is equivalent to the square of the wing rock frequency, which is positive. The last factor in $\frac{dA_1}{dL_{p_2}}$ expression is also positive due to the square operation. Thus, both derivatives are positive. Physically, this implies that increasing the values of L_{p_1} and L_{p_2}

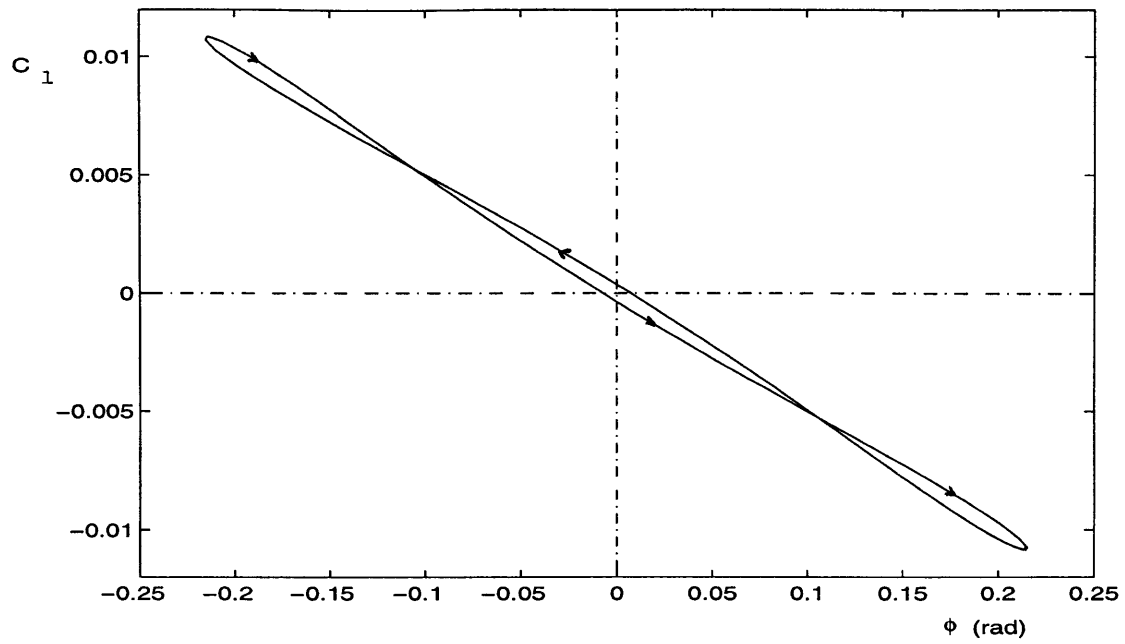

Figure 3-12: Histogram for $\alpha_0 = 30^o$ ($C_{l_{p_1}} = -0.043$, $C_{l_{p_2}} = -0.426$)

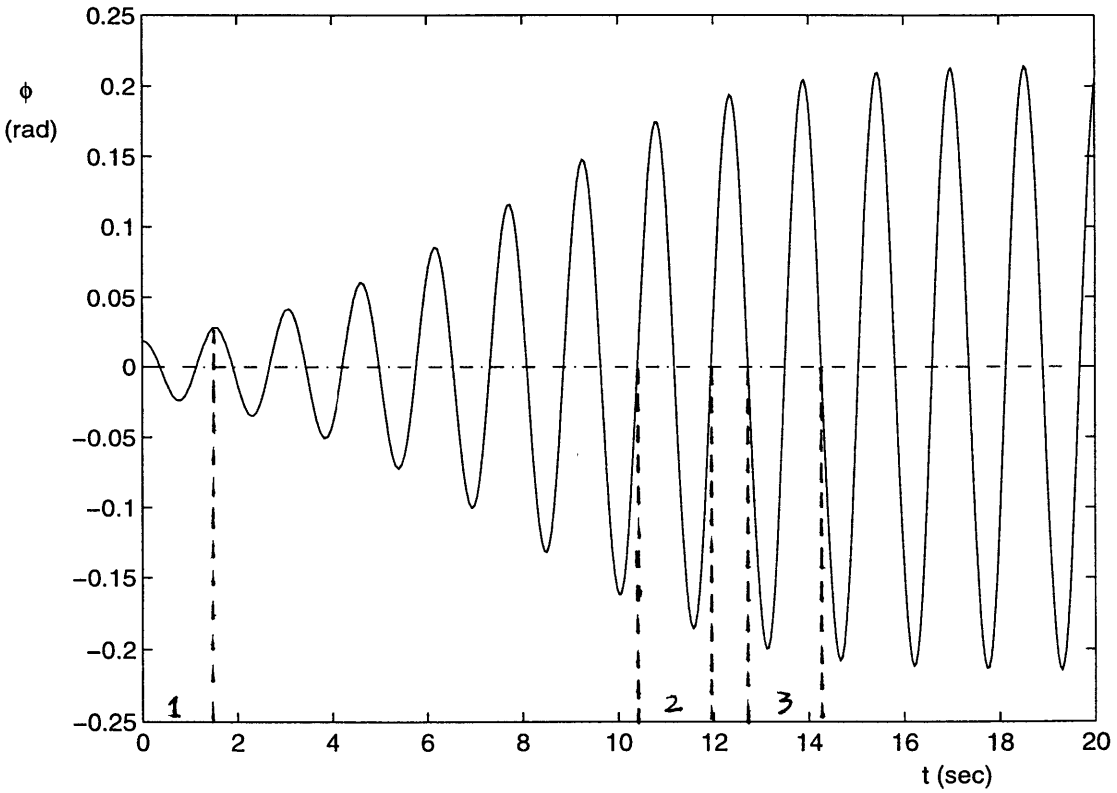

Figure 3-13: Motion simulation for initial conditions $(\phi, \dot{\phi}) = (0.02, 0)$ rad

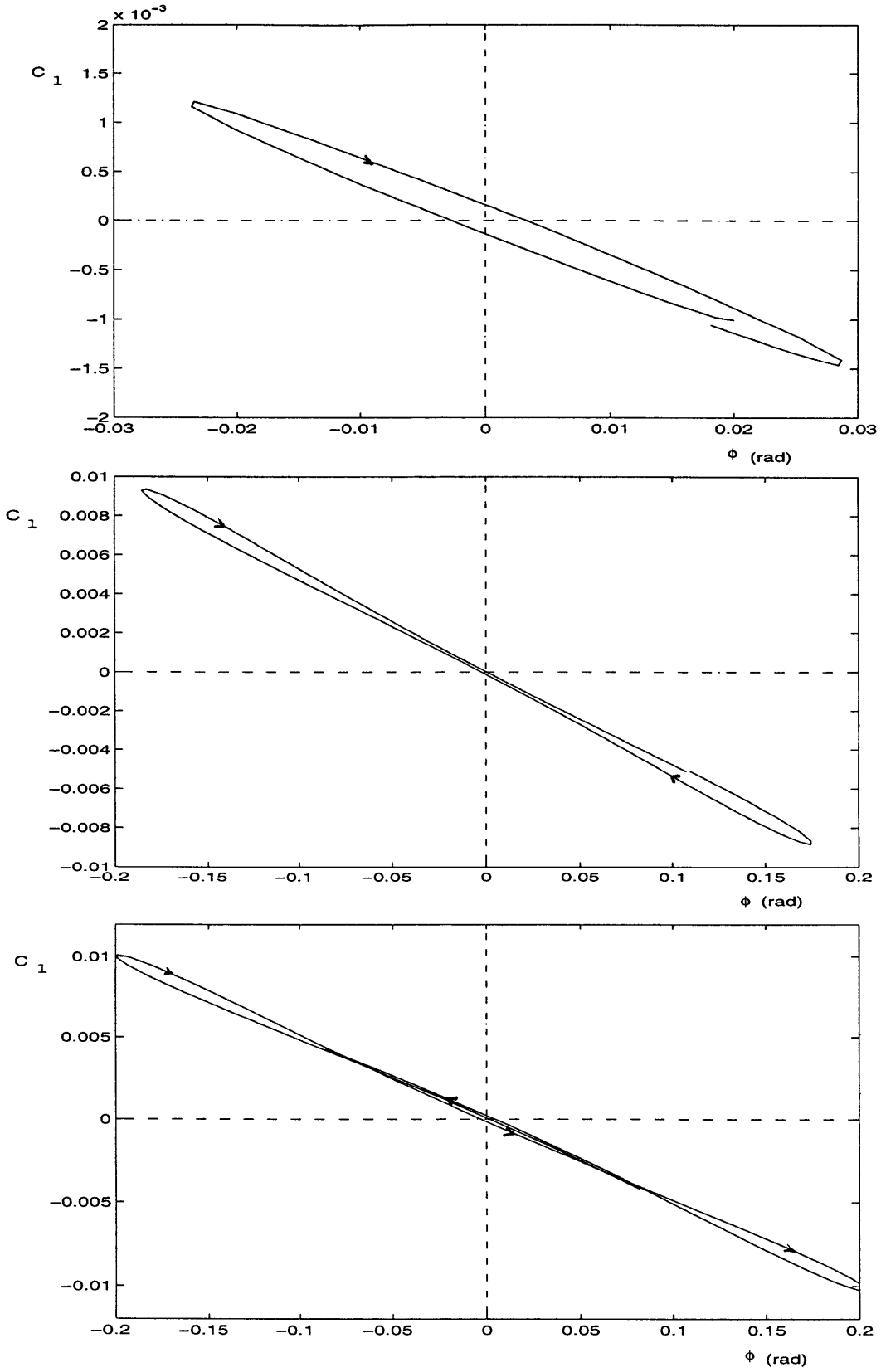

Figure 3-14: Histograms for cycle 1 (upper), 2 (middle), and 3 (bottom) of Figure 3.11

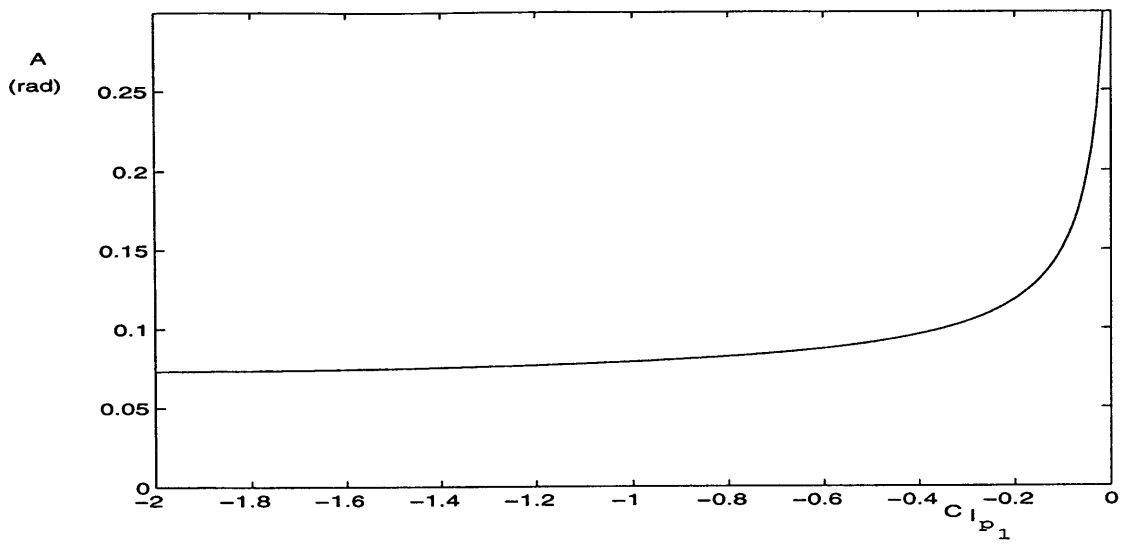

Figure 3-15: Variation of wing rock amplitude with L_{p_1}

increases the wing rock amplitude.

As an example, we consider the aircraft model from the previous section with all sources of nonlinearity being removed except for the nonlinearity in C_{l_p}. The changes of the wing rock amplitude at certain angle-of-attack as $C_{l_{p_1}}$ and $C_{l_{p_2}}$ vary are shown in Figure 3-15 and 3-16.

3.6.2 Effects of Cubic Variation of Rolling Moment with Sideslip

Nonlinearity in the variation of rolling moment with respect to sideslip angle is found in many fighter aircraft flying at high angles-of-attack. Some examples of such variation are given in Figures 3-17 and 3-18. This variation can be modeled fairly well using an odd order polynomial. The simplest model to incorporate such nonlinearity is using a cubic polynomial as follows

$$L = L_{p_0} p + L_{\beta_0} \beta + L_{\beta_1} \beta^3 + L_{\dot{\beta}_0} \dot{\beta} \tag{3.70}$$

The effect of L_{β_1} on the motion dynamics can now readily be looked at. When only such nonlinearity is present, the equation of motion becomes

$$\ddot{\phi} + \omega^2 \phi = \epsilon(\mu \dot{\phi} + c_1 \phi^3) \tag{3.71}$$

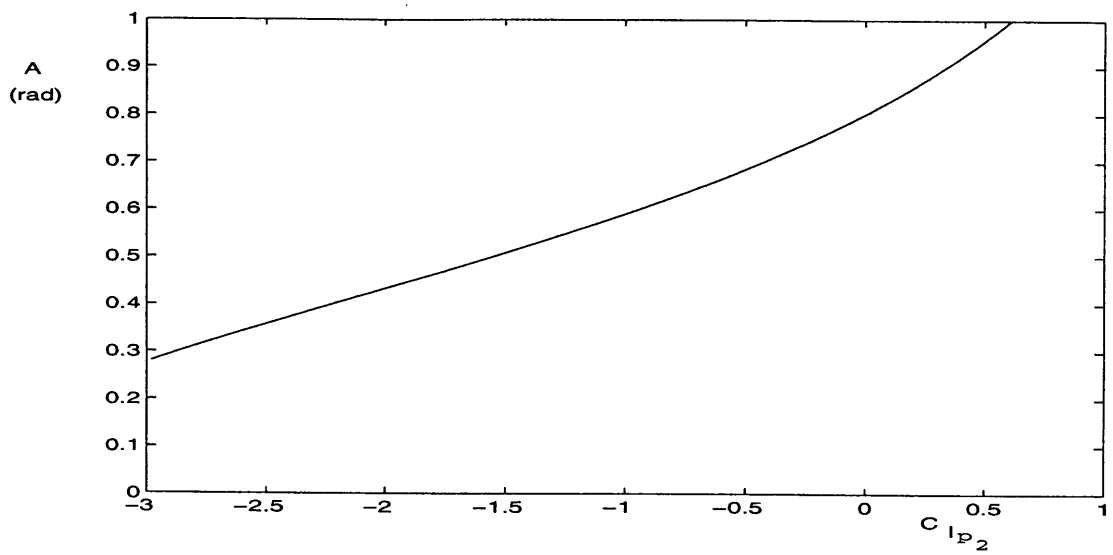

Figure 3-16: Variation of wing rock amplitude with L_{p_2}

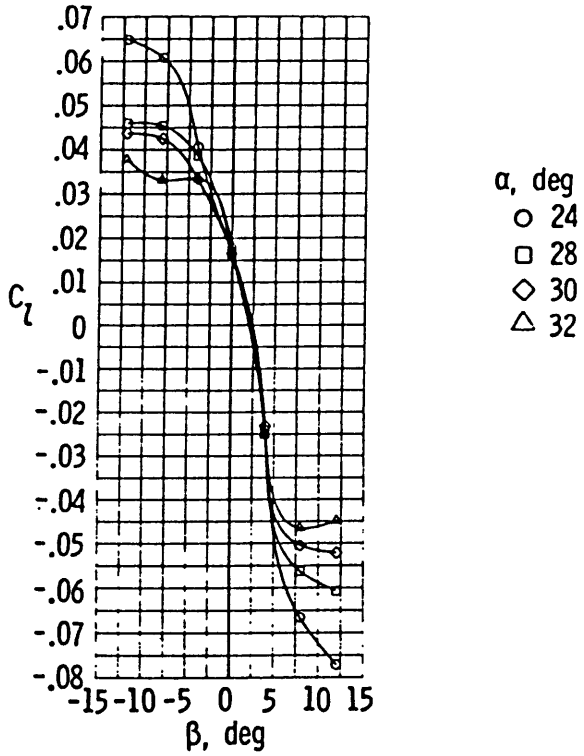

Figure 3-17: Variation of static lateral stability with sideslip for an 80° delta wing [15]

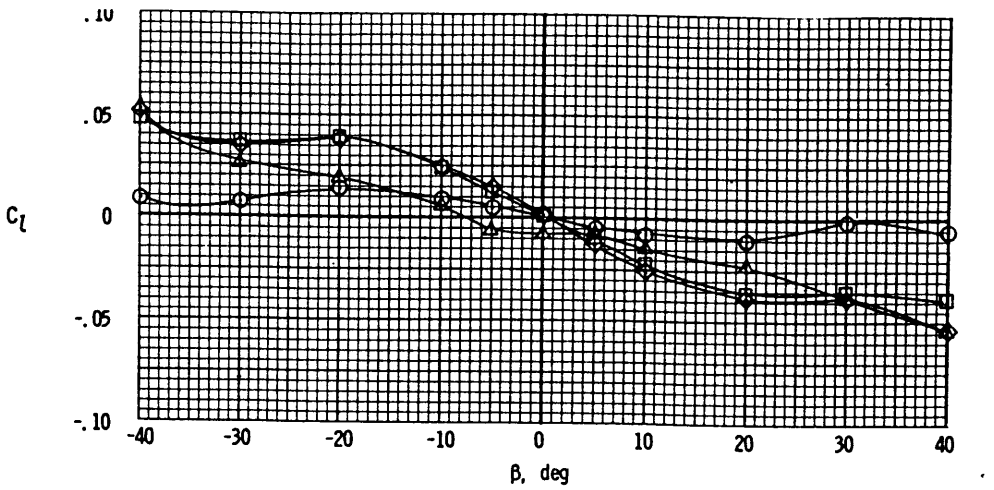

Figure 3-18: Variation of static lateral stability with sideslip for a twin jet fighter airplane [44]

which is a damped Duffing's type of equation. It is known (see [37]) that this type of equation does not possess a periodic solution for $\mu \neq 0$. The cubic variation of rolling moment with sideslip by itself does not cause wing rock. Comparison with Equation (3.18) yields

$$L_{\beta_1} = \bar{c}_4 \tag{3.72}$$

In Equation (3.44), L_{β_1} only contributes to p_2 through c_1. Therefore, this kind of nonlinearity only affects the phase or frequency of the roll motion but does not affect the roll amplitude history. Since

$$\frac{dp_2}{dL_{\beta_1}} = -\frac{3}{8}\frac{\bar{q}Sb}{I_{xx}}\omega \sin^3 \alpha \tag{3.73}$$

and the frequency correction varies proportionally with $-\epsilon p_2$, then we see that positive L_{β_1} causes a slight decrease in the frequency of motion and negative L_{β_1} causes a slight increase in frequency. See Figure 3-19. Positive L_{β_1} is analogous to the case of softening spring and negative L_{β_1} is analogous to the case of hardening spring. In case that wing rock occurs in the system (due to other types of nonlinearity), L_{β_1} affects the frequency of the wing rock motion in a similar way as described above.

3.7 Chapter Summary

Wing rock dynamics on an aircraft having only roll degree-of-freedom have been considered in this chapter. The development of the analytical solutions using the MTS method in conjunction with the bifurcation theory is discussed in detail. These solu-

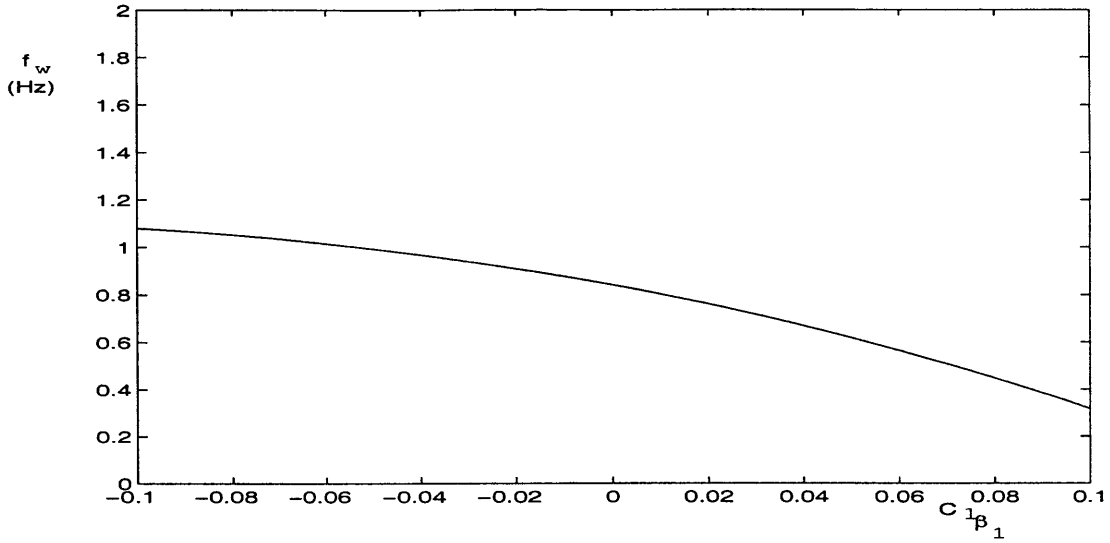

Figure 3-19: Variation of roll frequency with $C_{l_{\beta_1}}$

tions are shown to be in excellent agreement with the numerical integration results. The usefulness of our analysis is further demonstrated by the studying the effects of some specific nonlinearities on the resulting wing rock motion. Numerical approaches will only give us results for certain values of parameters, but the effect of a specific type of nonlinearity on the overall motion is not transparent. However, the analytical study allows us to see clearly how a certain parameter influences the overall dynamics of the aircraft. It can be understood that such results are very useful to alleviate undesirable wing rock behavior at the design stage and also to guide us to the right control strategy for the wing rock suppression.

Chapter 4

Two Degrees-of-Freedom Wing Rock

4.1 Introduction

Wing rock dynamics on an aircraft having only two rotational degrees-of-freedom in roll and pitch is discussed in this chapter. This assumption is good for an aircraft with negligible yaw dynamices during the motion of interest. This investigation shows the interdependence of the pitch degree-of-freedom and the wing rock motion. The analysis here also serves as an intermediate step before we treat the more complicated three degrees-of-freedom case. Again, an analytical approach using the multiple scales method in conjunction with the center manifold reduction and bifurcation theory is used in the analysis to obtain an approximate solution of the problem. This approach enables us to gain insight into the system dynamics and to identify the important parameters which influence the overall motion.

4.2 Equations of Motion

The axis systems used in deriving the equations of motion are described next. As our interest is in a flight condition which is symmetric nominally, then two axis systems are enough to describe the aircraft attitude during its perturbed motion. The first set of axes $(X_b Y_b Z_b)$ is called the body-fixed axis system. As the name implies, this axis system has its origin at the center of mass of the aircraft and is fixed to the aircraft body. The X_b axis points towards the nose of the aircraft, the Z_b axis is in

the aircraft vertical plane and perpendicular to X_b. The $X_b - Z_b$ plane is the vertical symmetry plane of the aircraft. The Y_b axis completes the righthanded axis system. The second set of axes $X_oY_oZ_o$ is referred to as the stability axis system. Its origin is at the center of mass of the aircraft and the orientation of the axes describes the nominal or unperturbed attitude of the aircraft. The X_o axis is oriented towards the nominal nose direction of the aircraft, the Z_o axis is in the nominal vertical plane of the aircraft pointing down and perperdicular to the X_o axis, while the Y_o axis completes the righthanded axis system. In the nominal flight condition, these two axis systems coincide with each other.

The expression for the aircraft angular rate in the body-fixed axes can be found by noting that the aircraft can be brought from its nominal position to the perturbed one by using two consecutive rotations, first in pitch and then in roll (see Fig. 1). Hence,

$$\begin{aligned} \boldsymbol{\omega} &= p\,\mathbf{i}_{x_b} + q\,\mathbf{i}_{y_b} + r\,\mathbf{i}_{z_b} \\ &= \dot{\theta}\,\mathbf{i}_{y_o} + \dot{\phi}\,\mathbf{i}_{x_b} \end{aligned} \tag{4.1}$$

where the notation $\mathbf{i}$ denotes the unit vector along the axis indicated by the subscript. Per usual convention, p, q, and r are the roll rate, pitch rate, and yaw rate respectively of the aircraft. ϕ and θ denote the roll and pitch angular perturbations from the nominal position. Since

$$\mathbf{i}_{y_o} = \cos\phi\,\mathbf{i}_{y_b} - \sin\phi\,\mathbf{i}_{z_b} \tag{4.2}$$

and by assuming that the perturbation angles are small, the following relations are obtained.

$$\begin{aligned} p &= \dot{\phi} \\ q &= \dot{\theta}\cos\phi \approx \dot{\theta} \\ r &= -\dot{\theta}\sin\phi \approx -\phi\dot{\theta} \end{aligned} \tag{4.3}$$

Note that r is not zero in this formulation, however its magnitude is one order of magnitude smaller than p and q.

We further assume that the aircraft body is vertically symmetric, which implies that the product of inertia $I_{xy} = I_{yz} = 0$. The rotational kinetic energy of the aircraft can then be expressed as follows.

$$T = \frac{1}{2}I_{xx}p^2 + \frac{1}{2}I_{yy}q^2 + \frac{1}{2}I_{zz}r^2 - I_{xz}pr$$

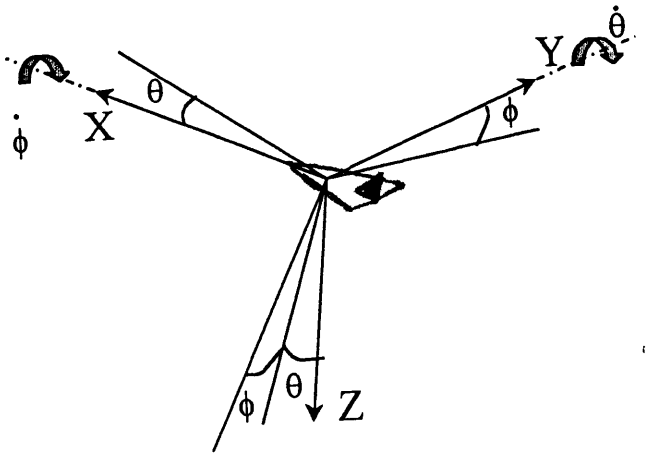

Figure 4-1: Transform angles and rotations between the stability and body-fixed axis systems

$$= \frac{1}{2}I_{xx}\dot{\phi}^2 + \frac{1}{2}I_{yy}\dot{\theta}^2 + \frac{1}{2}I_{zz}\phi^2\dot{\theta}^2 - I_{xz}\phi\dot{\phi}\dot{\theta} \tag{4.4}$$

where I_{xx}, I_{yy}, and I_{zz} are the moment of inertia of the aircraft about X_b, Y_b and Z_b, respectively. The Lagrange's equation is

$$\frac{d}{dt}\left(\frac{\partial T}{\partial \dot{\gamma}_i}\right) - \frac{\partial T}{\partial \gamma_i} = Q_i \;\; ; \;\; i = 1, 2 \tag{4.5}$$

where $\gamma_1 = \phi$, $\gamma_2 = \theta$ and the generalized force $Q_i = \dfrac{\delta W_i}{\delta \gamma_i}$, which is the variation of the work δW_i due to the variation of the displacement $\delta\gamma_i$. Substitution of Eq. 4.4 into Eq. 4.5 yields

$$I_{xx}\ddot{\phi} + I_{xz}\phi\ddot{\theta} + I_{xz}\dot{\phi}\dot{\theta} - I_{zz}\phi\dot{\theta}^2 = Q_1$$

$$(I_{yy} + I_{zz}\phi^2)\ddot{\theta} + I_{xz}\phi\ddot{\phi} + I_{xz}\dot{\phi}^2 + 2I_{zz}\phi\dot{\phi}\dot{\theta} = Q_2 \tag{4.6}$$

The generalized forces are assumed to be contributed solely by the aerodynamic moments. The effect of gravity is neglected in the current analysis. The derivation of the aerodynamic moments is performed next.

4.3 Derivation of the Aerodynamic Moments

The aerodynamic moments acting on the aircraft are derived under the assumption that the flow is incompressible and quasi-steady. For simplicity, modified strip theory aerodynamics is used in the derivation. In the usual strip theory, the local aerodynamic force is determined solely by the local force versus angle-of-attack properties of each aircraft segment and the gross angle-of-attack of the aircraft, with no con-

sideration of three-dimensional flow effects. Here, the aerodynamic model developed is general enough such that the three-dimensional effects of the flow can be taken into account. In this case, each segment of the aircraft may see a different effective angle-of-attack. We also assume that the aerodynamic forces are produced mainly by the wing and the horizontal tail planes. The aerodynamic forces on the fuselage is neglected. The fuselage does however have a significant presence, and contributes to three-dimensional effects especially in the unsymmetric flow case.

The purpose of this derivation is to find the appropriate mathematical expressions to represent the nonlinear aerodynamic moments to be used later in the analysis. The resulting moment expressions are expected to capture the parameters which have a significant impact on the system dynamics.

The aerodynamic forces on the wing are now considered. The derivation for the tail will then follow in a similar fashion. At each streamwise segment of the wing of width dy, the incremental lift and drag forces produced are

$$\begin{aligned} dL(y) &= \bar{q}c(y)c_L(y)dy \\ dD(y) &= \bar{q}c(y)c_D(y)dy \end{aligned} \tag{4.7}$$

where $\bar{q} = \frac{1}{2}\rho V^2$ is the dynamic pressure, $c(y)$ is the airfoil chord at location y along the Y_b axis, $c_L(y)$ and $c_D(y)$ are the local lift and drag coefficients, respectively. In this work, the dependence of the local lift and drag coefficients ($c_L(y)$ and $c_D(y)$) on the local effective angle-of-attack ($\alpha_e(y)$) is represented by a cubic polynomial.

$$\begin{aligned} c_L &= c_{L_0} + c_{L_1}\alpha_e + c_{L_2}\alpha_e^2 + c_{L_3}\alpha_e^3 \\ c_D &= c_{D_0} + c_{D_1}\alpha_e + c_{D_2}\alpha_e^2 + c_{D_3}\alpha_e^3 \end{aligned} \tag{4.8}$$

For notational simplicity, in the above equations, the dependence of the coefficients and α on the spanwise location has been dropped.

The effective angle-of-attack distribution along the wing span consists of several contributions. The following discussion describes the components building up the total distribution. The contribution of yaw rate r due to kinematic coupling is neglected, since its value is normally small in this two degrees-of-freedom aircraft model. Therefore, in this case, the angle-of-attack distribution depends on the nominal angle-of-attack, roll rate, sideslip rate, pitch rate, the rate of change of angle-of-attack and sideslip, and the deviation from the nominal angle-of-attack. As we only consider small deviations from the nominal condition, then the contributions of the above factors on the effective angle-of-attack distribution can be expressed using a linear

relation as follows.

$$\alpha_e(y) = \alpha_1(y) + \frac{\partial \alpha_e(y)}{\partial p} p + \frac{\partial \alpha_e(y)}{\partial \beta} \beta + \frac{\partial \alpha_e(y)}{\partial \dot{\beta}} \dot{\beta} + \frac{\partial \alpha_e(y)}{\partial \alpha} \alpha + \frac{\partial \alpha_e(y)}{\partial q} q + \frac{\partial \alpha_e(y)}{\partial \dot{\alpha}} \dot{\alpha} \quad (4.9)$$

or alternatively,

$$\alpha_e(y) = \alpha_1(y) + \alpha_2(y) + \alpha_3(y) + \alpha_4(y) + \alpha_5(y) + \alpha_6(y) + \alpha_7(y) \quad (4.10)$$

where $\alpha_1(y)$, $\alpha_2(y)$, $\alpha_3(y)$, $\alpha_4(y)$, $\alpha_5(y)$, $\alpha_6(y)$, and $\alpha_7(y)$ indicate the component of the effective angle-of-attack distribution due to the nominal angle-of-attack, roll rate, angle-of-sideslip, sideslip rate, the deviation from the nominal angle-of-attack, pitch rate, and the rate of change of angle-of-attack, respectively. $\alpha_1(y)$, $\alpha_2(y)$, $\alpha_3(y)$, and $\alpha_4(y)$ have been described in Chapter 3 and will not be repeated here. Brief discussions on the contribution of the other components are given next.

- The deviation from nominal angle-of-attack (α).
  Because of the assumption that the trajectory of the aircraft is unaltered due to its attitude motion, the change in the angle-of-attack means the change in pitch angle. The resulting spanwise angle-of-attack distribution due to the deviation from the nominal angle-of-attack is assumed symmetric and in general expressable as

  $$\alpha_5(y) = f_5(y)\alpha \quad (4.11)$$

  where $f_5(y)$ denotes an even function of y. As before $f_5(y)$ may take into account the effect of the three-dimensional air flow.

- Pitch rate (q).
  This effect normally contributes to a symmetric angle-of-attack distribution. It can be generally expressed as

  $$\alpha_6(y) = f_6(y)q \quad (4.12)$$

  where $f_6(y)$ is an even function of y. If the three-dimensional flow effect is negligible, then $f_6(y)$ can be approximated well using

  $$f_6(y) = -\cos\alpha_0 \frac{l(y)}{U} \quad (4.13)$$

  where U is the component of the aircraft speed on the X_b-axis and $l(y)$ denotes the distance between the center of mass of the aircraft and the aerodynamic center of the wing segment, positive if the center of mass lies behind the aero-

dynamic center. The negative sign in the equation is due to the fact that positive q contributes to negative angle-of-attack increment in the case where $l(y)$ is positive.

- The rate of change of angle-of-attack ($\dot{\alpha}$).
  The $\dot{\alpha}$ factor is mainly due to the lag of downwash experienced by the horizontal tail. The angle-of-attack increment distribution due to $\dot{\alpha}$ is assumed to be symmetric as follows

$$\alpha_{7_h}(y) = f_7(y)\dot{\alpha} \tag{4.14}$$

  with $f_7(y)$ is an even function of y. Often, $f_7(y)$ is approximated well using

$$f_7(y) = -\frac{l_h(y)}{U}\frac{d\epsilon}{d\alpha} \tag{4.15}$$

  where the subscript h indicates *the horizontal tail.* $l_h(y)$ is the distance from the center of mass of the aircraft to the aerodynamic center of the horizontal tail segment of interest.

The total effective angle-of-attack experienced by each streamwise segment of the wing is then given by summing up the effects from the components discussed previously, as follows.

$$\alpha(y) = \alpha_1(y) + f_2(y)p + f_3(y)\beta + f_4(y)\dot{\beta} + f_5(y)\alpha + f_6(y)q + f_7(y)\dot{\alpha} \tag{4.16}$$

The contribution of the horizontal and vertical tails on the overall aerodynamic moments experienced by the aircraft is neglected.

The substitution of Equations (4.16) into Equation (4.8) and then the substitution of the resulting equation into Equation (4.7) results in lengthy expressions involving the lift and drag forces on each segment of the wing and tail in terms of the variables p, β, $\dot{\beta}$, θ, q, and $\dot{\alpha}$. The work done by the aerodynamic forces for the displacements $\delta\phi$ and $\delta\theta$ can then be approximated by

$$\delta W = -\int_{a/c}(dL\cos\alpha_0 + dD\sin\alpha_0)y\delta\phi - \int_{a/c}(dL\cos\alpha_0 + dD\sin\alpha_0)l\,\delta\theta \tag{4.17}$$

Note that the integrations are performed along the wing and the horizontal tail span of the aircraft. The above equation can be expanded in terms of variables p, β, $\dot{\beta}$, q, α, $\dot{\alpha}$, and then integrated term by term. The process is not difficult, but it is lengthy and is shown in Appendix B. In general, the integrands can be divided into

two groups, the first contains the symmetric integrands and the second contains the antisymmetric ones. The antisymmetric integrands are integrated to zero and hence the final result is the contribution of the symmetric integrands only. Then by using $Q_i = \frac{\delta W_i}{\delta \gamma_i}$, the aerodynamic moments can be expressed as follows.

$$\begin{aligned}
\bar{Q}_1 &= \bar{c}_1\beta + \bar{c}_2 p + \bar{c}_3\dot{\beta} + \bar{c}_4\beta^3 + \bar{c}_5\beta^2 p + \bar{c}_6\beta^2\dot{\beta} + \bar{c}_7\beta p^2 + \bar{c}_8\beta\dot{\beta}^2 + \bar{c}_9\dot{\beta}^3 + \\
&\quad \bar{c}_{10}p^3 + \bar{c}_{11}\beta\alpha + \bar{c}_{12}\beta q + \bar{c}_{13}\beta\dot{\alpha} + \bar{c}_{14}\dot{\beta}\alpha + \bar{c}_{15}\dot{\beta}q + \bar{c}_{16}\dot{\beta}\dot{\alpha} + \bar{c}_{17}p\alpha + \\
&\quad \bar{c}_{18}pq + \bar{c}_{19}p\dot{\alpha} + \bar{c}_{20}\beta\alpha^2 + \bar{c}_{21}\beta q^2 + \bar{c}_{22}\beta\dot{\alpha}^2 + \bar{c}_{23}\dot{\beta}\alpha^2 + \bar{c}_{24}\dot{\beta}q^2 + \\
&\quad \bar{c}_{25}\dot{\beta}\dot{\alpha}^2 + \bar{c}_{26}p\alpha^2 + \bar{c}_{27}pq^2 + \bar{c}_{28}p\dot{\alpha}^2 + \bar{c}_{29}\beta\alpha q + \bar{c}_{30}p\alpha q + \bar{c}_{31}\dot{\beta}\alpha q + \\
&\quad \bar{c}_{32}\beta\alpha\dot{\alpha} + \bar{c}_{33}p\alpha\dot{\alpha} + \bar{c}_{34}\dot{\beta}\alpha\dot{\alpha} + \bar{c}_{35}\beta q\dot{\alpha} + \bar{c}_{36}pq\dot{\alpha} + \bar{c}_{37}\dot{\beta}q\dot{\alpha} + \bar{c}_{38}\beta\dot{\beta}p \\
\bar{Q}_2 &= \bar{d}_1\alpha + \bar{d}_2 q + \bar{d}_3\dot{\alpha} + \bar{d}_4\alpha^2 + \bar{d}_5\alpha q + \bar{d}_6\alpha\dot{\alpha} + \bar{d}_7 q^2 + \bar{d}_8 q\dot{\alpha} + \bar{d}_9\dot{\alpha}^2 + \\
&\quad \bar{d}_{10}\alpha^3 + \bar{d}_{11}\alpha^2 q + \bar{d}_{12}\alpha^2\dot{\alpha} + \bar{d}_{13}q^3 + \bar{d}_{14}q^2\alpha + \bar{d}_{15}\alpha\dot{\alpha}^2 + \bar{d}_{16}q\dot{\alpha}^2 + \\
&\quad \bar{d}_{17}q^2\dot{\alpha} + \bar{d}_{18}\dot{\alpha}^3 + \bar{d}_{19}\alpha q\dot{\alpha} + \bar{d}_{20}\alpha\beta^2 + \bar{d}_{21}\alpha\beta p + \bar{d}_{22}\alpha\beta\dot{\beta} + \bar{d}_{23}\alpha p^2 + \\
&\quad \bar{d}_{24}\alpha p\dot{\beta} + \bar{d}_{25}\alpha\dot{\beta}^2 + \bar{d}_{26}q\beta^2 + \bar{d}_{27}q\beta p + \bar{d}_{28}q\beta\dot{\beta} + \bar{d}_{29}qp^2 + \bar{d}_{30}qp\dot{\beta} + \\
&\quad \bar{d}_{31}q\dot{\beta}^2 + \bar{d}_{32}\dot{\alpha}\beta^2 + \bar{d}_{33}\dot{\alpha}\beta p + \bar{d}_{34}\dot{\alpha}\beta\dot{\beta} + \bar{d}_{35}\dot{\alpha}p^2 + \bar{d}_{36}\dot{\alpha}p\dot{\beta} + \bar{d}_{37}\dot{\alpha}\dot{\beta}^2 + \\
&\quad \bar{d}_{38}\beta^2 + \bar{d}_{39}\beta p + \bar{d}_{40}p^2 + \bar{d}_{41}\beta\dot{\beta} + \bar{d}_{42}\dot{\beta}^2
\end{aligned} \tag{4.18}$$

where $\bar{Q}_1 \equiv \frac{Q_1}{I_{xx}}$ and $\bar{Q}_2 \equiv \frac{Q_2}{I_{yy}}$.

The above expressions can be simplified by the use of stability derivatives as in the linear case, as follows.

$$\begin{aligned}
\frac{Q_1}{I_{xx}} &= \frac{L}{I_{xx}} = L_p p + L_\beta\beta + L_{\dot{\beta}}\dot{\beta} + L_q q + L_{\dot{\alpha}}\dot{\alpha} \\
\frac{Q_2}{I_{yy}} &= \frac{M}{I_{yy}} = M_q q + M_\alpha\alpha + M_{\dot{\beta}}\beta + M_p p + M_{\dot{\alpha}}\dot{\alpha}
\end{aligned} \tag{4.19}$$

where L and M are the usual notations for the aerodynamic rolling and pitching moments on the aircraft. It should be noted, however, that in the above expressions, the stability derivatives L_p, L_β, etc. are not constant. They may be functions of the variables β, p, q, α, $\dot{\beta}$, $\dot{\alpha}$ and in general, can be nonlinear. For example, by comparing Equations (4.18) and (4.19), we can write L_p as follows

$$\begin{aligned}
L_p &= \bar{c}_2 + \bar{c}_5\beta^2 + \bar{c}_7\beta p + \bar{c}_{17}\alpha + \bar{c}_{18}q + \bar{c}_{19}\dot{\alpha} + \bar{c}_{26}\alpha^2 + \bar{c}_{27}q^2 + \\
&\quad \bar{c}_{28}\dot{\alpha}^2 + \bar{c}_{30}\alpha q + \bar{c}_{33}\theta\dot{\alpha} + \bar{c}_{36}q\dot{\alpha} + \bar{c}_{38}\beta\dot{\beta}
\end{aligned} \tag{4.20}$$

4.4 Simplification of the Equations of Motion

The next step is to express the equations of motion in terms of two variables only, that is ϕ and θ. This can be done by using the following kinematic relations and approximations.

$$\begin{aligned} p &= \dot{\phi} \\ \beta &\approx \phi \sin\alpha_0 \\ \dot{\beta} &\approx \dot{\phi} \sin\alpha_0 \\ q &= \dot{\theta} \\ \alpha &\equiv \theta \\ \dot{\alpha} &\approx \dot{\theta} \end{aligned} \tag{4.21}$$

The equations of motion of the aircraft then become

$$\begin{aligned} \ddot{\phi} + n_1\phi\ddot{\theta} &= \hat{f}_1(\phi,\dot{\phi},\theta,\dot{\theta}) \\ (1+\frac{n_2}{n_3}\phi^2)\ddot{\theta} + n_2\phi\ddot{\phi} &= \hat{f}_2(\phi,\dot{\phi},\theta,\dot{\theta}) \end{aligned} \tag{4.22}$$

where n_i's are the inertia ratios defined as follows

$$\begin{aligned} n_1 &\equiv I_{xz}/I_{xx} \\ n_2 &\equiv I_{xz}/I_{yy} \\ n_3 &\equiv I_{xz}/I_{zz} \end{aligned} \tag{4.23}$$

and

$$\begin{aligned} \hat{f}_1(\phi,\dot{\phi},\theta,\dot{\theta}) &= \bar{Q}_1 - n_1\dot{\phi}\dot{\theta} + \frac{n_1}{n_3}\phi\dot{\theta}^2 \\ \hat{f}_2(\phi,\dot{\phi},\theta,\dot{\theta}) &= \bar{Q}_2 - n_2\dot{\phi}^2 - 2\frac{n_2}{n_3}\phi\dot{\phi}\dot{\theta} \end{aligned} \tag{4.24}$$

To facilitate the analysis, Eq. 4.22 will be expressed explicitly in $\ddot{\phi}$ and $\ddot{\theta}$. First, Eq. 4.22 is expressed in the matrix form as follows.

$$\begin{bmatrix} 1 & n_1\phi \\ n_2\phi & 1+\frac{n_2}{n_3}\phi^2 \end{bmatrix} \begin{pmatrix} \ddot{\phi} \\ \ddot{\theta} \end{pmatrix} = \begin{pmatrix} \hat{f}_1 \\ \hat{f}_2 \end{pmatrix} \tag{4.25}$$

Using the inverse operation, we get

$$\begin{pmatrix} \ddot{\phi} \\ \ddot{\theta} \end{pmatrix} = \frac{1}{1+(\frac{n_2}{n_3}-n_1n_2)\phi^2} \begin{bmatrix} 1+\frac{n_2}{n_3}\phi^2 & -n_1\phi \\ -n_2\phi & 1 \end{bmatrix} \begin{pmatrix} \hat{f}_1 \\ \hat{f}_2 \end{pmatrix} \tag{4.26}$$

Since we are only interested in small values of ϕ, then the following approximation is used.

$$\frac{1}{1+(\frac{n_2}{n_3}-n_1n_2)\phi^2} \approx 1-(\frac{n_2}{n_3}-n_1n_2)\phi^2 \tag{4.27}$$

This leads us to

$$\begin{aligned} \ddot{\phi} &= (1+\frac{n_2}{n_3}\phi^2)(1-(\frac{n_2}{n_3}-n_1n_2)\phi^2)\hat{f}_1 - n_1\phi(1-(\frac{n_2}{n_3}-n_1n_2)\phi^2)\hat{f}_2 \\ \ddot{\theta} &= -n_2\phi(1-(\frac{n_2}{n_3}-n_1n_2)\phi^2)\hat{f}_1 + (1-(\frac{n_2}{n_3}-n_1n_2)\phi^2)\hat{f}_2 \end{aligned} \tag{4.28}$$

In later analysis, only terms up to third order will be retained. Therefore, considering the fact that $\hat{f}_1$ and $\hat{f}_2$ consist of first and higher order terms, the above equations can be simplified further into

$$\begin{aligned} \ddot{\phi} &= (1+(\frac{n_2}{n_3}-n_1n_2)\phi^2)\hat{f}_1 - n_1\phi\hat{f}_2 \\ \ddot{\theta} &= -n_2\phi\hat{f}_1 + (1-(\frac{n_2}{n_3}-n_1n_2)\phi^2)\hat{f}_2 \end{aligned} \tag{4.29}$$

The substitution of $\hat{f}_1$ and $\hat{f}_2$ into the above equations yields

$$\begin{aligned} \ddot{\phi}+\omega^2\phi &= \tilde{\mu}\dot{\phi} + \tilde{c}_1\phi^3 + \tilde{c}_2\phi^2\dot{\phi} + \tilde{c}_3\phi\dot{\phi}^2 + \tilde{c}_4\dot{\phi}^3 + \tilde{c}_5\phi\theta + \tilde{c}_6\phi\dot{\theta} + \\ &\quad \tilde{c}_7\dot{\phi}\theta + \tilde{c}_8\dot{\phi}\dot{\theta} + \tilde{c}_9\phi\theta^2 + \tilde{c}_{10}\phi\dot{\theta}^2 + \tilde{c}_{11}\dot{\phi}\theta^2 + \tilde{c}_{12}\dot{\phi}\dot{\theta}^2 + \\ &\quad \tilde{c}_{13}\phi\theta\dot{\theta} + \tilde{c}_{14}\dot{\phi}\theta\dot{\theta} \\ \ddot{\theta}+\Omega^2\theta &= \tilde{\nu}\dot{\theta} + d_1\theta^2 + \tilde{d}_2\theta\dot{\theta} + \tilde{d}_3\dot{\theta}^2 + \tilde{d}_4\theta^3 + \tilde{d}_5\theta^2\dot{\theta} + \tilde{d}_6\theta\dot{\theta}^2 + \tilde{d}_7\dot{\theta}^3 + \\ &\quad \tilde{d}_8\theta\phi^2 + \tilde{d}_9\theta\phi\dot{\phi} + \tilde{d}_{10}\theta\dot{\phi}^2 + \tilde{d}_{11}\dot{\theta}\phi^2 + \tilde{d}_{12}\dot{\theta}\phi\dot{\phi} + \tilde{d}_{13}\dot{\theta}\dot{\phi}^2 + \\ &\quad \tilde{d}_{14}\phi^2 + \tilde{d}_{15}\phi\dot{\phi} + \tilde{d}_{16}\dot{\phi}^2 \end{aligned} \tag{4.30}$$

The relations between the coefficients in Equation (4.30) and Equation (4.18) are given in Appendix D. Dynamic analysis in the subsequent sections is based on the above equations.

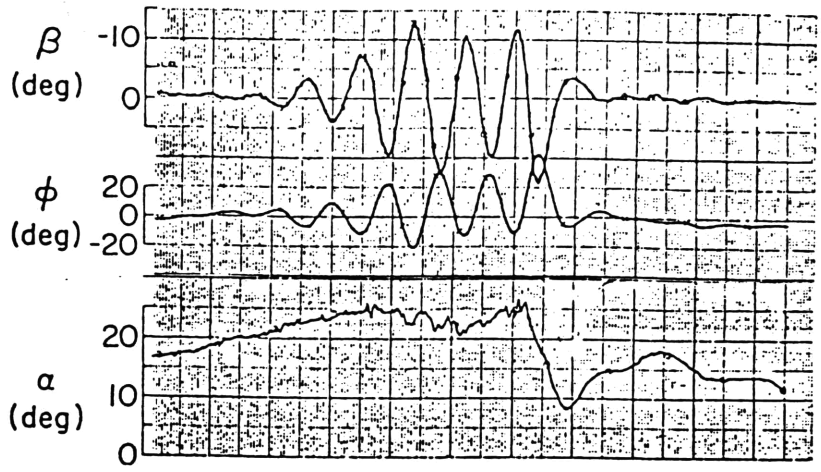

Figure 4-2: Wing rock motion on F-4 aircraft [4]

4.5 Motion Analysis

In the analysis, the Multiple Time Scales (MTS) Method is used to reduce the equations of motion into the so-called normal form, which is a set of first order equations for the amplitude and phase of the motion. Center manifold reduction techniques along with the bifurcation theory are then applied to this normal form to obtain the approximate solution and to assess the properties of the solution. Steady state and transient motion analysis are both performed and the results are compared with the ones obtained using numerical integration.

To facilitate our analysis, we focus on the small motions of the aircraft about its equilibrium conditions near wing rock situation. In such situations, for most aircrafts $\theta, \dot{\theta}$ are much smaller in magnitude than $\phi, \dot{\phi}$. An example of wing rock motion on a real aircraft is given in Figure 4-2 (from [4]). We can observe from this figure that that during the steady wing rock motion, the longitudinal oscillations are of much smaller amplitudes than the corresponding lateral oscillations. Mathematically, we express this as $O(|\mathbf{x_2}|) = O(|\mathbf{x_1}|^2)$, where $\mathbf{x_1^T} = \{\phi \ \dot{\phi}\}$ and $\mathbf{x_2^T} = \{\theta \ \dot{\theta}\}$. Because of the small motion assumption, in the ϕ-equation, we have

$$\lim_{\mathbf{x_1} \to \mathbf{0}} \frac{|f_1(\mathbf{x})|}{|\mathbf{x_1}|} = 0 \tag{4.31}$$

where $\mathbf{x} = \{\mathbf{x_1^T} \ \mathbf{x_2^T}\}^\mathbf{T}$ and $f_1(\mathbf{x})$ contains all the nonlinear terms in the ϕ-equation.

Similarly, for the θ-equation, we have

$$\lim_{\mathbf{x_2}\to\mathbf{0}} \frac{|f_2(\mathbf{x})|}{|\mathbf{x_2}|} = 0 \tag{4.32}$$

where $f_2(\mathbf{x})$ contains all the nonlinear terms in the θ-equation, except for the nonlinear terms of the form ϕ, $\phi\dot{\phi}$, and $\dot{\phi}^2$, since these terms will be of $O(|\mathbf{x_2}|)$ from the previous discussion in this paragraph. As in the single degree-of-freedom case and as we shall see later in the analysis, the roll damping parameter, $\tilde{\mu}$ plays an important role in the wing rock dynamics. Wing rock motion is normally caused by the loss of such damping. Since the analysis is focused on the aircraft motion in the vicinity of wing rock, hence this damping term is assumed to be small. The pitch damping parameter, $\tilde{\nu}$, is also assumed to be small in the current analysis. As we shall see later, relaxation of this assumption does not affect the final results. Hence, this assumption can be applied without loss of generality. Based on the above discussion and experience with numerical solutions of the problems, the following parameterization in terms of a small parameter, ϵ is found to be constructive.

$$\begin{aligned} \ddot{\phi} + \omega^2\phi &= \epsilon\left[\mu\dot{\phi} + f_1(\phi,\dot{\phi},\theta,\dot{\theta})\right] \\ \ddot{\theta} + \Omega^2\theta &= g(\phi,\dot{\phi}) + \epsilon\left[\nu\dot{\theta} + f_2(\phi,\dot{\phi},\theta,\dot{\theta})\right] \end{aligned} \tag{4.33}$$

where $0 < \epsilon << 1$, and

$$\begin{aligned} g(\phi,\dot{\phi}) &= d_{14}\phi^2 + d_{15}\phi\dot{\phi} + d_{16}\dot{\phi}^2 \\ f_1(\phi,\dot{\phi},\theta,\dot{\theta}) &= c_1\phi^3 + c_2\phi^2\dot{\phi} + c_3\phi\dot{\phi}^2 + c_4\dot{\phi}^3 + c_5\phi\theta + c_6\phi\dot{\theta} + \\ &\quad c_7\dot{\phi}\theta + c_8\dot{\phi}\dot{\theta} + c_9\phi\theta^2 + c_{10}\phi\dot{\theta}^2 + c_{11}\dot{\phi}\theta^2 + c_{12}\dot{\phi}\dot{\theta}^2 + \\ &\quad c_{13}\phi\theta\dot{\theta} + c_{14}\dot{\phi}\theta\dot{\theta} \\ f_2(\phi,\dot{\phi},\theta,\dot{\theta}) &= d_1\theta^2 + d_2\theta\dot{\theta} + d_3\dot{\theta}^2 + d_4\theta^3 + d_5\theta^2\dot{\theta} + d_6\theta\dot{\theta}^2 + d_7\dot{\theta}^3 + \\ &\quad d_8\theta\phi^2 + d_9\theta\phi\dot{\phi} + d_{10}\theta\dot{\phi}^2 + d_{11}\dot{\theta}\phi^2 + d_{12}\dot{\theta}\phi\dot{\phi} + d_{13}\dot{\theta}\dot{\phi}^2 \end{aligned} \tag{4.34}$$

The MTS method is now invoked. The independent variable, t, is extended into two time scales as follows.

$$\begin{aligned} t \to \{\tau_0, \tau_1\} \quad ; \quad \tau_0 &= t \\ \tau_1 &= \epsilon t \end{aligned} \tag{4.35}$$

In this case τ_0 is the fast time scale, while τ_1 is the slow one. The dependent variables

are also extended as

$$\begin{aligned} \phi(t) &\rightarrow \phi_0(\tau_0,\tau_1) + \epsilon\phi_1(\tau_0,\tau_1) + ... \\ \theta(t) &\rightarrow \theta_0(\tau_0,\tau_1) + \epsilon\theta_1(\tau_0,\tau_1) + ... \end{aligned} \tag{4.36}$$

The extended variables are then substituted into Eq. 4.33 and grouped according to the order of ϵ. Order by order analysis can then be performed by equating each group to zero.

Equations of leading order are given by

$$\begin{aligned} \frac{\partial^2\phi_0}{\partial\tau_0^2} + \omega^2\phi_0 &= 0 \\ \frac{\partial^2\theta_0}{\partial\tau_0^2} + \omega^2\theta_0 &= g(\phi_0,\dot{\phi}_0) \end{aligned} \tag{4.37}$$

The solution for the first equation is

$$\phi_0 = A_1(\tau_1)\sin\Psi_1 \;\; ; \;\; \Psi_1 \equiv \omega\tau_0 + B_1(\tau_1) \tag{4.38}$$

Then by substituting Eq 4.38 into the second equation in 4.37, we get

$$\theta_0 = A_2(\tau_1)\sin\Psi_2 + m_0A_1^2 + m_1A_1^2\cos 2\Psi_1 + m_2A_1^2\sin 2\Psi_1 \tag{4.39}$$

where

$$\begin{aligned} \Psi_2 &\equiv \Omega\tau_0 + B_2(\tau_1) \\ m_0 &= \frac{d_{14} + d_{16}\omega^2}{2\Omega^2} \\ m_1 &= \frac{-d_{14} + d_{16}\omega^2}{2(\Omega^2 - 4\omega^2)} \\ m_2 &= \frac{d_{15}\omega}{2(\Omega^2 - 4\omega^2)} \end{aligned} \tag{4.40}$$

The $O(\epsilon)$ analysis results in the following equations.

$$\begin{aligned} \frac{\partial^2\phi_1}{\partial\tau_0^2} + \omega^2\phi_1 &= \Big[-2\omega\frac{dA_1}{d\tau_1} + \mu\omega A_1 + (\frac{1}{4}c_2\omega + \frac{3}{4}c_4\omega^3 + \\ &\quad \frac{1}{2}m_2c_5 - m_1\omega c_6 + \frac{1}{2}c_7(2m_0 + m_1) + c_8m_2\omega^2)A_1^3 + \end{aligned}$$

$$
\begin{aligned}
& \frac{1}{2}\omega(c_{11}+c_{12}\Omega^2)A_1A_2^2\Big]\cos\Psi_1+\Big[2\omega A_1\frac{dB_1}{d\tau_1}+\frac{3}{4}c_1 \\
& +\frac{1}{4}c_3\omega^2+\frac{1}{2}c_5(2m_0-m_1)- \\
& c_6m_2\omega+\frac{1}{2}c_7m_2\omega-c_8m_1\omega^2]A_1^3+\frac{1}{2}c_9+ \\
& c_{10}\Omega^2)A_1A_2^2\Big]\sin\Psi_1+... \\
\frac{\partial^2\theta_1}{\partial\tau_0^2}+\omega^2\theta_1 &= \frac{1}{2}(d_1+d_3\Omega^2)A_2^3+\frac{1}{2}d_{15}A_1\frac{dA_1}{d\tau_1}+d_{16}\omega A_1^2\frac{dB_1}{d\tau_1}+ \\
& \Big[-2\Omega\frac{dA_2}{d\tau_1}+\nu\Omega A_2+\frac{1}{4}\Omega(d_5+3d_7\Omega^2)A_2^3+\Omega(d_2m_0+ \\
& \frac{1}{2}d_{11}+\frac{1}{2}d_{13}\omega^2)A_1^2A_2\Big]\cos\Psi_2+ \\
& \Big[2\Omega A_2\frac{dB_2}{d\tau_1}+\frac{1}{4}(3d_4+d_6\Omega^2)A_2^3+ \\
& \frac{1}{2}(4d_1m_0+d_8+d_{10})A_1^2A_2\Big]\sin\Psi_2+... \qquad (4.41)
\end{aligned}
$$

We concentrate on the case where there is no internal resonance, that is

$$
l_1\Psi_1\neq l_2\Psi_2 \qquad (4.42)
$$

where l_i's are arbitrary integers. In this case, we see from Eq. 4.41 that the coefficients of the first harmonic terms must be set to zero in order that no secular terms appear in the solution. By doing so, we get the following set of first order equations for the amplitude and phase.

$$
\begin{aligned}
\frac{dA_1}{d\tau_1} &= \frac{1}{2}\mu A_1+p_1A_1^3+p_2A_1A_2^2 \\
\frac{dA_2}{d\tau_1} &= \frac{1}{2}\nu A_2+q_1A_2^3+q_2A_1^2A_2 \\
\frac{dB_1}{d\tau_1} &= p_3A_1^2+p_4A_2^2 \\
\frac{dB_2}{d\tau_1} &= q_3A_1^2+q_4A_2^2 \qquad (4.43)
\end{aligned}
$$

where

$$
\begin{aligned}
p_1 &= \frac{1}{8}[c_2+3c_4\omega^2+\frac{2}{\omega}m_2c_5-4m_1c_6+ \\
& c_7(4m_0+2m_1)+4c_8m_2\omega]
\end{aligned}
$$

$$
\begin{aligned}
p_2 &= \frac{1}{4}(c_{11} + c_{12}\Omega^2) \\
p_3 &= -\frac{1}{8\omega}[3(c_1 + c_3)\omega^2 + c_5(4m_0 - 2m_1) - \\
&\quad 4c_6 m_2 \omega + 2c_7 m_2 \omega - 4c_8 m_1 \omega^2] \\
p_4 &= -\frac{1}{4\omega}[c_9 - n_1 d_1 + c_{10}\Omega^2] \\
q_1 &= \frac{1}{8}(d_5 + 3d_7\Omega^2) \\
q_2 &= \frac{1}{4}[2d_2 m_0 + d_{11} + d_{13}\omega^2] \\
q_3 &= -\frac{1}{4\Omega}[4d_1 m_0 + d_8 + d_{10}] \\
q_4 &= \frac{1}{8\Omega}(3d_4 + d_6\Omega^2)
\end{aligned} \tag{4.44}
$$

Note that the first two equations in (4.43) are the amplitude equations while the other two are the phase-correction equations. The amplitude equations determine the amplitude history of the motion. They determines whether the amplitudes of the motion decay or increase, hence the stability of the motion. The phase-correction equations give corrections to the frequency of the solution.

4.5.1 Local Stability Around the Origin

For stability analysis purposes, we need to consider only the amplitude equations. We will focus on the stability of the equilibrium point at the origin. Physically, this means that we are interested in the stability of the aircraft motion about a nominal flight condition. Throughout the discussion we assume $\nu < 0$, that is positive damping in pitch motion. The linearization of the amplitude equations around the origin is

$$
\begin{Bmatrix} \frac{dA_1}{d\tau_1} \\ \frac{dA_2}{d\tau_1} \end{Bmatrix} = \nabla \begin{Bmatrix} A_1 \\ A_2 \end{Bmatrix} \tag{4.45}
$$

with

$$
\nabla = \begin{Bmatrix} \frac{1}{2}\mu & 0 \\ 0 & \frac{1}{2}\nu \end{Bmatrix} \tag{4.46}
$$

It is clear that the eigenvalues of the Jacobian ∇ at the origin are $\mu/2$ and $\nu/2$. For $\nu < 0$, one of the eigenvalues $(\nu/2)$ is always negative. When $\mu < 0$, then both eigenvalues are negative, and so the origin is an asymptotically stable equilibrium.

When $\mu > 0$, then one of the eigenvalues of the system is positive and the origin is an unstable equilibrium. When $\mu = 0$, we cannot conclude anything about the stability of the origin from the Jacobian only. Higher order terms that are neglected in the linearization must be included in the analysis to determine the system stability for this particular case. As the system is of order two, then in general the analysis is very complicated. Reduction of order is possible using the center manifold approach, which is performed in the next subsection.

One should note that the above analysis is local. Once we move away from the origin, the nonlinear effects start to come into play. To obtain the whole dynamical picture of the system, the nonlinearity must be taken into account in the analysis. Since analysis of a nonlinear system having two or more cross-coupled equations is in general complicated, the reduction of the system order using the center manifold approach is very useful in making the analysis tractable.

4.5.2 Center Manifold Reduction and Bifurcation Analysis

In this section, we focus still on the amplitude equations. We seek a center manifold for this system when $\mu = 0$ and look at its properties. In case the exact center manifold cannot be easily found, an asymptotic approximation for it will be attempted. For $\mu \neq 0$ but sufficiently small, we can still use the approximation obtained to obtain the approximate solution of the system.

We will first focus on the case where $\mu = 0$. Let the center manifold for this system be

$$A_2 = h(A_1) \tag{4.47}$$

Then by using chain rule,

$$\frac{dA_2}{d\tau_1} = \frac{dh}{dA_1}\frac{dA_1}{d\tau_1} \tag{4.48}$$

By substituting the first two equations in (4.43) into Equation (4.48), we get

$$\frac{1}{2}\nu h + q_1 h^3 + q_2 A_1^2 h = \frac{dh}{dA_1}\left[\frac{1}{2}\mu A_1 + p_1 A_1^3 + p_2 A_1 h^2\right] \tag{4.49}$$

To find an approximation to the center manifold, we let

$$h(A_1) = A_{2_0} \exp(-\frac{k}{A_1^2}) \tag{4.50}$$

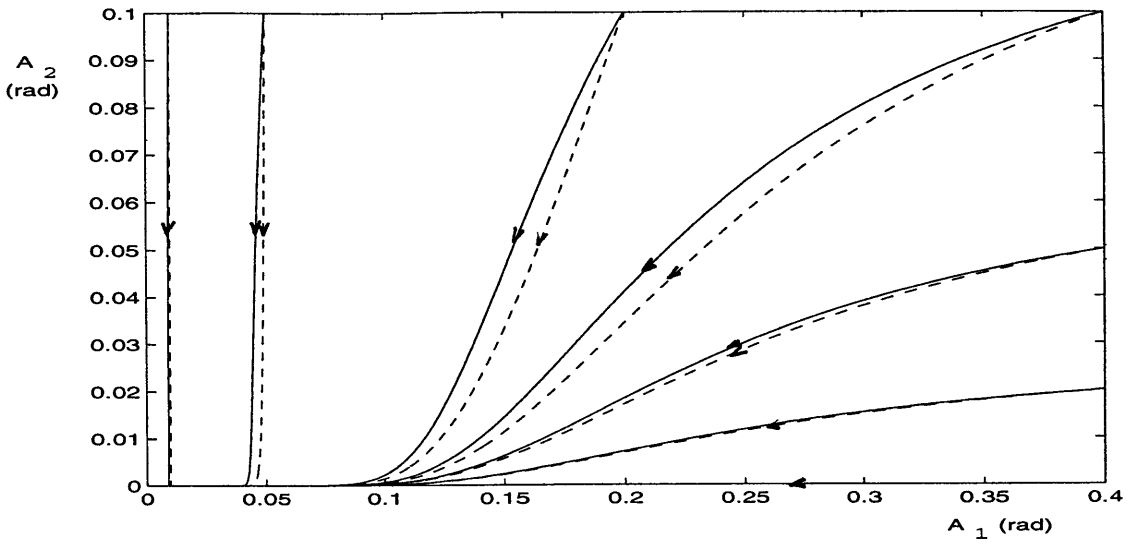

Figure 4-3: Center manifold

Note that this expression satisfies $h = \dfrac{dh}{d\tau_1} = 0$. By substituting the above expression into Equation (4.49), we get

$$\frac{\nu}{2}h = 2kA_1^{-3}p_1A_1^3h + O\left((|A_1| + |h|)^3\right) \tag{4.51}$$

Considering only the leading order terms in the equation (neglecting higher order terms), we obtain

$$\begin{aligned} \frac{\nu}{2} &= 2kp_1 \\ \Leftrightarrow k &= \frac{\nu}{4p_1} \end{aligned} \tag{4.52}$$

The substitution of this expression into Equation (4.50) results in the following approximate expression for the center manifold.

$$h(A_1) = A_{2_0}\exp(-\frac{\nu}{4p_1A_1^2}) \tag{4.53}$$

Note that this center manifold is non-analytic. Indeed, approximating the center manifold using Taylor series results in all zero terms. Figure 4-3 compares the exact center manifolds and their approximations as given by Equation (4.53) for various A_{2_0}. For practical purposes here, the above approximation can be considered very good.

One should also note that the center manifold is very flat near the origin. Hence if we are only interested in cases where $A_1, A_2 << 0$ then we can approximate the center manifold fairly well using

$$A_2 \approx 0 \tag{4.54}$$

For this reason, this approximation is used in further analysis. It can clearly be understood that this approximation considerably simplifies the analysis. As we shall see later, the accuracy of the approximation does not suffer within the assumption of small A_1.

With this approximation, the reduced system becomes

$$\frac{dA_1}{d\tau_1} = p_1 A_1^3 \tag{4.55}$$

This is a scalar first order differential equation, the solution of which can easily be found. According to *Theorem 2*, the stability properties of the system (4.43 are the same as the stability properties of the reduced system (4.65). Since the reduced system is quite simple, its stability properties can be studied without finding out its exact solution. Note that $\frac{dA_1}{d\tau_1}$ determines the slope of the $A_1(\tau_1)$. If $p_1 > 0$, $\frac{dA_1}{d\tau_1} > 0$ for all τ_1 and $A_1(\tau_1)$ increases monotonically with τ_1. In this case, the system is unstable. On the other hand, if $p_1 < 0$, $\frac{dA_1}{d\tau_1} < 0$ for all τ_1, which means that $A_1(\tau_1)$ decreases monotonically with τ_1. This implies that the system is stable for $p_1 < 0$. For $p_1 = 0$, the stability of the system can only be determined by looking at higher order terms. Since the case where $p_1 = 0$ is very rarely encountered, we will not explore this case further.

Next we will consider the case where μ is small but not equal zero. In this situation, the previous center manifold results cannot directly be applied. Some modification has to be made to put the problem into the center manifold framework. This is done by considering μ as a trivial dependent variable, as follows.

$$\begin{aligned}
\frac{dA_1}{d\tau_1} &= \frac{1}{2}\mu A_1 + p_1 A_1^3 + p_2 A_1 A_2^2 \\
\frac{dA_2}{d\tau_1} &= \frac{1}{2}\nu A_2 + q_1 A_2^3 + q_2 A_1^2 A_2 \\
\frac{d\mu}{d\tau_1} &= 0
\end{aligned} \tag{4.56}$$

Note that in this formulation, the term $\frac{1}{2}\mu A_1$ is considered nonlinear. The equilibrium point of interest is the origin $(A_1, A_2, \mu) = (0, 0, 0)$. The linearization of the system

(4.56) around the origin results in

$$\begin{aligned} \frac{dA_1}{d\tau_1} &= 0 \\ \frac{dA_2}{d\tau_1} &= \frac{1}{2}\nu A_2 \\ \frac{d\mu}{d\tau_1} &= 0 \end{aligned} \tag{4.57}$$

The eigenvalues of this linearized system are 0, ν, and 0. By the assumption $\nu < 0$, the A_2-axis is a stable manifold. In this case, we will find a center manifold

$$A_2 = h(A_1, \mu) \tag{4.58}$$

which satisfies $h(0,0) = \frac{dh}{dA_1}(0,0) = \frac{dh}{d\mu}(0,0) = 0$. Note that in order to satisfy this requirement, $h = O((|A_1| + |\mu|)^n)$; $n > 1$. By differentiating Equation (4.58) with respect to τ_1, we get

$$\frac{dA_2}{d\tau_1} = \frac{dh}{dA_1}\frac{dA_1}{d\tau_1} + \frac{dh}{d\mu}\frac{d\mu}{d\tau_1} \tag{4.59}$$

Then, by substituting $\frac{dA_1}{d\tau_1}$, $\frac{dA_2}{d\tau_1}$, and $\frac{d\mu}{d\tau_1}$ from Equation (4.56) into the above equation, we obtain

$$\frac{dh}{dA_1} = \frac{\frac{1}{2}\nu h + q_1 h^3 + q_2 A_1^2 h}{\frac{1}{2}\mu A_1 + p_1 A_1^3 + p_2 A_1 h^2} \tag{4.60}$$

Because solving this equation is very difficult, we simplify it by remembering that $h = O((|A_1| + |\mu|)^n)$, $n > 1$ and neglecting terms in the numerator and denominator of $O((|A_1| + |\mu|)^k)$, $k > 3$. Doing so, we get

$$\frac{dh}{dA_1} \approx \frac{\frac{1}{2}\nu h}{\frac{1}{2}\mu A_1 + p_1 A_1^3} \tag{4.61}$$

It can be shown that the solution of the simplified equation is

$$h(A_1, \mu) = C\left(\frac{A_1^2}{\frac{1}{2}\mu + p_1 A_1^2}\right)^{\frac{1}{2}\frac{\nu}{\mu}} \tag{4.62}$$

where C is a constant to be determined from the condition $h(0,0) = \frac{dh}{dA_1}(0,0) =$

$\frac{dh}{d\mu}(0,0) = 0$. This condition can only be satisfied when

$$C = 0 \tag{4.63}$$

Therefore, the center manifold of the system is

$$A_2 = 0 \tag{4.64}$$

which is the $A_1 - \mu$ plane.

The above result can also be deduced graphically. Figure 4-4 depicts the flows of A_2 vs. A_1 for $\mu < 0$ and for $\mu > 0$. In the figure, the exact flows, shown using the solid curves, are compared to the approximate ones given by Equation (4.62), represented by the dashed curves,. We can see that the approximate solutions follow the exact solutions fairly well. It can also easily seen from the figure that the only solution that always satisfies $h(0,0) = \frac{dh}{dA_1}(0,0) = \frac{dh}{d\mu}(0,0) = 0$ is $A_2 = 0$. It is clear then that $A_2 = 0$, that is the $A_1 - \mu$ plane, is the center manifold of the system.

The reduced system is then given by

$$\begin{aligned} \frac{dA_1}{d\tau_1} &= \frac{1}{2}\mu A_1 + p_1 A_1^3 \\ \frac{d\mu}{d\tau_1} &= 0 \end{aligned} \tag{4.65}$$

The equilibria of this system consist of the μ-axis and the parabola $\mu = -2p_1 A_1^2$. Since $\frac{d\mu}{d\tau_1} = 0$, the planes $\mu = constant$ are invariant. In a plane $\mu = constant \neq 0$, all of the equilibria are of hyperbolic type, and so their local stability properties can be assessed by looking at the eigenvalues of the linearized systems around the equilibria. The linearized system around the equilibria at μ-axis for $\mu = constant \neq 0$ is

$$\begin{Bmatrix} \frac{dA_1}{d\tau_1} \\ \frac{dA_2}{d\tau_1} \end{Bmatrix} = \begin{bmatrix} \frac{1}{2}\mu & 0 \\ 0 & \frac{1}{2}\nu \end{bmatrix} \begin{Bmatrix} A_1 \\ A_2 \end{Bmatrix} \tag{4.66}$$

The eigenvalues of the system are $\frac{1}{2}\mu$ and $\frac{1}{2}\nu$. Since ν is assumed to be negative, then the equilibria at μ-axis is asymptotically stable if $\mu < 0$ and unstable if $\mu > 0$. Similarly, the linearized system around the equilibria $\mu = -2p_1 A_1^2$ for $\mu = constant \neq$

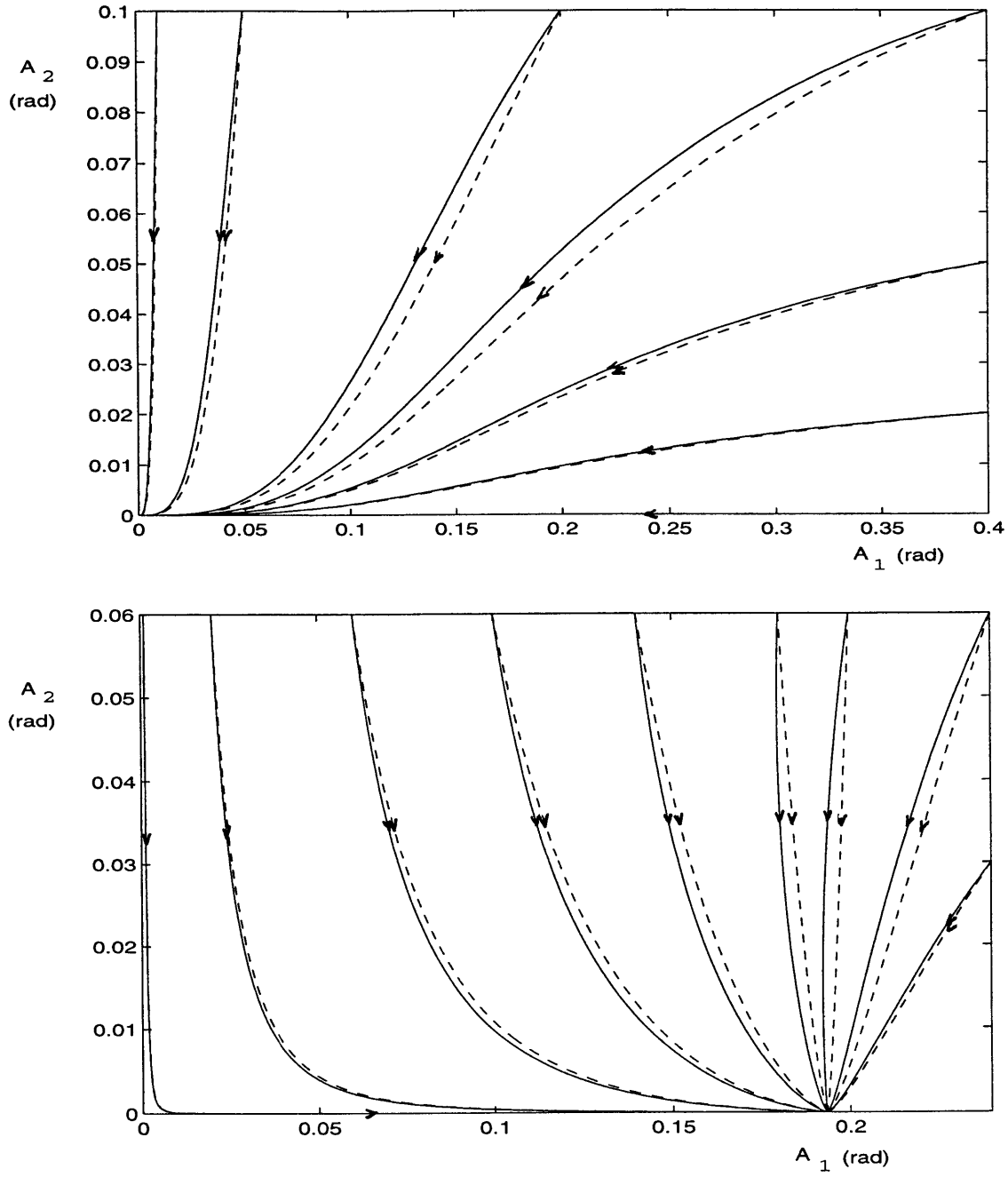

Figure 4-4: The flow of the system for $\mu < 0$ (upper) and for $\mu > 0$ (lower)

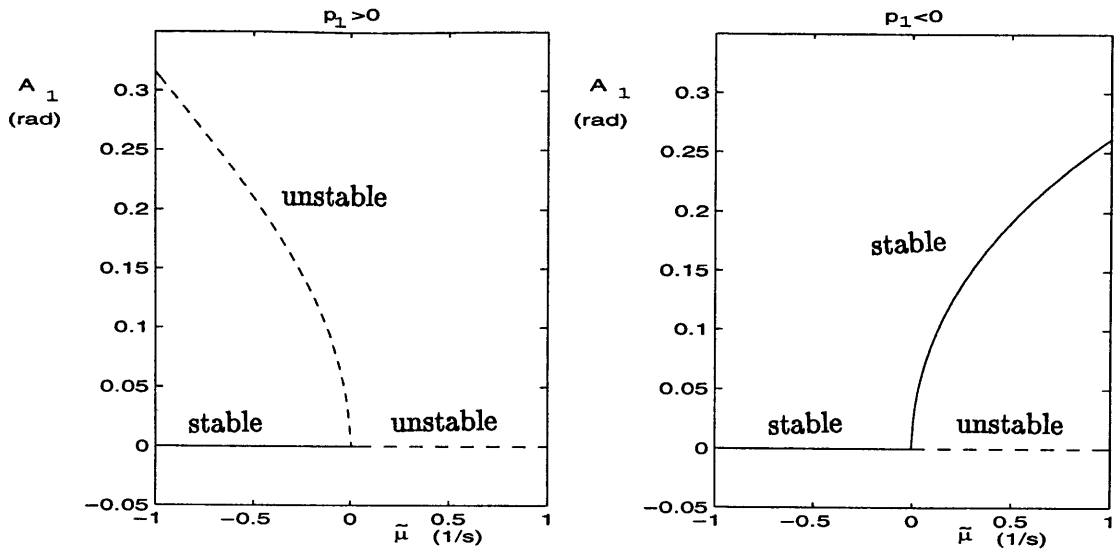

Figure 4-5: Bifurcation diagrams for (a) $p_1 > 0$ and (b) $p_1 < 0$

0 is given by

$$\begin{Bmatrix} \frac{dA_1}{d\tau_1} \\ \frac{dA_2}{d\tau_1} \end{Bmatrix} = \begin{Bmatrix} -\frac{1}{2}\mu & 0 \\ 0 & \frac{1}{2}\nu \end{Bmatrix} \begin{Bmatrix} A_1 \\ A_2 \end{Bmatrix} \tag{4.67}$$

Here, the eigenvalues of the system are $-\frac{1}{2}\mu$ and $\frac{1}{2}\nu$. Hence, the equilibria at $\mu = -2p_1 A_1^2$ are asymptotically stable for $\mu > 0$ and unstable if $\mu < 0$.

The above discussion shows that the properties of the solution of the system change as μ varies from negative to positive. For one, it is easy to see that the number of the equilibrium points changes across $\mu = 0$. Hence, $\mu = 0$ is the bifurcation point of the system. The bifurcation diagrams of this system for $p_1 > 0$ and $p_1 < 0$ are given in Figure 4-5. These diagrams indicate that there is a finite amplitude oscillation of the limit cycle type appearing or dissapearing in the system when μ is varied across $\mu = 0$. Hence, this is a Hopf type bifurcation. When $p_1 > 0$, a subcritical Hopf bifurcation occurs and no stable limit cycle in the system. When $p_1 < 0$, the Hopf bifurcation is supercritical and a stable limit cycle appears for $\mu > 0$. Physically this means that a sustained wing rock motion can be observed in the aircraft motion.

An alternative argument can also be used to infer the presence of Hopf bifurcation in the system. If we look at the eigenvalues of the linearized version of the equations of motion (4.33) as μ varies. In this case, there are two pairs of complex eigenvalues associated with the lateral and the longitudinal modes. Initially when $\mu < 0$, both pairs of the eigenvalues lie to the left of the imaginary axis (in the stable region). As

μ varies, the location of the eigenvalues changes. Exactly when $\mu = 0$, the pair of eigenvalues associated with the lateral mode lie on the imaginary axis. As μ increases further, these eigenvalues move to the right of the imaginary axis. The crossing of the imaginary axis occurs at a nonzero speed and based on the Theorem 2.5, this condition gives rise to the occurence of Hopf bifurcation. This type of analysis, however, does not tell us further whether the bifurcation is subcritical or supercritical.

In case where the stable limit cycle exists in the system, the amplitude of the limit cycle or in other words the amplitude of the wing rock motion is given by

$$A_1 = \sqrt{-\frac{\mu}{2p_1}} \tag{4.68}$$

The above analysis can be interpreted as a steady-state analysis. This implies that after some transient, the amplitudes A_1 and A_2 eventually reach the steady-state values $A_1 = \sqrt{-\frac{\mu}{2p_1}}$ and $A_2 = 0$. The steady-state correction to the phase then can be calculated from the last two equations in (4.43), which in this case become

$$\begin{aligned} \frac{dB_1}{d\tau_1} &= -p_3\frac{\mu}{2p_1} \\ \frac{dB_2}{d\tau_1} &= -q_3\frac{\mu}{2p_1} \end{aligned} \tag{4.69}$$

These equations can easily be integrated to obtain

$$\begin{aligned} B_1 &= -p_3\frac{\mu}{2p_1}\tau_1 \\ B_2 &= -q_3\frac{\mu}{2p_1}\tau_1 \end{aligned} \tag{4.70}$$

4.5.3 Analytical Approximation of the Solution

In this subsection, a closed form approximation of the system response is developed, which includes an approximation to the transients of the motion. We will start by looking at the amplitude and phase equations depicted in (4.43) and attempt to find a closed form solution to this set of first order differential equations. As can be observed, the phase correction equations can be solved once the amplitude equations are solved. Hence we focus initially on the amplitude differential equations. These equations are nonlinear and coupled and the exact solutions can only be obtained by treat them together. Since our goal is only to obtain approximation to the exact solutions, then

simplification of the system of equation is possible by applying Gronwall's Lemma to the always stable subset of the system, which in this case is represented by the second amplitude equation (recall the $\nu < 0$ assumption). This equation is rewritten as follows

$$\frac{dA_2}{d\tau_1} = \frac{1}{2}\nu A_2 + g(A_1, A_2) \tag{4.71}$$

where $g(A_1, A_2) \equiv (q_1 A_2^2 + q_2 A_1^2)$.
Now suppose that one can find $0 < \delta \ll 1$ and $0 < \gamma < |\frac{1}{2}\nu|$ such that for $A_1, A_2 < \delta$, one has $|g(A_1, A_2)| \leq \gamma A_2$. Since we only consider small amplitude motion, this condition can be easily satisfied. The integration of Equation (4.71) yields

$$A_2(\tau_1) = \exp(\frac{1}{2}\nu\tau_1)A_{2_0} + \int_0^{\tau_1} \exp(\frac{1}{2}\nu(\tau_1 - s))g(A_1, A_2)ds \tag{4.72}$$

By the condition imposed on $|g(A_1, A_2)|$, we can write

$$|A_2(\tau_1)| \leq A_{2_0} \exp(\frac{1}{2}\nu\tau_1) + \int_0^{\tau_1} \exp(\frac{1}{2}\nu(\tau_1 - s))\gamma|A_2|ds \tag{4.73}$$

Next, by multiplying both sides of the equation by $\exp(-\frac{1}{2}\nu\tau_1)$, we get

$$\exp(-\frac{1}{2}\nu\tau_1)|A_2(\tau_1)| \leq A_{2_0} + \int_0^{\tau_1} \gamma \exp(-\frac{1}{2}s)|A_2|ds \tag{4.74}$$

The statement of the Gronwall's lemma is given below. For proof, the reader may refer to [36].
Gronwall's lemma :
If

$$f(t) \leq K + \int_a^t f(s)g(s)ds \tag{4.75}$$

for $a \leq t \leq b$, then $f(t)$ is bounded by

$$f(t) \leq K \exp(\int_a^t g(s)ds) \tag{4.76}$$

We see that Equation (4.74) is in the form of Equation (4.75) with $f(s) \equiv \exp(-\frac{1}{2}\nu s)|A_2(s)|$, $g(s) \equiv \gamma$, and $K \equiv A_{2_0}$. Therefore, it follows from the lemma that

$$\exp(-\frac{1}{2}\nu\tau_1)|A_2(\tau_1)| \leq A_{2_0} \exp(\gamma\tau_1) \tag{4.77}$$

or by multiplying both sides with $\exp(\frac{1}{2}\nu\tau_1)$, we get

$$A_2(\tau_1) \leq A_{2_0} \exp((\frac{1}{2}\nu + \gamma)\tau_1) \tag{4.78}$$

This inequality provides the upper bound of the amplitude history of pitch motion θ.

When $g(A_1, A_2) = 0$, Equation (4.71) becomes linear and the amplitude history solution is (from Equation (4.72))

$$\bar{A}_2(\tau_1) = A_{2_0} \exp(\frac{1}{2}\nu\tau_1) \tag{4.79}$$

The deviation of the actual A_2-history from (4.79) depends on the magnitude of $g(A_1, A_2)$, which is reflected in its upper bound γ. As a measure, we can examine the difference between the upper bound of A_2 and the linear solution $\bar{A}_2$ to get an idea on the magnitude of the deviation.

$$\Delta^u_{A_2} \equiv A_2 - \bar{A}_2 \leq A_{2_0} \exp(\frac{1}{2}\nu\tau_1)(\exp(\gamma\tau_1) - 1) \tag{4.80}$$

which is equivalent to

$$\frac{\Delta^u_{A_2}}{\bar{A}_2} \leq \exp(\gamma\tau_1) - 1 \tag{4.81}$$

The smaller γ, the closer $\exp(\gamma\tau_1)$ is to 1, and the smaller $\Delta^u_{A_2}$ is. This means that for small γ, $\bar{A}_2$ is a good approximation to the actual A_2-history. Since we are only interested in small amplitude motions and $|g(A_1, A_2)|$ is of the order of square of the amplitudes, then γ can be taken to be very small. Therefore, for our purposes we will use $\bar{A}_2$ as the approximation to the A_2-history.

The substitution of $\bar{A}_2$ into the A_1 differential equation yields

$$\frac{dA_1}{d\tau_1} = a(\tau_1)A_1 + p_1 A_1^3 \tag{4.82}$$

where

$$a(\tau_1) = \frac{1}{2}\mu + p_2 A_{2_0}^2 \exp(\nu\tau_1) \tag{4.83}$$

Equation (4.82) is a first order nonlinear differential equation with a time-varying coefficient in $a(\tau_1)$. The exact solution to this equation can be found using the procedure outlined below.

We first multiply Equation (4.82) with a function $k(\tau_1)$ to be determined later. This function is the integrating factor of the differential equation. By this multipli-

cation, the differential equation becomes

$$k(\tau_1)\frac{dA_1}{d\tau_1} = a(\tau_1)k(\tau_1)A_1 + p_1 k(\tau_1)A_1^3 \tag{4.84}$$

which can also be written in the following way

$$\frac{d(k(\tau_1)A_1)}{d\tau_1} - \frac{dk(\tau_1)}{d\tau_1}A_1 = a(\tau_1)k(\tau_1)A_1 + \frac{p_1}{k^2(\tau_1)}(k(\tau_1)A_1)^3 \tag{4.85}$$

The above equation can be solved exactly if we equate the second term on the left-hand side of the equation with the first term on the right-hand side, that is

$$\frac{dk(\tau_1)}{d\tau_1} = -a(\tau_1)k(\tau_1) \tag{4.86}$$

This equation determines the integration factor $k(\tau_1)$ and is solvable exactly to give

$$k(\tau_1) = K\exp(-\int a(\tau_1)d\tau_1) \tag{4.87}$$

where K is an arbitrary constant.
Using this integrating factor, Equation (4.85) becomes

$$\frac{d(k(\tau_1)A_1)}{d\tau_1} = \frac{p_1}{k^2(\tau_1)}(k(\tau_1)A_1)^3 \tag{4.88}$$

Then, by using the separation of variable technique and by considering $k(\tau_1)A_1$ as one of the variables, Equation (4.88) can be put into a form which is readily integrable as follows.

$$\frac{d(k(\tau_1)A_1)}{(k(\tau_1)A_1)^3} = \frac{p_1}{k^2(\tau_1)}d\tau_1 \tag{4.89}$$

Note that in this form, the left-hand side only contains the variable $(k(\tau_1)A_1)$ and the right-hand side has τ_1 as its variable. Integration of both sides with respect to its own variables yields

$$-\frac{1}{2(k(\tau_1)A_1)^2} = \int \frac{p_1}{K^2}\exp(2\int a(\tau_1)d\tau_1)d\tau_1 + \bar{C}_1 \tag{4.90}$$

where $\bar{C}_1$ is a constant coming from the indefinite integration of the left-hand side of Equation (4.89). Written explicitly in A_1, the above equation becomes

$$A_1 = \frac{\exp(\int a(\tau_1)d\tau_1)}{\sqrt{C_1 - 2p_1\int\exp(2\int a(\tau_1)d\tau_1)d\tau_1}} \tag{4.91}$$

Note that the constants C_1 and $\bar{C}_1$ in Equations (4.91) and (4.90) differ by a constant factor. C_1 is determined from the initial condition. The integral $\int \exp(2\int a(\tau_1)d\tau_1)d\tau_1$ is not simple to obtain since $a(\tau_1)$ also contains an exponential term. Here we attempt to assess some of its properties without solving it.

From Equation (4.83), we observe that the second term on the right-hand side is of $O(A_{2_0}^2)$. Since we are only interested in small amplitude motion, then the effect of this term is generally small. Moreover, since $\nu < 0$, this term goes to zero exponentially as τ_1 increases. When $\tau_1 = 0$, then

$$\int \exp(2\int a(\tau_1)d\tau_1)d\tau_1 = 0 \tag{4.92}$$

For large τ_1,

$$\int \exp(2\int a(\tau_1)d\tau_1)d\tau_1 \approx \frac{2}{\mu}\exp(\frac{\mu}{2}\tau_1) \tag{4.93}$$

and as $\tau_1 \to \infty$,

$$\begin{aligned} \exp(\frac{\mu}{2}\tau_1) &\to 0 \quad for\ \mu < 0 \\ \exp(\frac{\mu}{2}\tau_1) &\to \infty \quad for\ \mu > 0 \end{aligned} \tag{4.94}$$

For $\mu = 0$, one can refer to the center manifold analysis result presented in the previous subsection for the motion stability.

From the above discussion, if we let the initial condition for A_1 to be A_{1_0}, then we get C_1 in terms of A_{1_0} from Equation (4.91) as follows.

$$A_{1_0}^2 = \frac{1}{C_1} \Longleftrightarrow C_1 = \frac{1}{A_{1_0}^2} \tag{4.95}$$

Hence, in terms of A_{1_0},

$$A_1 = A_{1_0}\frac{\exp(\int a(\tau_1)d\tau_1)}{\sqrt{1 - 2p_1A_{1_0}^2\int \exp(2\int a(\tau_1)d\tau_1)d\tau_1}} \tag{4.96}$$

From the previous discussion, we can then obtain the steady state condition of the A_1-history. As $\tau_1 \to \infty$, the second term in the denominator is much greater in magnitude than 1, and thus

$$A_1 \to 0 \quad for\ \mu < 0$$

$$A_1 \rightarrow \sqrt{-\frac{\exp(\mu\tau_1)}{2\frac{p_1}{\mu}\exp(\mu\tau_1)}} = \sqrt{-\frac{\mu}{2p_1}} \quad for\ \mu > 0 \tag{4.97}$$

4.6 Comparison with Numerical Results

A generic fighter aircraft model is used to demonstrate the dynamics of the aircraft motion in the vicinity of wing rock and to examine how good the approximations obtained analytically in the previous section. The model involves nonlinearity in many aspects of aircraft aerodynamics, that is nonlinear variation with angle-of-sideslip, rotation rate, and angle-of-attack.

The parameters of the aircraft and its aerodynamic model as used in the simulation are given in Table 4.1. This model is only valid for angle-of-attack in the range 20^o to 40^o, which is the range where transition to wing rock motion occurs.

$I_{xx} = 36610\ kg\,m^2$ $\qquad$ $b = 12\ m$
$I_{yy} = 162700\ kg\,m^2$ $\qquad$ $c = 4.8\ m$
$I_{zz} = 183000\ kg\,m^2$ $\qquad$ $S = 164.6\ m^2$
$I_{xz} = 6780\ kg\,m^2$
$\rho = 1.225\ kg/m^3$
$V = 100\ m/s$

$$\begin{aligned}
C_l = {} & (-0.295\alpha_0 + 0.1975\alpha_0^2)\beta + (-0.22 + 0.63\alpha_0 - \\
& 0.797\alpha_0^2 + 0.975\alpha_0^3)\frac{bp}{2V} + 0.4\beta^2\frac{bp}{2V} - 0.075(\frac{bp}{2V})^3 - \\
& -1.42\beta^2\frac{bp}{2V} - 0.011\dot{\beta} - 0.08\alpha\beta + \\
& 0.236\alpha^2\beta + 0.56\alpha\frac{bp}{2V} + 0.09\alpha^2\frac{bp}{2V} + 1.6\alpha\dot{\beta} - \\
& 6.1\alpha^2\dot{\beta} + 0.5\beta\frac{cq}{2V} + 30\alpha\beta\frac{cq}{2V} \\
C_m = {} & -0.68\alpha - 2\frac{cq}{2V} - 0.75\alpha^2 - 3.75\alpha^3 \\
& +0.7(\frac{cq}{2V})^3 + 0.58\alpha\frac{cq}{2V} + 3.564\alpha^2\frac{cq}{2V} + 0.4\beta\frac{cq}{2V} - \\
& 4.01\beta^2 + 0.26\alpha\beta^2 + 0.1\beta\frac{bp}{2V} + 0.5\alpha\beta\frac{bp}{2V}
\end{aligned}$$

Table 4.1: Generic fighter aircraft parameters for $10^o \leq \alpha_0 \leq 50^o$

For this aircraft, the variation of the wing rock damping parameter μ and the parameter p_1 with the nominal angle-of-attack are given in Figure 4-6.

Simulation of the aircraft response for nominal angle-of-attack of 32^o is shown in Figure 4-7. At this angle-of-attack, μ is positive and wing rock motion is developed,

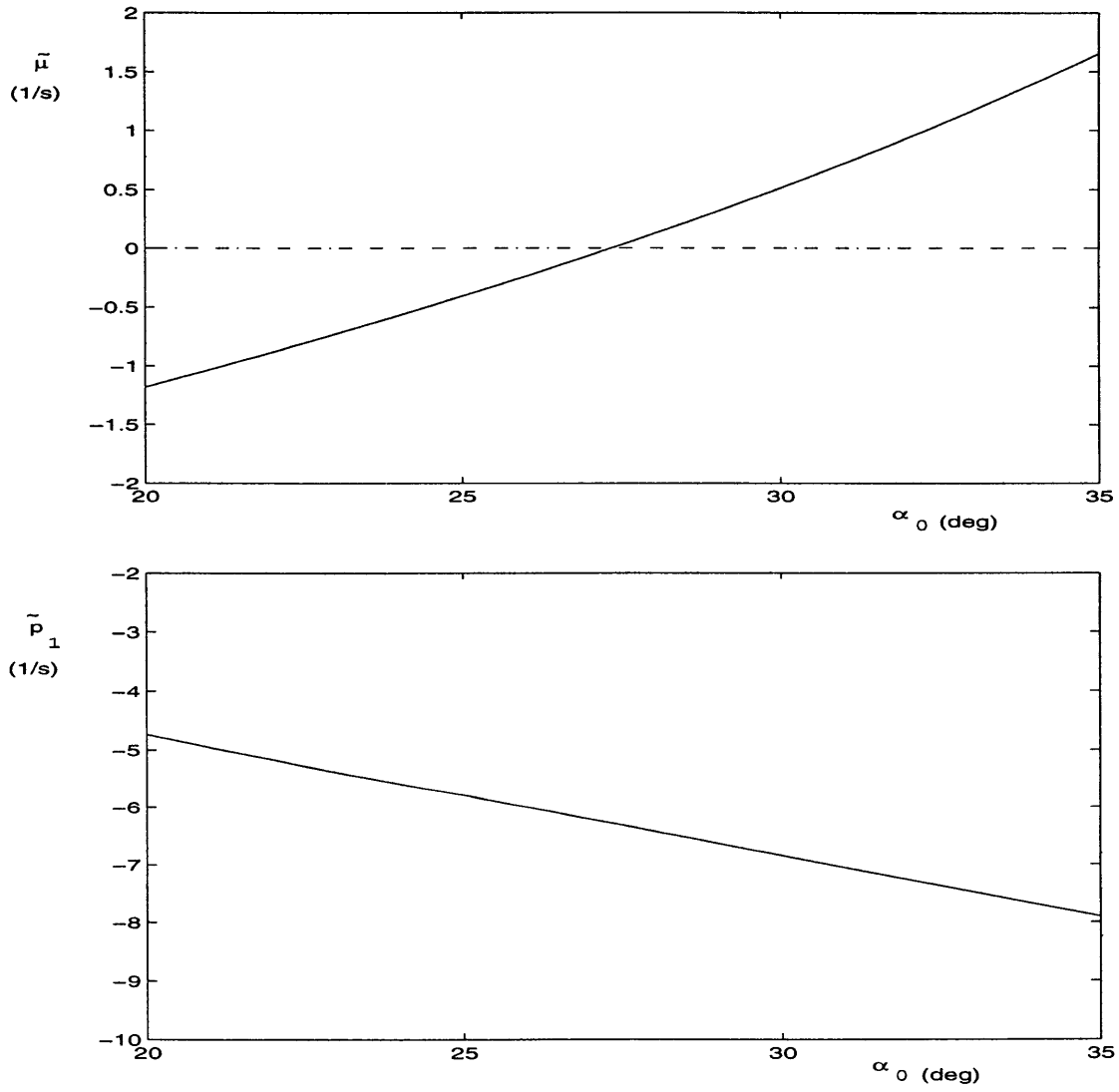

Figure 4-6: Variation of $\tilde{\mu}$ and $\tilde{p}_1$ with α_0

as can be seen from the Figure. Note that in the Figure, the analytical approximation obtained in the previous section is compared to the exact solution as obtained using numerical integration. In this case, the analytical approximation is in excellent agreement with the numerical integration result. The amplitude and phase history are predicted very well by the analytical result. Note also that for pitch motion, the analytical approximation correctly predicts the existence of the new equilibrium and the sustained oscillation with twice the frequency of the roll motion.

A useful tool to gain physical insight on the motion dynamics is the concept of energy exchange. Since no control action is assumed during the motion, the change in aerodynamic energy during a certain time interval is given by

$$\Delta E = \int_{t_1}^{t_2} \left(qSbC_l(t)\dot{\phi}(t) + qScC_m(t)\dot{\theta}(t) \right) dt \tag{4.98}$$

Through a change in integration variable, the above expression can be written as a line integral as follows

$$\Delta E = \int_{C_\phi} qSbC_l(\phi)d\phi + \int_{C_\theta} qScC_m(\theta)d\theta \tag{4.99}$$

where C_ϕ and C_θ are the curves of C_l versus ϕ and C_m versus θ for $t_1 \leq t \leq t_2$, respectively. Such curves are called histograms. In wing rock situation, C_ϕ and C_θ are closed curves over one oscillation cycle. The net energy change over a cycle is given by

$$\Delta E = \oint_{C_\phi} qSbC_l(\phi)d\phi + \oint_{C_\theta} qScC_m(\theta)d\theta \tag{4.100}$$

It is clear that the net aerodynamic energy exchange in a cycle is directly proportional to the areas contained within the histogram loops. For a clockwise loop, $\Delta E > 0$ or, in other words, energy is added to the system (destabilizing). Conversely, for a counter-clockwise loop, $\Delta E < 0$, which means that energy is extracted from the system (stabilizing).

In a sustained free wing rock motion, it is obvious that the system is in energy balance and so no energy is added or extracted from the system. In this situation, we will find that $\Delta E = 0$, which implies that the area within the clockwise loop must be the same as the area within the counter-clockwise loop. How the area is distributed within the clockwise and the counter-clockwise loops in a cycle can help us to gain some insights about the wing rock motion.

The histograms for the aircraft model at $\alpha_0 = 32^o$ are shown in Figure 4-8. In the C_l versus ϕ histogram (rolling moment histogram), a relatively large destabilizing loop

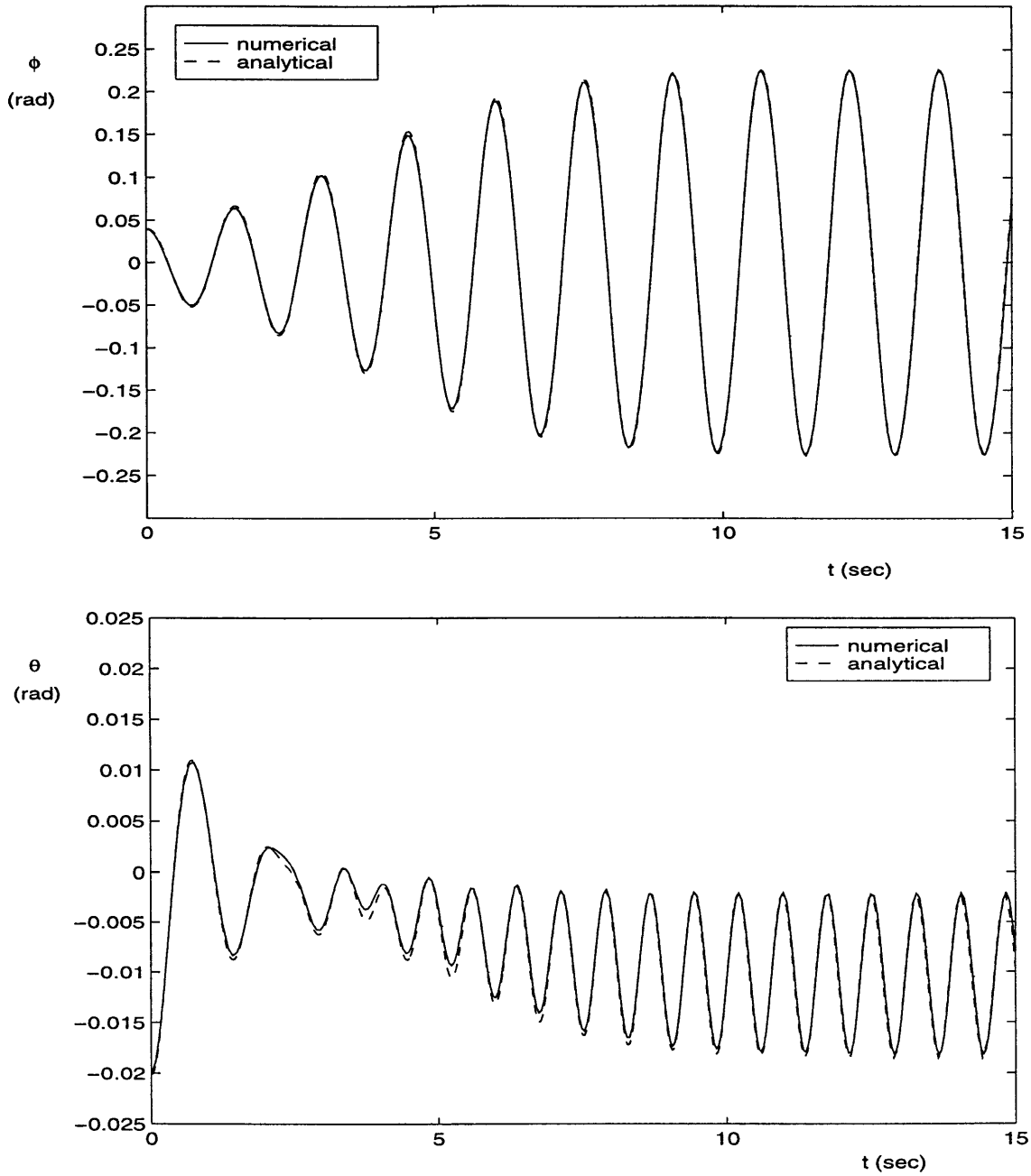

Figure 4-7: Roll and pitch angle response at $\alpha_0 = 31^o$ and initial condition $(\phi_0, \theta_0) = (0.04, -0.02)$ rad

(clockwise,$\Delta E > 0$) is observed around the origin for roll angle magnitudes less than 4^o (0.07 rad). Smaller stabilizing loops (counter-clockwise, $\Delta E < 0$) are observed for roll angle magnitudes greater than 4^o. For the pitching moment histogram C_m versus θ, only small single loop is seen and it is a stabilizing one. The net area within these loops are zero. From the rolling moment histogram, we see that for small roll angles, the rolling moment is destabilizing. From the pitching moment histogram, we can also observe that the pitching moment tends to stabilize the system, however its energy is so small and cannot overcome the destabilizing energy contributed by the roll moment. When the magnitude of the roll angle passes 4^o, the roll moment becomes stabilizing. The magnitude of the roll angle keeps increasing up to a point and then decreasing such that the stabilizing moment has enough energy to balance the destabilizing energy generated by the destabilizing rolling moment. When such energy balance is achieved, wing rock limit cycle is sustained in the aircraft system.

To examine the accuracy of the wing rock onset prediction, simulation of the aircraft responses slightly below and slightly above the onset point is performed. For the aircraft model, the wing rock onset is at $\alpha_0 = 27.34^o$. Numerical and analytical simulation of the system response for $\alpha_0 = 27.2^o$ and $\alpha_0 = 27.5^o$ are given in Figure 4-9. This example shows that our analytical development is capable of predicting the dynamics of the aircraft in the vicinity of wing rock very accurately. The aerodynamic model used in the example is quite complicated, yet the analytical approximation developed can predict the system response excellently.

The analysis performed here subsumes previous work, which only considers the effects of specific type of nonlinearity. For completeness and to gain more insight on how each specific type of nonlinearity affects the resulting wing rock dynamics, we will discuss some types of important nonlinearity individually in the next sections.

4.7 Effects of Specific Types of Aerodynamic Nonlinearity

4.7.1 Effects of Nonlinearity in Roll Damping Parameter With Sideslip and Roll Rate

As has been mentioned in Chapter3, the evidence of nonlinear variation of damping in roll with respect to angle-of-sideslip and roll rate has been reported in literature (see [1, 15]). An example of such nonlinearity is depicted in Figure 3-10 in Chapter

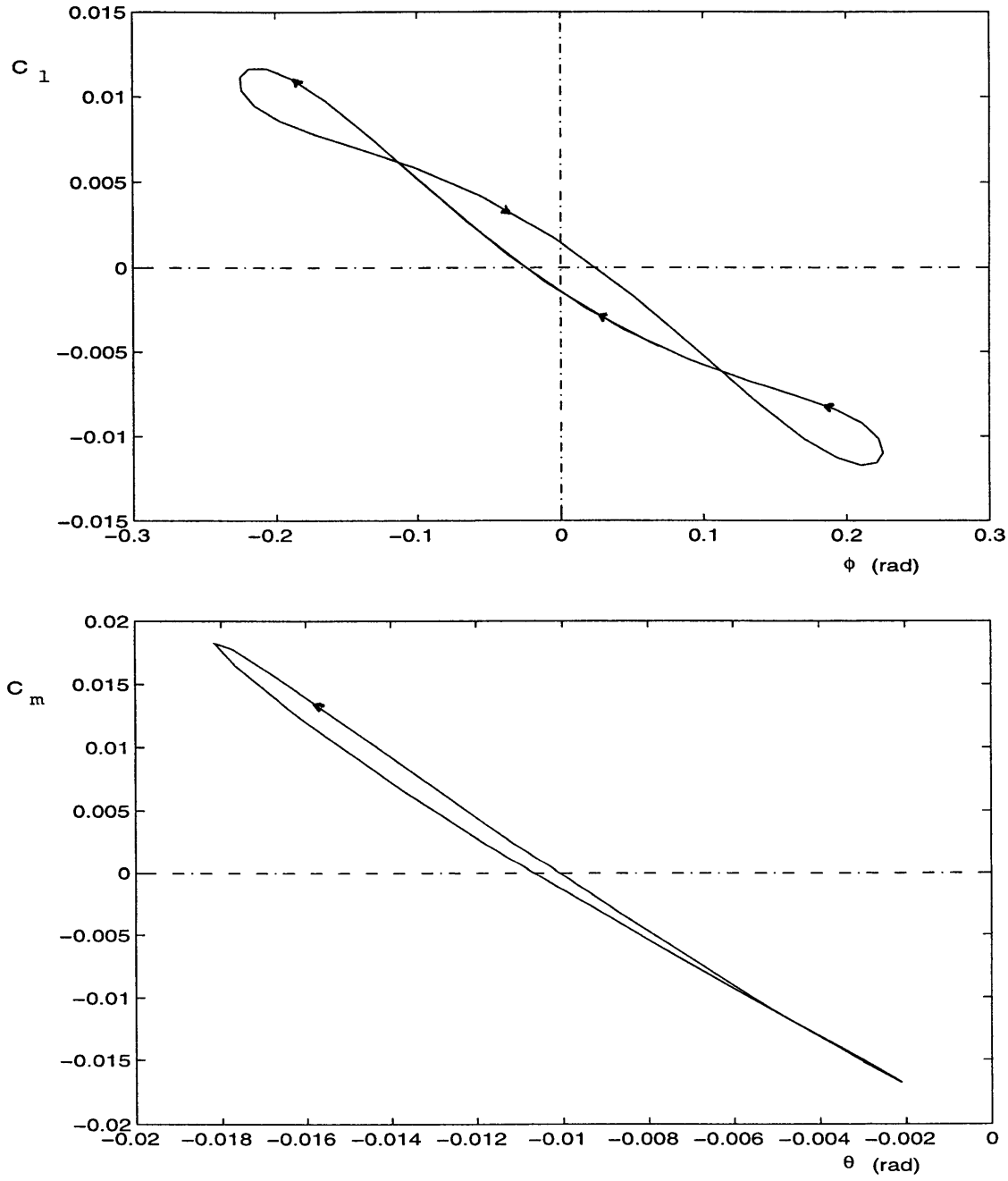

Figure 4-8: C_l vs ϕ and C_m vs θ for one cycle of wing rock at $\alpha_0 = 31^o$

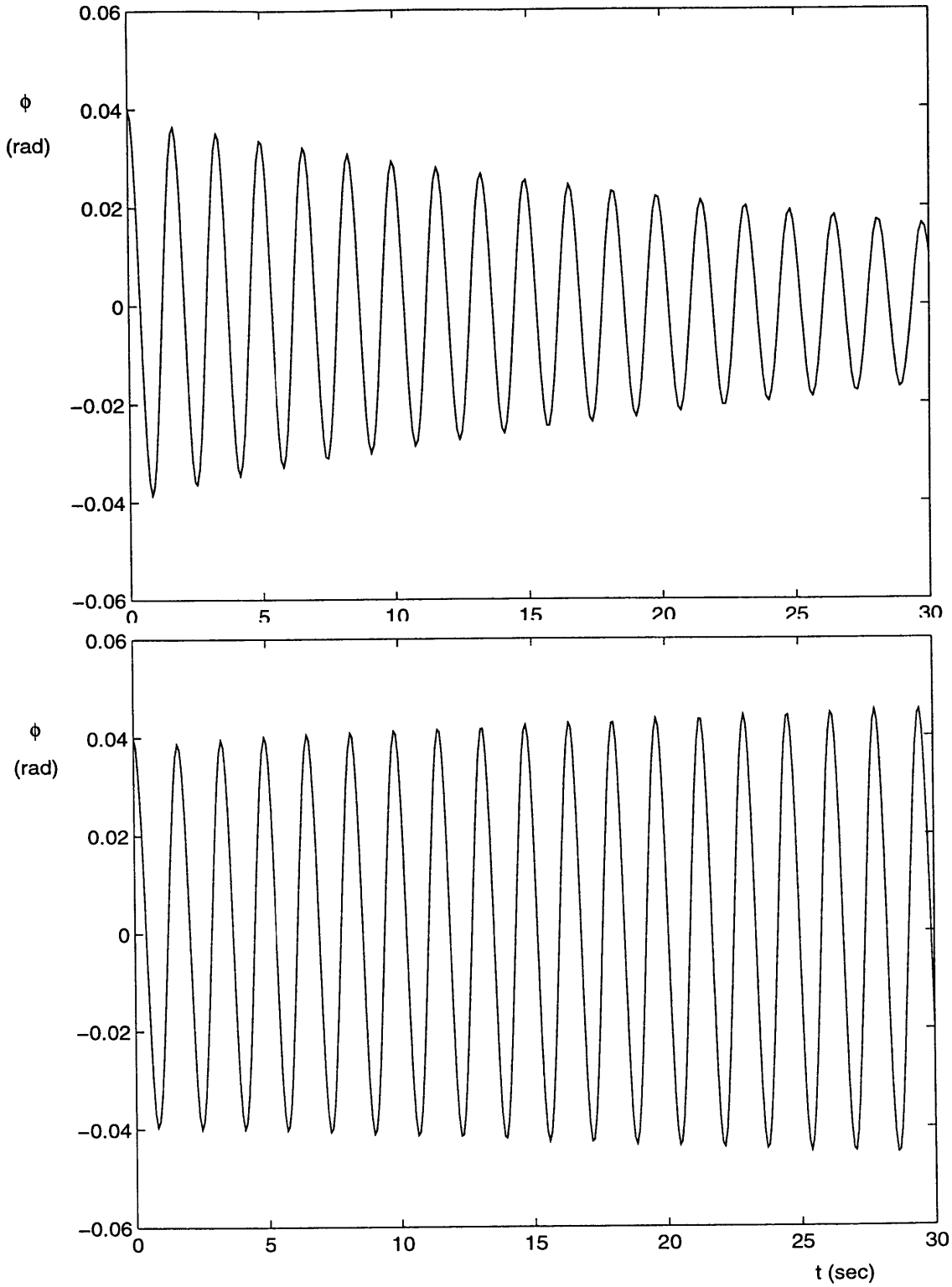

Figure 4-9: Aircraft response for $\alpha_0 = 27.2^o$ and $\alpha_0 = 27.5^o$

3. To examine this specific nonlinearity, a simplified aircraft model which includes only this type nonlinearity is employed. The other aerodynamic characteristics of the aircraft are assumed to be linear. Also, we assume that the nonlinearity due to the inertia cross coupling is negligible. To be more specific, we consider the aircraft with the following aerodynamic moments.

$$\begin{aligned} L &= L_p p + L_{\beta_0}\beta + L_{\dot{\beta}_0}\dot{\beta} \\ M &= M_{q_0} q + M_{\alpha_0}\alpha + M_{\dot{\alpha}_0}\dot{\alpha} \end{aligned} \tag{4.101}$$

The stability derivatives with subscript 0 are constant. They are the stability derivatives as usually used in the linear analysis. The nonlinear L_p model used here is the same as in Chapter 3 (for the reasoning for using this model, see explanation in 3.6.1), that is

$$L_p = L_{p_0} + L_{p_1} p^2 + L_{p_2}\beta^2 \tag{4.102}$$

Inserting this L_p model into Equation (4.101) and comparing the result with Equations (4.18), the following correspondence is observed.

$$\begin{aligned} [\bar{c}_1\ \bar{c}_2\ \bar{c}_3\ \bar{c}_5\ \bar{c}_{10}] &\equiv [L_{\beta_0}\ L_{p_0}\ L_{\dot{\beta}_0}\ L_{p_2}\ L_{p_1}] \\ [\bar{d}_1\ \bar{d}_2\ \bar{d}_3] &\equiv [M_{\alpha_0}\ M_{q_0}\ M_{\dot{\alpha}_0}] \end{aligned} \tag{4.103}$$

Next, by continuing the analysis in the same fashion as was done in Sections 4.4 and 4.5, the equations of motion of the aircraft become

$$\begin{aligned} \ddot{\phi} + \omega^2\phi &= \epsilon(\mu\dot{\phi} + c_2\phi^2\dot{\phi} + c_4\dot{\phi}^3) \\ \ddot{\theta} + \Omega^2\theta &= \epsilon\nu\dot{\theta} \end{aligned} \tag{4.104}$$

Thus, the lateral and longitudinal equations of motion are uncoupled when we only deal with this type of roll damping nonlinearity, and so they can be treated individually. As we have already mentioned, we only deal with $\nu < 0$ in current work, therefore the longitudinal dynamics is stable. The roll equation in this case is the same as in the single degree-of-freedom case, treated in 3.6.1. The analysis in that section is also valid here, hence it will not be repeated

In summary, this type of nonlinearity affects the amplitude of the wing rock motion. The variation of the wing rock amplitude with the variation of L_{p_1} and L_{p_2} can be seen in 3.6.1.

4.7.2 Cubic Variation of Rolling Moment with Sideslip

Nonlinearity in the variation of rolling moment with respect to sideslip angle is found in many fighter aircraft flying at high angles-of-attack. Examples of such variation are given in Figures 3-17 and 3-18 in the preceeding chapter. This variation can be modeled fairly well using odd order polynomial in β. Here, cubic variation of rolling moment with β is used to model this nonlinearity.

To examine specifically the effect of static lateral stability non linearity with sideslip, we consider an aircraft model where only such nonlinearity is present. All other nonlinearity is neglected in the equations of motion. Hence the aerodynamic moments on the aircraft are

$$\begin{aligned} L &= L_{\beta_0}\beta + L_{\beta_1}\beta^3 + L_{p_0}p + L_{\dot{\beta}_0}\dot{\beta} \\ M &= M_{q_0}q + M_{\alpha_0}\alpha + M_{\dot{\alpha}_0}\dot{\alpha} \end{aligned} \tag{4.105}$$

As in the earlier subsection, when we deal with only this type of nonlinearity, the roll and the pitch equations of motion become uncoupled and so we can treat them separately. The pitch motion is the same as in Equation (4.104), which is stable for $\nu < 0$. The roll equation assumes the same form as in Section 3.6.2, which is of the form of damped Duffing's type of equation. The discussion in Section 3.6.2 is also valid for this case, and will not be repeated here. In general, this type of nonlinearity by itself does not generate wing rock. Positive L_{β_1} causes a slight increase in the frequency of motion and negative L_{β_1} causes a slight decrease in frequency.

4.7.3 Effects of Dynamic Cross Coupling Derivatives

The effects of the cross coupling stability derivatives L_q and M_p on the wing rock dynamics are examined in this subsection. These derivatives give rise to nonlinear terms in the aircraft equations of motion. This is understandable since linearly their effects are negligible, which allows us to decouple between the longitudinal and the lateral equation of motion. Also, the cross coupling effects are only present when the attitude of the aircraft is non symmetrical, i.e. $\beta \neq 0$. From basic aerodynamic considerations, the variation of these cross coupling derivatives with the angle-of-sideslip β ideally is antisymmetrical. An example of C_{m_p} variations with respect to β is given in Figure 4-10.

A simple cross-coupling derivative model is utilized in current analysis. The model

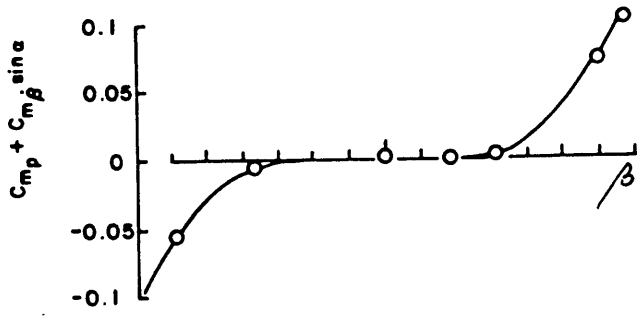

Figure 4-10: C_{m_p} variation due to β [1]

assumes linear variation of the derivatives with respect to β as follows

$$\begin{aligned} L_q &= L_{q_1}\beta \\ M_p &= M_{p_1}\beta \end{aligned} \tag{4.106}$$

Then, if we assume that

$$\begin{aligned} L &= L_{p_0}p + L_{\beta_0}\beta + L_{\dot\beta_0}\dot\beta + L_q q \\ M &= M_{q_0}q + M_{\alpha_0}\alpha + M_{\dot\alpha_0}\dot\alpha + M_p p \end{aligned} \tag{4.107}$$

where, as before, stability derivatives with subscript 0 are constant, we get

$$\begin{aligned} [\bar c_1\ \bar c_2\ \bar c_3\ \bar c_{12}] &\equiv [L_{\beta_0}\ L_{p_0}\ L_{\dot\beta_0}\ L_{q_1}] \\ [\bar d_1\ \bar d_2\ \bar d_3\ \bar d_{39}] &\equiv [M_{\alpha_0}\ M_{q_0}\ M_{\dot\alpha_0}\ M_{p_1}] \end{aligned} \tag{4.108}$$

If we only consider this type of nonlinearity and neglect the others, including the ones due to the inertia cross coupling, then $p_1 = 0$, and so no wing rock can occur in the system. If we include the nonlinearity due to the inertia cross coupling and consider only the nonlinearity due to the dynamic cross coupling derivatives in the aerodynamics, then the coefficients μ and p_1 of the amplitude equation (4.43) become

$$\begin{aligned} \tilde\mu \equiv \epsilon\mu &= L_{p_0} + L_{\dot\beta_0}\sin\alpha_0 \\ \tilde p_1 \equiv p_1 &= \frac{1}{8}\Big[n_1 n_2(L_{p_0} + L_{\dot\beta_0}\sin\alpha_0) - n_1 M_{p_1}\sin\alpha_0 + \\ &\quad \frac{n_1(M_{\alpha_0} - L_{\beta_0}\sin\alpha_0)(M_{p_1}\sin\alpha_0 - n_2(L_{p_0} + L_{\dot\beta_0}\sin\alpha_0))}{4L_{\beta_0}\sin\alpha_0 - M_{\alpha_0}} + \end{aligned}$$

$$4\,\frac{n_2 L_{\beta_0}\sin\alpha(L_{q_1}\sin\alpha_0 - n_1(M_{q_0}+M_{\dot{\alpha}_0}))}{4L_{\beta_0}\sin\alpha_0 - M_{\alpha_0}}\Bigg] \tag{4.109}$$

Since wing rock amplitude is defined by $\sqrt{-\frac{\mu}{2p_1}}$, clearly in this case, L_{q_1} and M_{p_1} influence the resulting wing rock amplitude.

Since μ is not influenced by the cross coupling derivatives, then wing rock can only occur if the values of such derivatives make $p_1 < 0$ when $\mu > 0$. This condition is satisfied when

$$L_{q_1} > \frac{n_1[n_2(L_{p_0}+L_{\dot{\beta}_0}\sin\alpha_0)+2n_2(M_{q_0}+M_{\alpha_0})-M_{p_1}\sin\alpha_0]}{2n_2\sin\alpha_0} \tag{4.110}$$

If the above condition is satisfied only marginally ($p_1 < 0$ but $|p_1|$ very small), then although theoretically wing rock can occur in the system, its amplitude is too large to be realistic. Besides, large amplitude motions destroy the ordering used in the analysis and thus the approximation obtained is not accurate for predicting the behavior of the motion.

Now suppose that wing rock occurs in the system. The derivative of the wing rock amplitude with respect to L_{q_1} and M_{p_1} are

$$\begin{aligned}
\frac{dA_1}{dL_{q_1}} &= \frac{dA_1}{dp_1}\frac{dp_1}{dL_{p_1}} = \frac{1}{2}\left(-\frac{\mu}{2p_1}\right)^{\frac{3}{2}}\left(\frac{\mu}{2p_1^2}\right)\left(-\frac{1}{2}\frac{n_2 L_{\beta_0}\sin^2\alpha_0}{4L_{\beta_0}\sin\alpha_0 - M_{\alpha_0}}\right)\\
\frac{dA_1}{dM_{p_1}} &= \frac{dA_1}{dp_1}\frac{dp_1}{dL_{p_2}} = \frac{1}{2}\left(-\frac{\mu}{2p_1}\right)^{\frac{3}{2}}\left(\frac{\mu}{2p_1^2}\right)\left(-\frac{2n_1 L_{\beta_0}\sin^2\alpha_0}{4L_{\beta_0}\sin\alpha_0 - M_{\alpha_0}}\right)
\end{aligned} \tag{4.111}$$

For an aircraft with $4L_{\beta_0}\sin\alpha_0 - M_{\alpha_0} < 0$ ($4\omega^2 > \Omega^2$), both $\frac{dA_1}{dL_{q_1}}$ and $\frac{dA_1}{dM_{p_1}}$ are negative. This implies that increasing the parameters L_{q_1} and M_{p_1} decreases the resulting roll angle limit cycle amplitude. It indicates that increasing L_{q_1} and M_{p_1} increases the amount of energy transferred from the lateral mode to the longitudinal mode. Note that in this model, if $I_{xz} = 0$ ($n_1 = n_2 = 0$), no energy transfer between the longitudinal and lateral modes possible. Figure 4-11 shows the variation of the amplitude of the wing rock motion with respect to L_{q_1} and M_{p_1} for the aircraft model in Table 4.1 with only cross coupling aerodynamic nonlinearity included.

We note that in many cases, the coupling between roll and pitch modes is weak. Hence, it is very rarely that wing rock occurs due to only this type of nonlinearity. This theoretical analysis demonstrates that in the case where strong coupling does occur in the aircraft system, such coupling is a potential cause of wing rock. However,

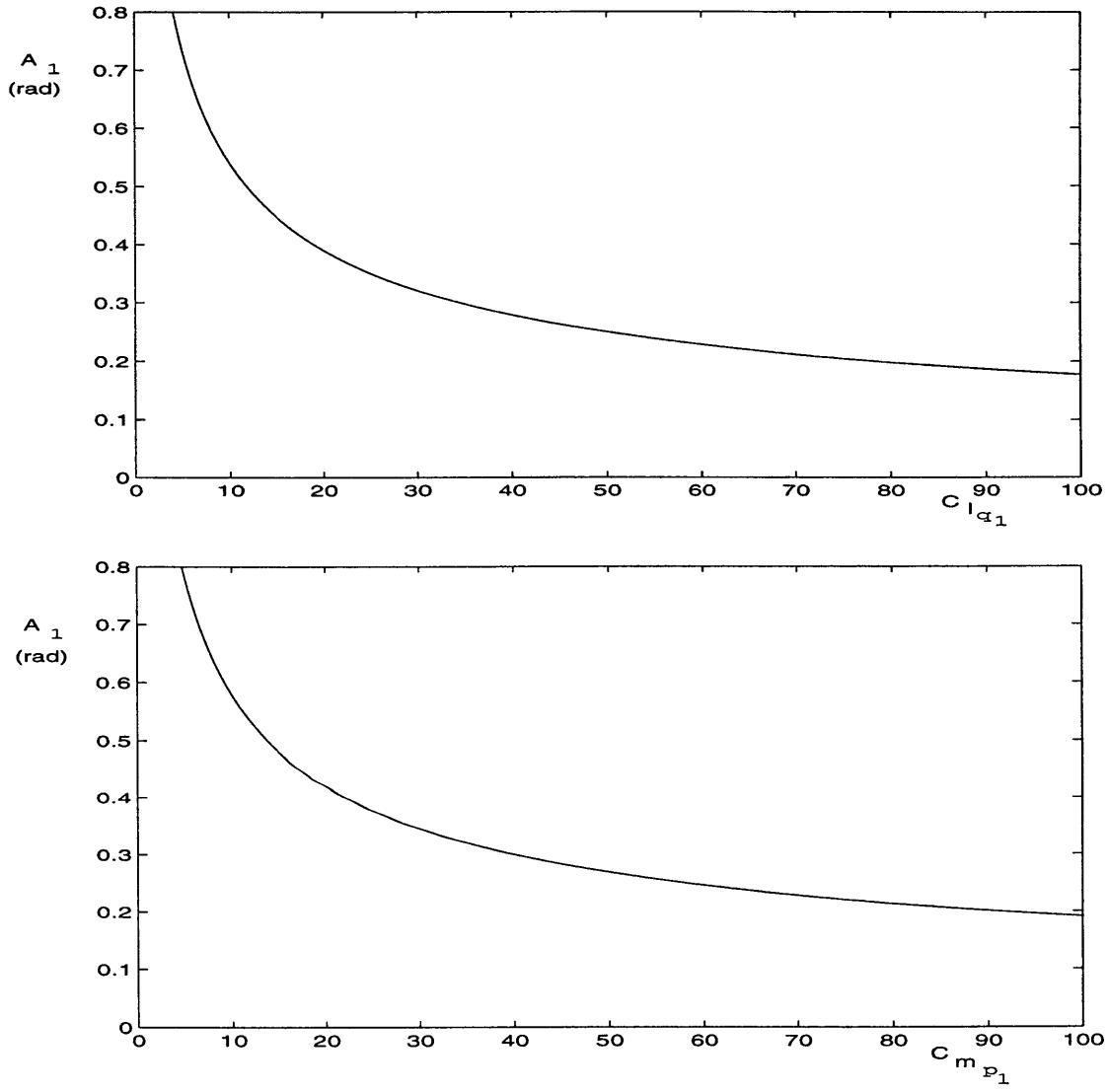

Figure 4-11: Variation of wing rock amplitude with L_{q_1} and M_{p_1}

one should be careful when dealing with a very strong coupling. As we have learned, the amplitude of steady state pitch oscillation is influenced by the cross coupling parameters. The increase in the cross coupling parameters (stronger coupling) will cause a larger pitch amplitude. Too strong cross coupling parameters can invalidate the analysis given in Section 4.5, since it is based on the assumption that the pitch motion is much smaller in magnitude than the roll motion. Therefore, further analysis might be necessary to uncover the dynamics of the system when there is such strong coupling.

4.8 Chapter Summary

Wing rock dynamics on an aircraft having two degrees-of-freedom in roll and pitch have been considered in this chapter. The analysis technique utilizing the MTS method, Center Manifold Reduction principle, and bifurcation theory describes the system dynamics successfully leading to the results in parametric form. In general, the onset of wing rock is not affected by the additional degree-of-freedom in pitch. However, the amplitude of the resulting wing rock motion in the two degrees-of-freedom case is generally different from the single degree-of-freedom one (for the same aircraft starting from the same nominal flight condition). The longitudinal and coupling parameters are shown to have some effects on the wing rock properties. An interesting aspect of the dynamics that is not captured by the single degree-of-freedom model is the steady state pitch oscillation around a *new* equilibrium with *twice* the frequency of the wing rock motion. All of these suggest that the simplified single degree-of-freedom model has to be used with caution, as it may not capture all the important aspects of the system dynamics. As we have seen in the examples treated in this chapter, the longitudinal dynamics may look insignificant compared to the lateral dynamics, however it has a quite significant effect on the wing rock properties in general.

Chapter 5

Three Degrees-of-Freedom Wing Rock

5.1 Introduction

This chapter considers wing rock dynamics on aircraft having three rotational degrees-of-freedom in roll, pitch, and yaw. As we shall see, the additional degree-of-freedom adds significant complexity and makes the analysis more lengthy than in the two degree-of-freedom case treated in the previous chapter. However, there are some physical phenomena captured by the model that are not found in the lower degrees-of-freedom models. The analysis technique combining the MTS method, Center Manifold reduction, and bifurcation theory is solves the problem systematically.

5.2 Equations of Motion

The derivation of the equations of motion is based on the assumption that the aircraft is rigid and has conventional configuration. Also we only consider small deviations of the aircraft attitudes from their nominal values. During the motion of interest, the trajectory of the center of mass of the aircraft is straight and horizontal and it is not affected by the aircraft's small attitude motion.

The same axis systems as the ones employed in the previous chapters are also used here. They are the body-fixed axis system ($X_bY_bZ_b$), which is fixed to the aircraft body, and the stability axis system ($X_oY_oZ_o$), which is used to describe the nominal

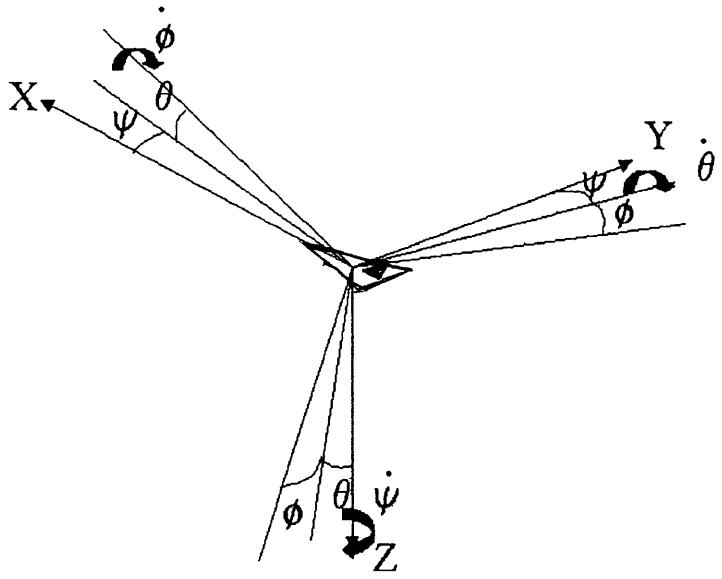

Figure 5-1: Transform angles and rotations between the stability and body-fixed axis systems

orientation of the aircraft. The description on the orientations of the these axis systems can be found in Chapter 4.

The aircraft can be brought from its nominal position to its perturbed position, described by the orientation of its body axes, by using three consecutive rotations in yaw, pitch, and then roll. This is illustrated in Figure 5-1. The angles describing these consecutive rotations are the Euler angles ψ, θ, and ϕ, which are called yaw angle, pitch angle, and roll angle, respectively. The angular rate of the aircraft in the body-fixed axes can be expressed in terms of the rate of change of the Euler angles by noting that

$$\begin{aligned} \boldsymbol{\omega} &= p\,\mathbf{i}_{x_b} + q\,\mathbf{i}_{y_b} + r\,\mathbf{i}_{z_b} \\ &= \dot{\psi}\mathbf{i}_{z_o} + \dot{\theta}\,\mathbf{i}_{y_1} + \dot{\phi}\,\mathbf{i}_{x_b} \end{aligned} \tag{5.1}$$

where as before the notation $\mathbf{i}$ denote the unity vector along the axis described in its subscript and per usual convention, p, q, and r are the roll rate, pitch rate, and yaw rate of the aircraft, respectively. The $X_1Y_1Z_1$ and $X_2Y_2Z_2$ are the intermediate axis systems for the rotations from the stability axes to the body-fixed axes. $X_1Y_1Z_1$ system is resulted by rotating the stability axis around its Z_o-axis through an angle ψ. Therefore, $Z_1 \equiv Z_o$. Similarly, $X_2Y_2Z_2$ system is resulted by rotating the $X_1Y_1Z_1$ axis system around its Y_1-axis through an angle θ. Hence, $Y_2 \equiv Y_1$ and $X_2 \equiv X_b$.

Then, by utilizing the kinematic relations

$$\begin{aligned}
\mathbf{i}_{y_1} &= \cos\phi\,\mathbf{i}_{y_b} - \sin\phi\,\mathbf{i}_{z_b} \\
\mathbf{i}_{z_2} &= \sin\phi\,\mathbf{i}_{y_b} + \cos\phi\,\mathbf{i}_{z_b} \\
\mathbf{i}_{z_o} &= -\sin\theta\,\mathbf{i}_{x_b} + \cos\theta\,\mathbf{i}_{z_2} \\
&= -\sin\theta\,\mathbf{i}_{x_b} + \cos\theta\sin\phi : \mathbf{i}_{y_b} + \cos\theta\cos\phi\mathbf{i}_{z_b}
\end{aligned} \tag{5.2}$$

we get

$$\begin{aligned}
p &= \dot{\phi} - \dot{\psi}\sin\theta \\
q &= \dot{\theta}\cos\phi + \dot{\psi}\cos\theta\sin\phi \\
r &= -\dot{\theta}\sin\phi + \dot{\psi}\cos\theta\cos\phi
\end{aligned} \tag{5.3}$$

If we only care about small angle and angular rate perturbations around the equilibrium position, the following approximations can be used.

$$\begin{aligned}
p &\approx \dot{\phi} - \theta\dot{\psi} \\
q &\approx \dot{\theta} + \phi\dot{\psi} \\
r &\approx \dot{\psi} - \phi\dot{\theta}
\end{aligned} \tag{5.4}$$

As before, since only aircraft with conventional configuration is considered in this analysis, we have $I_{xy} = I_{yz} = 0$. The rotational kinetic energy of the aircraft is then

$$\begin{aligned}
T &= \frac{1}{2}I_{xx}p^2 + \frac{1}{2}I_{yy}q^2 + \frac{1}{2}I_{zz}r^2 - I_{xz}pr \\
&= \frac{1}{2}I_{xx}\dot{\phi}^2 + \frac{1}{2}I_{yy}\dot{\theta}^2 + \frac{1}{2}I_{zz}\dot{\psi}^2 - I_{xz}\dot{\phi}\dot{\psi} - I_{xx}\dot{\phi}\theta\dot{\psi} + I_{yy}\phi\dot{\theta}\dot{\psi} - I_{zz}\phi\dot{\theta}\dot{\psi} + \\
&\quad I_{xz}\phi\dot{\phi}\dot{\theta} + I_{xz}\theta\dot{\psi}^2 + \frac{1}{2}I_{xx}\theta^2\dot{\psi}^2 + \frac{1}{2}I_{yy}\phi^2\dot{\psi}^2 + \frac{1}{2}I_{zz}\phi^2\dot{\theta}^2 - I_{xz}\phi\theta\dot{\theta}\dot{\psi}
\end{aligned} \tag{5.5}$$

where I_{xx}, I_{yy}, and I_{zz} are the moment of inertia of the aircraft about X_b, Y_b and Z_b, respectively. By inserting this kinetic energy expression into the Lagrange's equation

$$\frac{d}{dt}\left(\frac{\partial T}{\partial\dot{\gamma}_i}\right) - \frac{\partial T}{\partial\gamma_i} = Q_i \;\;;\;\; i = 1,2,3 \tag{5.6}$$

with $\gamma_1 = \phi$, $\gamma_2 = \theta$, and $\gamma_3 = \psi$, we get

$$\begin{aligned}
I_{xx}\ddot{\phi} \;+\; & I_{xz}\phi\ddot{\theta} - (I_{xz} + I_{xx}\theta)\ddot{\psi} - (I_{xx} + I_{yy} - I_{zz})\dot{\theta}\dot{\psi} - I_{yy}\phi\dot{\psi}^2 - \\
& I_{zz}\phi\dot{\theta}^2 + I_{xz}\theta\dot{\theta}\dot{\psi} = Q_1
\end{aligned}$$

$$
\begin{aligned}
(I_{yy} \;+\; & I_{zz}\phi^2)\ddot{\theta} + [(I_{yy} - I_{zz})\phi - I_{xz}\phi\theta]\,\ddot{\psi} + I_{xz}\phi\ddot{\phi} + (I_{xx} + I_{yy}I_{zz})\dot{\phi}\dot{\psi} + \\
& I_{xz}(\dot{\phi}^2 - \dot{\psi}^2) - I_{xx}\theta\dot{\psi}^2 + 2I_{zz}\phi\dot{\phi}\dot{\theta} - I_{xz}\dot{\phi}\theta\dot{\psi} = Q_2 \\
(I_{zz} \;+\; & 2I_{xz}\theta + I_{xx}\theta^2 + I_{yy}\phi^2)\ddot{\psi} - (I_{xz} + I_{xx}\theta)\ddot{\phi} + [(I_{yy} - I_{zz})\phi - I_{xz}\phi\theta]\,\ddot{\theta} - \\
& (I_{xx} - I_{yy} + I_{zz})\phi\dot{\theta} + 2I_{xz}\dot{\theta}\dot{\psi} - I_{xz}\phi\dot{\theta}^2 - I_{xz}\dot{\phi}\theta\dot{\theta} + \\
& 2I_{yy}\phi\dot{\phi}\dot{\psi} + 2I_{xx}\theta\dot{\theta}\dot{\psi} = Q_3
\end{aligned} \tag{5.7}
$$

where Q_1, Q_2, and Q_3 are the generalized forces. To simplify the notation, the following inertia ratios are defined.

$$
\begin{aligned}
n_1 &\equiv \frac{I_{xz}}{I_{xx}} \\
n_2 &\equiv \frac{I_{xz}}{I_{yy}} \\
n_3 &\equiv \frac{I_{xz}}{I_{zz}}
\end{aligned} \tag{5.8}
$$

By utilizing these definitions, Equations (5.7) become

$$
\begin{aligned}
\ddot{\phi} + n_1\phi\ddot{\theta} \;-\; & (n_1 + \theta)\ddot{\psi} - (1 + \frac{n_1}{n_2} - \frac{n_1}{n_3})\dot{\theta}\dot{\psi} - \frac{n_1}{n_2}\phi\dot{\psi}^2 - \frac{n_1}{n_3}\phi\dot{\theta}^2 + \\
& n_1\theta\dot{\theta}\dot{\psi} = \bar{Q}_1 \\
(1 + \frac{n_2}{n_3}\phi^2)\ddot{\theta} \;+\; & [(1 - \frac{n_2}{n_3})\phi - n_2\phi\theta]\ddot{\psi} + n_2\phi\ddot{\phi} + (\frac{n_2}{n_1} + 1 - \frac{n_2}{n_3})\dot{\phi}\dot{\psi} + \\
& n_2(\dot{\phi}^2 - \dot{\psi}^2) - \frac{n_2}{n_1}\theta\dot{\psi}^2 + 2\frac{n_2}{n_3}\phi\dot{\phi}\dot{\theta} - n_2\dot{\phi}\theta\dot{\psi} = \bar{Q}_2 \\
(1 + 2n_3\theta \;+\; & \frac{n_3}{n_1}\theta^2 + \frac{n_3}{n_2}\phi^2)\ddot{\psi} - (n_3 + \frac{n_3}{n_1}\theta)\ddot{\phi} + [(\frac{n_3}{n_2} - 1)\phi - n_3\phi\theta]\ddot{\theta} - \\
& (\frac{n_3}{n_1} - \frac{n_3}{n_2} + 1)\dot{\phi}\dot{\theta} + 2n_3\dot{\theta}\dot{\psi} - n_3\phi\dot{\theta}^2 - n_3\dot{\phi}\theta\dot{\theta} + \\
& 2\frac{n_3}{n_2}\phi\dot{\phi}\dot{\psi} + 2\frac{n_3}{n_1}\theta\dot{\theta}\,\dot{\psi} = \bar{Q}_3
\end{aligned} \tag{5.9}
$$

where $\bar{Q}_1 \equiv \dfrac{Q_1}{I_{xx}}$, $\bar{Q}_2 \equiv \dfrac{Q_2}{I_{yy}}$, and $\bar{Q}_3 \equiv \dfrac{Q_3}{I_{zz}}$. To facilitate our analysis later, we will express the equations of motion explicitly in terms of $\ddot{\phi}$, $\ddot{\theta}$, and $\ddot{\psi}$. Equations (5.9) can be written in matrix form as follows.

$$
\begin{bmatrix}
1 & n_1\phi & -(n_1 + \theta) \\
n_2\phi & 1 + \frac{n_2}{n_3}\phi^2 & (1 - \frac{n_2}{n_3})\phi - n_2\phi\theta \\
-(n_3 + \frac{n_3}{n_1}\theta) & (\frac{n_3}{n_2} - 1)\phi - n_3\phi\theta & (1 + 2n_3\theta + \frac{n_3}{n_1}\theta^2 + \frac{n_3}{n_2}\phi^2)
\end{bmatrix}
\begin{pmatrix} \ddot{\phi} \\ \ddot{\theta} \\ \ddot{\psi} \end{pmatrix}
=
\begin{pmatrix} \hat{f}_1 \\ \hat{f}_2 \\ \hat{f}_3 \end{pmatrix} \tag{5.10}
$$

where

$$\begin{aligned}
\hat{f}_1 &\equiv \bar{Q}_+(1+\frac{n_1}{n_2}+\frac{n_1}{n_3})\dot{\theta}\dot{\psi}+\frac{n_1}{n_2}\phi\dot{\psi}^2+\frac{n_1}{n_3}\phi\dot{\theta}^2-n_1\theta\dot{\theta}\dot{\psi} \\
\hat{f}_2 &\equiv \bar{Q}_2-(\frac{n_2}{n_1}+1-\frac{n_2}{n_3})\dot{\phi}\dot{\psi}-n_2(\dot{\phi}^2-\dot{\psi}^2)+\frac{n_2}{n_1}\theta\dot{\psi}^2-2\frac{n_2}{n_3}\phi\dot{\phi}\dot{\theta}+n_2\dot{\phi}\theta\dot{\psi} \\
\hat{f}_3 &\equiv \bar{Q}_3-(\frac{n_3}{n_1}\frac{n_3}{n_2}+1)\dot{\phi}\dot{\theta}-2n_3\theta\dot{\psi}-n_3\phi\dot{\theta}^2+n_3\dot{\phi}\theta\dot{\theta}-2\frac{n_3}{n_2}\phi\dot{\phi}\dot{\psi}-2\frac{n_3}{n_1}\theta\dot{\theta}\,\dot{\psi}
\end{aligned} \tag{5.11}$$

By using the matrix inverse operation and by neglecting the terms of fourth and higher order, we get

$$\begin{aligned}
\ddot{\phi} &= \frac{1}{D}\Big[(1+2n_3\theta+2\phi^2+\frac{n_3}{n_1}\theta^2)\hat{f}_1-[\frac{n_1n_3}{n_2}\phi+(n_1n_3+\frac{n_3}{n_2}-1)\phi\theta]\hat{f}_2+ \\
&\quad (n_1+\theta+n_1\phi^2)\hat{f}_3\Big] \\
\ddot{\theta} &= \frac{1}{D}\Big[-[n_3\phi+(n_2n_3+\frac{n_3}{n_1}-\frac{n_2}{n_1})\phi\theta]\hat{f}_1+(1-n_1n_3+\frac{n_3}{n_2}\phi^2)\hat{f}_2- \\
&\quad (n_1n_2+1-\frac{n_2}{n_3})\phi\hat{f}_3\Big] \\
\ddot{\psi} &= \frac{1}{D}\Big[(n_3+\theta+n_3\phi^2)\hat{f}_1-(n_1n_3+\frac{n_3}{n_2}-1)\phi\hat{f}_2+[1+(\frac{n_2}{n_3}-n_1n_2)\phi^2]\hat{f}_3\Big]
\end{aligned} \tag{5.12}$$

where D is the determinant of the matrix on the left hand side, given by

$$\begin{aligned}
D &= 1-n_1n_3+2(1-n_1n_3)\phi^2+(1-n_1n_3)\phi^4 \\
&= (1-n_1n_3)(1+\phi^2)^2
\end{aligned} \tag{5.13}$$

Since we are only interested in small motion around the nominal position, then we can use the following approximation.

$$\begin{aligned}
\frac{1}{D} &= \frac{1}{(1-n_1n_3)(1+\phi^2)^2} \\
&\approx \frac{1}{1-n_1n_3}(1-2\phi^2)
\end{aligned} \tag{5.14}$$

The Q_i's in the equations are assumed to come from the aerodynamics only, which will be derived next.

5.3 Aerodynamic Moments

The aerodynamic moments on the aircraft are derived in a similar way as in Chapter 4. The purpose of the derivation is to obtain the general forms of the appropriate aerodynamic nonlinearity to be included in the aircraft model. Therefore, it is by no means exhaustive. The aerodynamic flow around the aircraft is assumed incompressible and quasi-steady. For simplicity, modified strip theory, which takes into account the three dimensional effects, is utilized in the derivation.

It is assumed that only the aircraft's wings and horizontal tail are effective in generating the aerodynamic forces. As before, the incremental lift and drag produced at each streamwise segment of the wing or tail are

$$\begin{aligned} dL(y) &= \bar{q}c(y)c_L(y) \\ dD(y) &= \bar{q}c(y)c_D(y) \end{aligned} \tag{5.15}$$

where $\bar{q} = \frac{1}{2}\rho V^2$ is the dynamic pressure and $c(y)$ is the airfoil chord at location y along the Y_b axis. $c_L(y)$ and $c_D(y)$ are the local lift and drag coefficients, which are assumed to be cubic functions of local effective angle-of-attack, $\alpha_e(y)$, as follows.

$$\begin{aligned} c_L &= c_{L_0} + c_{L_1}\alpha_e + c_{L_2}\alpha_e^2 + c_{L_3}\alpha_e^3 \\ c_D &= c_{D_0} + c_{D_1}\alpha_e + c_{D_2}\alpha_e^2 + c_{D_3}\alpha_e^3 \end{aligned} \tag{5.16}$$

where in the above equations, the dependence of the coefficients and α on the spanwise location, y, has been dropped. In the two degrees-of-freedom case, the effective angle-of-attack distribution is influenced by the following factors :

- nominal angle-of-attack (α_0)
- roll rate (p)
- angle-of-sideslip (β)
- deviation from the nominal angle-of-attack (α)
- pitch rate (q)
- time dependent effects ($\dot{\alpha}$ and $\dot{\beta}$)

In addition to the above factors, the influence of yaw rate (r) is also important for the three degrees-of-freedom case. Positive yaw rate causes the left wing to see an

increase in the upcoming airspeed and the right wing to see a decrease in the upcoming airspeed. The change in airspeed seen by each wing segment varies depending upon the spanwise location of the segment. This contributes to the changes in angle-of-attack across the wing span. For simplicity, we assume that the angle-of-attack distribution due to yaw rate to be perfectly antisymmetric, that is

$$\alpha_8(y) = f_8(y)r \tag{5.17}$$

where $f_8(y)$ is an odd function of y.

With this additional factor, the total effective angle-of-attack experienced by each streamwise segment of the wing is given by

$$\alpha_e(y) = \alpha_1(y) + f_2(y)p + f_3(y)\beta + f_4(y)\alpha + f_5(y)q + f_6(y)\dot{\alpha} + f_7(y)\dot{\beta} + f_8(y)r \tag{5.18}$$

The substitution of Equation (5.18) into Equation (5.16) and then the substitution of the resulting equation into Eq. 5.15 results in some lengthy equations expressing the lift and drag forces in terms of the variables p, β, $\dot{\beta}$, α, q, $\dot{\alpha}$, and r. The work done by these aerodynamic forces for the displacements $\delta\phi$, $\delta\theta$, and $\delta\psi$ can then be approximated by

$$\begin{aligned}\delta W &= -\int_{a/c}(dL\cos\alpha_0 + dD\sin\alpha_0)y\delta\phi - \int_{a/c}(dL\cos\alpha_0 + dD\sin\alpha_0)l\ \delta\theta + \\ &\quad \int_{a/c}(dL\sin\alpha_0 - dD\cos\alpha_0)y\ \delta\psi\end{aligned} \tag{5.19}$$

This integration process is described in Appendix C. In general, the integrands can be grouped into the even and odd ones. The odd integrands are integrated to zero and so only the even integrands contribute to the result. By using $Q_i = \dfrac{\delta W_i}{\delta\gamma_i}$, the aerodynamic moments can be expressed as

$$\begin{aligned}\bar{Q}_1 &= \bar{c}_1\beta + \bar{c}_2p + \bar{c}_3\dot{\beta} + \bar{c}_4r + \bar{c}_5\beta^3 + \bar{c}_6\beta^2p + \bar{c}_7\beta^2r + \bar{c}_8\beta^2\dot{\beta} + \bar{c}_9\beta p^2 + \\ &\quad \bar{c}_10\beta r^2 + \bar{c}_{11}\beta\dot{\beta}^2 + \bar{c}_{12}p^3 + \bar{c}_{13}\dot{\beta}^3 + \bar{c}_{14}r^3 + \bar{c}_{15}p^2r + \bar{c}_{16}pr^2 + \bar{c}_{17}\dot{\beta}^2r + \\ &\quad \bar{c}_{18}\dot{\beta}r^2 + \bar{c}_{19}p^2\dot{\beta} + \bar{c}_{20}p\dot{\beta}^2 + \bar{c}_{21}\beta\alpha + \bar{c}_{22}\beta q + \bar{c}_{23}p\alpha + \bar{c}_{24}pq + \\ &\quad \bar{c}_{25}\dot{\beta}\alpha + \bar{c}_{26}\dot{\beta}q + \bar{c}_{27}\alpha r + \bar{c}_{28}qr + \bar{c}_{29}\beta\alpha^2 + \bar{c}_{30}\beta q^2 + \bar{c}_{31}p\alpha^2 + \\ &\quad \bar{c}_{32}pq^2 + \bar{c}_{33}\dot{\beta}\alpha^2 + \bar{c}_{34}\dot{\beta}q^2 + \bar{c}_{35}\alpha^2r + \bar{c}_{36}q^2r + \bar{c}_{37}\beta pr + \bar{c}_{38}\beta\dot{\beta}r + \\ &\quad \bar{c}_{39}\beta\dot{\beta}p + \bar{c}_{40}\dot{\beta}pr + \bar{c}_{41}\beta\alpha q + \bar{c}_{42}p\alpha q + \bar{c}_{43}\dot{\beta}\alpha q + \bar{c}_{44}\alpha qr \\ \bar{Q}_2 &= \bar{d}_1\alpha + \bar{d}_2q + \bar{d}_3\dot{\alpha} + \bar{d}_4\alpha^2 + \bar{d}_5\alpha q + \bar{d}_6\alpha\dot{\alpha} + \bar{d}_7q^2 + \bar{d}_8q\dot{\alpha} + \bar{d}_9\dot{\alpha}^2 + \\ &\quad \bar{d}_{10}\alpha^3 + \bar{d}_{11}\alpha^2q + \bar{d}_{12}\alpha^2\dot{\alpha} + \bar{d}_{13}q^3 + \bar{d}_{14}q^2\alpha + \bar{d}_{15}q^2\dot{\alpha} + \bar{d}_{16}\alpha\dot{\alpha}^2 +\end{aligned}$$

$$
\begin{aligned}
&\bar{d}_{17}q\dot{\alpha}^2 + \bar{d}_{18}\dot{\alpha}^3 + \bar{d}_{19}\alpha q\dot{\alpha} + \bar{d}_{20}\alpha\beta^2 + \bar{d}_{21}\theta p^2 + \bar{d}_{22}\alpha\dot{\beta}^2 + \bar{d}_{23}\alpha r^2 + \\
&\bar{d}_{24}q\beta^2 + \bar{d}_{25}qp^2 + \bar{d}_{26}q\dot{\beta}^2 + \bar{d}_{27}qr^2 + \bar{d}_{28}\dot{\alpha}p^2 + \bar{d}_{29}\alpha\beta p + \bar{d}_{30}\alpha\beta\dot{\beta} + \\
&\bar{d}_{31}\alpha\beta r + \bar{d}_{32}\alpha p\dot{\beta} + \bar{d}_{33}\alpha\dot{\beta}r + \bar{d}_{34}\alpha pr + \bar{d}_{35}q\beta p + \bar{d}_{36}q\beta\dot{\beta} + \bar{d}_{37}qp\dot{\beta} + \\
&\bar{d}_{38}q\beta r + \bar{d}_{39}q\dot{\beta}r + \bar{d}_{40}qpr + \bar{d}_{41}\beta^2 + \bar{d}_{42}\beta p + \bar{d}_{43}\beta\dot{\beta} + \bar{d}_{44}\beta r + \\
&\bar{d}_{45}p^2 + \bar{d}_{46}p\dot{\beta} + \bar{d}_{47}pr + \bar{d}_{48}\dot{\beta}^2 + \bar{d}_{49}\dot{\beta}r + \bar{d}_{50}r^2
\end{aligned}
$$

$$
\begin{aligned}
\bar{Q}_3 = \; & \bar{e}_1\beta + \bar{e}_2p + \bar{e}_3\dot{\beta} + \bar{e}_4r + \bar{e}_5\beta^3 + \bar{e}_6\beta^2p + \bar{e}_7\beta^2r + \bar{e}_8\beta^2\dot{\beta} + \bar{e}_9\beta p^2 + \\
& \bar{e}_10\beta r^2 + \bar{e}_{11}\beta\dot{\beta}^2 + \bar{e}_{12}p^3 + \bar{e}_{13}\dot{\beta}^3 + \bar{e}_{14}r^3 + \bar{e}_{15}p^2r + \bar{e}_{16}pr^2 + \bar{e}_{17}\dot{\beta}^2r + \\
& \bar{e}_{18}\dot{\beta}r^2 + \bar{e}_{19}p^2\dot{\beta} + \bar{e}_{20}p\dot{\beta}^2 + \bar{e}_{21}\beta\alpha + \bar{e}_{22}\beta q + \bar{e}_{23}p\alpha + \bar{e}_{24}pq + \\
& \bar{e}_{25}\dot{\beta}\alpha + \bar{e}_{26}\dot{\beta}q + \bar{e}_{27}\alpha r + \bar{e}_{28}qr + \bar{e}_{29}\beta\alpha^2 + \bar{e}_{30}\beta q^2 + \bar{e}_{31}p\alpha^2 + \\
& \bar{e}_{32}pq^2 + \bar{e}_{33}\dot{\beta}\alpha^2 + \bar{e}_{34}\dot{\beta}q^2 + \bar{e}_{35}\alpha^2r + \bar{e}_{36}q^2r + \bar{e}_{37}\beta pr + \bar{e}_{38}\beta\dot{\beta}r + \\
& \bar{e}_{39}\beta\dot{\beta}p + \bar{e}_{40}\dot{\beta}pr + \bar{e}_{41}\beta\alpha q + \bar{e}_{42}p\alpha q + \bar{e}_{43}\dot{\beta}\alpha q + \bar{e}_{44}\alpha qr
\end{aligned} \tag{5.20}
$$

where $\bar{Q}_1 \equiv \dfrac{Q_1}{I_{xx}}$, $\bar{Q}_2 \equiv \dfrac{Q_2}{I_{yy}}$, and $\bar{Q}_3 \equiv \dfrac{Q_3}{I_{zz}}$

The above equations can be expressed in terms of stability derivatives as follows.

$$
\begin{aligned}
\frac{Q_1}{I_{xx}} &= \frac{L}{I_{xx}} = L_pp + L_rr + L_\beta\beta + L_{\dot{\beta}}\dot{\beta} + L_qq + L_{\dot{\alpha}}\dot{\alpha} \\
\frac{Q_2}{I_{yy}} &= \frac{M}{I_{yy}} = M_qq + M_\alpha\alpha + M_\beta\beta + M_pp + M_rr + M_{\dot{\alpha}}\dot{\alpha} \\
\frac{Q_3}{I_{xx}} &= \frac{N}{I_{xx}} = N_pp + N_rr + N_\beta\beta + N_{\dot{\beta}}\dot{\beta} + N_qq + N_{\dot{\alpha}}\dot{\alpha}
\end{aligned} \tag{5.21}
$$

where L, M, and N are the usual notation for the aerodynamic rolling, pitching, and yawing moments, respectively. As before, the stability derivatives L_β, N_β, etc. are not constant, but may be functions of the variables β, p, q, r, α, $\dot{\beta}$, and $\dot{\alpha}$. By substituting the aerodynamic moments in (5.20) into Equations (5.11) and (5.12), the complete system equations of motion are obtained.

5.4 Simplification of the Equations of Motion

The equations of motion obtained in the previous section are still very complicated and involve many variables. Since we only have three equations, we simplify the equations of motion by using kinematic relations and utilizing the motion constraint so that only three motion variables are left.

By the assumption that the aircraft trajectory is not influenced by the attitude

motion, we can use the following approximations :

$$\begin{aligned} \alpha &\approx \theta \\ \dot{\alpha} &\approx q \\ \dot{\beta} &\approx p\sin\alpha_0 - r\cos\alpha_0 + \frac{g}{V}\phi\cos\alpha_0 \end{aligned} \tag{5.22}$$

These approximations together with the kinematic relations (5.3) are then used to express the equations of motion in three variables only, that is β, ϕ, and θ. For this purpose, we need to express the other variables in terms of these three variables.

From the last of the three equation in (5.3), we get

$$\dot{\psi} = r + \phi\dot{\theta} \tag{5.23}$$

Therefore, to second order the first equation in (5.3) becomes

$$p = \dot{\phi} - \theta r \tag{5.24}$$

By substituting Equation (5.24) into β equation in (5.22) and then expressing explicitly for r, we obtain

$$r = -\frac{1}{\cos\alpha_0 + \sin\alpha_0\,\theta}\left[\dot{\beta} - \sin\alpha_0\,\dot{\phi} - \frac{g}{V}\cos\alpha_0\,\phi\right] \tag{5.25}$$

Note that the above equation expresses r explicitly in terms of variables β and ϕ.

By differentiating the β equation in (5.22) once with respect to time, we get

$$\ddot{\beta} = \sin\alpha_0\,\dot{p} - \cos\alpha_0\,\dot{r} + \frac{g}{V}\cos\alpha_0\dot{\phi} \tag{5.26}$$

Then by replacing $\dot{p}$ and $\dot{r}$ in the above equation with

$$\begin{aligned} \dot{p} &= \ddot{\phi} - \theta\ddot{\psi} - \dot{\theta}\dot{\psi} \\ \dot{r} &= \ddot{\psi} - \phi\ddot{\theta} - \dot{\phi}\dot{\theta} \end{aligned} \tag{5.27}$$

and using Equations (5.23) and (5.25), Equation (5.26) becomes

$$\begin{aligned} \ddot{\beta} = {} & \sin\alpha_0\,\ddot{\phi} - (\cos\alpha_0 + \sin\alpha_0\,\theta)\ddot{\psi} + \cos\alpha_0\,\phi\ddot{\theta} + \frac{g}{V}\cos\alpha_0\,\dot{\phi} + \frac{g}{V}\sin\alpha_0\,\phi\dot{\theta} + \\ & (\cos\alpha_0 - \sin\alpha_0\tan\alpha_0)\dot{\phi}\dot{\theta} + \tan\alpha_0\,\dot{\beta}\dot{\theta} - \sin\alpha_0\,\phi\dot{\theta}^2 + \frac{g}{V}\sin\alpha_0\tan\alpha_0\,\phi\theta\dot{\theta} + \\ & \sin\alpha_0\tan^2\alpha_0\,\dot{\phi}\theta\dot{\theta} - \tan^2\alpha_0\,\dot{\beta}\theta\dot{\theta} \end{aligned} \tag{5.28}$$

Next by substituting the equations for $\ddot{\phi}$, $\ddot{\theta}$, and $\ddot{\psi}$ from (5.12 into the above equation and also by doing the necessary substitutions such that Equation (5.11) are expressed in terms of variables β, ϕ, and θ, we obtain the following simplified equations of motion.

$$
\begin{aligned}
\ddot{\beta} + \omega_1^2\beta &= \tilde{\eta}_1\dot{\beta} + \tilde{\kappa}_2\phi + \tilde{\eta}_2\dot{\phi} + \\
&\quad \tilde{e}_1\phi^3 + \tilde{e}_2\phi^2\dot{\phi} + \tilde{e}_3\phi\dot{\phi}^2 + \tilde{e}_4\dot{\phi}^3 + \tilde{e}_5\beta^3 + \tilde{e}_6\beta^2\dot{\beta} + \\
&\quad \tilde{e}_7\beta\dot{\beta}^2 + \tilde{e}_8\dot{\beta}^3 + \tilde{e}_9\phi^2\beta + \tilde{e}_{10}\phi^2\dot{\beta} + \tilde{e}_{11}\dot{\phi}^2\beta + \tilde{e}_{12}\dot{\phi}^2\dot{\beta} + \\
&\quad \tilde{e}_{13}\phi\beta^2 + \tilde{e}_{14}\phi\dot{\beta}^2 + \tilde{e}_{15}\dot{\phi}\beta^2 + \tilde{e}_{16}\dot{\phi}\dot{\beta}^2 + \tilde{e}_{17}\phi\theta + \tilde{e}_{18}\phi\dot{\theta} + \\
&\quad \tilde{e}_{19}\dot{\phi}\theta + \tilde{e}_{20}\dot{\phi}\dot{\theta} + \tilde{e}_{21}\theta\beta + \tilde{e}_{22}\theta\dot{\beta} + \tilde{e}_{23}\dot{\theta}\beta + \tilde{e}_{24}\dot{\theta}\dot{\beta} + \\
&\quad \tilde{e}_{25}\phi\theta^2 + \tilde{e}_{26}\phi\dot{\theta}^2 + \tilde{e}_{27}\dot{\phi}\theta^2 + \tilde{e}_{28}\dot{\phi}\dot{\theta}^2 + \tilde{e}_{29}\theta^2\beta + \tilde{e}_{30}\theta^2\dot{\beta} + \\
&\quad \tilde{e}_{31}\dot{\theta}^2\beta + \tilde{e}_{32}\dot{\theta}^2\dot{\beta} + \tilde{e}_{33}\phi\dot{\phi}\beta + \tilde{e}_{34}\phi\dot{\phi}\dot{\beta} + \tilde{e}_{35}\phi\beta\dot{\beta} + \\
&\quad \tilde{e}_{36}\dot{\phi}\beta\dot{\beta} + \tilde{e}_{37}\phi\theta\dot{\theta} + \tilde{e}_{38}\dot{\phi}\theta\dot{\theta} + \tilde{e}_{39}\theta\dot{\theta}\beta + \tilde{e}_{40}\theta\dot{\theta}\dot{\beta} \\
\ddot{\phi} &= \tilde{\kappa}_1\beta + \tilde{\kappa}_3\phi + \tilde{\xi}_1\dot{\phi} + \tilde{\xi}_2\dot{\beta} + \\
&\quad \tilde{c}_1\phi^3 + \tilde{c}_2\phi^2\dot{\phi} + \tilde{c}_3\phi\dot{\phi}^2 + \tilde{c}_4\dot{\phi}^3 + \tilde{c}_5\beta^3 + \tilde{c}_6\beta^2\dot{\beta} + \\
&\quad \tilde{c}_7\beta\dot{\beta}^2 + \tilde{c}_8\dot{\beta}^3 + \tilde{c}_9\phi^2\beta + \tilde{c}_{10}\phi^2\dot{\beta} + \tilde{c}_{11}\dot{\phi}^2\beta + \tilde{c}_{12}\dot{\phi}^2\dot{\beta} + \\
&\quad \tilde{c}_{13}\phi\beta^2 + \tilde{c}_{14}\phi\dot{\beta}^2 + \tilde{c}_{15}\dot{\phi}\beta^2 + \tilde{c}_{16}\dot{\phi}\dot{\beta}^2 + \tilde{c}_{17}\phi\theta + \tilde{c}_{18}\phi\dot{\theta} + \\
&\quad \tilde{c}_{19}\dot{\phi}\theta + \tilde{c}_{20}\dot{\phi}\dot{\theta} + \tilde{c}_{21}\theta\beta + \tilde{c}_{22}\theta\dot{\beta} + \tilde{c}_{23}\dot{\theta}\beta + \tilde{c}_{24}\dot{\theta}\dot{\beta} + \\
&\quad \tilde{c}_{25}\phi\theta^2 + \tilde{c}_{26}\phi\dot{\theta}^2 + \tilde{c}_{27}\dot{\phi}\theta^2 + \tilde{c}_{28}\dot{\phi}\dot{\theta}^2 + \tilde{c}_{29}\theta^2\beta + \tilde{c}_{30}\theta^2\dot{\beta} + \\
&\quad \tilde{c}_{31}\dot{\theta}^2\beta + \tilde{c}_{32}\dot{\theta}^2\dot{\beta} + \tilde{c}_{33}\phi\dot{\phi}\beta + \tilde{c}_{34}\phi\dot{\phi}\dot{\beta} + \tilde{c}_{35}\phi\beta\dot{\beta} + \\
&\quad \tilde{c}_{36}\dot{\phi}\beta\dot{\beta} + \tilde{c}_{37}\phi\theta\dot{\theta} + \tilde{c}_{38}\dot{\phi}\theta\dot{\theta} + \tilde{c}_{39}\theta\dot{\theta}\beta + \tilde{c}_{40}\theta\dot{\theta}\dot{\beta} \\
\ddot{\theta} + \Omega^2\theta &= \tilde{\nu}\dot{\theta} + \tilde{d}_4\phi^2 + \tilde{d}_5\phi\dot{\phi} + \tilde{d}_6\dot{\phi}^2 + \tilde{d}_7\beta^2 + \tilde{d}_8\beta\dot{\beta} + \tilde{d}_9\dot{\beta}^2 + \\
&\quad \tilde{d}_{10}\phi\beta + \tilde{d}_{11}\phi\dot{\beta} + \tilde{d}_{12}\dot{\phi}\beta + \tilde{d}_{13}\dot{\phi}\dot{\beta} + \\
&\quad \tilde{d}_1\theta^2 + \tilde{d}_2\theta\dot{\theta} + \tilde{d}_3\dot{\theta}^2 + \tilde{d}_{14}\theta^3 + \tilde{d}_{15}\theta^2\dot{\theta} + \tilde{d}_{16}\theta\dot{\theta}^2 + \tilde{d}_{17}\dot{\theta}^3 + \\
&\quad \tilde{d}_{18}\phi^2\theta + \tilde{d}_{19}\phi^2\dot{\theta} + \tilde{d}_{20}\dot{\phi}^2\theta + \tilde{d}_{21}\dot{\phi}^2\dot{\theta} + \tilde{d}_{22}\theta\beta^2 + \tilde{d}_{23}\theta\dot{\beta}^2 + \\
&\quad \tilde{d}_{24}\dot{\theta}\beta^2 + \tilde{d}_{25}\dot{\theta}\dot{\beta}^2 + \tilde{d}_{26}\phi\dot{\phi}\theta + \tilde{d}_{27}\phi\dot{\phi}\dot{\theta} + \tilde{d}_{28}\theta\beta\dot{\beta} + \\
&\quad \tilde{d}_{29}\dot{\theta}\beta\dot{\beta} + \tilde{d}_{30}\phi\theta\beta + \tilde{d}_{31}\phi\theta\dot{\beta} + \tilde{d}_{32}\phi\dot{\theta}\beta + \tilde{d}_{33}\phi\dot{\theta}\dot{\beta} + \\
&\quad \tilde{d}_{34}\dot{\phi}\theta\beta + \tilde{d}_{35}\dot{\phi}\theta\dot{\beta} + \tilde{d}_{36}\dot{\phi}\dot{\theta}\beta + \tilde{d}_{37}\dot{\phi}\dot{\theta}\dot{\beta}
\end{aligned}
\tag{5.29}
$$

Analysis of system dynamics based on these equations is performed in the next section.

5.5 Motion Analysis

As in the previous chapter, Multiple Time Scales (MTS) Method is used for this analysis to reduce the complicated equations of motion to a form where center manifold reduction techniques and bifurcation theory can readily be applied. To facilitate the application of the MTS method, we first parameterize the system's equations of motion.

The parameterization is based on several observations. First, since we only consider small motions around the equilibrium conditions, then for each equation we have

$$\lim_{\mathbf{x}\to\bar{\mathbf{0}}} \frac{|N(\mathbf{x})|}{|\mathbf{x}|} \to 0 \tag{5.30}$$

where $\mathbf{x} = \{\beta\ \phi\ \theta\ \dot{\beta}\ \dot{\phi}\ \dot{\theta}\}^{\mathbf{T}}$ and $N(\mathbf{x})$ contains all the nonlinear terms in the equation. This is equivalent to saying that $N(\mathbf{x}) = \mathbf{O}(\epsilon)$, where $0 < \epsilon \ll 1$. Second, we use the fact that in the vicinity of the onset of wing rock, the magnitudes of the lateral motion are much larger than those of the longitudinal motion. This means that mathematically $O(\phi) = O(\beta) = O(\epsilon)$ and $O(\theta) = O(\epsilon^2)$. Third, in near wing rock case, the damping terms are usually small. Finally, we assume that the term $\frac{g}{\omega V}$ is small ($O(\epsilon)$), where ω denotes the dominant frequency of the rotational motion. This ratio can be interpreted as describing the ratio of the translational motion time scale with that of the rotational motion. The above assumption basically states that the rotational motion time scale is much faster than the translational time scale. This is consistent with our previous assumption that the translational motion is not influenced by the rotational motion. With the above observations and assumptions, the equations of motion can be written in a parameterized form as follows.

$$\begin{aligned}
\ddot{\beta} + \omega_1^2\beta &= \epsilon\left[\eta_1\dot{\beta} + \kappa_2\phi + \eta_2\dot{\phi} + f_1(\beta,\dot{\beta},\phi,\dot{\phi},\theta,\dot{\theta})\right] \\
\ddot{\phi} &= \kappa_1\beta + \epsilon\left[\kappa_3\phi + \xi_1\dot{\phi} + \xi_2\dot{\beta} + f_2(\beta,\dot{\beta},\phi,\dot{\phi},\theta,\dot{\theta})\right] \\
\ddot{\theta} + \Omega^2\theta &= g(\beta,\dot{\beta},\phi,\dot{\phi}) + \epsilon\left[\nu\dot{\theta} + f_3(\beta,\dot{\beta},\phi,\dot{\phi},\theta,\dot{\theta})\right]
\end{aligned} \tag{5.31}$$

where

$$\begin{aligned}
g(\beta,\dot{\beta},\phi,\dot{\phi}) &= d_4\phi^2 + d_5\phi\dot{\phi} + d_6\dot{\phi}^2 + d_7\beta^2 + d_8\beta\dot{\beta} + d_9\dot{\beta}^2 + \\
&\quad d_{10}\phi\beta + d_{11}\phi\dot{\beta} + d_{12}\dot{\phi}\beta + d_{13}\dot{\phi}\dot{\beta} \\
f_1(\beta,\dot{\beta},\phi,\dot{\phi},\theta,\dot{\theta}) &= e_1\phi^3 + e_2\phi^2\dot{\phi} + e_3\phi\dot{\phi}^2 + e_4\dot{\phi}^3 + e_5\beta^3 + e_6\beta^2\dot{\beta} + \\
&\quad e_7\beta\dot{\beta}^2 + e_8\dot{\beta}^3 + e_9\phi^2\beta + e_{10}\phi^2\dot{\beta} + e_{11}\dot{\phi}^2\beta + e_{12}\dot{\phi}^2\dot{\beta} +
\end{aligned}$$

$$
\begin{aligned}
& e_{13}\phi\beta^2 + e_{14}\phi\dot{\beta}^2 + e_{15}\dot{\phi}\beta^2 + e_{16}\dot{\phi}\dot{\beta}^2 + e_{17}\phi\theta + e_{18}\phi\dot{\theta} + \\
& e_{19}\dot{\phi}\theta + e_{20}\dot{\phi}\dot{\theta} + e_{21}\theta\beta + e_{22}\theta\dot{\beta} + e_{23}\dot{\theta}\beta + e_{24}\dot{\theta}\dot{\beta} + \\
& e_{25}\phi\theta^2 + e_{26}\phi\dot{\theta}^2 + e_{27}\dot{\phi}\theta^2 + e_{28}\dot{\phi}\dot{\theta}^2 + e_{29}\theta^2\beta + e_{30}\theta^2\dot{\beta} + \\
& e_{31}\dot{\theta}^2\beta + e_{32}\dot{\theta}^2\dot{\beta} + e_{33}\phi\dot{\phi}\beta + e_{34}\phi\dot{\phi}\dot{\beta} + e_{35}\phi\beta\dot{\beta} + \\
& e_{36}\dot{\phi}\beta\dot{\beta} + e_{37}\phi\theta\dot{\theta} + e_{38}\dot{\phi}\theta\dot{\theta} + e_{39}\theta\dot{\theta}\beta + e_{40}\theta\dot{\theta}\dot{\beta}
\end{aligned}
$$

$$
\begin{aligned}
f_2(\beta,\dot{\beta},\phi,\dot{\phi},\theta,\dot{\theta}) = {} & c_1\phi^3 + c_2\phi^2\dot{\phi} + c_3\phi\dot{\phi}^2 + c_4\dot{\phi}^3 + c_5\beta^3 + c_6\beta^2\dot{\beta} + \\
& c_7\beta\dot{\beta}^2 + c_8\dot{\beta}^3 + c_9\phi^2\beta + c_{10}\phi^2\dot{\beta} + c_{11}\dot{\phi}^2\beta + c_{12}\dot{\phi}^2\dot{\beta} + \\
& c_{13}\phi\beta^2 + c_{14}\phi\dot{\beta}^2 + c_{15}\dot{\phi}\beta^2 + c_{16}\dot{\phi}\dot{\beta}^2 + c_{17}\phi\theta + c_{18}\phi\dot{\theta} + \\
& c_{19}\dot{\phi}\theta + c_{20}\dot{\phi}\dot{\theta} + c_{21}\theta\beta + c_{22}\theta\dot{\beta} + c_{23}\dot{\theta}\beta + c_{24}\dot{\theta}\dot{\beta} + \\
& c_{25}\phi\theta^2 + c_{26}\phi\dot{\theta}^2 + c_{27}\dot{\phi}\theta^2 + c_{28}\dot{\phi}\dot{\theta}^2 + c_{29}\theta^2\beta + c_{30}\theta^2\dot{\beta} + \\
& c_{31}\dot{\theta}^2\beta + c_{32}\dot{\theta}^2\dot{\beta} + c_{33}\phi\dot{\phi}\beta + c_{34}\phi\dot{\phi}\dot{\beta} + c_{35}\phi\beta\dot{\beta} + \\
& c_{36}\dot{\phi}\beta\dot{\beta} + c_{37}\phi\theta\dot{\theta} + c_{38}\dot{\phi}\theta\dot{\theta} + c_{39}\theta\dot{\theta}\beta + c_{40}\theta\dot{\theta}\dot{\beta}
\end{aligned}
$$

$$
\begin{aligned}
f_3(\beta,\dot{\beta},\phi,\dot{\phi},\theta,\dot{\theta}) = {} & d_1\theta^2 + d_2\theta\dot{\theta} + d_3\dot{\theta}^2 + d_{14}\theta^3 + d_{15}\theta^2\dot{\theta} + d_{16}\theta\dot{\theta}^2 + d_{17}\dot{\theta}^3 + \\
& d_{18}\phi^2\theta + d_{19}\phi^2\dot{\theta} + d_{20}\dot{\phi}^2\theta + d_{21}\dot{\phi}^2\dot{\theta} + d_{22}\theta\beta^2 + d_{23}\theta\dot{\beta}^2 + \\
& d_{24}\dot{\theta}\beta^2 + d_{25}\dot{\theta}\dot{\beta}^2 + d_{26}\phi\dot{\phi}\theta + d_{27}\phi\dot{\phi}\dot{\theta} + d_{28}\theta\beta\dot{\beta} + \\
& d_{29}\dot{\theta}\beta\dot{\beta} + d_{30}\phi\theta\beta + d_{31}\phi\theta\dot{\beta} + d_{32}\phi\dot{\theta}\beta + d_{33}\phi\dot{\theta}\dot{\beta} + \\
& d_{34}\dot{\phi}\theta\beta + d_{35}\dot{\phi}\theta\dot{\beta} + d_{36}\dot{\phi}\dot{\theta}\beta + d_{37}\dot{\phi}\dot{\theta}\dot{\beta}
\end{aligned} \tag{5.32}
$$

The relations between the coefficients in Equation (5.31) and Equation (5.29) are given in Appendix E.

We will attempt to the *principle of minimal simplification* (subsection 2.2.3) to determine the appropriate time scales for the system. The form of the longitudinal equation is the same as in the two degrees-of-freedom case, and as we have already seen, a simple time scales ordering works (t, ϵt,...). Therefore, the time scales for this system are determined mainly by the two lateral equations. For convenience, we first decouple the linear part of the lateral equations. The decoupling process is not difficult, but it is rather lengthy. The result of linearly decoupling these equations is given below.

$$
\dddot{\dddot{\phi}} + \epsilon v_1 \dddot{\phi} + (v_2 + \epsilon v_3 + \epsilon^2 v_4)\ddot{\phi} + (\epsilon v_5 + \epsilon^2 v_6)\dot{\phi} + \epsilon v_7 \phi = \epsilon F_1 + \epsilon^2 F_2 \tag{5.33}
$$

where

$$
\begin{aligned}
v_1 &= -(\eta_1 + \xi_1) & v_5 &= -(\kappa_1\eta_2 + \omega_1^2\xi_1) \\
v_2 &= \omega_1^2 & v_6 &= -(\xi_2\kappa_2 - \eta_1\kappa_3) \\
v_3 &= -\kappa_3 & v_7 &= -(\kappa_1\kappa_2 + \omega_1^2\kappa_3) \\
v_4 &= -(\eta_2\xi_2 - \eta_1\xi_1) & & \\
F_1 &= \kappa_1 f_1 + \omega_1^2 f_2 + \ddot{f}_2 & & \\
F_2 &= \xi_2 \dot{f}_1 - \eta_1 \dot{f}_2 & &
\end{aligned}
\tag{5.34}
$$

The independent variable is then extended as follows

$$
\begin{aligned}
t \rightarrow \{\tau_0, \tau_1\} \qquad & \tau_0 = t \\
& \tau_1 = \epsilon^\sigma t
\end{aligned}
\tag{5.35}
$$

With this extension, the differential equation (5.33) becomes a partial differential equation as follows.

$$
\begin{aligned}
&\frac{\partial^4\phi}{\partial\tau_0^4} + \epsilon^\sigma 4\frac{\partial^4\phi}{\partial\tau_0^3\partial\tau_1} + \epsilon^{2\sigma}6\frac{\partial^4\phi}{\partial\tau_0^2\partial\tau_1^2} + \epsilon^{3\sigma}4\frac{\partial^4\phi}{\partial\tau_0\partial\tau_1^3} + \epsilon^{4\sigma}\frac{\partial^4\phi}{\partial\tau_1^4} + \\
&\epsilon v_1\frac{\partial^3\phi}{\partial\tau_0^3} + \epsilon^{1+\sigma}3v_1\frac{\partial^3\phi}{\partial\tau_0^2\partial\tau_1} + \epsilon^{1+2\sigma}3v_1\frac{\partial^3\phi}{\partial\tau_0\partial\tau_1^2} + \epsilon^{1+3\sigma}v_1\frac{\partial^3\phi}{\partial\tau_1^3} + \\
&(v_2 + \epsilon v_3 + \epsilon^2 v_4)\frac{\partial^2\phi}{\partial\tau_0^2} + \epsilon^\sigma 2(v_2 + \epsilon v_3 + \epsilon^2 v_4)\frac{\partial^2\phi}{\partial\tau_0\partial\tau_1} + \\
&\epsilon^{2\sigma}(v_2 + \epsilon v_3 + \epsilon^2 v_4)\frac{\partial^2\phi}{\partial\tau_1^2} + (\epsilon v_5 + \epsilon^2 v_6)\frac{\partial\phi}{\partial\tau_0} + \epsilon^\sigma(\epsilon v_5 + \epsilon^2 v_6)\frac{\partial\phi}{\partial\tau_1} + \\
&\epsilon v_7\phi = \epsilon F_1 + \epsilon^2 F_2
\end{aligned}
\tag{5.36}
$$

In general, each term in (5.36) is of the form $\epsilon^{c_0+c_1\sigma}(\cdot)$, where the terms in $(\cdot)$ are assumed to be of $O(1)$.

However, in this situation, the principle of minimal simplification does not yield meaningful information. Therefore, we need to use the extensions of this idea, and invoke Ramnath's *principle of subminimal simplification* [32]. This leads to the choice

$$
\sigma = 1 \tag{5.37}
$$

which basically suggests simple time scales ordering for the system ($\{t, \epsilon t, ...\}$). However, continuing the MTS analysis using these time scales leads us into mathematical difficulty, and one has to go to the next rank of simplification to get a meaningful result.

Continuing this idea, we are led to the choice

$$\sigma = \frac{1}{2} \tag{5.38}$$

This result is equivalent to the time scales ordering $\{t, \epsilon^{\frac{1}{2}}t, \epsilon t, ...\}$. As we shall see later, this result leads to a meaningful result and so, the analysis that follows is based on these time scales. Three time scales are used in the analysis, since the use of two time scales only is not enough to capture all the essential dynamics of the system. Also, instead of using the linearly decoupled fourth order lateral equation, we use the original coupled second order equations, because the mathematics is more compact and they both lead to the same result.

To formalize the previous result, the independent variable is extended according to

$$\begin{aligned} t \rightarrow \{\tau_0, \tau_1, \tau_2\} \qquad & \tau_0 = t \\ & \tau_1 = \epsilon^{\frac{1}{2}}t \\ & \tau_2 = \epsilon t \end{aligned} \tag{5.39}$$

The dependent variables are extended as

$$\begin{aligned} \beta(t) &\rightarrow \beta_0(\tau_0, \tau_1, \tau_2) + \epsilon\beta_1(\tau_0, \tau_1, \tau_2) + ... \\ \phi(t) &\rightarrow \phi_0(\tau_0, \tau_1, \tau_2) + \epsilon\phi_1(\tau_0, \tau_1, \tau_2) + ... \\ \theta(t) &\rightarrow \theta_0(\tau_0, \tau_1, \tau_2) + \epsilon\theta_1(\tau_0, \tau_1, \tau_2) + ... \end{aligned} \tag{5.40}$$

These extended variables are substituted into Equation (5.31) and then grouped according to their orders. This process is not difficult although it is quite lengthy. Order by order analysis can then be performed by equating each group to zero.

The dominant order group ($O(1)$) yields

$$\begin{aligned} \frac{\partial^2\beta_0}{\partial\tau_0^2} + \omega_1^2\beta_0 &= 0 \\ \frac{\partial^2\phi_0}{\partial\tau_0^2} &= \kappa_1\beta_0 \\ \frac{\partial^2\theta_0}{\partial\tau_0^2} + \Omega^2\theta_0 &= g(\beta_0, \dot{\beta}_0, \phi_0, \dot{\phi}_0) \end{aligned} \tag{5.41}$$

The solution of the first equation in (5.41) is

$$\beta_0 = A_1(\tau_1, \tau_2) \sin \Psi_1 \ ; \ \ \Psi_1 \equiv \omega_1 \tau_0 + B_1(\tau_1) \tag{5.42}$$

The substitution of this solution into the second equation in (5.41) yields

$$\phi_0 = -\frac{\kappa_1}{\omega_1^2} A_1(\tau_1, \tau_2) \sin \Psi_1 + C(\tau_1, \tau_2) + D(\tau_1, \tau_2)\tau_0 \tag{5.43}$$

The last term in the above equation is a *secular* term, which destroys the accuracy of the asymptotic approximation for long times [41]. The existence of such a term is not uncommon in an asymptotic expansion. However, appropriate counterterms can be constructed to cancel this term. The construction is based on the compatibility conditions that must be satisfied by the expansion. A detailed discussion on this subject is presented in [41]. Mathematical elaboration on this point is not done here, however it is clear from the physical reason that $D(\tau_1, \tau_2)$ must be dropped in order to get a meaningful result. Therefore,

$$\phi_0 = \phi_{0_1} + \phi_{0_2} \tag{5.44}$$

where

$$\begin{aligned} \phi_{0_1} &= -\frac{\kappa_1}{\omega_1^2} A_1(\tau_1, \tau_2) \sin \Psi_1 \\ \phi_{0_2} &= C(\tau_1, \tau_2) \end{aligned} \tag{5.45}$$

ϕ_{0_1} and ϕ_{0_2} are treated as two independent solutions. Although we are dealing with a nonlinear system, this treatment is justifiable, since these solutions are obtained from a set of linear partial differential equations. We will deal first with ϕ_{0_1}.

The substitution of β_0 and ϕ_{0_1} obtained above into the third equation in (5.41) results in

$$\theta_0 = \theta_{0_1} + \theta_{0_2} \tag{5.46}$$

where

$$\begin{aligned} \theta_{0_1} &= A_2(\tau_1, \tau_2) \sin \Psi_2 \quad ; \quad \Psi_2 \equiv \Omega \tau_0 + B_2(\tau_1, \tau_2) \\ \theta_{0_2} &= m_0 A_1^2(\tau_1, \tau_2) + m_1 A_1^2(\tau_1, \tau_2) \cos 2\Psi_1 + m_2 A_1^2(\tau_1, \tau_2) \sin 2\Psi_1 \end{aligned} \tag{5.47}$$

with

$$
\begin{aligned}
m_0 &= \frac{1}{2\Omega^2}\left[\left(\frac{\kappa_1}{\omega_1^2}\right)^2(d_1+d_3\omega_1^2)+(d_4+d_6\omega_1^2)-\left(\frac{\kappa_1}{\omega_1^2}\right)(d_7+d_{10}\omega_1^2)\right] \\
m_1 &= \frac{1}{2(\Omega^2-\omega_1^2)}\left[-\left(\frac{\kappa_1}{\omega_1^2}\right)^2(d_1-d_3\omega_1^2)-(d_4-d_6\omega_1^2)+\left(\frac{\kappa_1}{\omega_1^2}\right)(d_7-d_{10}\omega_1^2)\right] \\
m_2 &= \frac{1}{2(\Omega^2-\omega_1^2)}\left[\left(\frac{\kappa_1}{\omega_1^2}\right)^2 d_2\omega_1+d_5\omega_1-\left(\frac{\kappa_1}{\omega_1^2}\right)(d_8+d_9)\right] \qquad (5.48)
\end{aligned}
$$

In Equation (5.46), θ_{0_1} and θ_{0_2} are the homogeneous and the particular solutions of the dominant longitudinal equation, respectively.

Continuing the analysis to the next order ($O(\epsilon^{\frac{1}{2}})$) we get

$$
\begin{aligned}
\frac{\partial^2\beta_0}{\partial\tau_0\partial\tau_1} &= 0 \\
\frac{\partial^2\phi_0}{\partial\tau_0\partial\tau_1} &= 0 \\
\frac{\partial^2\theta_0}{\partial\tau_0\partial\tau_1} &= d_2\phi_0\frac{\partial\phi_0}{\partial\tau_1}+2d_3\frac{\partial\phi_0}{\partial\tau_0}\frac{\partial\phi_0}{\partial\tau_1}+d_5\beta_0\frac{\partial\beta_0}{\partial\tau_1}+2d_6\frac{\partial\beta_0}{\partial\tau_0}\frac{\partial\beta_0}{\partial\tau_1}+ \\
&\quad d_8\phi_0\frac{\partial\beta_0}{\partial\tau_1}+d_9\beta_0\frac{\partial\phi_0}{\partial\tau_1}+d_{10}\frac{\partial\phi_0}{\partial\tau_0}\frac{\partial\beta_0}{\partial\tau_1}+d_{10}\frac{\partial\phi_0}{\partial\tau_1}\frac{\partial\beta_0}{\partial\tau_0} \qquad (5.49)
\end{aligned}
$$

The substitution of β_0 and ϕ_0 from Equations (5.42) and (5.44) into the first two equations in (5.49) leads to the following equation.

$$\frac{\partial A_1}{\partial\tau_1}\cos\Psi_1-A_1\frac{\partial B_1}{\partial\tau_1}\sin\Psi_1=0 \qquad (5.50)$$

The above equation can only be satisfied when

$$\frac{\partial A_1}{\partial\tau_1}=\frac{\partial B_1}{\partial\tau_1}=0 \qquad (5.51)$$

This implies that A_1 and B_1 are not functions of τ_1 ($A_1, B_1 \neq f(\tau_1)$). We now look at the third equation in (5.49). Notice that due to the above result, the righthand side of this equation becomes zero. Then, by substituting θ_0 in (5.46) into the equation, we get

$$\frac{\partial A_2}{\partial\tau_1}\cos\Psi_2-A_2\frac{\partial B_2}{\partial\tau_1}\sin\Psi_2=0 \qquad (5.52)$$

This equation is satisfied only when

$$\frac{\partial A_2}{\partial \tau_1} = \frac{\partial B_2}{\partial \tau_1} = 0 \tag{5.53}$$

which means that A_2 and B_2 are not functions of τ_1. It is clear from the above development that A_1, B_1, A_2, and B_2 are functions of τ_2 only.

Next order analysis on β equation yields

$$\begin{aligned} O(\epsilon) \; : \; \frac{\partial^2 \beta_1}{\partial \tau_0^2} + \omega_1^2 \beta_1 &= -2\frac{\partial^2 \beta_0}{\partial \tau_0 \partial \tau_2} - \frac{\partial^2 \beta_0}{\partial \tau_1^2} + \eta_1 \frac{\partial \beta_0}{\partial \tau_0} + \kappa_2 \phi_0 + \\ &\quad \eta_1 \frac{\partial \phi_0}{\partial \tau_0} + f_{1_0} \\ &= [Coef_1] \cos \Psi_1 + [Coef_2] \sin \Psi_1 + ... \end{aligned} \tag{5.54}$$

where f_{1_0} is the extended version of the nonlinear function f_1 of $O(1)$. Note that in the above equation, fourth and higher order terms are neglected. It can be observed from the above equation that the presence of the nonzero $\cos \Psi_1$ and $\sin \Psi_1$ terms on the righthand side will give rise to the secular terms in the β_1 solution and this makes the approximation obtained nonuniform. To obtain a uniform approximation, we set the coefficients of these terms to zero. By doing so, we get

$$\begin{aligned} \frac{dA_1}{d\tau_2} &= \frac{\mu}{2} A_1 + p_1 A_1^3 + p_2 A_1 A_2^2 \\ \frac{dB_1}{d\tau_1} &= p_3 + p_4 A_1^2 + p_5 A_2^2 \end{aligned} \tag{5.55}$$

where

$$\begin{aligned} \mu &= \frac{1}{2}\left(\eta_1 - \frac{\kappa_1}{\omega_1^2}\eta_2\right) \\ p_1 &= -\frac{1}{8}\frac{\kappa_1^3}{\omega_1^6}e_2 - \frac{3}{8}\frac{\kappa_1^3}{\omega_1^4}e_4 + \frac{1}{8}e_6 + \frac{3}{8}\omega_1^2 e_8 + \frac{1}{8}\frac{\kappa_1^2}{\omega_1^4}e_{10} + \frac{3}{8}\frac{\kappa_1^2}{\omega_1^2}e_{12} - \frac{1}{8}\frac{\kappa_1}{\omega_1^2}e_{15} - \\ &\quad \frac{3}{8}\kappa_1 e_{16} - \frac{1}{4}\frac{\kappa_1 m_3}{\omega_1^3(\Omega^2 - 4\omega_1^2)}e_{17} + \frac{1}{2}\frac{\kappa_1 m_2}{\omega_1^2(\Omega^2 - 4\omega_1^2)}e_{18} - \frac{1}{2}\left(\frac{\kappa_1 m_1}{\omega_1^2 \Omega^2} + \right. \\ &\quad \left.\frac{1}{2}\frac{\kappa_1 m_2}{\omega_1^2(\Omega^2 - 4\omega_1^2)}\right)e_{19} - \frac{1}{2}\frac{\kappa_1 m_3}{\omega_1(\Omega^2 - 4\omega_1^2)}e_{20} + \frac{1}{4}\frac{m_3}{\omega_1(\Omega^2 - 4\omega_1^2)}e_{21} + \\ &\quad \frac{1}{2}\left(\frac{m_1}{\Omega^2} + \frac{m_2}{\Omega^2 - 4\omega_1^2}\right)e_{22} - \frac{1}{2}\frac{m_2}{(\Omega^2 - 4\omega_1^2)}e_{23} + \frac{1}{2}\frac{m_3\omega_2}{(\Omega^2 - 4\omega_1^2)}e_{24} + \\ &\quad \frac{1}{8}\frac{\kappa_1^2}{\omega_1^4}e_{33} - \frac{1}{8}\frac{\kappa_1}{\omega_1^2}e_{35} \end{aligned}$$

$$
\begin{aligned}
p_2 &= -\frac{1}{4}\frac{\kappa_1}{\omega_1^2}e_{27} - \frac{1}{4}\frac{\kappa_1\Omega^2}{\omega_1^2}e_{28} + \frac{1}{4}e_{30} + \frac{1}{4}\Omega^2 e_{32} \\
p_3 &= -\frac{1}{4}\frac{\kappa_1}{\omega_1^2}e_2 - \frac{3}{4}\frac{\kappa_1\omega_1^2}{\omega_1^2}e_4 + \frac{1}{4}e_{10} + \frac{1}{4}\omega_1^2 e_{12} \\
p_4 &= \frac{\kappa_1\kappa_2}{2\omega_1^3} \\
p_5 &= \frac{3}{8}\frac{\kappa_1^3}{\omega_1^7}e_1 + \frac{1}{8}\frac{\kappa_1^3}{\omega_1^5}e_3 - \frac{3}{8}\frac{1}{\omega_2}e_5 - \frac{1}{4}\omega_2 e_7 - \frac{3}{8}\frac{\kappa_1^2}{\omega_1^5}e_9 - \frac{1}{8}\frac{\kappa_1^2}{\omega_1^3}e_{11} + \frac{3}{8}\frac{\kappa_1}{\omega_1^3}e_{13} + \\
&\quad \frac{1}{8}\frac{\kappa_1}{\omega_1}e_{14} + \frac{1}{2}\left(\frac{\kappa_1 m_1}{\omega_1^3\Omega^2} - \frac{1}{2}\frac{\kappa_1 m_2}{\omega_1^3(\Omega^2 - 4\omega_1^2)}\right)e_{17} - \frac{1}{2}\frac{\kappa_1 m_3}{\omega_1^2(\Omega^2 - 4\omega_1^2)}e_{18} - \\
&\quad -\frac{1}{2}\left(\frac{m_1}{\omega_1\Omega^2} - \frac{m_2}{\omega_1(\Omega^2 - 4\omega_1^2)}\right)e_{21} - \frac{1}{2}\frac{\kappa_1 m_2}{\omega_1(\Omega^2 - 4\omega_1^2)}e_{20} - \\
&\quad \frac{1}{4}\frac{m_3}{\Omega^2 - 4\omega_1^2}e_{22} + \frac{1}{2}\frac{m_3}{\Omega^2 - 4\omega_1^2}e_{23} + \frac{1}{2}\frac{\omega_1 m_2}{\Omega^2 - 4\omega_1^2}e_{24} - \frac{1}{8}\frac{\kappa_1^2}{\omega_1^3}e_{34} + \\
&\quad \frac{1}{8}\frac{\kappa_1}{\omega_2}e_{36} + \frac{1}{4}\frac{\kappa_1 m_3}{\omega_1^2(\Omega^2 - 4\omega_1^2)}e_{19}
\end{aligned} \tag{5.56}
$$

The first equation in (5.55) is the lateral amplitude equation while the second one gives the phase correction of this lateral oscillation. These equations describe the slowly changing behavior of the amplitude and phase of this particular mode. Notice that these differential equations depend on the longitudinal mode through A_2. The equations that govern the amplitude and the phase correction of the homogeneous longitudinal mode are derived next.

The $O(\epsilon)$ terms in the longitudinal equation leads to the following.

$$
\begin{aligned}
O(\epsilon) : \frac{\partial^2\theta_1}{\partial\tau_0^2} + \Omega_1^2\theta_1 &= -2\frac{\partial^2\theta_0}{\partial\tau_0\partial\tau_2} + \nu\frac{\partial\theta_0}{\partial\tau_0} + g_2 + f_{3_0} \\
&= [Coef_3]\cos\Psi_2 + [Coef_4]\sin\Psi_2 + ...
\end{aligned} \tag{5.57}
$$

As before, the terms involving $\cos\Psi_2$ and Ψ_2 on the righthand side of the equation contribute to the secular terms in the solution. Therefore, for a uniform approximation, the coefficients of these terms are set to zero. Therefore,

$$
\begin{aligned}
\frac{dA_2}{d\tau_2} &= \frac{1}{2}\nu A_2 + q_1 A_2^3 + q_2 A_1^2 A_2 \\
\frac{dB_2}{d\tau_2} &= q_3 A_1^2 + q_4 A_2^2
\end{aligned} \tag{5.58}
$$

where

$$
\begin{aligned}
q_1 &= \frac{1}{8}d_{15} + \frac{3}{8}\Omega^2 d_{17} \\
q_2 &= \frac{1}{4}\frac{\kappa_1\Omega}{\omega_1^4}d_{19} + \frac{1}{4}\frac{\kappa_1^2}{\omega_1^2}d_{21} + \frac{1}{4}d_{24} + \frac{1}{4}\omega_1^2 d_{25} - \frac{1}{4}\frac{\kappa_1}{\omega_1^2}d_{32} - \\
&\quad \frac{1}{4}\kappa_1 d_{37} + \frac{1}{2}\frac{m_1}{\Omega^2} \\
q_3 &= -\frac{m_1}{\Omega^3}d_1 - \frac{1}{4}\frac{\kappa_1^2}{\Omega\omega_1^4}d_{18} - \frac{1}{4}\frac{1}{\Omega}d_{22} + \frac{1}{4}\frac{\kappa_1}{\Omega\omega_1^2}d_{30} - \frac{1}{4}\frac{\kappa_1^2}{\Omega\omega_1^2}d_{20} - \\
&\quad \frac{1}{4}\frac{\omega_1^2}{\Omega}d_{23} + \frac{1}{4}\frac{\kappa_1}{\Omega}d_{35} \\
q_4 &= -\frac{3}{8}\frac{1}{\Omega}d_{14} - \frac{1}{8}\Omega d_{16}
\end{aligned}
\tag{5.59}
$$

Equation (5.58) describes the amplitude and phase correction history of the homogeneous longitudinal mode. This set of first order differential equations together with the one in Equation (5.55) form a complete set of differential equations that need to be solved in order to get the amplitude and phase correction history of the dominant lateral and longitudinal modes. Exact solutions of this set of equations are very difficult to obtain, however they are in the form where the center manifold reduction technique can readily be applied. We will look into more detail on the application of the technique later.

We now focus on the other mode that appears on the roll mode, denoted previously by ϕ_{0_2}. The governing equation for this particular mode can be obtained by examining the $O(\epsilon)$ ϕ-equation as follows.

$$
\begin{aligned}
\frac{\partial^2\phi_1}{\partial\tau_0^2} &= \kappa_1\beta_1 + \kappa_3\phi_0 - 2\frac{\partial^2\phi_0}{\partial\tau_0\partial\tau_2} - \frac{\partial^2\phi_0}{\partial\tau_1^2} + \\
&\quad \xi_1\frac{\partial\phi_0}{\partial\tau_0} + \xi_2\frac{\partial\beta_0}{\partial\tau_0} + f_{2_0}
\end{aligned}
\tag{5.60}
$$

The substitution of ϕ_{0_2} into ϕ in the above equation results in an equation of the following form.

$$
\frac{\partial^2\phi_1}{\partial\tau_0^2} = f(\tau_1,\tau_2) + P(\tau_0,\tau_1,\tau_2) \tag{5.61}
$$

where $P(\tau_0,\tau_1,\tau_2)$ contains periodic terms in τ_0. These periodic terms in general generate periodic terms after integration. On the other hand, after integration $f(\tau_1,\tau_2)$ results in

$$
k_1(\tau_1,\tau_2) + k_2(\tau_1,\tau_2)\tau_0 + \frac{1}{2}f(\tau_1,\tau_2)\tau_0^2 \tag{5.62}
$$

which is secular and destroys the uniformity of the approximation. Hence, to maintain uniformity, we must set

$$f(\tau_1, \tau_2) = 0 \tag{5.63}$$

which gives

$$\frac{\partial^2 C}{\partial \tau_1^2} + \omega_2^2 C + u_1 C^3 = 0 \tag{5.64}$$

where

$$\begin{aligned} \omega_2^2 &= \kappa_3 + \frac{\kappa_1 \kappa_2}{\omega_1^2} \\ u_1 &= c_1 + c_{17}\frac{d_1}{\Omega^2} + \frac{\kappa_1}{\omega_1^2}\left(e_1 + e_{17}\frac{d_1}{\Omega^2}\right) \end{aligned} \tag{5.65}$$

The derivation of the solution of this equation follows. By considering that the amplitude of the equation varies with the slower time scale τ_2 and $\frac{\partial C}{\partial \tau_1} = 0$ at the the amplitude, then Equation (5.64) can be integrated to yield

$$\frac{1}{2}\left(\frac{\partial C}{\partial \tau_1}\right)^2 + \frac{1}{2}\omega_2^2 C^2 + \frac{1}{4}u_1 C^4 = \frac{1}{2}\omega_2^2 A_3^2(\tau_2) + \frac{1}{4}u_1 A_3^4(\tau_2) \tag{5.66}$$

or

$$\left(\frac{\partial C}{\partial \tau_1}\right)^2 = \frac{u_1}{2}(A_3^2(\tau_2) - C^2)(\frac{2\omega_2^2}{u_1} + A_3^2(\tau_2) + C^2) \tag{5.67}$$

where $A_3(\tau_2)$ is the amplitude of the motion. By separating the variables and then integrating, we obtain the solution in terms of elliptic integrals as follows.

$$\tau_1 = \sqrt{\frac{2}{u_1}} \int \frac{dC}{\sqrt{(A_3^2(\tau_2) - C^2)(\frac{2\omega_2^2}{u_1} + A_3^2(\tau_2) + C^2)}} \tag{5.68}$$

Using the table of elliptic integrals in [42], the above solution can be expressed in terms of elliptic function as follows.

$$\tau_1 = \frac{1}{\omega_2\sqrt{1 + \frac{u_1}{\omega_1^2}A_3^2(\tau_2)}} cn^{-1}\left(\frac{C}{A_3(\tau_2)}, k\right) \tag{5.69}$$

where k is the modulus, which in this case is given by

$$k = \frac{A_3^2(\tau_2)}{\frac{2\omega_2^2}{u_1} + 2A_3^2(\tau_2)} \tag{5.70}$$

The inversion of Equation (5.69) yields

$$C(\tau_1, \tau_2) = A_3(\tau_2) cn\left(\omega_2 \sqrt{1 + \frac{u_1}{\omega_1^2} A_3^2(\tau_2)}\, \tau_1\right) \tag{5.71}$$

The period of the oscillation is given by (see [43])

$$P = \frac{4\chi}{\omega_2 \sqrt{1 + \frac{u_1}{\omega_1^2} A_3^2}} \tag{5.72}$$

where

$$\chi = \frac{1}{2}\pi \left[1 + \left(\frac{1}{2}\right)^2 k^2 + \left(\frac{1 \cdot 3}{2 \cdot 4}\right)^2 k^4 + ...\right] \tag{5.73}$$

If we only consider small amplitude motions, then the modulus, k, is small, and χ can be approximated very well using

$$\chi \approx \frac{1}{2}\pi \left[1 + \left(\frac{1}{2}\right)^2 k^2\right] \tag{5.74}$$

Using this approximation, we get

$$\chi = \frac{1}{2}\pi \left[1 + \frac{1}{8}\frac{u_1}{\omega_2^2} A_3^2(\tau_2)\right] \tag{5.75}$$

The period of the oscillation can then be expressed as

$$P = 2\pi \frac{1 + \frac{1}{8}\frac{u_1}{\omega_2^2} A_3^2(\tau_2)}{\omega_2 \sqrt{1 + \frac{u_1}{\omega_2^2} A_3^2(\tau_2)}} \tag{5.76}$$

The angular frequency can be written as

$$\omega_3 = \frac{2\pi}{P}$$

$$= \frac{\omega_2\sqrt{1+\frac{u_1}{\omega_2^2}A_3^2(\tau_2)}}{1+\frac{1}{8}\frac{u_1}{\omega_2^2}A_3^2(\tau_2)} \tag{5.77}$$

Then, by using binomial expansion, we obtain

$$\begin{aligned}\omega_3 &\approx \omega_2\left(1+\frac{1}{2}\frac{u_1}{\omega_2^2}A_3^2(\tau_2)\right)\left(1-\frac{1}{8}\frac{u_1}{\omega_2^2}A_3^2(\tau_2)\right)\\ &\approx \omega_2\left(1+\frac{3}{8}\frac{u_1}{\omega_2^2}A_3^2(\tau_2)\right)\end{aligned} \tag{5.78}$$

As we have mentioned previously, the modulus, k, of the elliptic function is small for the case of interest. This implies that the departure of the elliptic function from the elementary sinusoidal function (sine or cosine) is also small. In general, for small k, we can approximate the elliptic function (5.71) fairly well using the sinusoidal function with the same frequency as follows.

$$C(\tau_1,\tau_2) = A_3(\tau_2)\sin\left[\omega_2(1+\frac{3}{8}\frac{u_1}{\omega_2^2}A_3^2(\tau_2))\tau_1 + B_3(\tau_2)\right] \tag{5.79}$$

where A_3 and B_3 represent the amplitude and phase-correction of the solution, respectively. We will use this representation in the rest of the analysis.

The amplitude variation and the phase-correction can be found using the next order group of terms in the expansion of Equation (5.31). Substituting $C(\tau_1,\tau_2)$ in place of ϕ_0 into the $O(\epsilon^{\frac{3}{2}})$ terms results in

$$2\frac{\partial^2 C}{\partial\tau_1\partial\tau_2} = \left(\xi_2+\frac{\kappa_1\eta_2}{\omega_1^2}\right)\frac{\partial C}{\partial\tau_1} + c_2C^2\frac{\partial C}{\partial\tau_1} \tag{5.80}$$

Inserting C from (5.79) into the above equation and then equating the coefficient of the $\cos\omega_2\tau_1$ to zero, we obtain

$$\begin{aligned}\frac{dA_3}{d\tau_2} &= \frac{1}{2}\left(\xi_2+\frac{\kappa_1\eta_2}{\omega_1^2}\right)A_3 + \frac{1}{8}c_2A_3^3\\ \frac{dB_3}{d\tau_2} &= 0\end{aligned} \tag{5.81}$$

Note that in obtaining this equation, we use the simplifying assumption that the part of the frequency that is amplitude-dependent can be neglected since we only deal with small amplitude motions. Equation (5.81) is the governing equation for A_3 and

B_3. The amplitude equation determines the stability of this particular mode. We will continue our analysis by considering the stability of the nominal conditions based on our results so far.

5.5.1 Local Stability of the Nominal Conditions

To see the stability of the nominal conditions, only the amplitude equations need to be considered. Specifically, for local stability purposes, the linearization of the amplitude equations around the point $(A_1, A_2, A_3) = (0, 0, 0)$ is examined. We refer to this point as the origin, since it is naturally represented by the origin of the $A_1A_2A_3$ axis system. From the previous result, the linearization of the amplitude equations around the origin yields

$$\left\{ \begin{array}{c} \frac{dA_1}{d\tau_2} \\ \frac{dA_2}{d\tau_2} \\ \frac{dA_3}{d\tau_2} \end{array} \right\} = \nabla \left\{ \begin{array}{c} A_1 \\ A_2 \\ A_3 \end{array} \right\} \tag{5.82}$$

where

$$\nabla = \left\{ \begin{array}{ccc} \frac{1}{2}\mu & 0 & 0 \\ 0 & \frac{1}{2}\nu & 0 \\ 0 & 0 & \frac{1}{2}\vartheta \end{array} \right\} \tag{5.83}$$

with $\vartheta = \left(\xi_2 + \frac{\kappa_1\eta_2}{\omega_1^2}\right)$. The eigenvalues of the Jacobian ∇ at the origin are given by $\frac{1}{2}\mu$, $\frac{1}{2}\nu$, and $\frac{1}{2}\vartheta$.

From the linear stability theory, the nominal condition is locally stable if $\mu < 0$, $\nu < 0$, and $\vartheta < 0$. If at least one of these three parameters becomes positive, the nominal condition is unstable. Note, however, that if one of the parameters is zero while the others are negative, the stability of the system is cannot be concluded from this linear representation. In this case, one has to examine the stability of the system by including the nonlinear terms.

In the rest of the discussion we assume $\nu < 0$, that is positive damping in pitch motion. Therefore, pitch motion is always stable in the subsequent treatment. We limit the current study on the effects of stable pitch motion on the wing rock dynamics, because that is what we will normally find in real life situation.

5.5.2 Center Manifold Reduction and Bifurcation Analysis

This analysis is performed on the amplitude equations of the system. The purpose is to find the branching of the system equilibria and to examine if periodic solutions exist in the system.

We first look at the A_3 equation given in (5.81), which is uncoupled to the other amplitude equations. For conventional aircraft, the coefficient c_2 can be approximated very well using

$$c_2 = -\frac{n_1 n_3}{n_2} d_2 \tan \alpha_0 \tag{5.84}$$

Note that in the above equation n_i's are positive. and $\tan \alpha_0$ are positived_2 is the dominant contribution to the pitch damping parameter. As we have stated previously, we only consider the case where $\nu < 0$, and $\nu = \frac{\bar{q}c}{I_{yy}}(d_2 + d_3)$ (from the definition of ν). The coefficients d_2 and d_3 depend on the stability derivatives C_{m_q} and $C_{m_{\dot{\alpha}}}$, respectively. In most situation, the contribution of $C_{m_{\dot{\alpha}}}$ to ν is much smaller than C_{m_q}. Therefore, the sign of ν is mostly contributed by d_2. The assumption that $\nu < 0$ almost always implies that $d_2 < 0$. Therefore, we assume d_2 be negative here and for the rest of the discussion. This then implies that $c_2 > 0$.

The equilibria for the A_3 equation consists of $A_3 = 0$ and $A_3 = \sqrt{-\frac{4\vartheta}{c_2}}$, where $\vartheta = \left(\xi_2 + \frac{\kappa_1 \eta_2}{\omega_1^2}\right)$ In $A_3 - \vartheta$ diagram, the equilibria of the equation consist of the ϑ-axis and the parabola $\vartheta = \frac{1}{4} c_2 A_3^2$. The linearization of the equation about the equilibria at $A_3 = 0$ is

$$\frac{dA_3}{d\tau_2} = \frac{1}{2}\vartheta A_3 \tag{5.85}$$

It is clear that the eigenvalue of the linearized equation in this case is $\frac{1}{2}\vartheta$, which is positive for $\vartheta > 0$ and negative for $\vartheta < 0$. In other words, around the equilibrium $A_3 = 0$, this specific mode is stable if $\vartheta < 0$ and unstable if $\vartheta > 0$. About the equilibria at $\vartheta = -\frac{1}{4} c_2 A_3^2$, the linearization of the equation is given by

$$\frac{dA_3}{d\tau_2} = -\vartheta A_3 \tag{5.86}$$

The eigenvalue of this linearized equation is $-\vartheta$, which is positive for $\vartheta < 0$ and negative for $\vartheta > 0$. Physically this means that the equilibria $\vartheta = -\frac{1}{4} c_2 A_3^2$ are stable for $\vartheta > 0$ and unstable for $\vartheta < 0$. This is summarized in the bifurcation diagram depicted in Figure 5-2, which is a subcritical Hopf bifurcation. The only stable

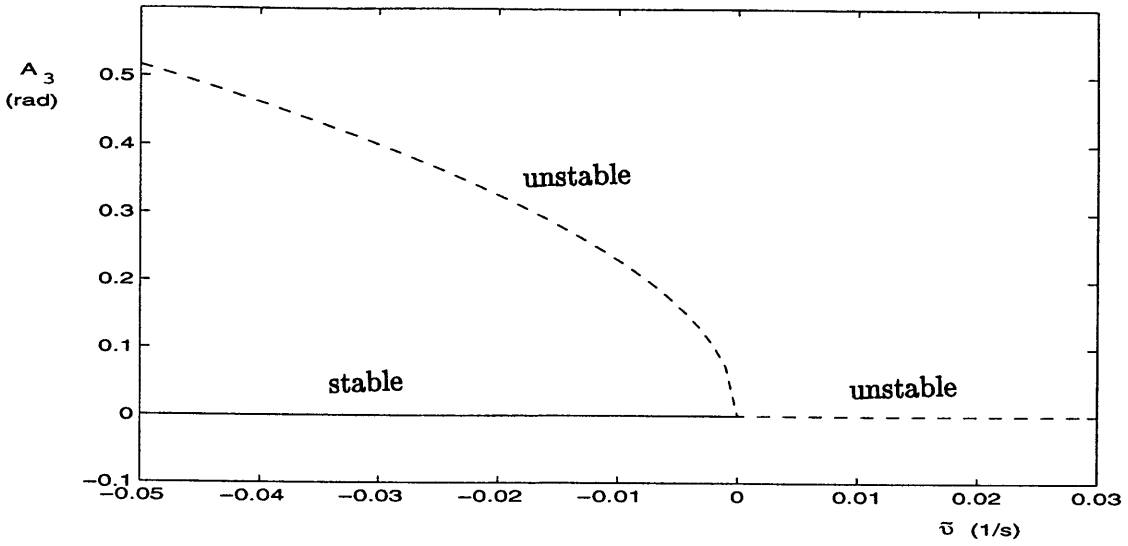

Figure 5-2: Bifurcation diagram for A_3 equation

branch of equilibria is the the one on the negative ϑ-axis. The nominal condition of the aircraft is stable when $\vartheta < 0$. The aircraft motion diverges when $\vartheta > 0$.

Next we consider the coupled A_1 and A_2 equations as given in (5.55) and (5.58), as follows.

$$\begin{aligned} \frac{dA_1}{d\tau_2} &= \frac{\mu}{2}A_1 + p_1 A_1^3 + p_2 A_1 A_2^2 \\ \frac{dA_2}{d\tau_2} &= \frac{1}{2}\nu A_2 + q_1 A_2^3 + q_2 A_1^2 A_2 \end{aligned} \tag{5.87}$$

We consider the case where μ is small but not zero. The case where $\mu = 0$ can be treated in the same way as described in Chapter 4. However, since this is a very degenerate situation, we will not discuss it further here. We will focus on the case where $\mu \neq 0$. To put Equation (5.87) into the center manifold analysis framework, μ is treated as a trivial dependent variable, as follows.

$$\begin{aligned} \frac{dA_1}{d\tau_2} &= \frac{1}{2}\mu A_1 + p_1 A_1^3 + p_2 A_1 A_2^2 \\ \frac{dA_2}{d\tau_2} &= \frac{1}{2}\nu A_2 + q_1 A_2^3 + q_2 A_1^2 A_2 \\ \frac{d\mu}{d\tau_2} &= 0 \end{aligned} \tag{5.88}$$

Note that in this formulation, the term $\frac{1}{2}\mu A_1$ is considered nonlinear. The equilibrium

point of interest is the origin $(A_1, A_2, \mu) = (0, 0, 0)$. The linearization of the system (4.56) around the origin results in

$$\begin{aligned} \frac{dA_1}{d\tau_2} &= 0 \\ \frac{dA_2}{d\tau_2} &= \frac{1}{2}\nu A_2 \\ \frac{d\mu}{d\tau_2} &= 0 \end{aligned} \tag{5.89}$$

The eigenvalues of this linearized system are 0, ν, and 0. By the assumption $\nu < 0$, the A_2-axis is a stable manifold. It is clear then that $A_2 = 0$, that is the $A_1 - \mu$ plane, is the center manifold of the system. The reduced system is then given by

$$\begin{aligned} \frac{dA_1}{d\tau_2} &= \frac{1}{2}\mu A_1 + p_1 A_1^3 \\ \frac{d\mu}{d\tau_2} &= 0 \end{aligned} \tag{5.90}$$

The equilibria of this system consist of the μ-axis and the parabola $\mu = -2p_1 A_1^2$. Since $\frac{d\mu}{d\tau_1} = 0$, the planes $\mu = constant$ are invariant. In a plane $\mu = constant \neq 0$, all of the equilibria are of hyperbolic type, and so their local stability properties can be assessed by looking at the eigenvalues of the linearized systems around the equilibria. The linearized system around the equilibria at μ-axis for $\mu = constant \neq 0$ is

$$\begin{Bmatrix} \frac{dA_1}{d\tau_2} \\ \frac{dA_2}{d\tau_2} \end{Bmatrix} = \begin{Bmatrix} \frac{1}{2}\mu & 0 \\ 0 & \frac{1}{2}\nu \end{Bmatrix} \begin{Bmatrix} A_1 \\ A_2 \end{Bmatrix} \tag{5.91}$$

The eigenvalues of the system are $\frac{1}{2}\mu$ and $\frac{1}{2}\nu$. Since ν is assumed to be negative, then the equilibria at μ-axis is asymptotically stable if $\mu < 0$ and unstable if $\mu > 0$. Similarly, the linearized system around the equilibria $\mu = -2p_1 A_1^2$ for $\mu = constant \neq 0$ is given by

$$\begin{Bmatrix} \frac{dA_1}{d\tau_2} \\ \frac{dA_2}{d\tau_2} \end{Bmatrix} = \begin{Bmatrix} -\frac{1}{2}\mu & 0 \\ 0 & \frac{1}{2}\nu \end{Bmatrix} \begin{Bmatrix} A_1 \\ A_2 \end{Bmatrix} \tag{5.92}$$

Here, the eigenvalues of the system are $-\frac{1}{2}\mu$ and $\frac{1}{2}\nu$. Hence, the equilibria at $\mu = -2p_1 A_1^2$ are asymptotically stable for $\mu > 0$ and unstable if $\mu < 0$.

The bifurcation diagrams depicting the above description are given in Figure 5-3.

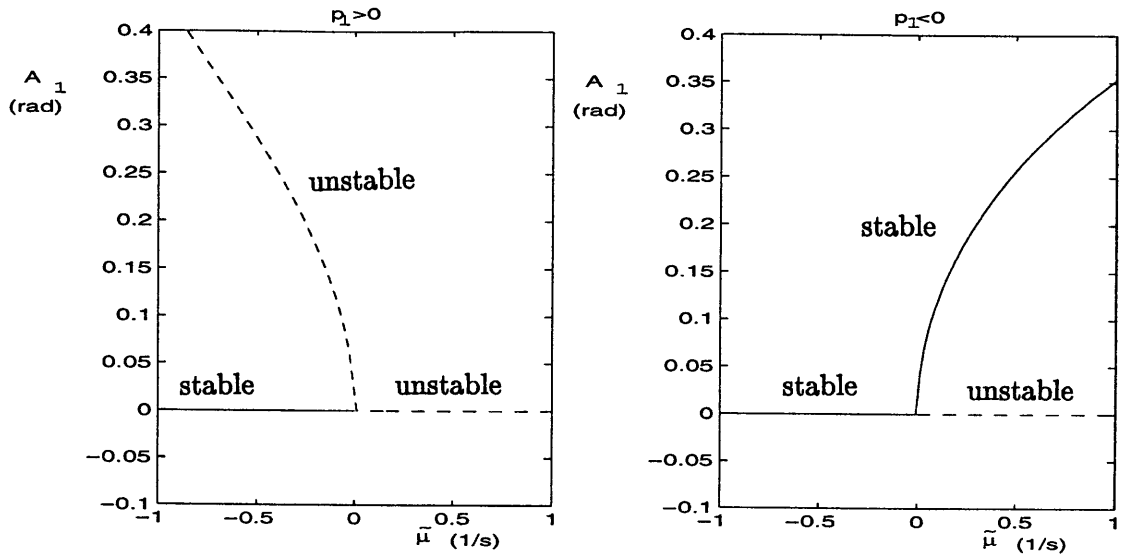

Figure 5-3: Bifurcation diagrams for (a) $p_1 > 0$ and (b) $p_1 < 0$

These diagrams show that there is a finite amplitude oscillation of limit cycle type appearing and dissappearing in the system as μ varies across $\mu = 0$ (Hopf bifurcation). However, only for $p_1 < 0$, the system sustains a stable limit cycle. Physically, this means that only for this situation, the sustained wing rock motion can exist.

In case where the stable limit cycle exists in the system, the amplitude of the limit cycle or in other words the amplitude of the wing rock motion is given by

$$A_1 = \sqrt{-\frac{\mu}{2p_1}} \tag{5.93}$$

The above analysis can be interpreted as a steady-state analysis. This implies that after some transient, the amplitudes A_1 and A_2 eventually reach the steady-state values $A_1 = \sqrt{-\frac{\mu}{2p_1}}$ and $A_2 = 0$. The steady-state correction to the phase then can be calculated from the last two equations in (4.43), which in this case become

$$\begin{aligned} \frac{dB_1}{d\tau_2} &= -p_3 \frac{\mu}{2p_1} \\ \frac{dB_2}{d\tau_2} &= -q_3 \frac{\mu}{2p_1} \end{aligned} \tag{5.94}$$

These equations can easily be integrated to obtain

$$\begin{aligned} B_1 &= -p_3 \frac{\mu}{2p_1} \tau_1 \\ B_2 &= -q_3 \frac{\mu}{2p_1} \tau_1 \end{aligned} \tag{5.95}$$

5.5.3 Analytical Approximation of the Solutions

The analytical solutions of the system are derived here from the amplitude and phase-correction equations obtained earlier. We start by considering the amplitude equation A_3, since this is the easiest and it is not coupled with the other amplitude or phase equations. Multiplying both sides of Equation (5.81) with A_3, we get

$$\begin{aligned} & A\frac{dA_3}{d\tau_2} = \frac{1}{2}\vartheta A_3^2 + \frac{1}{8}c_2 A_3^4 \\ \Leftrightarrow \quad & \frac{dA_3^2}{d\tau_2} = \vartheta A^2 + \frac{1}{4}c_2 A_3^4 \end{aligned} \tag{5.96}$$

By separating the variables and then integrating both sides of the equation, we obtain

$$\begin{aligned} & \frac{dA_3^2}{A_3^2\left(\vartheta + \frac{1}{4}c_2 A_3^2\right)} = d\tau_2 \\ \Leftrightarrow \quad & \int \left(\frac{\frac{1}{\vartheta}}{A_3^2} - \frac{\frac{c_2}{4\vartheta}}{\vartheta + \frac{1}{4}c_2 A_3^2} \right) dA_3^2 = \int d\tau_2 \\ \Leftrightarrow \quad & \frac{A_3^2}{\vartheta + \frac{1}{4}c_2 A_3^2} = K_1 \exp(\vartheta \tau_2) \end{aligned} \tag{5.97}$$

Expressing A_3 explicitly, we find

$$A_3 = \frac{\sqrt{K_1 \vartheta}\exp(\frac{\vartheta}{2}\tau_2)}{\sqrt{1 - \frac{1}{4}K_1 c_2 \exp(\vartheta \tau_2)}} \tag{5.98}$$

where K_1 is a constant determined from the initial condition.

Examination of the properties of the A_3 solution follows. If we talk about A_3 as departure from the equilibrium condition, then from (5.97), $K_1 < 0$ for $\vartheta < 0$ and $K_1 > 0$ for $\vartheta > 0$. Note that the assumption $c_2 > 0$ is imbedded in the previous statement. For $\vartheta < 0$, the numerator of Equation (5.98) goes to zero as $\tau_2 \to \infty$. Therefore, $A_3 \to 0$ as $\tau_2 \to \infty$. For $\vartheta > 0$, the denominator of Equation (5.98) becomes smaller as τ_2 increases, while the value of the numerator increases. Hence,

A_3 increases as τ_2 increases and at some τ_2, $A_3 \to \infty$. In other words, the solution diverges for $\vartheta > 0$.

Next we consider the coupled $A_1 - A_2$ equation. As in the previous chapter, Gronwall's lemma can be used to justify the approximation of A_2 in the following form.

$$\bar{A}_2(\tau_2) = A_{2_0} \exp(\frac{1}{2}\nu\tau_1) \tag{5.99}$$

Using this approximation for A_2, we are left with the following equation

$$\frac{dA_1}{d\tau_2} = a(\tau_2)A_1 + p_1 A_1^3 \tag{5.100}$$

where

$$a(\tau_1) = \frac{1}{2}\mu + p_2 A_{2_0}^2 \exp(\nu\tau_2) \tag{5.101}$$

Again, as in Chapter 4, the exact solution of Equation (5.100) can be derived. Since the derivation is the same, it is not repeated here. The result is as follows.

$$A_1 = \frac{\exp(\int a(\tau_2)d\tau_2)}{\sqrt{K_2 - 2p_1 \int \exp(2\int a(\tau_2)d\tau_2)d\tau_2}} \tag{5.102}$$

The constant K_2 depends on the initial condition. The integral $\int \exp(2\int a(\tau_2)d\tau_2)d\tau_2$ is not simple to obtain since $a(\tau_2)$ also contains an exponential term. However, for integration limit from 0 to τ_2, the integral has the following properties.

$$\int_0^{\tau_2} \exp(2\int_0^{\tau_2} a(\tau_2)d\tau_2)d\tau_2 = 0 \quad ; \quad \tau_2 = 0 \tag{5.103}$$

$$\int_0^{\tau_2} \exp(2\int_0^{\tau_2} a(\tau_2)d\tau_2)d\tau_2 \approx \frac{2}{\mu}\exp(\frac{\mu}{2}\tau_2) \quad ; \quad \tau_2 \gg 1 \tag{5.104}$$

As $\tau_1 \to \infty$,

$$\begin{aligned} \exp(\frac{\mu}{2}\tau_2) &\to 0 \ \ for\ \mu < 0 \\ \exp(\frac{\mu}{2}\tau_2) &\to \infty \ \ for\ \mu > 0 \end{aligned} \tag{5.105}$$

Based on this, we obtain

$$\begin{aligned} A_1 &\to 0 \quad for\ \mu < 0 \\ A_1 &\to \sqrt{-\frac{\exp(\mu\tau_1)}{2\frac{p_1}{\mu}\exp(\mu\tau_1)}} = \sqrt{-\frac{\mu}{2p_1}} \quad for\ \mu > 0 \end{aligned} \tag{5.106}$$

5.6 Comparison With Numerical Results

To demonstrate the accuracy of the analytical prediction, comparison with numerical results is shown in this section. As before, a generic fighter aircraft model is used for this purpose. The parameters and the nonlinear aerodynamic models for this aircraft are given in Table 5.1. For this aircraft the variations of the parameters μ, p_1, and ϑ with the nominal angle-of-attack are shown in Figure 5-4. We can see from the figure that the onset of wing rock ($\mu = 0$) in this case is 29.23^o.

$I_{xx} = 36610\ kg\,m^2$ $\qquad$ $b = 12\ m$
$I_{yy} = 162700\ kg\,m^2$ $\qquad$ $c = 4.8\ m$
$I_{zz} = 183000\ kg\,m^2$ $\qquad$ $S = 164.6\ m^2$
$I_{xz} = 6780\ kg\,m^2$
$\rho = 1.225\ kg/m^3$
$V = 100\ m/s$

$$
\begin{aligned}
C_l = {} & (-1.18\alpha_0 + 0.79\alpha_0^2)\beta + 0.4\beta^3 - 0.08\alpha\beta + 0.236\alpha^2\beta - 0.1\beta p \\
& +(-0.22 + 0.63\alpha_0 + 0.797\alpha_0^2 + 0.975\alpha_0^3)p - 0.006p^3 \\
& -1.42\beta^2 p + 0.56\alpha p + 0.09\alpha^2 p + 0.5\beta q - 3\alpha\beta q \\
& -0.011\dot{\beta} + 1.6\alpha\dot{\beta} - 6.1\alpha^2\dot{\beta} + 0.05r - 0.03\beta^2 r \\
& +0.1r^3 + 1.43\alpha r + 2.29\alpha^2 r \\
C_m = {} & -0.68\alpha - 0.75\alpha^2 - 3.75\alpha^3 + 0.1p^2 - 8.02\alpha\beta + 0.26\beta^2 \\
& +0.1\beta p + 5\alpha\beta p - 2q + 0.58\alpha q + 3.564\alpha^2 q + 0.1q^2 \\
& -0.5\dot{\alpha} + 0.5\beta r \\
C_n = {} & 0.25\beta - 0.19\alpha\beta - 0.7\alpha^2\beta - 0.025\beta^3 + 0.1p + 0.02p^3 - 3.19\beta^2 p \\
& -0.07\alpha p + 2.8\alpha^2 p - 0.3r - 2\beta^2 r - 0.01r^3 + \alpha r - 3.19\alpha^2 r \\
& -0.1\dot{\beta} - 0.2\beta q + 0.5\alpha\beta q
\end{aligned}
$$

Table 5.1: Generic fighter aircraft parameters for $10^o \leq \alpha_0 \leq 50^o$

We first examine the accuracy of the wing rock onset prediction. As before, this is done by simulating the aircraft response slightly above and slightly below the onset point. From Figure 5-4, the wing rock onset is at $\alpha_0 = 29.23^o$. Numerical simulations of the aircraft response at $\alpha_0 = 29.1^o$ and $\alpha_0 = 29.4^o$ are depicted in Figure 5-5. Stable response for nominal angle-of-attack below the onset and wing rock response for nominal angle-of-attack above the onset are observed. This shows that the analytical result is accurate in predicting the onset of wing rock from the model.

Comparison of the analytical and numerical results for $\alpha_0 = 31^o$ is given in Figure 5-6. The analytical result predicts the amplitude history and the limit cycle frequency very well. The existence of the new equilibrium and sustained oscillation in the longitudinal mode with frequency twice of the lateral motion is correctly pre-

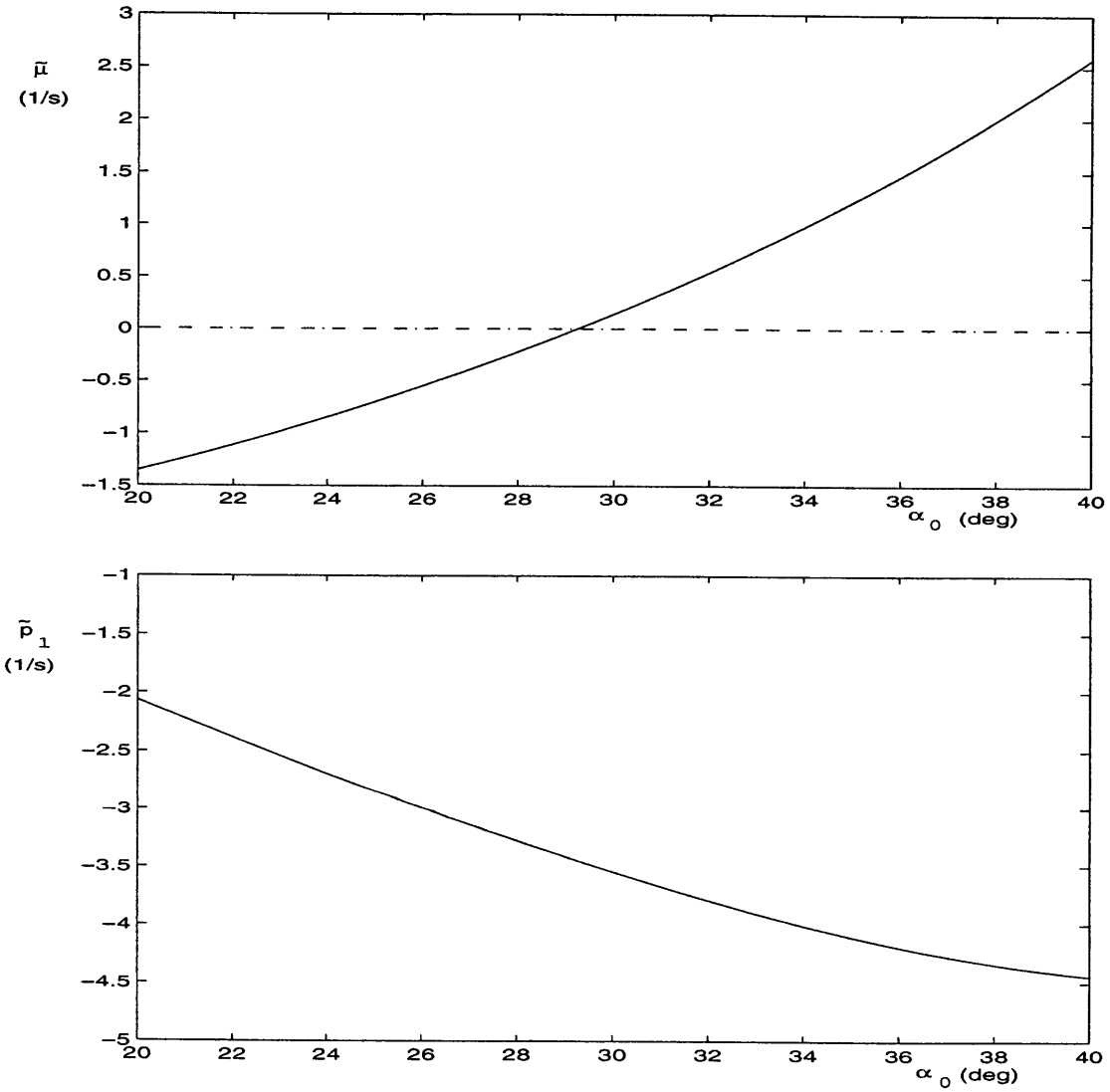

Figure 5-4: Variation of $\tilde{\mu}$ and $\tilde{p}_1$ with α_0

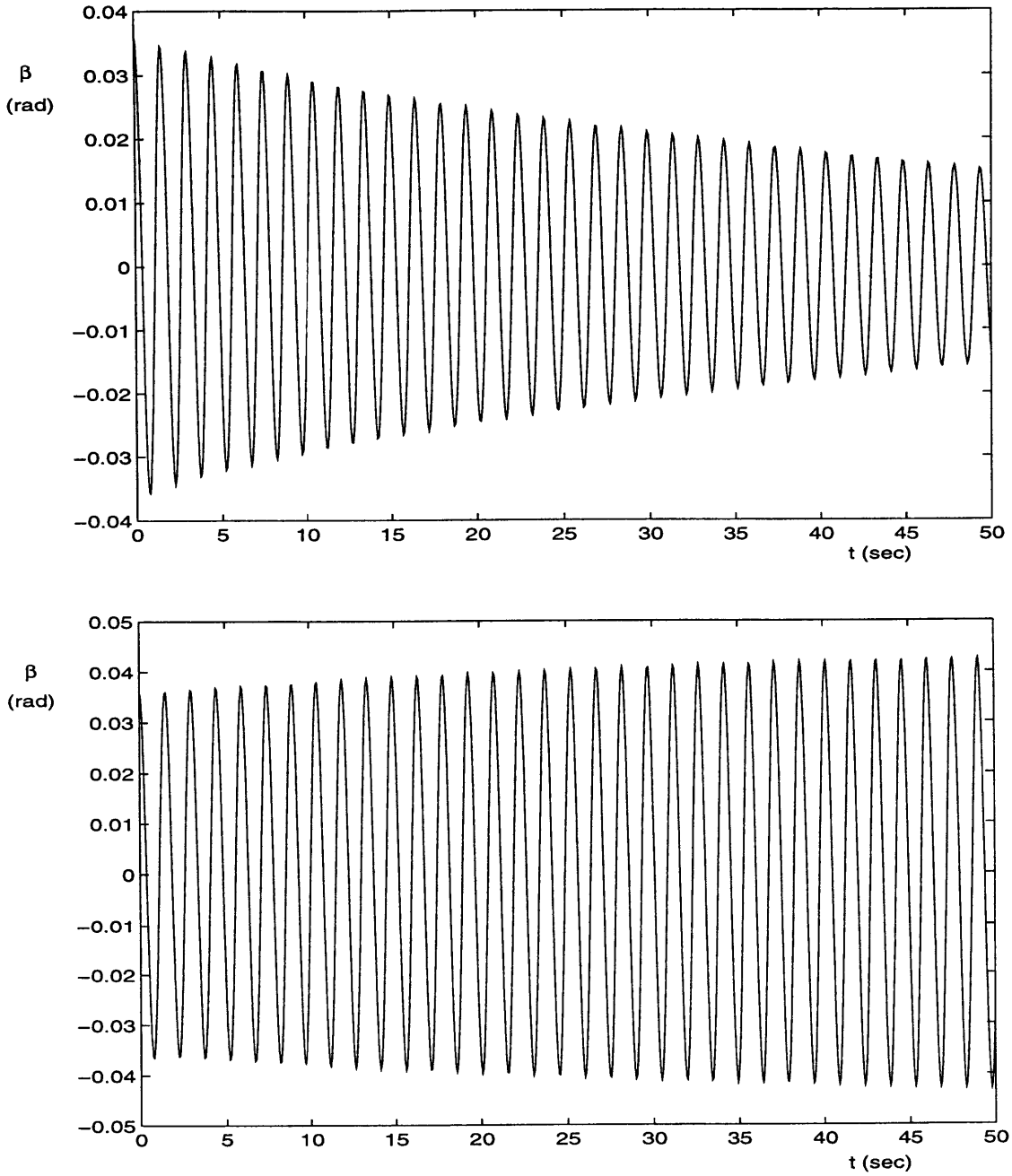

Figure 5-5: Aircraft response for $\alpha_0 = 29.1^o$ and $\alpha_0 = 29.4^o$

dicted by the analytical approximation. Also note that initially the roll motion is not symmetrical about its equilibrium. This asymmetry is caused by the presence of the third mode in the system ($C(t)$). To see specifically this particular mode, we plot this mode together with the overall roll response of the aircraft in Figure 5-7. This mode is slower than the other modes of the aircraft, which is also predicted correctly by the analytical method.

The above examples demonstrate that the analytical analysis is able to predict the dynamics of the aircraft accurately. Considering that we start with a very complicated aircraft model, these results show the power of the analysis. More importantly, the analysis obtains solution in parametric forms, which are very useful in assessing the effects of aircraft parameters on the overall aircraft dynamics. Unlike numerical analysis, this analytical technique enables us to see explicitly the dependence of the resulting aircraft dynamics on the system parameters. To gain a better understanding on the wing rock mechanism in this three degrees-of-freedom case, energy exchange concept will be utilized next.

5.6.1 Energy Exchange Concept

For this three degrees-of-freedom case, the change in aerodynamic energy during a certain time interval is given by

$$\Delta E = \int_{t_1}^{t_2} \left(qSbC_l(t)\dot{\phi}(t) + qScC_m(t)\dot{\theta}(t) + qSbC_n(t)\dot{\psi}(t) \right) dt \tag{5.107}$$

By changing the integration variables, the above equation can be written as

$$\Delta E = \int_{C_\phi} qSbC_l(\phi)d\phi + \int_{C_\theta} qScC_m(\theta)d\theta + \int_{C_\psi} qSbC_n(\psi)d\psi \tag{5.108}$$

where C_ϕ, C_θ, and C_ψ are the curves of C_l versus ϕ, C_m versus θ, and C_n versus ψ for $t_1 \leq t \leq t_2$, respectively (histograms). The net energy change over a cycle is given by

$$\Delta E = \oint_{C_\phi} qSbC_l(\phi)d\phi + \oint_{C_\theta} qScC_m(\theta)d\theta + \oint_{C_\psi} qSbC_n(\psi)d\psi \tag{5.109}$$

In wing rock situation, C_ϕ, C_θ, and C_ψ are closed curves and the net aerodynamic energy exchange in a cycle is directly proportional to the areas contained within the histogram loops. As a remainder, for a clockwise loop, $\Delta E > 0$ or, in other words, energy is added to the system (destabilizing). Conversely, for a counter-clockwise loop, $\Delta E < 0$, which indicates that energy is extracted from the system (stabilizing).

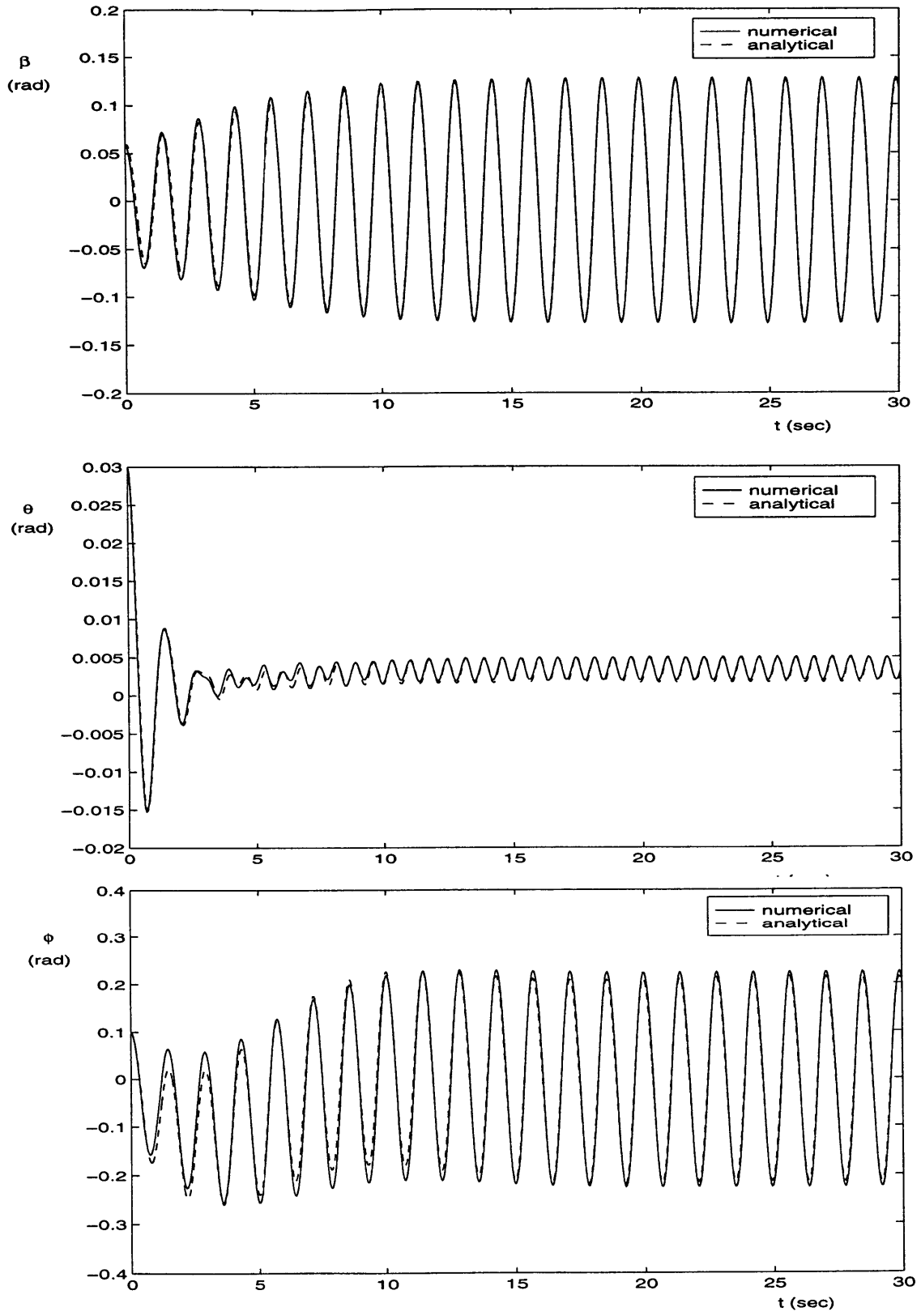

Figure 5-6: Aircraft response at $\alpha_0 = 31^o$ and initial condition $(\beta_0, \phi_0, \theta_0) = (0.058, 0.1, 0.03)$ rad

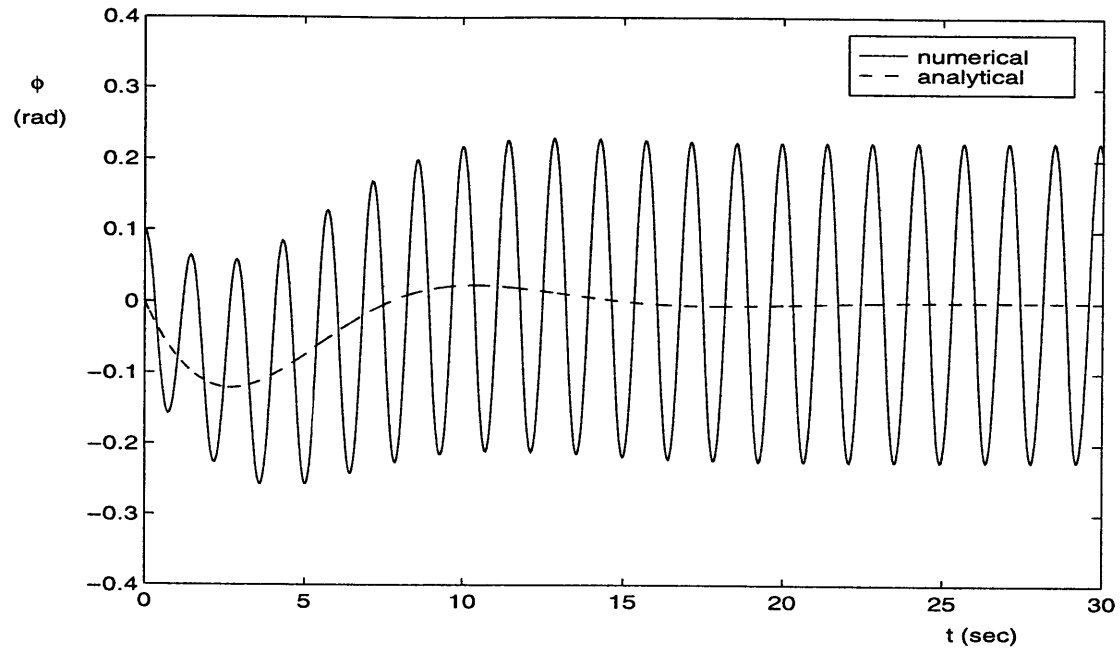

Figure 5-7: Third mode of the motion compared to roll response at $\alpha_0 = 31^o$

In a free wing rock motion, the system is in energy balance, hence $\Delta E = 0$.

The histograms of the aircraft model for one cycle of wing rock at $\alpha_0 = 31^o$ are depicted in Figure 5-8. In the histogram C_l vs ϕ, there is a destabilizing loop for small roll angles ($\phi < 0.1$ rad). For roll angles larger than 0.1 rad, stabilizing loops appear in the system. It can also be observed from the figure that the area inside the stabilizing loops is larger than the area inside the destabilizing loop. Hence, the balance of energy is not achieved by this mode alone. The destabilizing loops from the other modes (see Figure 5-8) help in achieving the energy balance needed for a sustained wing rock motion.

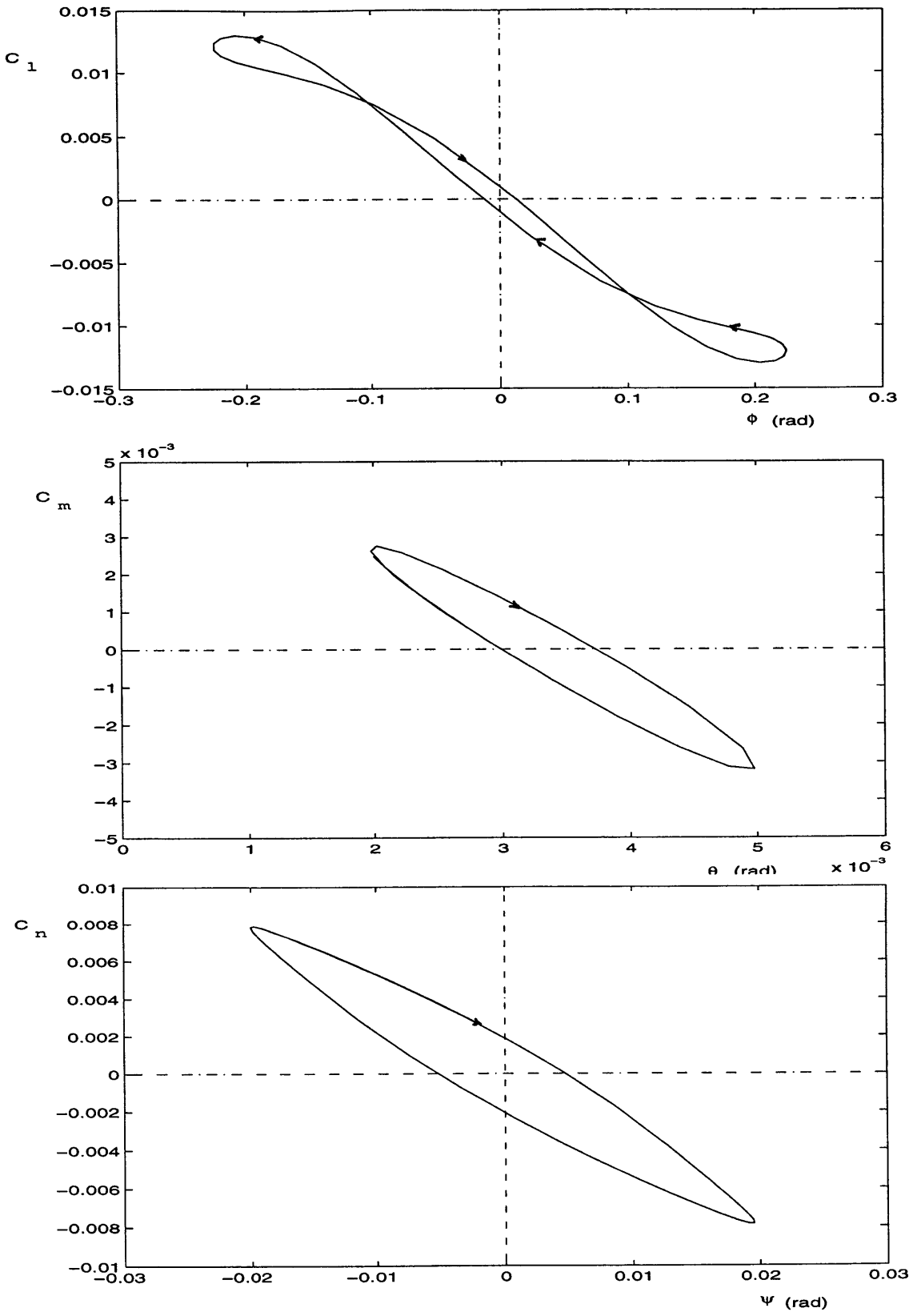

Figure 5-8: Histograms for one cycle of wing rock motion at $\alpha_0 = 31^o$

5.7 Effects of Specific Types of Aerodynamic Nonlinearity

5.7.1 Nonlinear Variations of Lateral Damping Derivatives with Angle-of-Sideslip

To examine specifically the effects of the lateral damping derivatives with the angle-of-sideslip, we consider a simplified aircraft model with negligible nonlinearity due to inertia and has the following aerodynamic moments.

$$\begin{aligned} L &= L_p(\beta)p + L_{\beta_0}\beta + L_{r_0}r + L_{\dot{\beta}_0}\dot{\beta} \\ M &= M_{q_0}q + M_{\alpha_0}\alpha + M_{\dot{\alpha}_0}\dot{\alpha} \\ N &= N_r(\beta)r + N_{\beta_0}\beta + N_{p_0}p + N_{\dot{\beta}_0}\dot{\beta} \end{aligned} \tag{5.110}$$

In the above equations, stability derivatives with subscript *0* are constant for specific angle-of-attack. The roll and yaw damping derivatives are not constant, they are functions of the angle-of-sideslip. As can be expected from basic aerodynamic considerations, the variations of these damping derivatives should be symmetrical with respect to zero angle-of-sideslip. This is confirmed in delta wing experiment (Figure 3-10) for roll damping derivative variation with angle-of-sideslip. In this analysis, we assume

$$\begin{aligned} L_p(\beta) &= L_{p_0} + L_{p_1}\beta^2 \\ N_r(\beta) &= N_{r_0} + N_{r_1}\beta^2 \end{aligned} \tag{5.111}$$

where L_{p_0}, L_{p_1}, N_{r_0} and N_{r_1} are all constants. Note from Equation (5.110) that since the nonlinearity due to inertia is neglected, the longitudinal and the lateral equations of motion become uncoupled. Because we always assume stable longitudinal motion, then we can look only at the lateral equations in this analysis.

Comparing Equation (5.110) with Equation (5.20), the following correspondence is observed.

$$\begin{aligned} [\bar{c}_1\ \bar{c}_2\ \bar{c}_3\ \bar{c}_4\ \bar{c}_6] &\equiv [L_{\beta_0}\ L_{p_0}\ L_{\dot{\beta}_0}\ L_{r_0}\ L_{p_1}] \\ [\bar{d}_1\ \bar{d}_2\ \bar{d}_3] &\equiv [M_{\alpha_0}\ M_{q_0}\ M_{\dot{\alpha}_0}] \\ [\bar{e}_1\ \bar{e}_2\ \bar{e}_3\ \bar{e}_4\ \bar{e}_8] &\equiv [N_{\beta_0}\ N_{p_0}\ N_{\dot{\beta}_0}\ N_{r_0}\ N_{r_1}] \end{aligned} \tag{5.112}$$

With only the above derivatives present in the system, the lateral equations of motion

become

$$\begin{aligned}
\ddot{\beta} + \omega_1^2 \beta &= \epsilon \left[\eta_1 \dot{\beta} + \kappa_2 \phi + \eta_2 \dot{\phi} + e_6 \beta^2 \dot{\beta} + e_{13} \phi \beta^2 + e_{15} \dot{\phi} \dot{\beta}^2 \right] \\
\ddot{\phi} &= \kappa_1 \beta + \epsilon \left[\kappa_3 \phi + \xi_1 \dot{\phi} + \xi_2 \dot{\beta} + c_6 \beta^2 \dot{\beta} + c_{13} \phi \beta^2 + c_{15} \dot{\phi} \beta^2 \right] \quad (5.113)
\end{aligned}$$

The above set of equations are much simpler than the original complete equations of motion (5.31). By continuing the analysis using the described technique, we will find the following amplitude and phase equations

$$\begin{aligned}
\frac{dA_1}{d\tau_2} &= \frac{\mu}{2} A_1 + p_1 A_1^3 \\
\frac{dB_1}{d\tau_2} &= p_3 + p_4 A_1^2 \\
\frac{dA_3}{d\tau_2} &= \frac{\vartheta}{2} A_3 \qquad (5.114)
\end{aligned}$$

For a more detailed analysis, we express μ, p_1, p_3, and p_4 in terms of the stability derivatives, as follows.

$$\begin{aligned}
\tilde{\mu} &= -\frac{(\sin\alpha_0 - n_3 \cos\alpha_0)(L_{\beta_0} + n_1 N_{\beta_0})}{-\sin\alpha_0 (L_{\beta_0} + n_1 N_{\beta_0}) + \cos\alpha_0 (N_{\beta_0} + n_3 L_{\beta_0})} L_{p_0} + \\
&\left(n_3 - \tan\alpha_0 - \frac{(\sin\alpha_0 - n_3 \cos\alpha_0) \tan\alpha_0 (L_{\beta_0} + n_1 N_{\beta_0})}{-\sin\alpha_0 (L_{\beta_0} + n_1 N_{\beta_0}) + \cos\alpha_0 (N_{\beta_0} + n_3 L_{\beta_0})} \right) L_{r_0} - \\
&\frac{(n_1 \sin\alpha_0 - \cos\alpha_0)(L_{\beta_0} + n_1 N_{\beta_0})}{-\sin\alpha_0 (L_{\beta_0} + n_1 N_{\beta_0}) + \cos\alpha_0 (N_{\beta_0} + n_3 L_{\beta_0})} N_{p_0} + (\sin\alpha_0 - n_3 \cos\alpha_0) L_{\dot{\beta}_0} + \\
&\left(1 - n_1 \tan\alpha_0 - \frac{(n_1 \sin\alpha_0 - \cos\alpha_0) \tan\alpha_0 (L_{\beta_0} + n_1 N_{\beta_0})}{-\sin\alpha_0 (L_{\beta_0} + n_1 N_{\beta_0}) + \cos\alpha_0 (N_{\beta_0} + n_3 L_{\beta_0})} \right) N_{r_0} + \\
&(n_1 \sin\alpha_0 - \cos\alpha_0) N_{\dot{\beta}_0} - \frac{g \cos\alpha_0}{V} \frac{L_{\beta_0} + n_1 N_{\beta_0}}{-\sin\alpha_0 (L_{\beta_0} + n_1 N_{\beta_0}) + \cos\alpha_0 (N_{\beta_0} + n_3 L_{\beta_0})} \\
\tilde{p}_1 &= -\frac{1}{8} \frac{(\sin\alpha_0 - n_3 \cos\alpha_0)(L_{\beta_0} + n_1 N_{\beta_0})}{-\sin\alpha_0 (L_{\beta_0} + n_1 N_{\beta_0}) + \cos\alpha_0 (N_{\beta_0} + n_3 L_{\beta_0})} L_{p_1} + \\
&\frac{1}{8} \left(1 - n_1 \tan\alpha_0 - \frac{(n_1 \sin\alpha_0 - \cos\alpha_0) \tan\alpha_0 (L_{\beta_0} + n_1 N_{\beta_0})}{-\sin\alpha_0 (L_{\beta_0} + n_1 N_{\beta_0}) + \cos\alpha_0 (N_{\beta_0} + n_3 L_{\beta_0})} \right) N_{r_1} \\
\tilde{p}_3 &= \frac{g}{V} \frac{(L_{\beta_0} + n_1 N_{\beta_0})((\sin\alpha_0 n_3 \cos\alpha_0) L_{r_0} - (\cos\alpha_0 - n_1 \sin\alpha_0) N_{r_0}}{(-\sin\alpha_0 (L_{\beta_0} + n_1 N_{\beta_0}) + \cos\alpha_0 (N_{\beta_0} + n_3 L_{\beta_0}))^3} \\
\tilde{p}_4 &= \frac{3}{8} \frac{g}{V} \frac{(L_{\beta_0} + n_1 N_{\beta_0})(-\cos\alpha_0 + n_1 \sin\alpha_0)}{(-\sin\alpha_0 (L_{\beta_0} + n_1 N_{\beta_0}) + \cos\alpha_0 (N_{\beta_0} + n_3 L_{\beta_0}))^{\frac{3}{2}}} \qquad (5.115)
\end{aligned}$$

It is clear from the above representation, that the parameter L_{p_1} affect the value of p_1 only, hence it affects the amplitude of the wing rock oscillation. On the other

hand, N_{r_1} influences not only p_1, but also p_5, therefore it affects both the wing rock amplitude and frequency.

Variation of the wing rock amplitudes with L_{p_1} and N_{r_1} can be examined by looking at the derivatives of the amplitude with respect to those parameters. They are

$$\begin{aligned}
\frac{dA_1}{dL_{p_1}} &= \frac{1}{2}\left(-\frac{\mu}{2p_1}\right)^{\frac{3}{2}}\left(\frac{\mu}{2p_1^2}\right)\left(-\frac{1}{8}\right)\frac{(\sin\alpha_0 - n_3\cos\alpha_0)(L_{\beta_0}+n_1N_{\beta_0})}{-\sin\alpha_0(L_{\beta_0}+n_1N_{\beta_0})+\cos\alpha_0(N_{\beta_0}+n_3L_{\beta_0})} \\
\frac{dA_1}{dN_{r_1}} &= \frac{1}{2}\left(-\frac{\mu}{2p_1}\right)^{\frac{3}{2}}\left(\frac{\mu}{2p_1^2}\right)\frac{1}{8}\Bigg(1 - n_1\tan\alpha_0 - \\
&\qquad \frac{(n_1\sin\alpha_0 - \cos\alpha_0)\tan\alpha_0(L_{\beta_0}+n_1N_{\beta_0})}{-\sin\alpha_0(L_{\beta_0}+n_1N_{\beta_0})+\cos\alpha_0(N_{\beta_0}+n_3L_{\beta_0})}\Bigg)
\end{aligned} \tag{5.116}$$

Using the same reasoning as in the previous chapter, the sign of the above derivatives is determined by the sign of the last factor. The examination of the sign of the last factor is in order. We use the fact that the inertia ratios n_1, n_2, and n_3 are small. Due to this fact, the denominator of the last factor in both equations can be approximated by $-\sin\alpha_0 L_{\beta_0} + \cos\alpha_0 N_{\beta_0}$. For a statically stable aircraft, which is the case considered here, $L_{\beta_0} < 0$ and $N_{\beta_0} > 0$. For the range of angle-of-attack of interest ($0^o \leq \alpha_0 \leq 90^o$), $\sin\alpha_0$ and $\cos\alpha_0$ are both positive. Therefore, for most aircraft, the denominator of the last factors is positive. The numerator of the last factor in the first expression can be approximated by $\frac{-1}{8}\sin\alpha_0 L_{\beta_0}$, which is positive. Hence, the wing rock amplitude increases monotonically with L_{p_1}. The last factor of the second expression in (5.116) can be approximated by $\dfrac{1}{8}\dfrac{-\cot\alpha_0\left(\frac{N_{\beta_0}}{L_{\beta_0}}\right)}{1-\cot\alpha_0\left(\frac{N_{\beta_0}}{L_{\beta_0}}\right)}$. Since for a statically stable aircraft, $\dfrac{N_{\beta_0}}{L_{\beta_0}} < 0$ and $\cot\alpha_0 > 0$ for the range of angle-of-attack of interest, then this factor is also positive. Thus, at specific angle-of-attack, the wing rock amplitude increases monotonically with N_{r_1}. Figure 5-9 shows the variation of the wing rock amplitude for the aircraft model described in the previous section as L_{p_1} and N_{r_1} vary.

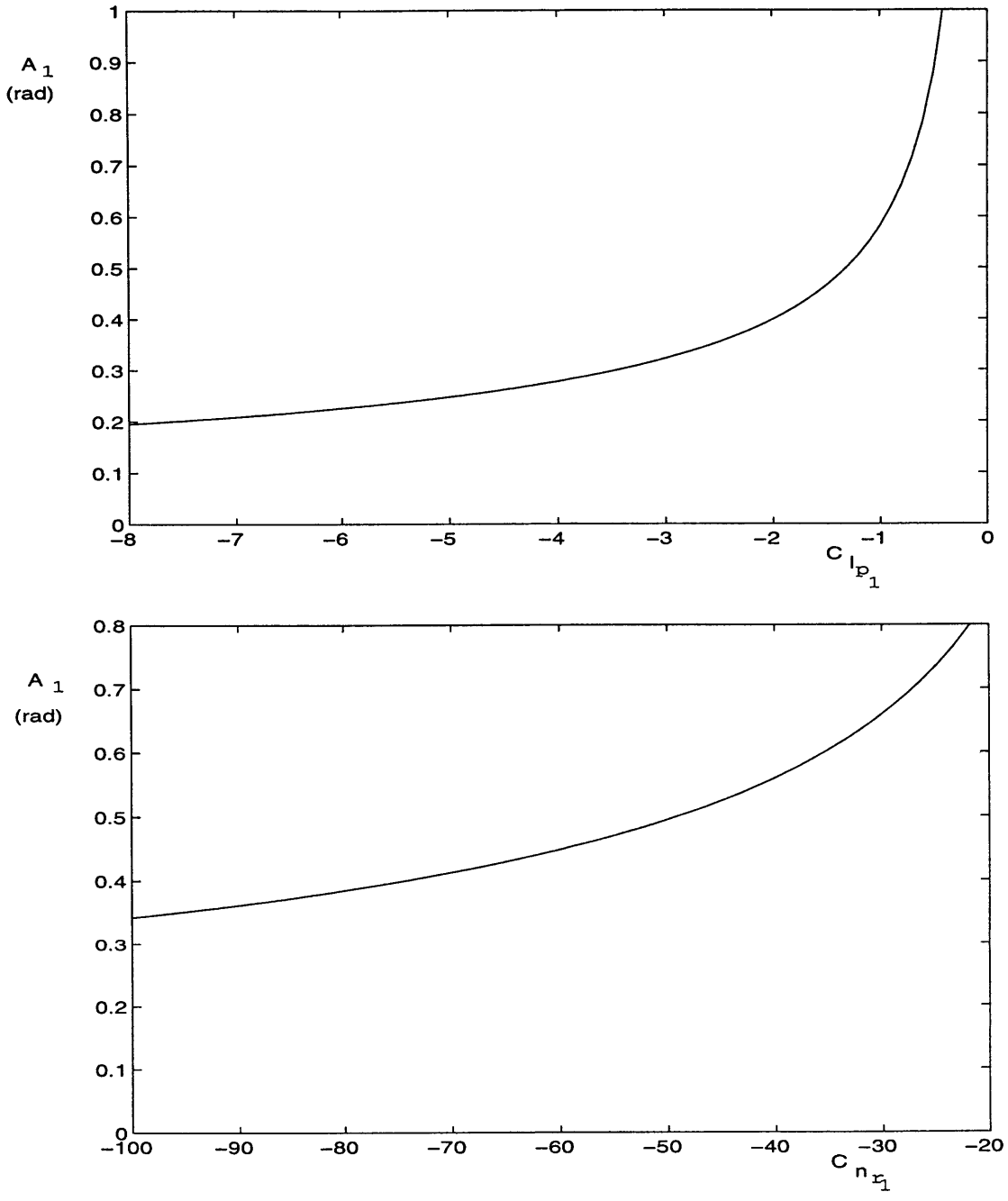

Figure 5-9: Variation of wing rock amplitude with L_{p_1} and N_{r_1}

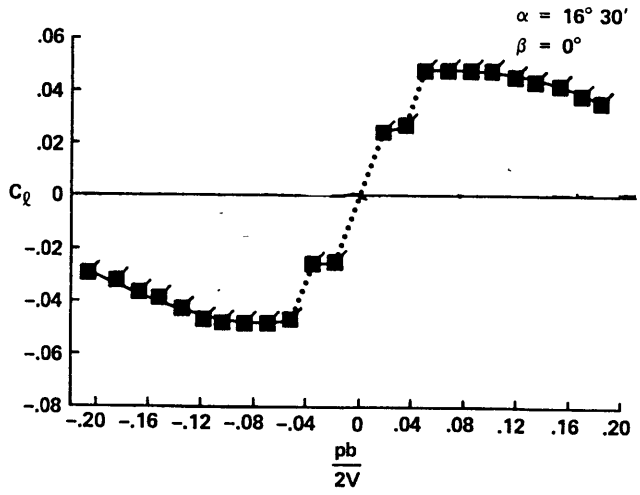

Figure 5-10: Nonlinear variations of rolling moment coefficient with roll rate [45]

5.7.2 Nonlinear Variations of Lateral Moments with Roll Rate

At this subsection, the effects of nonlinear variations of lateral aerodynamic moments with roll rate are examined. Evidence of such nonlinearity has been observed from wind tunnel experiments. Figure 5-10 depicts an example that shows this type of nonlinearity. Although nonlinear variations of lateral moments with yaw rate have also been observed, we will not include this case here, since for the wing rock situation, yaw rate is normally an order of magnitude smaller than roll rate, as can be observed from the example in the previous section.

As before, we consider an aircraft model that possesses only this type of nonlinearity. All other sources of nonlinearity are assumed to be absent. Because of this assumption, the longitudinal and the lateral modes are uncoupled, and so we can look only at the lateral modes of the aircraft in current analysis. In this case, the lateral aerodynamic moments acting on the aircraft are as follows.

$$\begin{aligned} L &= L_{p_0}p + L_{p_2}p^3 + L_{\beta_0}\beta + L_{r_0}r + L_{\dot{\beta}_0}\dot{\beta} \\ N &= N_{p_0}p + N_{p_2}p^3 + N_{\beta_0}\beta + N_{r_0}r + N_{\dot{\beta}_0}\dot{\beta} \end{aligned} \tag{5.117}$$

The lateral equations of motion then become

$$\begin{aligned} \ddot{\beta} + \omega_1^2\beta &= \epsilon\left[\eta_1\dot{\beta} + \kappa_2\phi + \eta_2\dot{\phi} + e_3\phi\dot{\phi}^2 + e_4\dot{\phi}^3 + e_{12}\dot{\phi}^2\dot{\beta}\right] \\ \ddot{\phi} &= \kappa_1\beta + \epsilon\left[\kappa_3\phi + \xi_1\dot{\phi} + \xi_2\dot{\beta} + c_3\phi\dot{\phi}^2 + c_4\dot{\phi}^3 + c_{12}\dot{\phi}^2\dot{\beta}\right] \end{aligned} \tag{5.118}$$

Again, in this case, the form of the amplitude and phase equations are as given

in (5.114), with

$$
\begin{aligned}
\tilde{\mu} &= -\frac{(\sin\alpha_0 - n_3\cos\alpha_0)(L_{\beta_0} + n_1 N_{\beta_0})}{-\sin\alpha_0(L_{\beta_0} + n_1 N_{\beta_0}) + \cos\alpha_0(N_{\beta_0} + n_3 L_{\beta_0})} L_{p_0} + \\
&\left(n_3 - \tan\alpha_0 - \frac{(\sin\alpha_0 - n_3\cos\alpha_0)\tan\alpha_0(L_{\beta_0} + n_1 N_{\beta_0})}{-\sin\alpha_0(L_{\beta_0} + n_1 N_{\beta_0}) + \cos\alpha_0(N_{\beta_0} + n_3 L_{\beta_0})}\right) L_{r_0} - \\
&\frac{(n_1\sin\alpha_0 - \cos\alpha_0)(L_{\beta_0} + n_1 N_{\beta_0})}{-\sin\alpha_0(L_{\beta_0} + n_1 N_{\beta_0}) + \cos\alpha_0(N_{\beta_0} + n_3 L_{\beta_0})} N_{p_0} + (\sin\alpha_0 - n_3\cos\alpha_0) L_{\dot{\beta}_0} + \\
&\left(1 - n_1\tan\alpha_0 - \frac{(n_1\sin\alpha_0 - \cos\alpha_0)\tan\alpha_0(L_{\beta_0} + n_1 N_{\beta_0})}{-\sin\alpha_0(L_{\beta_0} + n_1 N_{\beta_0}) + \cos\alpha_0(N_{\beta_0} + n_3 L_{\beta_0})}\right) N_{r_0} + \\
&(n_1\sin\alpha_0 - \cos\alpha_0) N_{\dot{\beta}_0} - \frac{g\cos\alpha_0}{V}\frac{L_{\beta_0} + n_1 N_{\beta_0}}{-\sin\alpha_0(L_{\beta_0} + n_1 N_{\beta_0}) + \cos\alpha_0(N_{\beta_0} + n_3 L_{\beta_0})} \\
\tilde{p}_1 &= -\frac{3}{8}\frac{(\sin\alpha_0 - n_3\cos\alpha_0)(L_{\beta_0} + n_1 N_{\beta_0}^3}{[-\sin\alpha_0(L_{\beta_0} + n_1 N_{\beta_0} + \cos\alpha_0(N_{\beta_0} + n_3 L_{\beta_0})]^2} L_{p_2} - \\
&\frac{3}{8}\frac{(n_1\sin\alpha_0 - \cos\alpha_0)(L_{\beta_0} + n_1 N_{\beta_0}^3}{[-\sin\alpha_0(L_{\beta_0} + n_1 N_{\beta_0} + \cos\alpha_0(N_{\beta_0} + n_3 L_{\beta_0})]^2} N_{p_2} \\
\tilde{p}_3 &= \frac{g}{V}\frac{(L_{\beta_0} + n_1 N_{\beta_0})((\sin\alpha_0 n_3\cos\alpha_0) L_{r_0} - (\cos\alpha_0 - n_1\sin\alpha_0) N_{r_0}}{(-\sin\alpha_0(L_{\beta_0} + n_1 N_{\beta_0}) + \cos\alpha_0(N_{\beta_0} + n_3 L_{\beta_0}))^3} \\
\tilde{p}_4 &= 0
\end{aligned}
\tag{5.119}
$$

The parameter L_{p_2} affects only p_1, while N_{p_2} affects p_1 and p_5. Therefore, L_{p_2} affects the amplitude of the wing rock oscillations, while N_{p_2} affects both the amplitude and the frequency of the oscillations.

The effects of the parameters L_{p_2} and N_{p_2} on the amplitude of the wing rock motion can be inferred by examining the first derivative of the amplitude with respect to these parameters. They are

$$
\begin{aligned}
\frac{dA_1}{dL_{p_2}} &= \frac{1}{2}\left(-\frac{\mu}{2p_1}\right)^{\frac{3}{2}}\left(\frac{\mu}{2p_1^2}\right)\left(-\frac{3}{8}\right)\frac{(\sin\alpha_0 - n_3\cos\alpha_0)(L_{\beta_0} + n_1 N_{\beta_0})^3}{[-\sin\alpha_0(L_{\beta_0} + n_1 N_{\beta_0}) + \cos\alpha_0(N_{\beta_0} + n_3 L_{\beta_0})]^2} \\
\frac{dA_1}{dN_{p_2}} &= \frac{1}{2}\left(-\frac{\mu}{2p_1}\right)^{\frac{3}{2}}\left(\frac{\mu}{2p_1^2}\right)\left(-\frac{3}{8}\right)\frac{(n_1\sin\alpha_0 - \cos\alpha_0)(L_{\beta_0} + n_1 N_{\beta_0})^3}{[-\sin\alpha_0(L_{\beta_0} + n_1 N_{\beta_0}) + \cos\alpha_0(N_{\beta_0} + n_3 L_{\beta_0})]^2}
\end{aligned}
\tag{5.120}
$$

Again, we will examine the last factors in the above equations, because these factors determine the sign of the derivatives. The denominators of the last factor in both equations are the same and have a positive sign due to the square operation. The terms in the numerator will determine the sign of the expression. By using the facts that the inertia ratios are small, the numerator in the last factor of the first

expression can be approximated by $-\frac{3}{8}\sin\alpha_0 L_{\beta_0}$. Because we are only interested in the statically stable aircraft flying in an angle-of-attack between 0^o and 90^o, then this last factor is positive, which means that increasing L_{p_2} will increase the amplitude of wing rock. Similarly, for the second expression, the numerator of the last factor can be approximated by $\frac{3}{8}\cos\alpha_0 L_{\beta_0}$, which for a statically stable aircraft is negative. This implies that the amplitude of wing rock decreases monotonically with N_{p_2}. Variations of wing rock amplitude with L_{p_2} and N_{p_2} are shown in Figure 5-11.

5.7.3 Nonlinear Variations of Lateral Moments with Angle-of-Sideslip

Figure 5-12 shows an example of nonlinear variations in lateral moment coefficients with respect to angle-of-sideslip. The variations shown in the Figure are typical for fighter aircraft, although the strength of the variations may vary with configurations. As can be seen from the figure, in the simplest way, this nonlinearity can be expressed using cubic polynomial in β. The use of this simple nonlinearity representation leads us to the following lateral moments.

$$\begin{aligned} L &= L_{\beta_0}\beta + L_{\beta_1}\beta^3 + L_{p_0}p + L_{r_0}r + L_{\dot{\beta}_0}\dot{\beta} \\ N &= N_{\beta_0}\beta + N_{\beta_1}\beta^3 + N_{p_0}p + N_{r_0}r + N_{\dot{\beta}_0}\dot{\beta} \end{aligned} \tag{5.121}$$

All other nonlinearities in the system are neglected in current analysis. In this formulation, the longitudinal and the lateral modes of the aircraft become uncoupled and we can analyze the lateral modes separately.

Using the above lateral moments, the lateral equations of motion of the aircraft become (see Appendix E)

$$\begin{aligned} \ddot{\beta} + \omega_1^2\beta &= \epsilon\left[\eta_1\dot{\beta} + \kappa_2\phi + \eta_2\dot{\phi} + e_5\beta^3\right] \\ \ddot{\phi} &= \kappa_1\beta + \epsilon\left[\kappa_3\phi + \xi_1\dot{\phi} + \xi_2\dot{\beta} + c_5\beta^3\right] \end{aligned} \tag{5.122}$$

In this case, we will arrive at the following amplitude and phase-correction equations :

$$\begin{aligned} \frac{dA_1}{d\tau_2} &= \frac{\mu}{2}A_1 \\ \frac{dB_1}{d\tau_2} &= p_3 + p_4 A_1^2 \end{aligned}$$

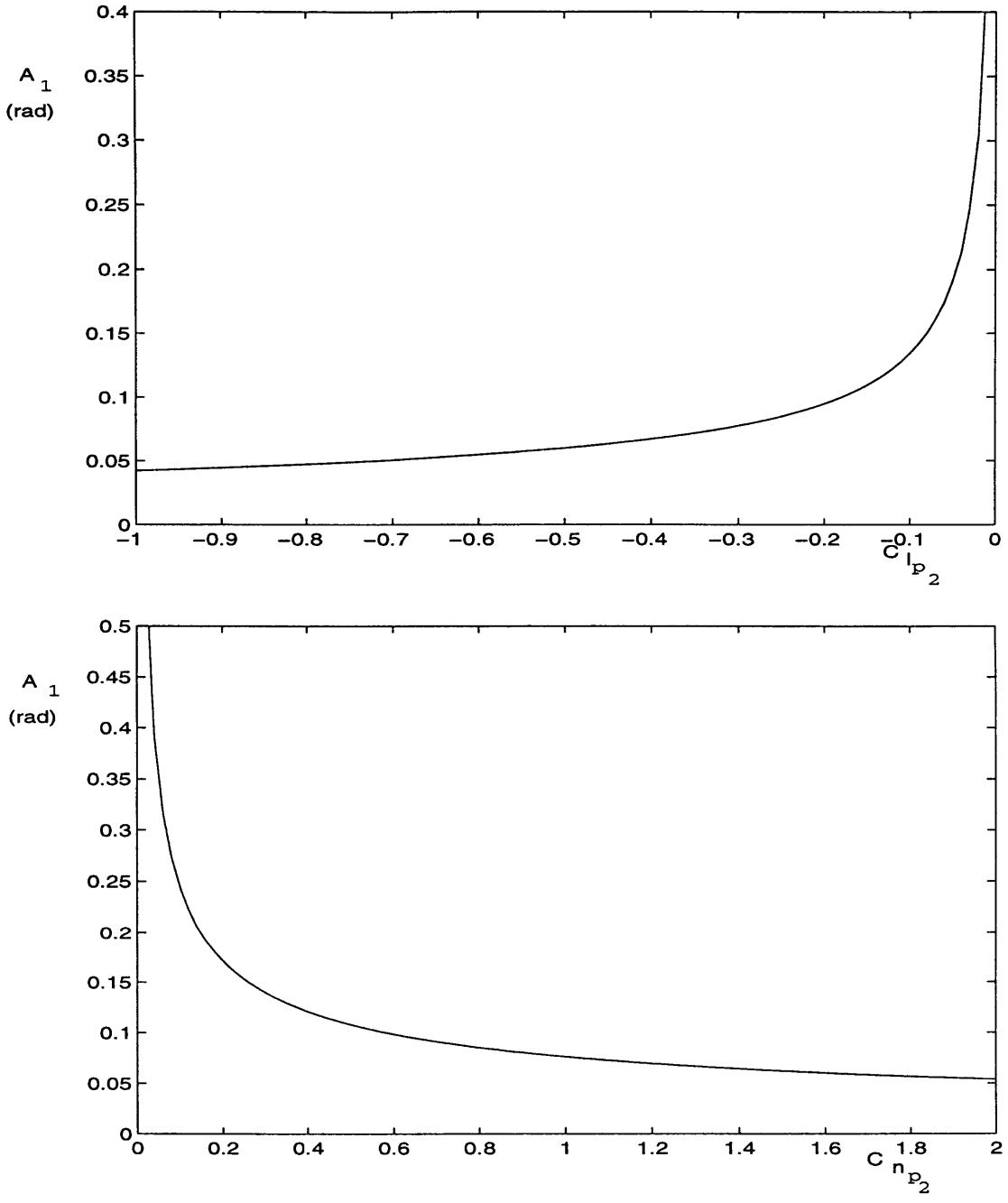

Figure 5-11: Variation of wing rock amplitude with L_{p_2} and N_{p_2}

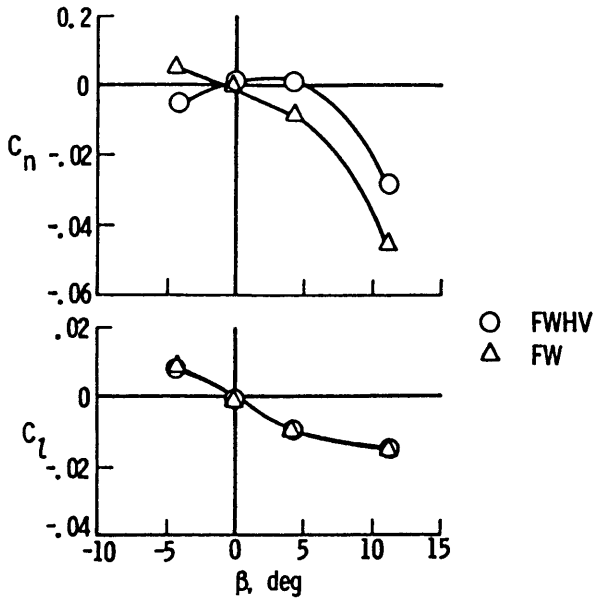

Figure 5-12: Variation of lateral moment coefficients with sideslip [46]

$$\frac{dA_3}{d\tau_2} = \frac{\vartheta}{2}A_3 \tag{5.123}$$

Note that in this case $p_1 = 0$. Hence the amplitude equation for A_1 becomes linear. It is clear then that limit cycles cannot occur in the system. A_1 diverges when $\mu > 0$ and decays to zero when $\mu < 0$. L_{β_1} and N_{β_1} only affect the frequency of the motion.

An interesting case arises when the nonlinearity due to L_{β_1} and N_{β_1} becomes stronger. In this case, we can no longer put the terms $e_5\beta^3$ and $c_5\beta^3$ in the $O(\epsilon)$ group. However, since we only consider small deviations from the nominal conditions, the nonlinearity keeps these terms to be smaller than $O(1)$ terms. This can be formulated mathematically as follows.

$$\begin{aligned} \ddot{\beta} + \omega_1^2\beta &= e_5\beta^3 + \epsilon\left[\eta_1\dot{\beta} + \kappa_2\phi + \eta_2\dot{\phi}\right] \\ \ddot{\phi} &= \kappa_1\beta + c_5\beta^3 + \epsilon\left[\kappa_3\phi + \xi_1\dot{\phi} + \xi_2\dot{\beta}\right] \end{aligned} \tag{5.124}$$

where $0 < \epsilon \ll< 1$. The MTS method can be invoked to the above equation. Three time scales are used in the analysis, as follows.

$$\begin{aligned} t \rightarrow \{\tau_0, \tau_1, \tau_2\} \qquad & \tau_0 = t \\ & \tau_1 = \epsilon^{\frac{1}{2}}t \\ & \tau_2 = \epsilon t \end{aligned} \tag{5.125}$$

The dependent variables are extended as follows

$$\begin{aligned} \beta(t) &\rightarrow \beta(\tau_0, \tau_1, \tau_2) \\ \phi(t) &\rightarrow \phi(\tau_0, \tau_1, \tau_2) \end{aligned} \tag{5.126}$$

By these extensions, Equation (5.124) becomes partial differential equations as follows.

$$\begin{aligned} \frac{\partial^2\beta}{\partial\tau_0^2} &+ \omega_1^2\beta + \epsilon^{\frac{1}{2}}\left(2\frac{\partial^2\beta}{\partial\tau_0\partial\tau_1}\right) + \epsilon\left(2\frac{\partial^2\beta}{\partial\tau_0\partial\tau_2} + \frac{\partial^2\beta}{\partial\tau_1^2}\right) + \epsilon^{\frac{3}{2}}\left(2\frac{\partial^2\beta}{\partial\tau_1\partial\tau_2}\right) + \ldots = \\ & e_5\beta^3 + \epsilon\left(\eta_1\frac{\partial\beta}{\partial\tau_0} + \kappa_2\phi + \eta_2\frac{\partial\phi}{\partial\tau_0}\right) + \epsilon^{\frac{3}{2}}\left(\eta_1\frac{\partial\beta}{\partial\tau_1} + \eta_2\frac{\partial\phi}{\partial\tau_1}\right) + \ldots \\ \frac{\partial^2\phi}{\partial\tau_0^2} &+ \epsilon^{\frac{1}{2}}\left(2\frac{\partial^2\phi}{\partial\tau_0\partial\tau_1}\right) + \epsilon\left(2\frac{\partial^2\phi}{\partial\tau_0\partial\tau_2} + \frac{\partial^2\phi}{\partial\tau_1^2}\right) + \epsilon^{\frac{3}{2}}\left(2\frac{\partial^2\phi}{\partial\tau_1\partial\tau_2}\right) + \ldots = \\ & \kappa_1\beta + c_5\beta^3 + \epsilon\left(\kappa_3\phi + \xi_1\frac{\partial\phi}{\partial\tau_0} + \xi_2\frac{\partial\beta}{\partial\tau_0}\right) + \epsilon^{\frac{3}{2}}\left(\xi_1\frac{\partial\phi}{\partial\tau_1} + \xi_2\frac{\partial\beta}{\partial\tau_1}\right) + \ldots \end{aligned} \tag{5.127}$$

Order by order analysis is then performed on the above equation. We start by considering the leading order β-equation, which is

$$O(1) \quad : \quad \frac{\partial^2\beta}{\partial\tau_0^2} + \omega_1^2\beta = e_5\beta^3 \tag{5.128}$$

This equation is of similar form to C-equation found in Section 5.5. This equation is known to have oscillatory solution and this solution can be expressed in term of elliptic integrals or elliptic functions. The derivation of the solution is described below. Since Equation (5.128) is a partial differential equation, we allow the constant of integration to vary with other independent variables, which are the slower time scales, τ_1 and τ_2. In this case, we will use the fact that at the amplitude of oscillation, $\frac{\partial\beta}{\partial\tau_0} = 0$. By multiplying Equation (5.128) with $\frac{\partial\beta}{\partial\tau_0}$ and then integrating, we get

$$\frac{1}{2}\left(\frac{\partial\beta}{\partial\tau_0}\right)^2 + \frac{1}{2}\omega_1^2\beta^2 - \frac{1}{4}e_5\beta^4 = \frac{1}{2}\omega_1^2 A_1^2(\tau_1, \tau_2) - \frac{1}{4}e_5 A_1^4(\tau_1, \tau_2) \tag{5.129}$$

or

$$\left(\frac{\partial\beta}{\partial\tau_0}\right)^2 = \frac{e_5}{2}(A_1^2(\tau_1, \tau_2)\beta^2)(\frac{2\omega_1^2}{e_5}A_1^2(\tau_1, \tau_2) - \beta^2) \tag{5.130}$$

where $A_1(\tau_1, \tau_2)$ is the slowly varying amplitude of the motion. To simplify the notation, we will suppress the dependence of A_1 on τ_1 and τ_2 for the rest of the derivation. It should be clear to the reader that A_1 is slowly varying amplitude and not a constant. Separating the variables and then integrating, we obtain

$$\tau_0 = \sqrt{\frac{2}{e_5}} \int \frac{d\beta}{\sqrt{(A_1^2 - \beta^2)(\frac{2\omega_1^2}{e_5} - A_1^2 - \beta^2)}} \tag{5.131}$$

Using the table of elliptic integrals in [42], the above solution can be expressed in terms of elliptic function as follows.

$$\tau_0 = \frac{1}{\omega_1 \sqrt{1 - \frac{e_5}{\omega_1^2} A_1^2}} sn^{-1}\left(\frac{\beta}{A_1}, k\right) \tag{5.132}$$

where the modulus, k, is given by

$$k = \frac{A_1^2}{\frac{2\omega_1^2}{e_5} - A_1^2} \tag{5.133}$$

Equation (5.132) can be inverted to yield

$$\beta = A_1(\tau_1, \tau_2) sn\left(\omega_1 \sqrt{1 - \frac{e_5}{2\omega_1^2} A_1^2(\tau_1, \tau_2)}\ \tau_0\right) \tag{5.134}$$

The period of oscillation is given by

$$P = \frac{4\chi}{\omega_1 \sqrt{1 - \frac{e_5}{2\omega_1^2} A_1^2(\tau_1, \tau_2)}} \tag{5.135}$$

where for small amplitude motions (small k),

$$\chi = \frac{1}{2}\pi \left[1 + \frac{1}{8}\frac{e_5}{\omega_1^2} A_1^2\right] \tag{5.136}$$

The period of the oscillation can then be written as

$$P = 2\pi \frac{1 + \frac{1}{8}\frac{e_5}{\omega_1^2}A_1^2}{\omega_1\sqrt{1 - \frac{e_5}{2\omega_1^2}A_1^2}} \tag{5.137}$$

The angular frequency of the motion can be expressed as

$$\begin{aligned} \bar{\omega}_1 &= \frac{2\pi}{P} \\ &= \frac{\omega_1\sqrt{1 - \frac{e_5}{2\omega_1^2}A_1^2}}{1 + \frac{1}{8}\frac{e_5}{\omega_1^2}A_1^2} \end{aligned} \tag{5.138}$$

Applying binomial expansion to the above equation, we obtain

$$\begin{aligned} \bar{\omega}_1 &\approx \omega_1\left(1 - \frac{1}{4}\frac{e_5}{\omega_1^2}A_1^2\right)\left(1 - \frac{1}{8}\frac{e_5}{\omega_1^2}A_1^2\right) \\ &\approx \omega_1\left(1 - \frac{3}{8}\frac{e_5}{\omega_1^2}A_1^2\right) \end{aligned} \tag{5.139}$$

Rather than dealing with non-elementary functions, in current analysis, we will find an approximation to the above solution in terms of elementary functions. For small k, we can approximate the elliptic function (5.134) fairly well using the sinusoidal function with the same frequency as follows [42, 43]

$$\beta(\tau_0, \tau_1, \tau_2) = A_1(\tau_1, \tau_2)\sin\left[\bar{\omega}_1\tau_0 + B_1(\tau_1, \tau_2)\right] \tag{5.140}$$

where B_1 represent the phase-correction of the solution. This representation simplifies further analysis, since we do not have to deal with the mathematical operations involving the non-elementary functions.

The solution (5.140) indicates that the frequency of the solution is dependent upon its amplitude. This is a consequence of approximating a non-elementary solution in terms of elementary functions. The dependence of the frequency on the amplitudes complicates the analysis of the higher order terms. This complication can be avoided by remembering that only small amplitude motions are of interest ($A_1 << 1$). Therefore, the variation of $\bar{\omega}_1$ due to A_1 can be neglected. $\bar{\omega}$ is then assumed to be constant in the subsequent order analysis. The effect of the dependence of frequency on the

amplitude will be invoked on the final result.

From Equation (5.127), the leading order terms in ϕ-equation yield

$$\frac{\partial^2 \phi}{\partial \tau_0^2} = \kappa_1 \beta + c_5 \beta^3 \tag{5.141}$$

By substituting Equation (5.140) into the above equation and then integrating twice with respect to τ_0, we get

$$\begin{aligned} \phi(\tau_0, \tau_1, \tau_2) &= -\left(\frac{\kappa_1}{\bar{\omega}_1^2} A_1(\tau_1, \tau_2) + \frac{3}{4}\frac{c_5}{\bar{\omega}_1^2} A_1^3(\tau_1, \tau_2)\right) \sin\Theta_1 + \\ & \frac{1}{36}\frac{c_5}{\bar{\omega}^2} A_1^3(\tau_1, \tau_2) \sin 3\Theta_1 + G(\tau_1, \tau_2) + H(\tau_1, \tau_2)\tau_0 \end{aligned} \tag{5.142}$$

As before, the last term is secular and destroys the ordering of the expansion. The appearance of such term is common in an asymptotic expansion. This term appears here because the above equation is a degenerate second order differential equation. However, a counter term can be constructed to eliminate such term, as discussed in [41]. Based on this reason, we will not include the last term in the subsequent analysis. This leaves us with $G(\tau_1, \tau_2)$ as the only homogeneous solution of the equation. As we will see, the detail form of this solution is found from the $O(\epsilon)$ analysis.

We now continue with the $O(\epsilon^{\frac{1}{2}})$ terms.

$$\begin{aligned} O(\epsilon^{\frac{1}{2}}) \; : \; \frac{\partial^2 \beta}{\partial \tau_0 \partial \tau_1} &= 0 \\ \frac{\partial^2 \phi}{\partial \tau_0 \partial \tau_1} &= 0 \end{aligned} \tag{5.143}$$

The substitution of Equations (5.140) and (5.142) into the above equation yields

$$\frac{\partial A_1}{\partial \tau_1} = \frac{\partial B_1}{\tau_1} = 0 \tag{5.144}$$

This means that

$$A_1, B_1 \neq f(\tau_1) \tag{5.145}$$

or in other words, A_1 and B_1 are functions of τ_2 only.

The $O(\epsilon)$ terms of the β-equation gives

$$O(\epsilon) \; : \; 2\frac{\partial^2 \beta}{\partial \tau_0 \partial \tau_2} + \frac{\partial^2 \beta}{\partial \tau_1^2} - \eta_1 \frac{\partial \beta}{\partial \tau_0} - \kappa_2 \phi - \eta_2 \frac{\partial \phi}{\partial \tau_0} = 0 \tag{5.146}$$

By substituting Equations (5.140) and (5.142) into Equation (5.146) and by considering only the first harmonic, we obtain

$$\begin{aligned}\left[2\bar{\omega}_1\frac{dA_1}{d\tau_2} - \bar{\omega}_1\left(\eta_1 - \frac{\kappa_1}{\bar{\omega}_1^2}\eta_2\right)A_1 + \frac{3}{4}\bar{\omega}_1\left(\eta_2\frac{c_5}{\bar{\omega}_1^2}\right)A_1^3\right]\cos\Theta_1 - \\ 2\left[\bar{\omega}_1 A_1\frac{dB_1}{d\tau_2} + \frac{\kappa_1}{\bar{\omega}_1^2}\kappa_2 A_1 + \kappa_2\frac{c_5}{\bar{\omega}_1^2}A_1^3\right]\sin\Theta_1 = 0\end{aligned} \tag{5.147}$$

which leads to the following amplitude and phase-correction equations.

$$\begin{aligned}\frac{dA_1}{d\tau_2} &= \frac{1}{8\bar{\omega}_1^2}\left[\left(\eta_1\bar{\omega}_1^2 - \kappa_1\eta_2\right)A_1 - 3c_5\eta_2 A_1^3\right] \\ \frac{dB_1}{d\tau_2} &= \frac{1}{\bar{\omega}_1^4}\left[-\frac{1}{2}\kappa_1\kappa_2\bar{\omega}_1 + \kappa_2 c_5\bar{\omega}_1 A_1^2\right]\end{aligned} \tag{5.148}$$

Note that the above equations still contain $\bar{\omega}_1$, which is a function of A_1. The equations are simplified using the following approximations.

$$\bar{\omega}_1^2 \approx \omega^2 - \frac{3}{4}e_5 A_1^2 \tag{5.149}$$

By substituting the above approximations into Equation (5.148) and retaining only terms up to third order in A_1, we get

$$\begin{aligned}\frac{dA_1}{d\tau_2} &= \frac{1}{2}\mu A_1 + p_1 A_1^3 \\ \frac{dB_1}{d\tau_2} &= p_3 + p_4 A_1^2\end{aligned} \tag{5.150}$$

where

$$\begin{aligned}\mu &= \eta_1 - \frac{\kappa_1}{\omega^2}\eta_2 \\ p_1 &= -\frac{3}{8}\left(\eta_2 c_5 + \eta_1 e_5\right) \\ p_3 &= -\frac{1}{2}\frac{\kappa_1\kappa_2}{\omega_1^3} \\ p_4 &= \frac{\kappa_2 c_5}{\omega_1^3}\end{aligned} \tag{5.151}$$

We have put Equation (5.150) in the same notation as in the previous sections to show that the analysis of the equation can follow the same framework. Note that μ expression is the same as in the previous sections, which suggests that the type of nonlinearity considered does not change the onset of wing rock.

We focus first on the amplitude equation. For $\mu < 0$, the system is asymptotically stable. As μ varies from negative to positive value, the system will undergo the Hopf bifurcation. $\mu = 0$ is the onset of bifurcation. The nature of the Hopf bifurcation is determined by the sign of p_1. If $p_1 > 0$, the bifurcation is of the subcritical type and the aircraft will undergo divergent motion. If $p_1 < 0$, a limit cycle type of oscillation is developed (wing rock). The amplitude history of the wing rock motion is given by the solution of the amplitude equation (5.150), that is

$$A = \frac{\sqrt{K\frac{\mu}{2}}\exp(\frac{\mu}{2}\tau_1)}{\sqrt{1 - Kp_1\exp(\mu\tau_1)}} \tag{5.152}$$

As can be observed, this solution has the following properties.

$$\begin{aligned} A_1 &\rightarrow 0 \quad for\ \mu < 0 \\ A_1 &\rightarrow \sqrt{-\frac{\exp(\mu\tau_1)}{2\frac{p_1}{\mu}\exp(\mu\tau_1)}} = \sqrt{-\frac{\mu}{2p_1}} \quad for\ \mu > 0 \end{aligned} \tag{5.153}$$

as $t \rightarrow \infty$. The second expression determines the steady wing rock amplitude. The amplitude depends on p_1 which, in this case, consists of L_{β_1} and N_{β_1}. Thus, the degree of the nonlinearity in angle-of-sideslip determines the resulting amplitude of the wing rock motion.

The homogeneous ϕ solution ($G(\tau_1, \tau_2)$) can be found using the $O(\epsilon)$ analysis of the ϕ-equation, that is

$$2\frac{\partial^2\phi}{\partial\tau_0\partial\tau_2} + \frac{\partial^2\phi}{\partial\tau_1^2} - \kappa_3\phi - \xi_1\frac{\partial\phi}{\partial\tau_0} - \xi_2\frac{\partial\beta}{\partial\tau_0} = 0 \tag{5.154}$$

By substituting $\phi = G(\tau_1, \tau_2)$ into the above equation, we get

$$\frac{\partial G}{\partial\tau_1^2} - \kappa_3 G = 0 \tag{5.155}$$

The solution of this equation is

$$G(\tau_1, \tau_2) = A_2(\tau_2)\sin\Theta_2 \quad ; \quad \Theta_2 \equiv \sqrt{-\kappa_3}\tau_1 + B_2(\tau_2) \tag{5.156}$$

The $O(\epsilon^{\frac{3}{2}})$ analysis then yields

$$2\frac{\partial^2\phi}{\partial\tau_1\partial\tau_2} - \xi_1\frac{\partial\phi}{\partial\tau_1} - \xi_2\frac{\partial\beta}{\partial\tau_1} = 0$$

$$\Leftrightarrow \quad \left[2\sqrt{-\kappa_3}\frac{dA_2}{d\tau_2} - \xi_1\sqrt{-\kappa_3}A_2\right]\cos\Theta_2 - 2\sqrt{-\kappa_3}A_2\frac{dB_2}{d\tau_2}\sin\Theta_2 = 0 \quad (5.157)$$

This leads to the following amplitude and phase-correction equations.

$$\begin{aligned} \frac{dA_2}{d\tau_2} &= \frac{\xi_1}{2}A_2 \\ \frac{dB_2}{d\tau_2} &= 0 \end{aligned} \quad (5.158)$$

The solutions of these simple equations are as follows.

$$\begin{aligned} A_2 &= A_{2_0}\exp(\frac{\xi_1}{2}\tau_2) \\ B_2 &= \text{constant} \end{aligned} \quad (5.159)$$

It is obvious then that the stability of this specific mode is determined by the sign of ξ_1. This mode is asymptotically stable if $\xi_1 < 0$ and unstable if $\xi_1 > 0$.

The comparison between the analytical result with the numerical integration result is depicted in Figure 5-13. As we can see, the analytical solution predicts the steady state amplitude of wing rock motion accurately. A slight amount of phase error is observed on the analytical solution. The phase shift becomes obvious after several oscillations. The transient part of the roll motion is also not predicted very accurately by the analytical solution. Considering the simplicity of the form of the analytical solution, however, we can say that the analytical solution predicts the overall motion fairly well.

The effects of L_{β_1} and N_{β_1} on the amplitude of the wing rock motion for the aircraft model considered are shown in Figure 5-14.

5.7.4 Variations of the Dynamics Cross Coupling Derivatives With Angle-of-Sideslip

The effects of the variations of the dynamics cross coupling derivatives due to the angle-of-sideslip are studied in this subsection. Such variation produces nonlinear terms in the aerodynamic moment expressions. As before, other nonlinearities are neglected in the analysis. Therefore, the aerodynamic moments in the equation of motion have the following form.

$$L = L_{p_0}p + L_{\beta_0}\beta + L_{r_0}r + L_{\dot{\beta}_0}\dot{\beta} + L_q(\beta)q$$

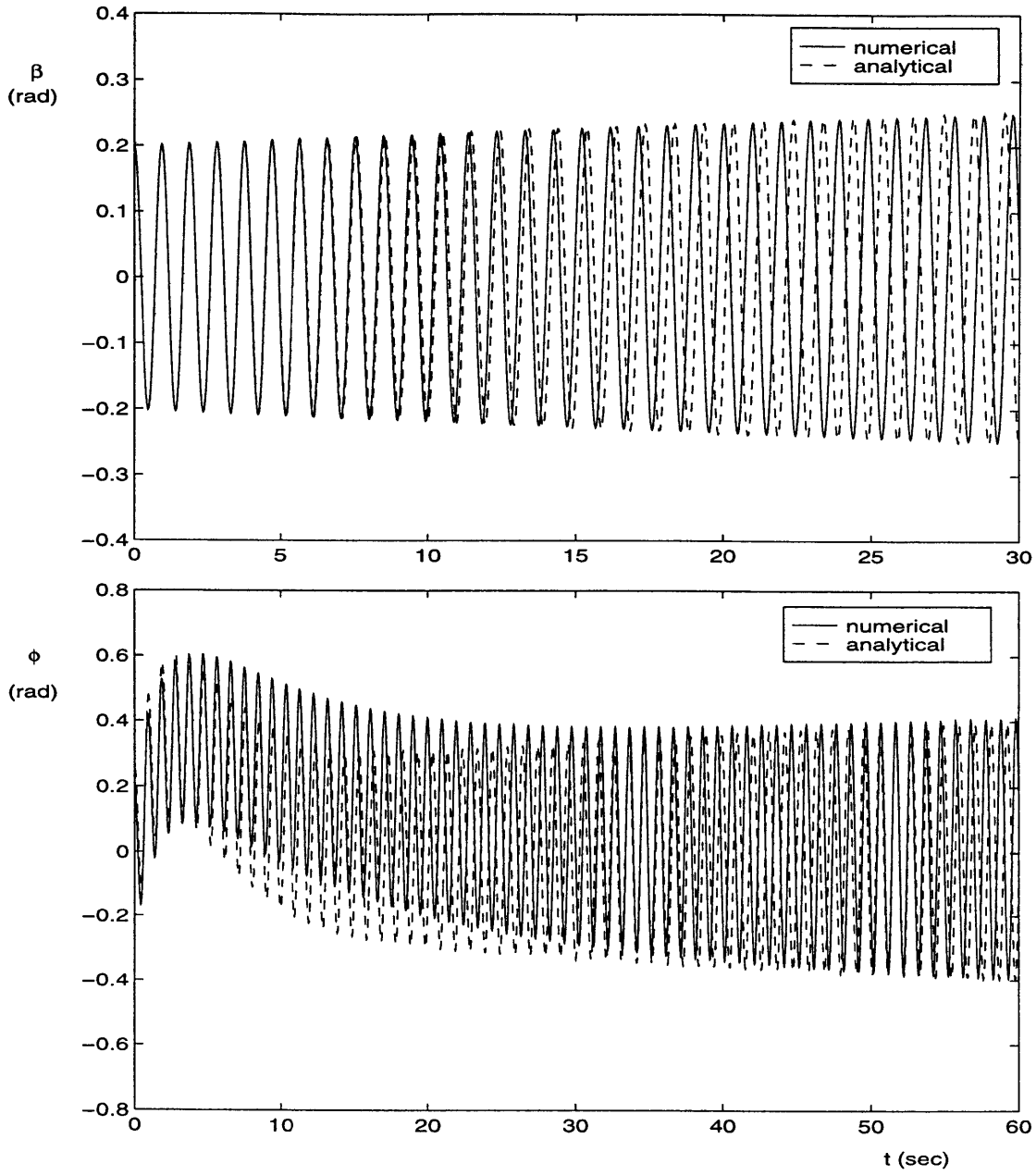

Figure 5-13: Analytical vs numerical-integration result at $\alpha_0 = 31^o$ with $C_{l_{\beta_1}} = -5$ and $C_{n_{\beta_1}} = -2$

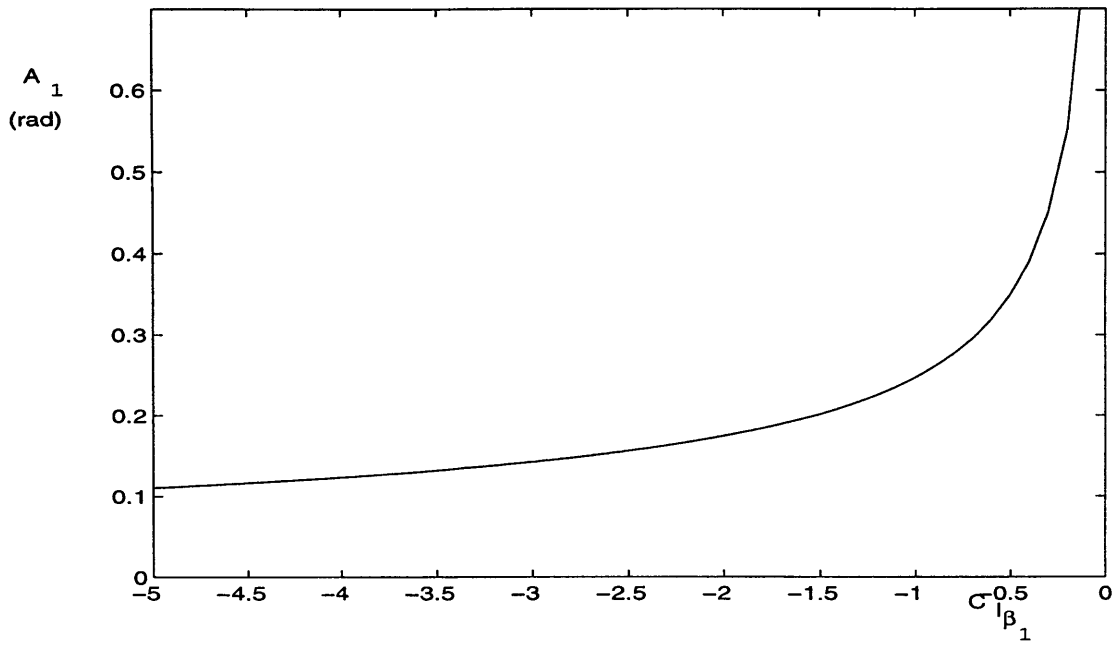

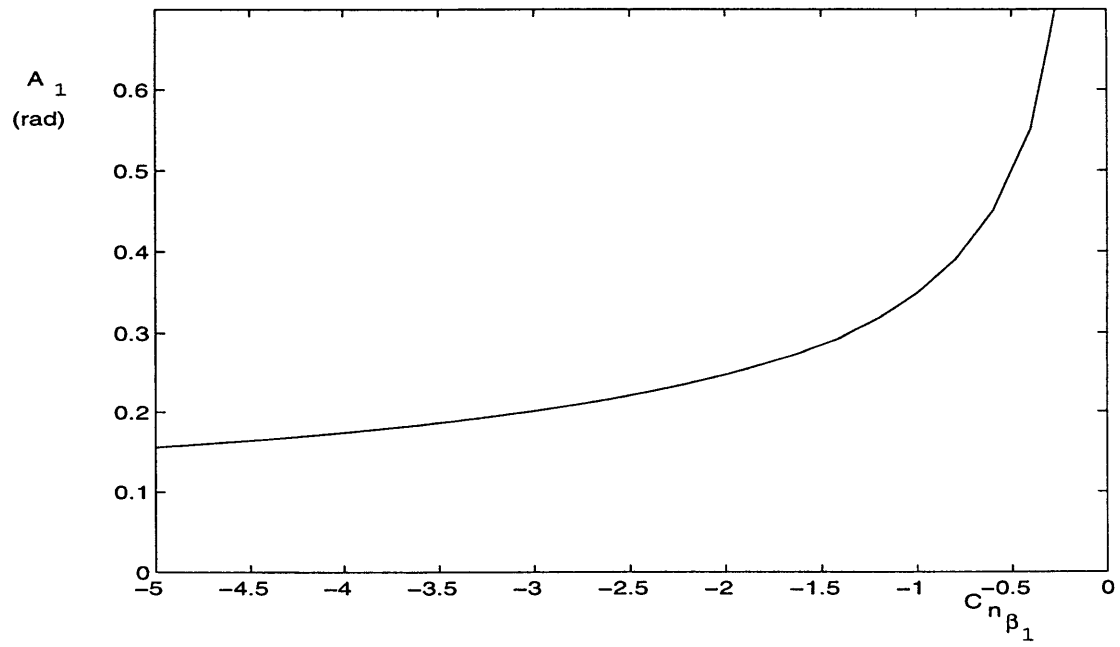

Figure 5-14: Variation of wing rock amplitude with L_{β_1} and N_{β_1}

$$
\begin{aligned}
M &= M_{\alpha_0}\alpha + M_{q_0}q + M_{\dot{\alpha}_0}\dot{\alpha} + M_p(\beta)p + M_r(\beta)r \\
N &= N_{r_0}r + N_{\beta_0}\beta + N_p p + N_{\dot{\beta}_0}\dot{\beta} + N_q(\beta)q
\end{aligned} \tag{5.160}
$$

As indicated in the equations, only the cross coupling derivatives L_q, M_p, M_r, and N_q are functions of β, while the others are constant. From the basic aerodynamics, which is also confirmed by several flight data, the variations of these cross coupling derivatives with respect to the angle-of-sideslip are antisymmetric. To capture the antisymmetricity, while maintaining the model to be as simple as possible, we model the variation as follows.

$$
\begin{aligned}
L_q &= L_{q_1}\beta \\
M_p &= M_{p_1}\beta \\
M_r &= M_{r_1}\beta \\
N_q &= N_{q_1}\beta
\end{aligned} \tag{5.161}
$$

Substituting these expression into Equation (5.160) and then comparing the resulting equation to Equation (5.20), the following correspondences are hold.

$$
\begin{gathered}
[\bar{c}_1\ \bar{c}_2\ \bar{c}_3\ \bar{c}_4\ \bar{c}_{22}] \equiv [L_{\beta_0}\ L_{p_0}\ L_{\dot{\beta}_0}\ L_{r_0}\ L_{q_1}] \\
[\bar{d}_1\ \bar{d}_2\ \bar{d}_3\ \bar{d}_{42}\ \bar{d}_{44}] \equiv [M_{\alpha_0}\ M_{q_0}\ M_{\dot{\alpha}_0}\ M_{p_1}\ M_{r_1}] \\
[\bar{e}_1\ \bar{e}_2\ \bar{e}_3\ \bar{e}_4\ \bar{e}_{22}] \equiv [N_{\beta_0}\ N_{p_0}\ N_{\dot{\beta}_0}\ N_{r_0}\ N_{q_1}]
\end{gathered} \tag{5.162}
$$

For this simplified case, the equations of motion (5.31) become

$$
\begin{aligned}
\ddot{\beta} + \omega_1^2\beta &= \epsilon\left[\eta_1\dot{\beta} + \kappa_2\phi + \eta_2\dot{\phi} + e_3\phi\dot{\phi}^2 + e_{23}\beta\dot{\theta} + e_{33}\phi\dot{\phi}\beta + e_{35}\phi\beta\dot{\beta}\right] \\
\ddot{\theta} + \Omega^2\theta &= d_8\beta\dot{\beta} + d_{10}\beta\phi + d_{12}\beta\dot{\phi} + \epsilon\left[\nu\dot{\theta}\right] \\
\ddot{\phi} &= \kappa_1\beta + \epsilon\left[\kappa_3\phi + \xi_1\dot{\phi} + \xi_2\dot{\beta} + c_{23}\beta\dot{\theta} + c_{33}\phi\dot{\phi}\beta + c_{35}\phi\beta\dot{\beta}\right]
\end{aligned} \tag{5.163}
$$

Then following the same analysis procedure, we get the following amplitude and phase-correction equations.

$$
\begin{aligned}
\frac{dA_1}{d\tau_2} &= \frac{1}{2}\mu A_1 + p_1 A_1^3 + p_2 A_1 A_2^2 \\
\frac{dA_2}{d\tau_2} &= \frac{1}{2}\nu A_2 \\
\frac{dB_1}{d\tau_2} &= p_3 + p_4 A_1^2
\end{aligned}
$$

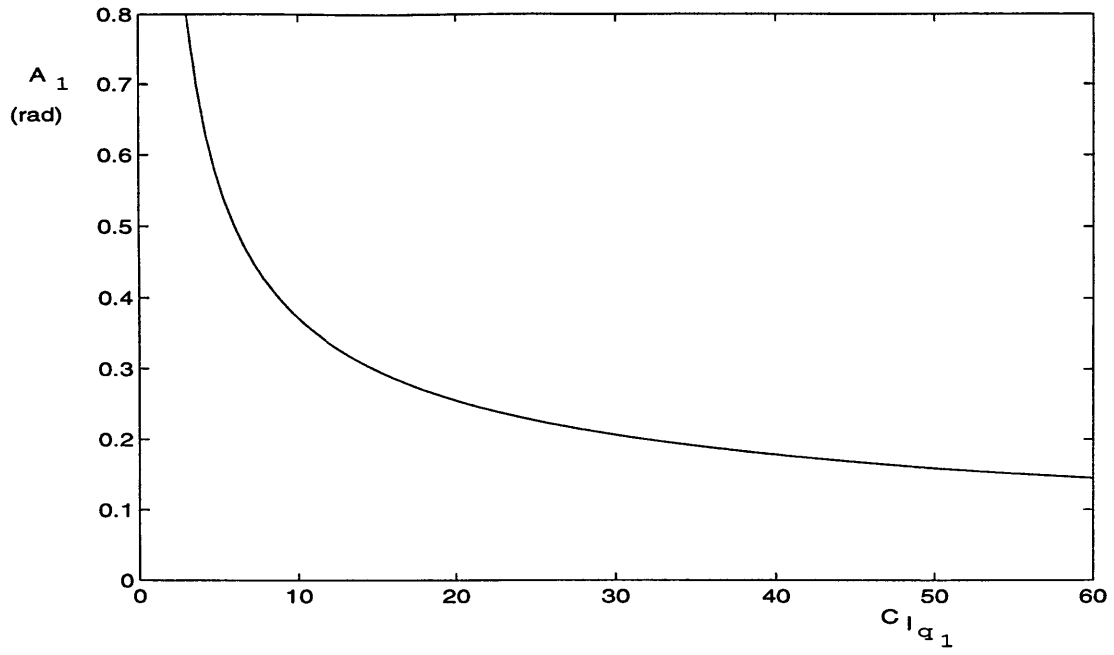

Figure 5-15: Variation of wing rock amplitude with L_{q_1}

$$\frac{dB_2}{d\tau_2} = q_3 A_1^2 \tag{5.164}$$

The parameters L_{q_1}, N_{q_1}, M_{p_1}, and M_{r_1} affect the coefficients of the above equations through d_8, d_{10}, d_{12}, e_{23}, e_{33}, e_{35}, c_{23}, c_{33}, c_{35}. Hence, from Equations 5.56) and (5.59), we see that these parameters L_{q_1}, N_{q_1}, M_{p_1}, and M_{r_1} affect both the amplitude and the frequency of wing rock. Figures 5-15, 5-16, 5-17, and 5-18 show the variation of the wing rock amplitude for the generic fighter model in our example with respect to L_{q_1}, N_{q_1}, M_{p_1}, and M_{r_1}, respectively. In obtaining each figure, we only consider the associated parameter as the only source of nonlinearity. In general, the larger the magnitude of the parameters, the smaller the wing rock amplitude is. This implies that the larger the magnitude of the parameters, the more energy is transferred from the lateral modes to the longitudinal mode of motion.

5.8 Chapter Summary

Wing rock dynamics of an aircraft having three degrees-of-freedom in roll, pitch, and yaw has been analyzed in this chapter. The additional degree-of-freedom in yaw adds significant complexity to the analysis as compared to the two degree-of-

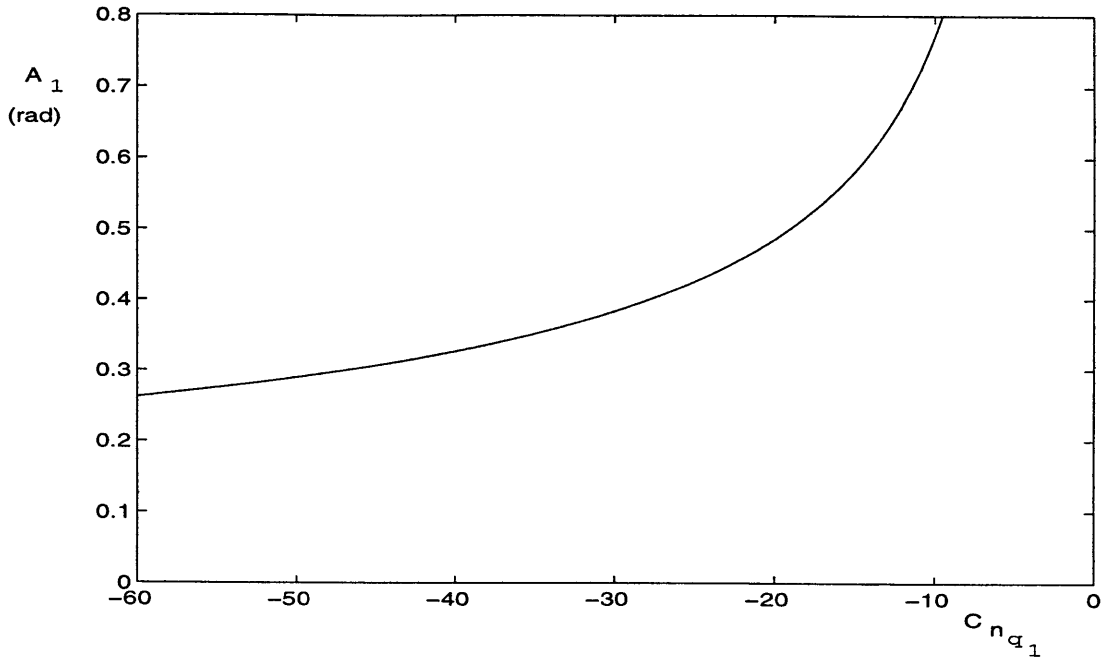

Figure 5-16: Variation of wing rock amplitude with N_{q_1}

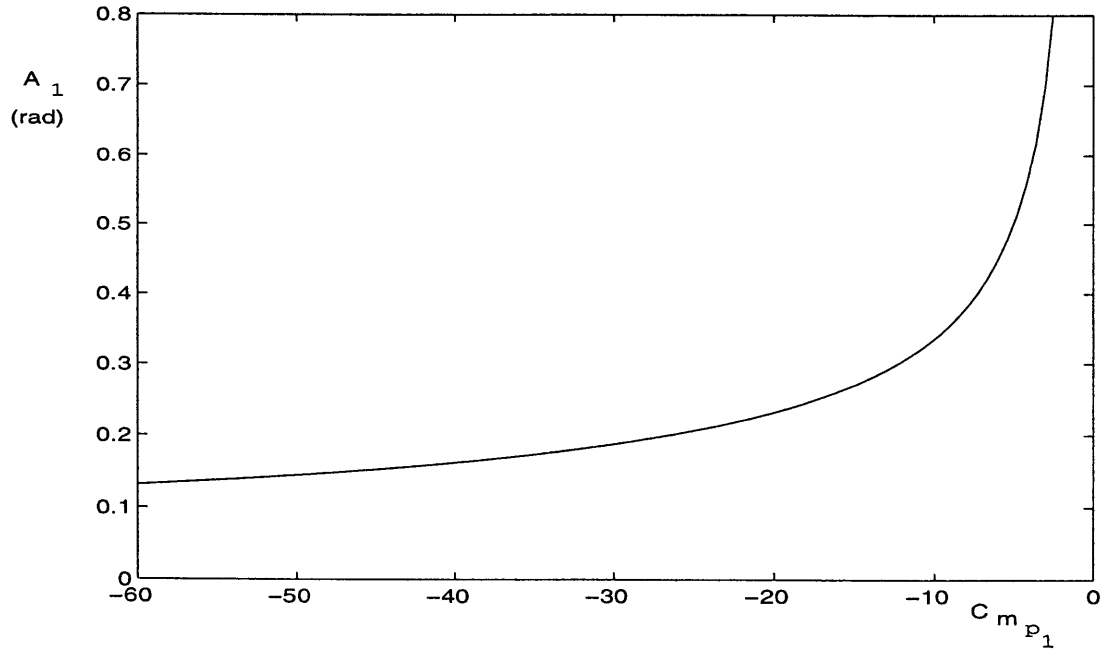

Figure 5-17: Variation of wing rock amplitude with M_{p_1}

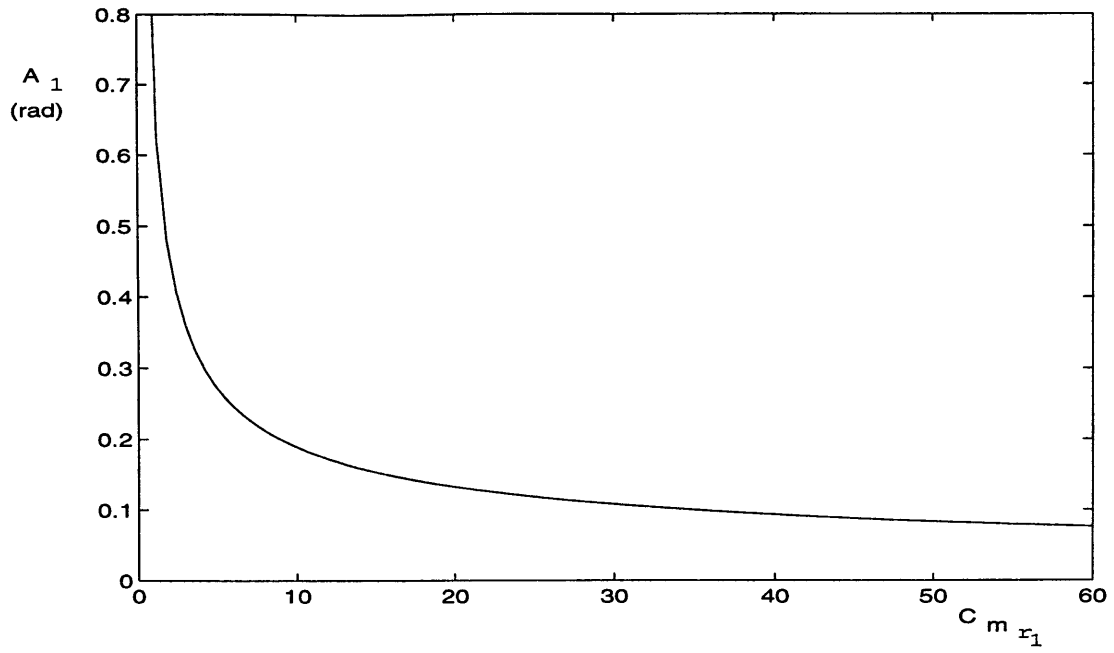

Figure 5-18: Variation of wing rock amplitude with M_{r_1}

freedom case. There are more parameters involved in determining the properties of wing rock motion. However, the result can be formulated using the same analytical forms as in the lower degrees-of-freedom cases. It should be noted that although more complex, the model captures more physical phenomena than the lower degrees-of-freedom models. Examples of the phenomena that are not observed in the lower degrees-of-freedom models are the presence of the mode due to roll yaw coupling in the roll response and the potential cause of wing rock due to strong cubic variation of lateral moments with sideslip. The analytical results have also been shown to compare very well with the numerical results.

Chapter 6

Wing Rock Alleviation

6.1 Introduction

The wing rock dynamics of aircraft have been considered in the previous chapters for single and multiple degrees-of-freedom cases. Based on the results, some control strategies to alleviate wing rock motion are developed in this chapter. Such alleviation is necessary to achieve the enhanced performance requirements imposed on modern fighter aircraft.

Since wing rock motion is normally encountered at high angles-of-attack, the control power needed to perform the alleviation becomes an important issue. This is due to the fact that the conventional aerodynamic control surfaces (elevators, ailerons, and rudders) loose their effectiveness, or in other words, loose their power, at high angles-of-attack. Figure 6-1 illustrates typical control moment coefficients from the conventional aerodynamic control surfaces (ailerons and rudders). The magnitude of these coefficients drops significantly at high angles-of-attack.

Wing rock alleviation by using only conventional control surfaces will now be discussed in detail, along with the potential limitations. Some techniques to overcome the control power requirements for the wing rock suppression will also be described. These techniques involve the use of the advanced controls, such as thrust vectoring and forebody strakes, to increase the control power of the aircraft. As we shall see later, a proper implementation of such techniques can eliminate fully or partially the control power limitations of the conventional controls.

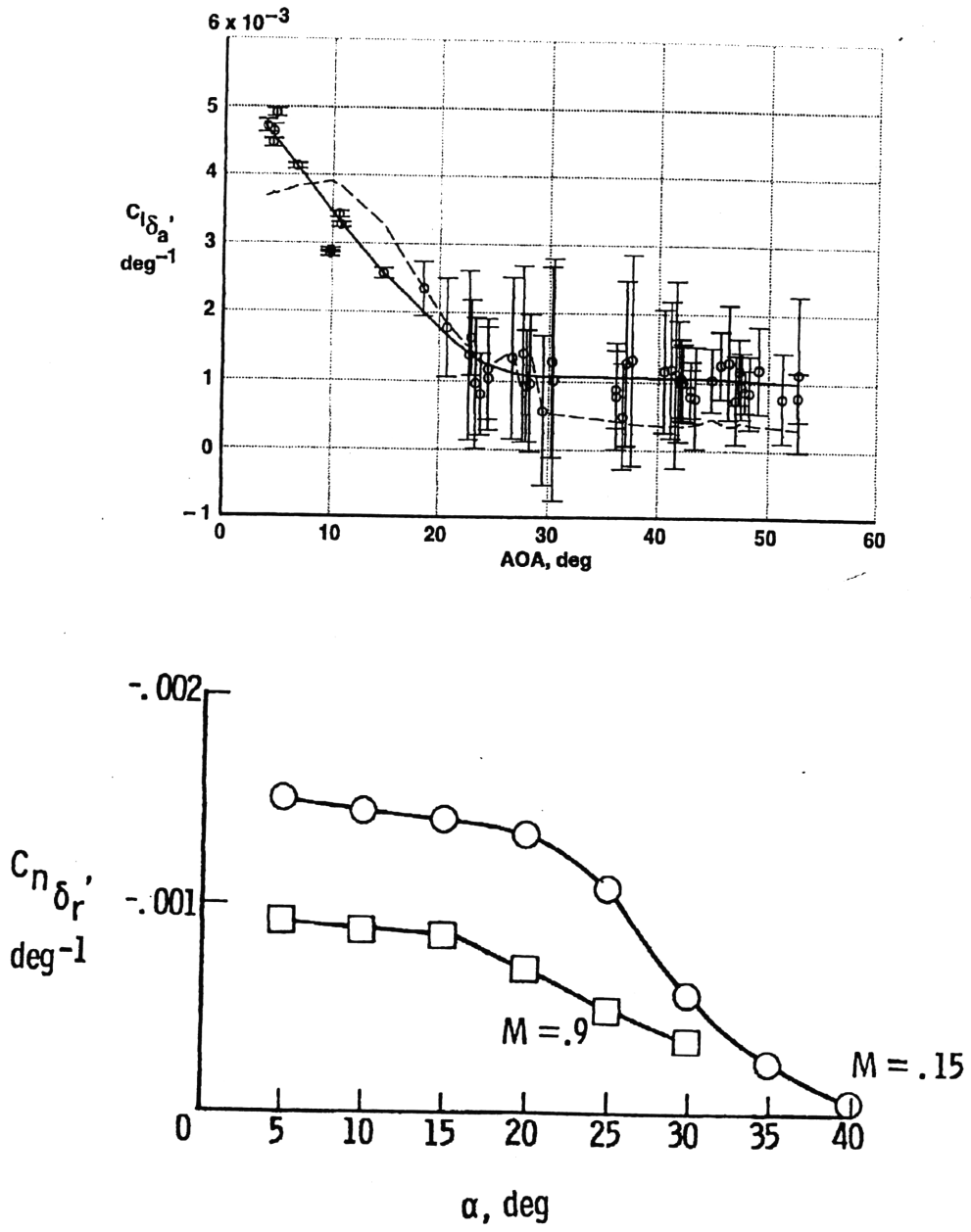

Figure 6-1: Roll and yaw control moment derivatives for conventional controls [47, 48]

6.2 Control Approach

As can be seen from the previous chapters, wing rock motion occurs when the aircraft system undergoes the supercritical Hopf bifurcation. It should also be remembered, that a subcritical Hopf bifurcation can occur instead, for certain combinations of parameter values. Such a condition leads to divergent motions, which are more catastrophic than the wing rock. In all cases, the parameters defined as μ and p_1 determine asymptotically which situation the aircraft will encounter. The control approach taken here is to modify these parameters such that a satisfactory dynamics can be achieved. The elaboration on what we mean by *satisfactory dynamics* is given in the next paragraphs.

Dynamic analysis of single, two, and three degrees-of-freedom cases (see Chapters 3, 4, and 5) has led to a unified governing equation for the amplitude of wing rock motion of the form

$$\frac{dA}{d\tau^*} = \frac{1}{2}\mu A + p_1 A^3 \tag{6.1}$$

where A indicates the amplitude of motion and τ^* indicates the slow time scale, ϵt, with $0 < \epsilon << 1$. This equation can tell us whether wing rock occurs in the system and can predict the amplitude of the motion. As we have stated earlier, the amplitude of the wing rock motion is usually used as a measure of the severity of the motion. Hence, the unified result as given by Equation (6.1) is very useful and will be utilized to guide us to the appropriate control strategy.

The onset of wing rock is determined by the parameter μ. When $\mu < 0$, the nominal flight condition is asymptotically stable, and when $\mu > 0$, wing rock or divergent motion can occur. In this case, the parameter p_1 determines whether the aircraft will undergo wing rock ($p_1 < 0$) or divergent motion ($p_1 > 0$). In the case where wing rock occurs in the system, the amplitude of the roll angle limit cycle is asymptotically determined by $\sqrt{-\frac{\mu}{2p_1}}$. Ideally, the goal of the control system is to achieve an asymptotically stable system at any possible flight condition. This implies that the control law should be designed such that $\mu < 0$ for all flight conditions of interest. However, this is not always possible, because there may not be enough control power to generate the necessary control moments. This is especially true for an aircraft equipped only with the conventional aerodynamic control surfaces, as we shall show later. In the situation where μ cannot be kept negative by the available controls, then the supercritical Hopf bifurcation case is preferable to the subcritical one. This is because in the supercritical Hopf bifurcation case, the aircraft motion is still bounded (wing rock), as opposed to the unbounded motion in the subcritical

Hopf bifurcation case (divergent motion). However, to be considered satisfactory, the amplitude of the wing rock motion should be kept as small as possible. Again, the control power issue may come into play here.

To summarize, the ideal goal of the control system is to avoid wing rock (wing rock avoidance), which can be achieved by making $\mu < 0$. In the case where wing rock cannot be avoided, then the control system should suppress the wing rock amplitude as much as possible (wing rock suppression). This can be achieved by making the ratio of μ to p_1 as small as possible. Figure 6-2 illustrates the concept of wing rock avoidance and suppression. The first part of the figure indicates the amplitude of wing rock motion as a function of the nominal angle-of-attack when no control is applied. The onset of wing rock in this figure is denoted by α^*. For the nominal angles-of-attack below α^*, wing rock does not occur and the motion of the aircraft is asymptotically stable. The second part of the figure describes the concept of avoidance. Suppose that the maximum operational angle-of-attack of the aircraft is $\hat{\alpha}$. The avoidance system delays the onset of wing rock to an angle-of-attack higher than $\hat{\alpha}$, so that in its whole operational angle-of-attack range, the aircraft will not undergo wing rock. The last part of the figure illustrate the concept of suppression. Here, the aircraft will still experience wing rock at some angles-of-attack within its operational range, however the control system will suppress the amplitude of the wing rock motion to the level which is considered acceptable. We will next discuss the wing rock avoidance/suppression systems in more detail.

6.2.1 Wing Rock Avoidance

The onset of wing rock occurs at the angle-of-attack associated with $\mu = 0$. If $\mu < 0$, no wing rock motion can occur and if $\mu > 0$, the aircraft can develop wing rock or divergent motion. Therefore, keeping the parameter μ to be negative for any flight condition of interest is the goal of the wing rock avoidance system. We will now consider μ in more detail, and especially examine the parameters that influence its value for the cases considered here. It should be noted that for all these cases, μ depends only on the constant parts of some stability derivatives.

For the single and two degrees-of-freedom cases, μ has the same form, that is (expressed in terms of linear stability derivatives)

$$\tilde{\mu} \equiv \epsilon\mu = L_{p_0} + L_{\dot{\beta}_0} \sin\alpha_0 \tag{6.2}$$

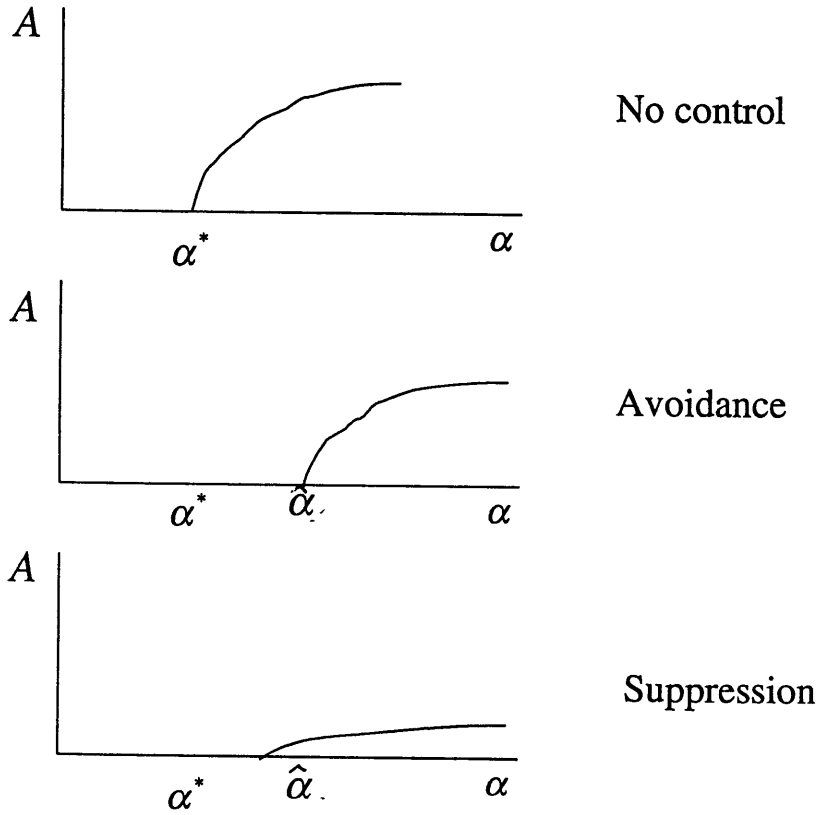

Figure 6-2: Illustration of wing rock avoidance and suppression

The combination of the parameters $L_{p_0} + L_{\dot{\beta}_0} \sin\alpha_0$ is called *the dynamic roll damping parameter* in the literature. Thus, in this case, the wing rock damping parameter is the same as the dynamic roll damping parameter. $L_{\dot{\beta}_0}$ is difficult to modify by a simple control, as it is normally highly dependent on the aircraft configuration. L_{p_0}, on the other hand, can be easily modified using control, such as by a roll damper system. However, it should be noted that the level of ease of the L_{p_0} modification varies with flight regimes.

For the three degrees-of-freedom case, μ is more complicated. It is defined by

$$\tilde{\mu} \equiv \epsilon\mu = \eta_1 - \frac{\kappa_1}{\omega_1^2}\eta_2 \tag{6.3}$$

where (in terms of the linear stability derivatives)

$$\begin{aligned}
\tilde{\eta}_1 &= \frac{1}{1 - n_1 n_3}\left[\left(L_{\dot{\beta}_0} - \frac{L_{r_0}}{\cos\alpha_0}\right)(\sin\alpha_0 - n_3\cos\alpha_0) - \right. \\
&\quad \left.\left(N_{\dot{\beta}_0} - \frac{N_{r_0}}{\cos\alpha_0}\right)(\cos\alpha_0 - n_1\sin\alpha_0)\right] \\
\frac{\kappa_1}{\omega_1^2} &= -\frac{L_{\beta_0} + n_1 N_{\beta_0}}{(L_{\beta_0} + n_1 N_{\beta_0})\sin\alpha_0 - (N_{\beta_0} + n_3 L_{\beta_0})\cos\alpha_0} \\
\tilde{\eta}_2 &= \frac{g}{V}\cos\alpha_0 + \frac{1}{1 - n_1 n_3}\left[(L_{p_0} + L_{r_0}\tan\alpha_0)(\sin\alpha_0 - n_3\cos\alpha_0) - \right. \\
&\quad \left.(N_{p_0} + N_{r_0}\tan\alpha_0)(\cos\alpha_0 - n_1\sin\alpha_0)\right]
\end{aligned} \tag{6.4}$$

μ for this case is influenced by more aerodynamic stability derivatives than for the single and two degrees-of-freedom cases. In addition to L_{p_0} and $L_{\dot{\beta}_0}$, μ is also affected by L_{β_0}, N_{β_0}, L_{r_0}, N_{p_0}, N_{r_0}, and $N_{\dot{\beta}_0}$. Among these parameters, L_{p_0} and N_{r_0} are the easiest ones to control. In a conventional aircraft system, L_{p_0} is modified using a roll damper system (feedback of roll rate to the aileron) and N_{r_0} is usually modified using a yaw damper system (feedback of yaw rate to the rudder). Due to the lateral cross-control effects, L_{r_0} and N_{p_0} are usually modified when there is roll rate or yaw rate feedback. However, we will assume that the cross-control effects are small and do not have significant effects on the dynamics. Although in theory L_{β_0} and N_{β_0} can be modified by β-feedback, in practice, this is normally not feasible, since the β measurement is noisy. Similar reasoning applies to $L_{\dot{\beta}_0}$ and $N_{\dot{\beta}_0}$. Thus, the modification of these derivatives by using feedback will not be considered here.

The above discussion clearly shows that μ depends only on the constant parts of the stability derivatives of the aircraft, which are normally used in the linear treatment of aircraft dynamics. Therefore, a linear control law can be used to modify μ to avoid

wing rock. In this work, wing rock avoidance is performed by modifying L_{p_0} and N_{r_0} through the use of either conventional or advanced controls.

6.2.2 Wing Rock Suppression

Wing rock suppression system is normally employed when there is not enough control power to avoid the onset of the Hopf bifurcation within the flight envelope of the aircraft. The idea is to avoid the divergent motion (subcritical Hopf bifurcation) by allowing the aircraft to encounter the wing rock motion with small amplitudes. This is done by making $p_1 < 0$ and keeping the ratio of μ to p_1 to be as small as possible. As we shall see later, this usually requires the use of a nonlinear control law, since p_1 consists of the nonconstant parts of the stability derivatives.

Wing rock avoidance/suppression systems by using conventional and advanced controls are studied next.

6.3 Wing Rock Alleviation Using Conventional Aerodynamic Controls

Alleviation of wing rock by using only conventional aerodynamic controls is described in this section. Since wing rock motion is mostly lateral in nature, then the only effective aerodynamic controls to suppress it are ailerons and rudders. As has been mentioned previously, control power is an important issue to consider when utilizing these controls at high angles-of-attack, which is the flight regimes of interest here. Both ailerons and rudders lose their effectiveness at high angles-of-attack. Without loss of generality, for the fighter aircraft model used in the previous numerical examples, the variations of the lateral direct control derivatives with the angle-of-attack are assumed to be well approximated by piecewise linear functions (Figure 6-3). The trends of the variation are typical, as can also be seen in Figure 6-1.

Next, we will examine in detail the avoidance/suppression of wing rock using the conventional aerodynamic controls for each case considered in Chapter 3, 4 and 5.

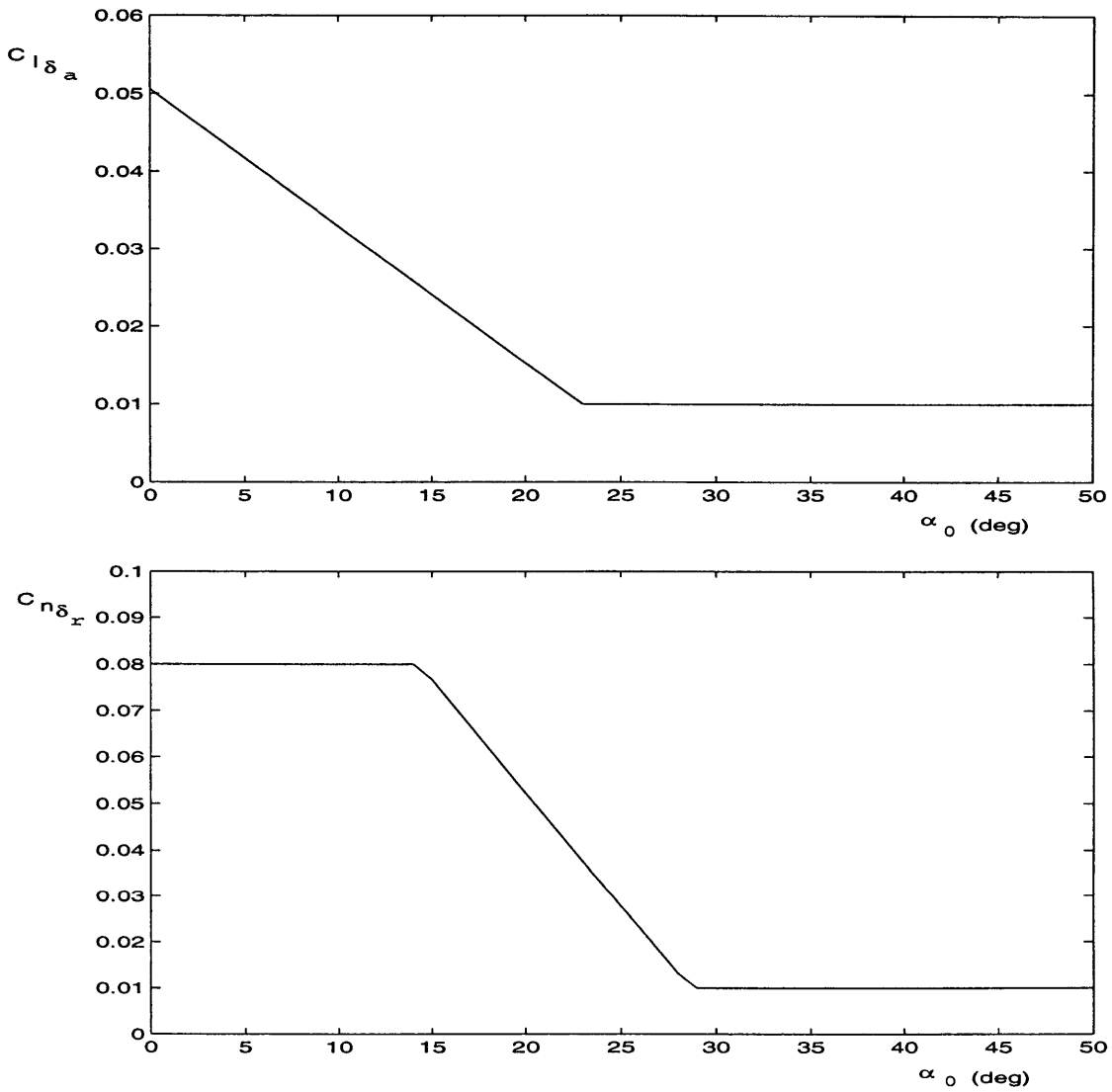

Figure 6-3: Assumed variation of direct lateral control derivatives with angle-of-attack

6.3.1 Single Degree-of-Freedom Case

In the single degree-of-freedom case, the only aerodynamic surfaces utilized for the wing rock suppression are the ailerons. The equation of motion of the aircraft system with control, expressed in terms of stability derivatives, becomes (see Chapter 3 for the uncontrolled case)

$$\ddot{\phi} = L_p p + L_\beta \beta + L_{\dot{\beta}} \dot{\beta} + L_{\delta_a} \delta_a \tag{6.5}$$

where δ_a denotes the aileron deflection and L_{δ_a} indicates the aileron rolling control derivative. Note that in the above equation, all the stability and control derivatives can be nonlinear. The constant parts of the derivatives, which normally appear in the linear aircraft dynamics analysis, will be denoted by the subscript '0', as before. Expressed in this way, the above equation of motion becomes

$$\ddot{\phi} = L_{p_0} p + L_{\beta_0} \beta + L_{\dot{\beta}_0} \dot{\beta} + L_{NL} + L_{\delta_{a_0}} \delta_a \tag{6.6}$$

where L_{NL} represents the nonlinear parts of the rolling moment which do not come from the application of control. We will first consider the use of linear control law to avoid the occurence of wing rock in the system.

As has been explained in the previous section, we apply a control law that will augment L_{p_0}. A simple gain control law of the following form is studied here.

$$\delta_a = -K_{p_1} \, p \tag{6.7}$$

For the implementation of this control law, the measurement of roll rate by using a roll rate sensor is fedback to command a certain aileron deflection. With this control law, the wing rock damping parameter is modified to

$$\tilde{\mu} = \bar{L}_p + L_{\dot{\beta}_0} \sin \alpha_0 \tag{6.8}$$

where

$$\bar{L}_p = L_{p_0} - K_{p_1} L_{\delta_{a_0}} \tag{6.9}$$

To avoid wing rock, μ has to be kept negative. This requirement produces the minimum bound for the gain K_{p_1} to yield an asymptotically stable system, as follows.

$$\begin{aligned} L_{p_0} \; - \; & K_{p_1} L_{\delta_{a_0}} + L_{\dot{\beta}_0} \sin \alpha_0 < 0 \\ \Leftrightarrow \quad & K_{p_1} L_{\delta_{a_0}} > L_{p_0} + L_{\dot{\beta}_0} \sin \alpha_0 \end{aligned}$$

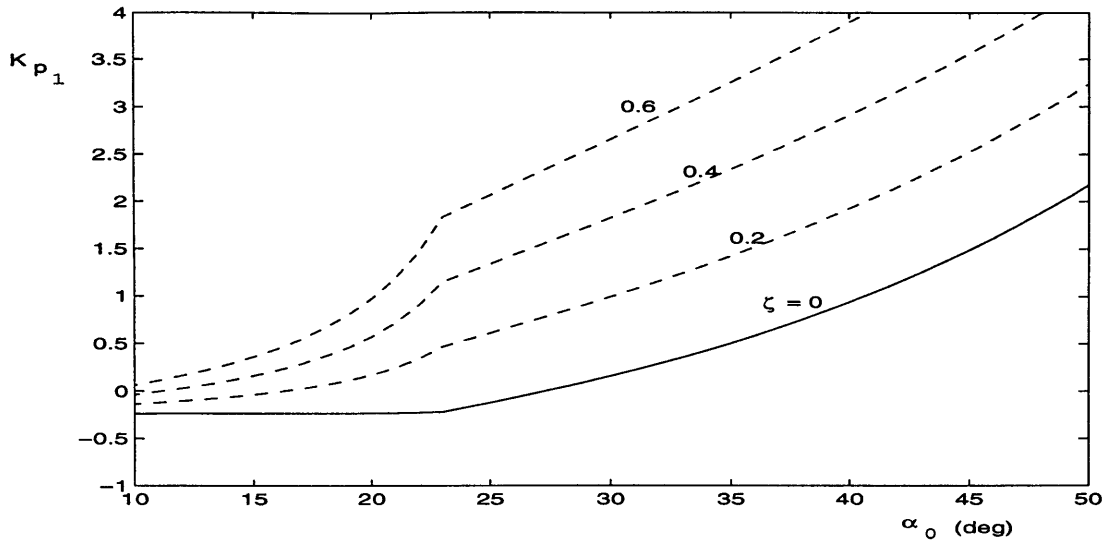

Figure 6-4: Lower bound of the gain for stability (solid line) and the gain to achieve the damping ratio of 0.2, 0.4, and 0.6 (dashed line) in the avoidance system

$$\Leftrightarrow \qquad K_{p_1} > \frac{L_{p_0} + L_{\dot{\beta}_0} \sin \alpha_0}{L_{\delta_{a_0}}} \tag{6.10}$$

For the fighter aircraft model used in the numerical example in Chapter 1, this bound is shown in Figure 6-4. The gain K is adjusted such that the resulting closed loop system has desirable dynamics. Since in our case, $\mu = -2\zeta\omega$ with ζ the damping ratio of the system and $\omega = \sqrt{-L_{\beta_0} \sin \alpha_0}$, then the gain K_{p_1} to obtain a system with damping ratio ζ is given by

$$\begin{aligned} -2\zeta\omega &= L_{p_0} - K_{p_1} L_{\delta_{a_0}} + L_{\dot{\beta}_0} \sin \alpha_0 \\ \Leftrightarrow \qquad K_{p_1} &= \frac{L_{p_0} + L_{\dot{\beta}_0} \sin \alpha_0 + 2\zeta\sqrt{-L_{\beta_0} \sin \alpha_0}}{L_{\delta_{a_0}}} \end{aligned} \tag{6.11}$$

The gains to achieve certain damping ratio is shown by the dashed lines in Figure 6-4.

The figure suggests the use of low gain at low angles-of-attack and high gain at high angles-of-attack. Based on this, it can be understood that the use of a constant gain for the whole angle-of-attack range will not be optimal. In fact, if we try to compensate for the wing rock by using high gain control for the whole angle-of-attack range, the system will be highly overdamped at low angles-of-attack, hence it has a very sluggish roll response. This is undesirable, especially for a fighter aircraft. In order to avoid this problem, some sort of gain-scheduling based on angles-of-attack can be devised. The simplest scenario would be to use low or zero gain at low angles-

of-attack and to use high gain control at high angles-of-attack.

The discussion in the previous paragraph has not taken into account the range of the aileron deflections. In most aircraft, aileron deflections are limited to $\pm 30^o$ or $\pm 40^o$. Also, the maximum rate of deflection of the ailerons is usually limited. Too high a gain can easily drive the ailerons to their limits. Therefore, this physical restriction limits the potential dynamics achievable by the control system.

The simulations of the aircraft responses without and with the aileron deflection and rate limitations are shown in Figures 6-5 and 6-6. We see from the figures, that theoretically, the specified gain produces an asymptotically stable system. However, due to the aileron limitations, wing rock motion cannot be avoided. Physically, this failure is attributed to the high gain control requirement to avoid wing rock, which then leads the ailerons to their maximum limits. This high gain requirement is driven by the loss of control power (low $C_{l_{\delta_a}}$) at high angles-of-attack.

We will consider now the suppression of the resulting wing rock amplitude. Since, the amplitude of the wing rock motion is asymptotically determined by $\sqrt{-\frac{\mu}{2p_1}}$, then the suppression is achieved by minimizing the ratio $\frac{\mu}{p_1}$. At this point, we assume that the wing rock avoidance using the linear control law (6.7) can only be accomplished up to a certain angle-of-attack and we are interested in the nominal flight condition at an angle-of-attack higher than the avoidance range. Hence, the option we have is to ensure that $p_1 < 0$ (to avoid the divergent case) and to increase its magnitude as much as possible such that the ratio $\frac{\mu}{p_1}$ is as small as possible within the limitation of the controls. For the single degree-of-freedom case, p_1 is defined by

$$\tilde{p}_1 \equiv \epsilon p_1 = \frac{1}{8}(\tilde{c}_2 + 3\tilde{c}_4\omega^2) \tag{6.12}$$

The measurement of β is usually noisy, and thus is not used in the feedback system. Based on this, p_1 will be modified by feeding back p^3 into the ailerons. In this case, the control law is nonlinear and is given by

$$\delta_a = -K_{p_1}p - K_{p_3}p^3 \tag{6.13}$$

The nonlinear part of the control law augments the parameter c_4 so that p_1 becomes

$$\tilde{p}_1 = \frac{1}{8}[\tilde{c}_2 + 3(\tilde{c}_4 - K_{p_3}L_{\delta_a})\omega^2] \tag{6.14}$$

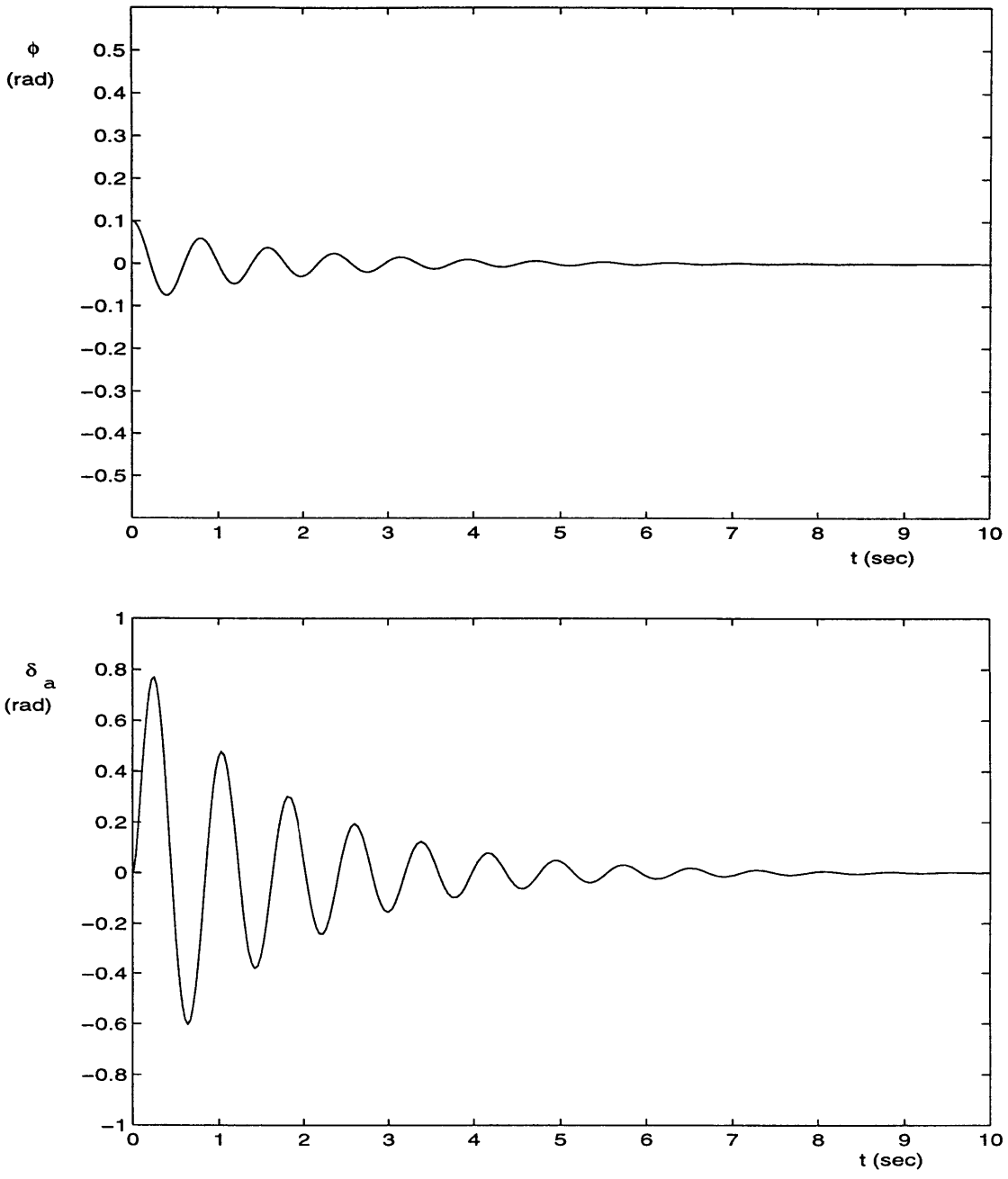

Figure 6-5: Aircraft responses without aileron limitations for specific value of control gain

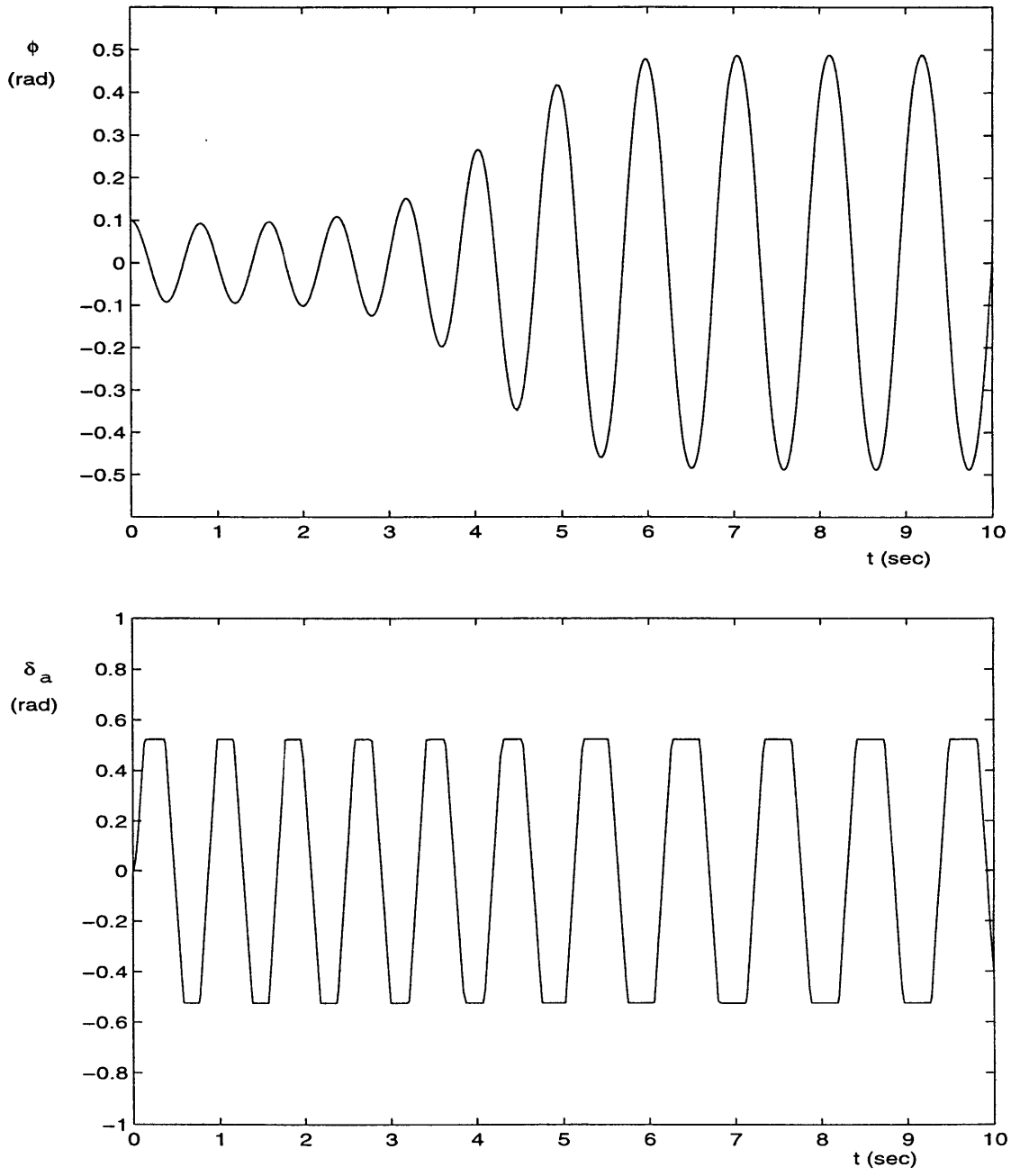

Figure 6-6: Aircraft responses with aileron limitations for specific value of control gain

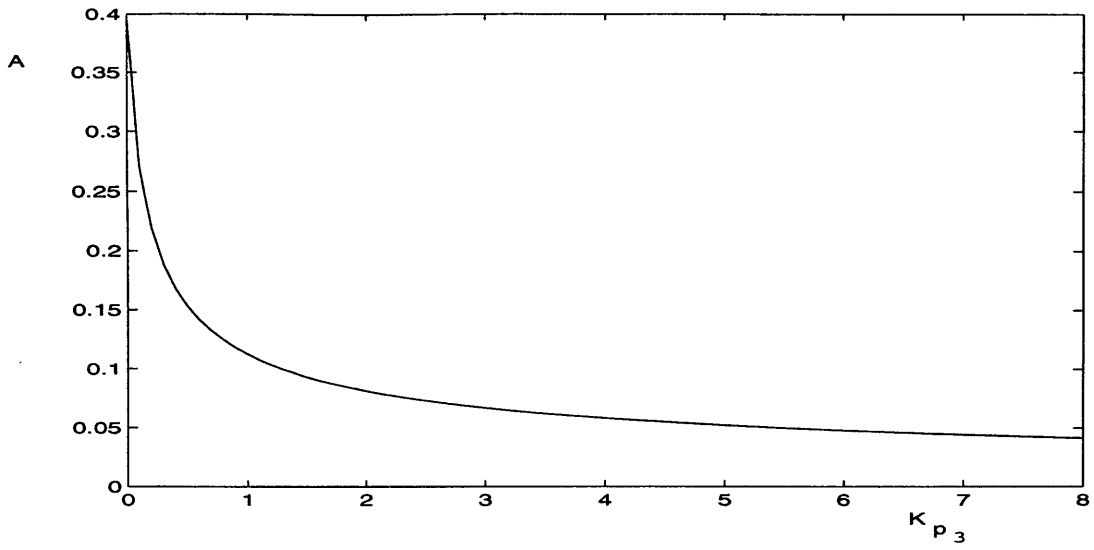

Figure 6-7: Effect of K_{p_3} on wing rock amplitude

The effect of K_{p_3} on the wing rock amplitude is summarized in Figure 6-7. Theoretically, K_{p_3} can be selected so that the maximum amplitude of wing rock is within a certain bound. Practically, the freedom in the selection of K_{p_3} is limited by the available control power and the physical limitations of the ailerons. Figure 6-8 compares the theoretical and practical suppression of wing rock at a specific angle-of-attack for a certain K_{p_1} and K_{p_3} combination. We see that although theoretically we can suppress the wing rock amplitude very well, due to the aileron physical limitations, the suppression is not successful. Therefore, the control gains have to be selected very carefully for a successful wing rock alleviation.

6.3.2 Two Degrees-of-Freedom Case

Because μ in the two degrees-of-freedom case is the same as in the single degree-of-freedom one, the discussion on wing rock avoidance in the previous subsection can again be applied here. The additional degree-of-freedom in pitch does not necessitate one to use a different avoidance strategy. The reader may refer to the previous subsection for the discussion on this matter.

The parameter p_1 in this case is more complicated than in the single degree-of-freedom case. It contains some additional terms due to the presence of the longitudinal degree-of-freedom. We may expect that such terms due to the longitudinal coupling are small. Therefore, it is clear that the wing rock suppression control law (6.13) can

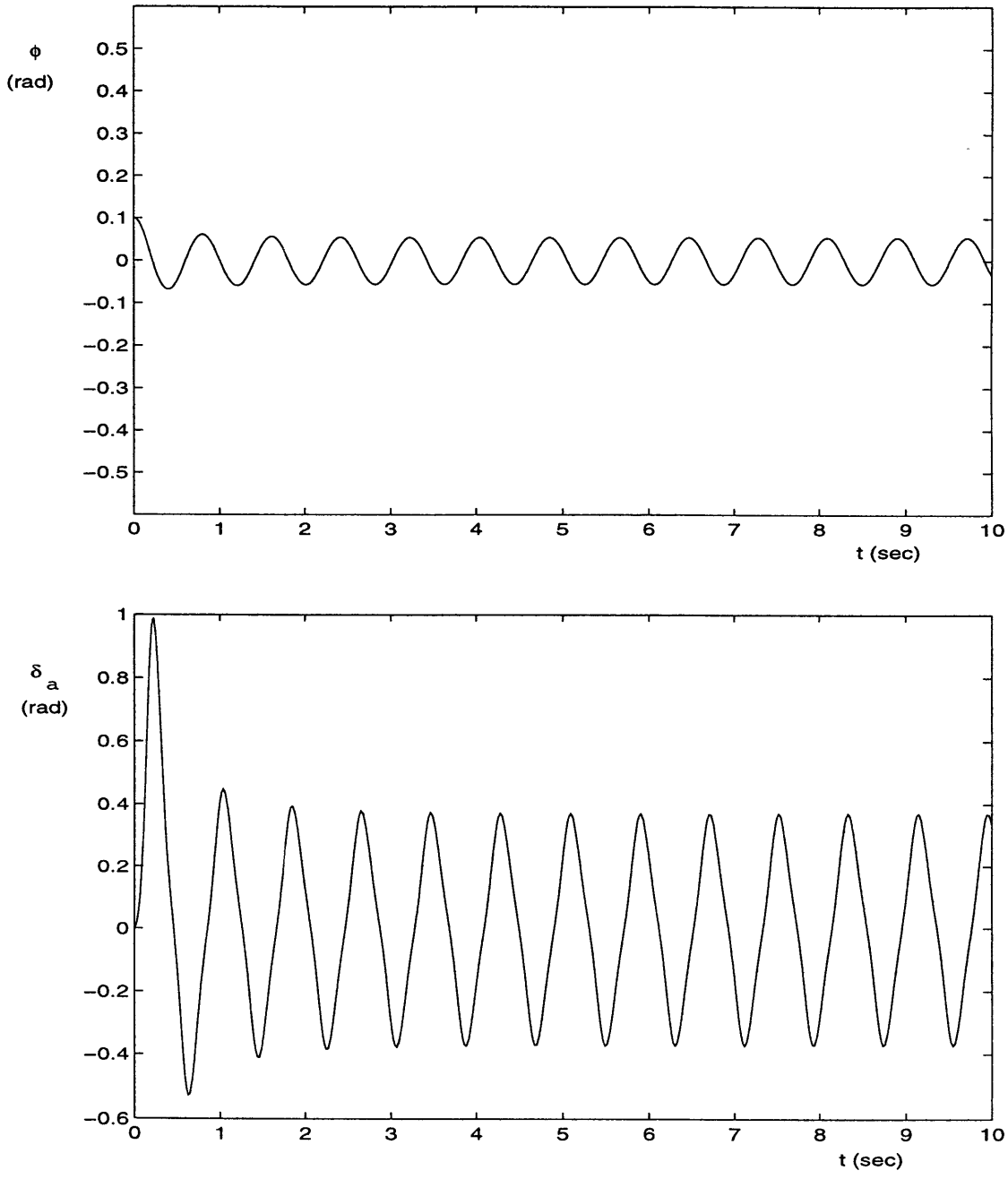

Figure 6-8: Wing rock suppression result without aileron limitations for specific values of control gains ($K_{p_1} = .5$ and $K_{p_3} = 2$)

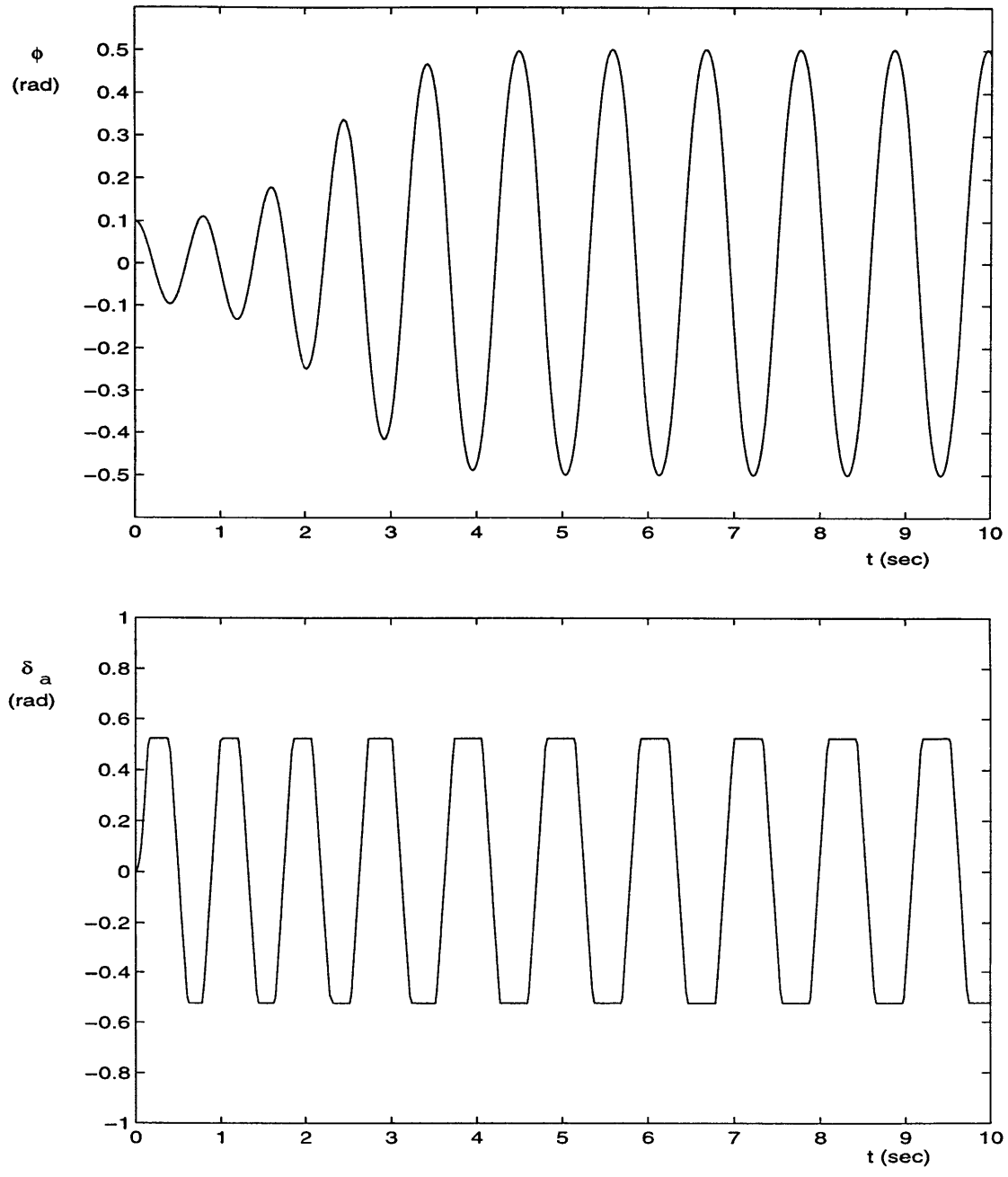

Figure 6-9: Wing rock suppression result with aileron limitations for specific values of control gains ($K_{p_1} = .5$ and $K_{p_3} = 2$)

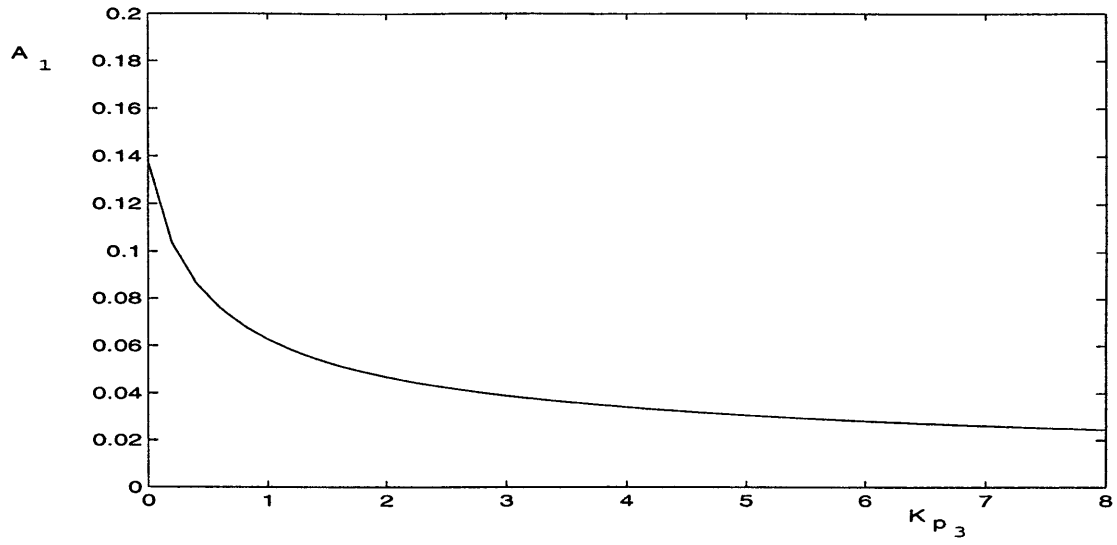

Figure 6-10: Effect of K_{p_3} on wing rock amplitude for $\alpha_0 = 35^o$

be applied also for this case. The typical effect of K_{p_3} on the wing rock amplitude for specific angle-of-attack is shown in Figure 6-10. The effect is similar to the single degree-of-freedom case.

6.3.3 Three Degrees-of-Freedom Case

As mentioned earlier, the wing rock avoidance system for the three degrees-of-freedom case is based on the modification of L_{p_0} and N_{r_0} through the use of linear feedback. L_{p_0} is modified by the feedback of roll rate to the ailerons (roll damper), while N_{r_0} can be modified by the feedback of yaw rate to the rudder (yaw damper), that is

$$\begin{aligned} \delta_a &= K_{p_1} p \\ \delta_r &= K_{r_1} r \end{aligned} \tag{6.15}$$

Such a feedback augments the linear roll and yaw damping derivatives to become

$$\begin{aligned} \bar{L}_p &= L_{p_0} - K_{p_1} L_{\delta_a} \\ \bar{N}_r &= N_{r_0} - K_{r_1} N_{\delta_r} \end{aligned} \tag{6.16}$$

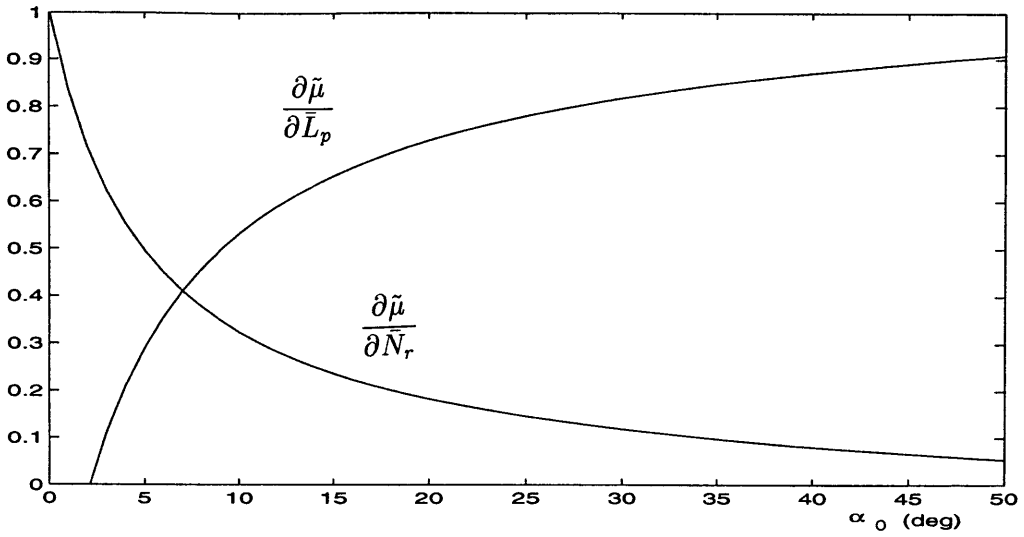

Figure 6-11: Sensitivity of μ to the augmentation of roll and yaw damping

The sensitivity of $\tilde{\mu}$ to the augmentation is described by the partial derivative of $\tilde{\mu}$ with respect to $\bar{L}_p$ and $\bar{N}_r$. From Equations (6.3) and (6.4),

$$\begin{aligned}
\frac{\partial\tilde{\mu}}{\partial\bar{L}_p} &= \frac{1}{1-n_1n_3}(\sin\alpha_0 - n_3\cos\alpha_0)\frac{L_{\beta_0}+n_1N_{\beta_0}}{\sin\alpha_0(L_{\beta_0}+n_1N_{\beta_0})-\cos\alpha_0(N_{\beta_0}+n_3L_{\beta_0}}) \\
\frac{\partial\tilde{\mu}}{\partial\bar{N}_r} &= \frac{1}{1-n_1n_3}(1-n_1\tan\alpha_0)\left[1-\frac{(L_{\beta_0}+n_1N_{\beta_0})\sin\alpha_0}{\sin\alpha_0(L_{\beta_0}+n_1N_{\beta_0})-\cos\alpha_0(N_{\beta_0}+n_3L_{\beta_0}}\right]
\end{aligned} \tag{6.17}$$

The plots of the above derivatives as a function of the nominal angle-of-attack for the generic aircraft model treated in Chapter 5 are given in Figure 6-11. We see that the sensitivity of μ to the augmentation in roll damping increases with angle-of-attack, while the sensitivity to the augmentation in yaw damping decreases with angle-of-attack. Hence, in the high angle-of-attack regimes, the roll damper is more effective for wing rock control than the yaw damper, because a certain amount of change in roll damping affects μ more than the same amount of change in yaw damping. Physically, this is due to the fact that the aircraft dynamics is dominated by roll oscillations in this flight regime.

The sensitivity of μ with respect to the control gains K_{p_1} and K_{r_1} depends on the efficiency of the aerodynamic controls, as follows

$$\frac{\partial\tilde{\mu}}{\partial K_{p_1}} = \frac{\partial\tilde{\mu}}{\partial\bar{L}_p}\frac{\partial\bar{L}_p}{\partial K_{p_1}} = -\frac{\partial\tilde{\mu}}{\partial\bar{L}_p}L_{\delta_a}$$

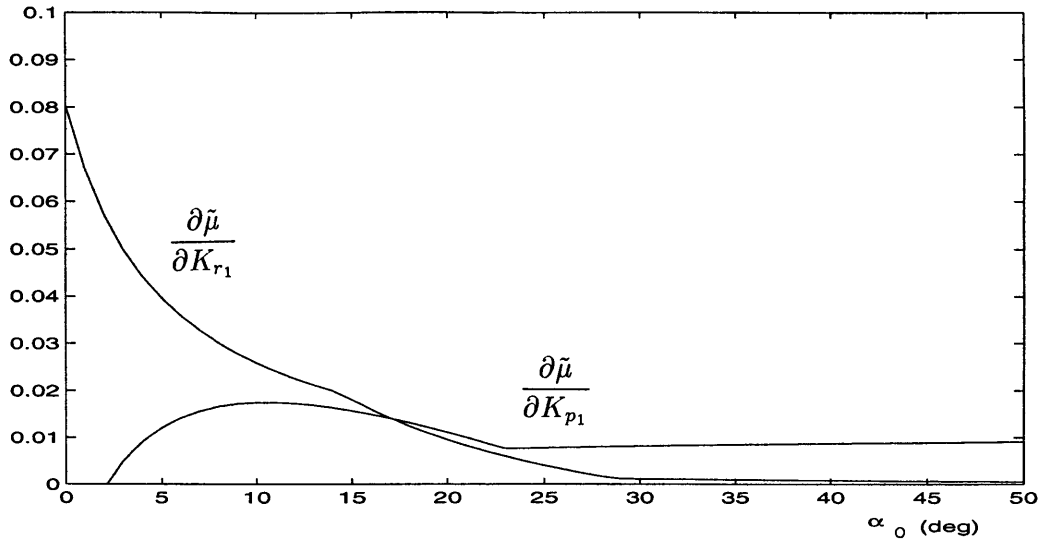

Figure 6-12: Variation of μ sensitivity to the control gains

$$\frac{\partial \tilde{\mu}}{\partial K_{r_1}} = \frac{\partial \tilde{\mu}}{\partial \bar{N}_r}\frac{\partial \bar{N}_r}{\partial K_{r_1}} = -\frac{\partial \tilde{\mu}}{\partial \bar{N}_r}N_{\delta_r} \tag{6.18}$$

where $\frac{\partial \tilde{\mu}}{\partial \bar{L}_p}$ and $\frac{\partial \tilde{\mu}}{\partial \bar{N}_r}$ are given by Equation (6.17). By using the control derivative variations given in Figure 6-3, the variations of the μ sensitivity with respect to the control gains are shown in Figure 6-12. We see here that the μ is more sensitive to roll control gain K_{p_1} than to the yaw control gain K_{r_1}. Hence, if only single channel control is implemented, the roll damper system is a better choice of the two. However, the fact that yaw damper has effect on the parameter μ can be utilized to our advantage. Yaw damper can reduce the task of the roll damper to avoid wing rock. It can be interconnected with the roll channel and be used as an integral part of the wing rock avoidance system.

When only the roll damper is present, the lower bound of the control gain K_{p_1} to avoid wing rock is shown by the solid line in Figure 6-13. If the yaw damper is also implemented in the system, the bound of K_{p_1} for wing rock avoidance becomes lower. The higher the gain of the yaw damper, the lower the gain of the roll damper needed to avoid wing rock. Similarly, Figure 6-14 depicts the lower bound of the yaw damper gain K_{r_1} for wing rock avoidance with and without the presence of the roll damper in the system. Note that the needed gains for the yaw damper are relatively higher than the gains for the roll damper. This is because the effectiveness of the rudder is very low at high angles-of-attack.

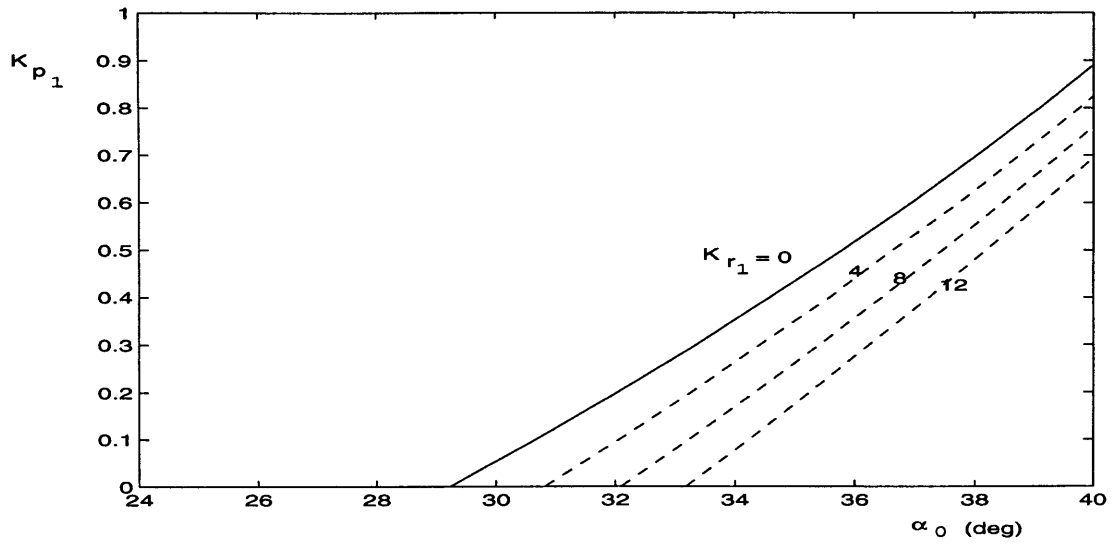

Figure 6-13: Lower bound of K_{p_1} for wing rock avoidance

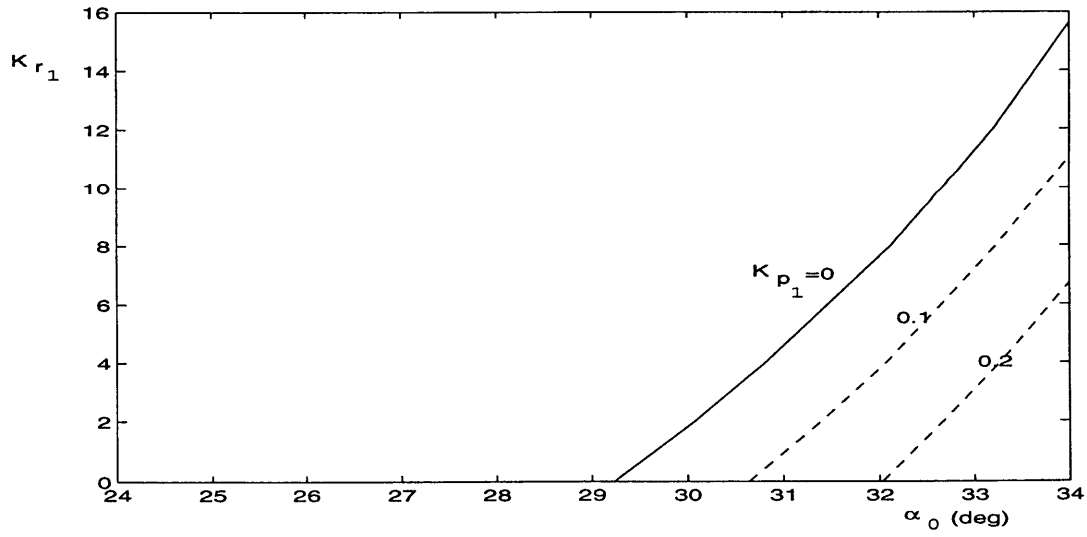

Figure 6-14: Lower bound of K_{r_1} for wing rock avoidance

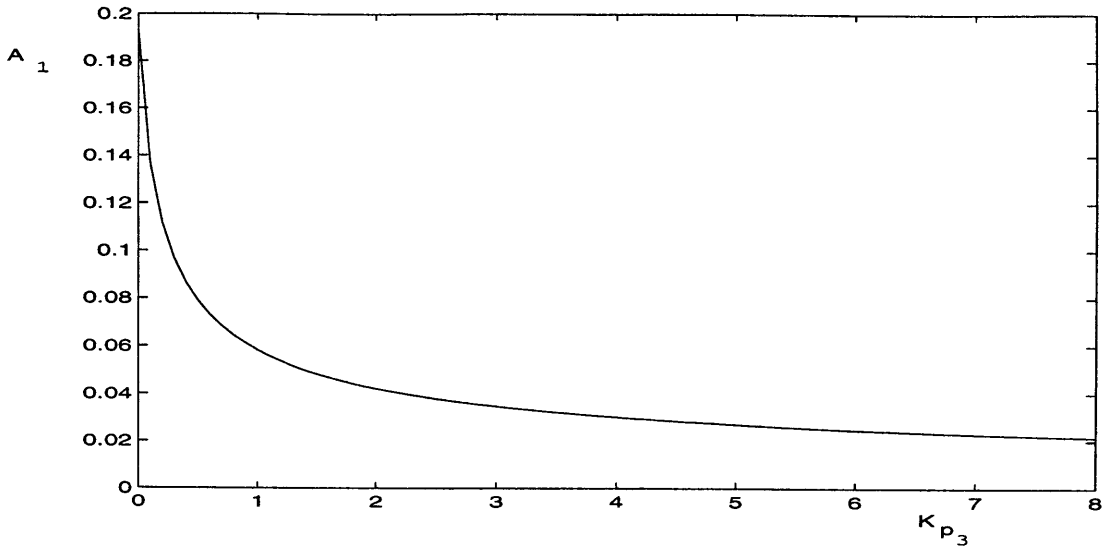

Figure 6-15: Wing rock amplitude as a function of K_{p_3} for $\alpha_0 = 33^o$

As has been discussed, the control power limitation might force us to use a wing rock suppression system rather than the avoidance system. In the previous cases, the suppression is performed by the feedback of p^3 to the ailerons. It is natural here to also consider the feedback of r^3 to the rudder for the wing rock suppression. However, since in this case the rudder effectiveness to the aircraft dynamics is very low (see Figure 6-11) the r^3 feedback to the rudder is not utilized. We will only consider the feedback of p_3 to the ailerons as in the previous cases. Hence, the wing rock suppression control laws used here are as follows.

$$\begin{aligned} \delta_a &= K_{p_1} p + K_{p_3} p^3 \\ \delta_r &= K_{r_1} r \end{aligned} \tag{6.19}$$

For specific angle-of-attack, the effect of K_{p_3} on the resulting wing rock amplitude is shown in Figure 6-15. We see that within the limitations of the control surfaces, such a feedback is quite effective in suppressing the wing rock motion.

6.4 Advanced Control Concepts

We have shown in the previous sections, that theoretically, conventional controls are sufficient to alleviate wing rock. However, limitations in the power of the conventional controls, especially at high angles-of-attack, may force us to explore other means of

control for a successful alleviation. Several advanced control techniques have been studied and applied and have been shown to be effective at high angle-of-attack operations. Some of them, which will be described briefly here, are thrust vectoring [49, 50, 51], forebody flow control [53, 54, 55]. The purpose of the description is to show the potential advantages of these techniques for high angle-of-attack control. One way to utilize these advanced control techniques is to schedule the control law with angle-of-attack such that the most effective control is used most at certain region of angles-of-attack.

6.4.1 Thrust Vectoring

As the name implies, in thrust vectoring control, the engine thrust vector is directed such that a desired control moment is obtained. Figure 6-16 illustrates this concept. Thrust vectoring is usually effective up to a very high angle-of-attack. An aircraft equipped with the thrust vectoring capability has additional control moments over the ones provided by the conventional aerodynamic control surfaces. In the high angle-of-attack region, where the aerodynamic control surfaces are usually not effective, the additional control moments from thrust vectoring are very useful. In general, thrust vectoring expands the control power envelope of the aircraft, especially at high angles-of-attack. An example of the expanded control power achieved by thrust vectoring on the F-18 HARV aircraft is given in Figure 6-17. Note that the F-18 HARV is only equipped with pitch and yaw thrust vectoring only (no roll thrust vectoring capability). In the figure, the origin represents the condition where no thrust vectoring is used. We can see that significant pitch and yaw moments can be generated by vectoring the thrust. The yaw thrust vectoring, specifically, can be very useful for wing rock alleviation.

6.4.2 Forebody Flow Control

Concepts of generating control moments by controlling the forebody flow of the aircraft have been studied (see e.g. [53]). The manipulation of the forebody flow can be performed either pneumatically (forebody blowing) or mechanically (deflectable forebody strakes). Brief look at these two forebody flow control techniques is given next.

Figure 6-18 illustrate the concept of forebody blowing. In this case, high pressure air is blown from the aircraft forebody to the surrounding airflow. The idea is to

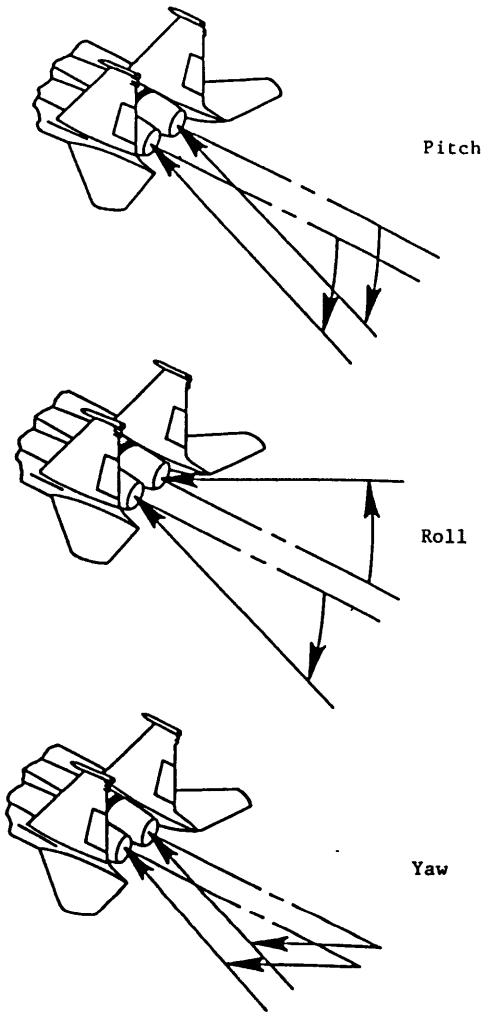

Figure 6-16: Thrust vector control moments [49]

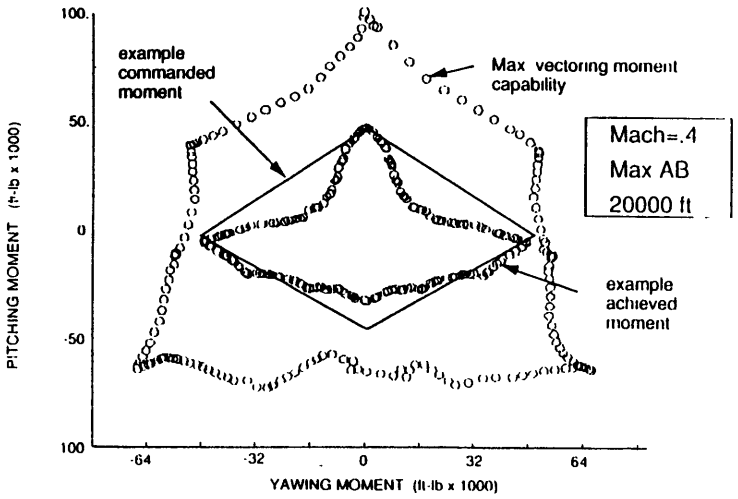

Figure 6-17: Additional moments from thrust vectoring on the F-18 HARV [52]

generate a desired vortex flow which is useful for producing aerodynamic moments. Experiment to demonstrate the effectiveness of the method on a generic fighter aircraft configuration has been performed [53, 54]. Figure 6-19 shows the effects of tangential blowing on the yawing moment of the aircraft. We can see that the blowing is especially effective at high angles-of-attack, where the rudder has become non-effective.

The use of deflectable forebody strakes for forebody flow control has been reported [53, 55]. See Figure 6-20 for an illustration of deflectable strakes. The strakes are used to produce useful vortex flow for generating desired control moments, especially at high angles-of-attack. The effectiveness of the strakes in generating yawing moment for a generic fighter configuration is given in Figure 6-21. The figure shows that the strakes can produce significant yawing moment at high angles-of-attack, which can be useful for control.

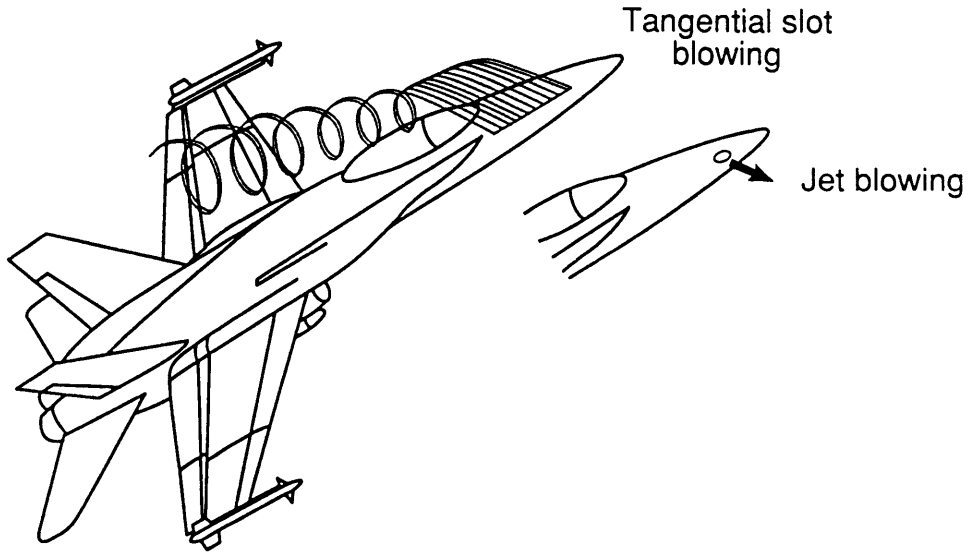

Figure 6-18: Forebody blowing concept [53]

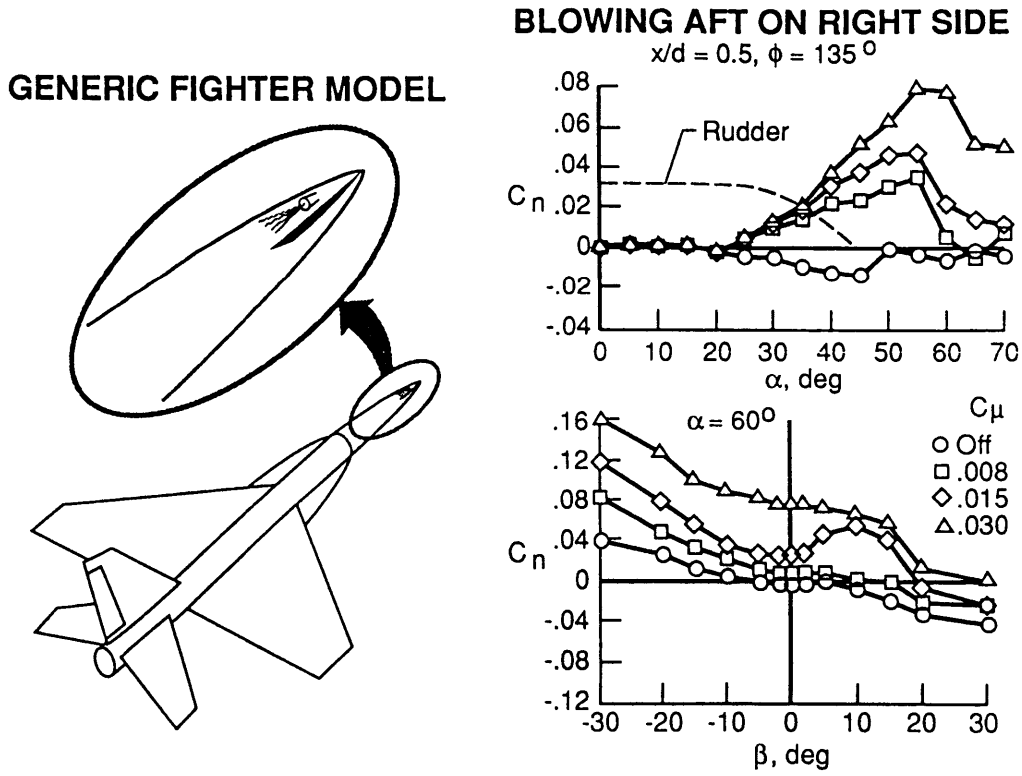

Figure 6-19: The effects of tangential forebody blowing on the yawing moment [53]

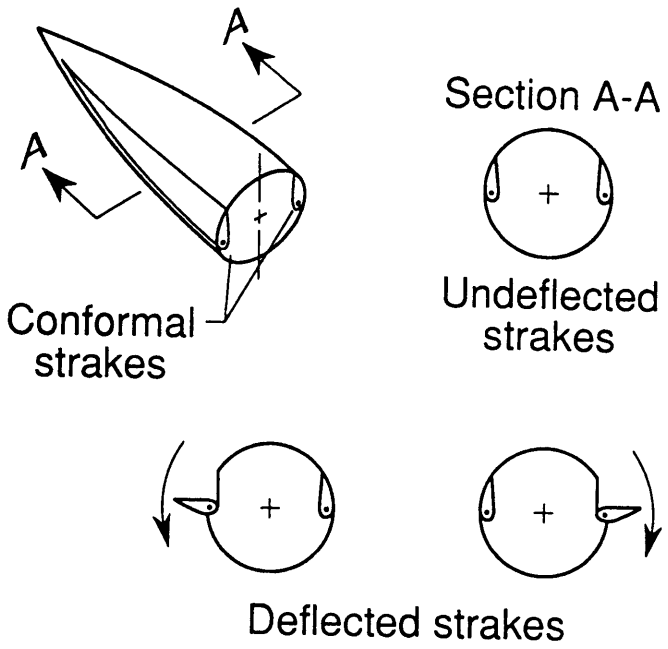

Figure 6-20: Deflectable forebody strakes [53]

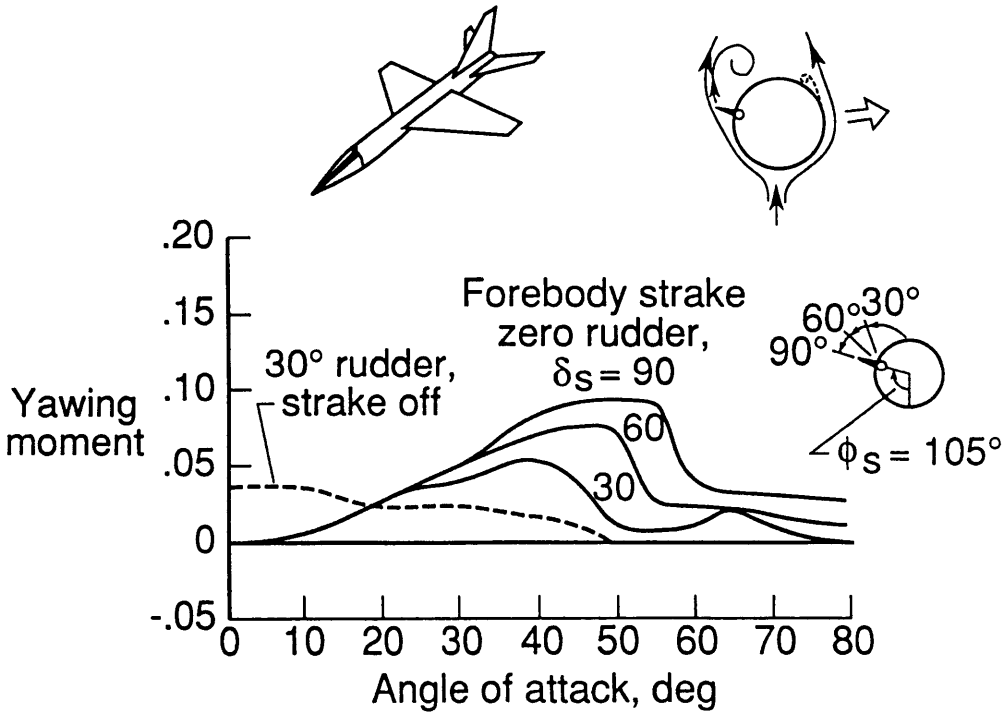

Figure 6-21: The effectiveness of forebody strakes on yawing moment [53]

Chapter 7

Conclusions and Recommendations

7.1 Conclusions

The conclusions drawn from the work presented in the previous chapters can be divided into three major groups. The grouping is based on whether the conclusions are related to wing rock dynamics, wing rock control, or the technique used for the analysis.

7.1.1 Conclusions Related to Wing Rock Dynamics

- For the three cases considered (single, two, and three degrees-of-freedom cases), the amplitude history of wing rock motion is governed asymptotically by the same form of nonlinear first order ordinary differential equation which involves the parameters μ and p_1 (see Equations (3.44), (4.65), (5.90)). Note that although the form of the equation is the same, the definitions of μ and p_1 vary from case to case, and so do the contributing parameters. Assuming that the other modes of motion are stable, then both μ and p_1 determine whether wing rock occurs in the system. μ determines the onset of wing rock and is called the wing rock damping parameter. The ratio of μ and p_1 determines the steady state amplitude of wing rock motion. Wing rock can only occur in the aircraft system when $\mu > 0$ and $p_1 < 0$.

- In general, the onset of wing rock is mainly determined by the dynamic lateral damping parameters (in linear flight dynamics sense) and to some extent by the lateral static stability parameters and lateral coupling parameters (also in

linear flight dynamics sense). In the single and two degrees-of-freedom cases, it is determined only by the dynamic roll damping parameter ($L_{p_0} + L_{\dot{\beta}_0} \sin \alpha_0$). However, in the three degrees-of-freedom case, it is not only influenced by the roll damping parameter, but also by yaw damping parameter ($N_{r_0} + N_{\dot{\beta}_0} \cos \alpha_0$), dynamic lateral coupling parameters (L_{r_0}, N_{p_0}), and static stability parameters (L_{β_0}, N_{β_0}).

- The amplitude of the wing rock motion is determined by the balance between the stabilizing and destabilizing energy from the aerodynamic moments. The stabilizing energy mainly comes from the aerodynamic nonlinearities, the parameters of which are reflected in p_1. The parameters contributing to p_1, hence affect the wing rock amplitude, can be identified to come from nonlinear terms with odd power of rate variables and from the longitudinal and lateral cross coupling nonlinearity. Strong cubic variation of lateral moments with sideslip can also have an effect on the wing rock amplitude in the three degrees-of-freedom case.

- The frequency of wing rock oscillations is mostly affected by the lateral static stability parameters of the aircraft (L_{β_0} and N_{β_0}). In the single and two degrees-of-freedom cases considered, the wing rock frequency is determined mostly by the static roll stability parameter (dihedral effect). In the three degrees-of-freedom case, the static yaw stability parameter also contributes to the wing rock frequency.

- In wing rock situation involving the longitudinal degree-of-freedom, the pitch angle goes to a new equilibrium and in steady state oscillate around the new equilibrium with a constant amplitude and twice the wing rock frequency. At specific angle-of-attack, the constant amplitude is proportional to the square of the wing rock amplitude. In general, the properties of the steady pitch oscillation during wing rock are influenced mainly by the aerodynamic cross coupling derivatives.

- Certain phenomena cannot be captured by the lower degrees-of-freedom models. For example, strong cubic variation of lateral moments with sideslip cannot cause wing rock in the single and two degrees-of-freedom cases, however it can give rise to wing rock in the three degrees-of-freedom case. Another example is the potential of wing rock due to the variation of the dynamic cross coupling derivatives with sideslip, which is not captured in the single degree-of-freedom model. In selecting which model to use in the analysis, the trade-off is between the accuracy in modeling the physical phenomena and the analysis complexity.

A higher degree-of-freedom model is more accurate in modeling the physical phenomena at the expense of a more complex analysis.

7.1.2 Conclusions Related to Wing Rock Control

- In this work, both linear and nonlinear control laws for the alleviation of wing rock have been developed. In a conventional aircraft system, feedback of roll rate to the ailerons has been shown to be effective for wing rock alleviation. For best results, nonlinear control laws need to be implemented. Linear feedback of roll rate is effective for delaying the onset of wing rock. Additional feedback of cubic of roll rate helps in suppressing the resulting wing rock amplitude.
- Feedback of yaw rate to the rudder helps in alleviating wing rock. When combined with roll rate feedback, it helps in reducing the aileron workload for this specific task.
- Due to control power limitations of conventional aerodynamic control surfaces at high angles-of-attack, advanced controls, such as thrust vectoring and forebody flow control, may need to be utilized for wing rock alleviation. Such advanced controls are used to increase the overall control power of the aircraft at high angles-of-attack.

7.1.3 Conclusions Related to the Analysis Technique

- The technique of analysis used, which is a combination of the Multiple Time Scales method, center manifold reduction principle, and bifurcation theory, is very effective in systematically uncovering the dynamics of the multiple degrees-of-freedom cases analytically. Moreover, the technique is able to obtain solutions in analytical form, which enable us to see how the parameters affect the system behavior. In contrast, numerical analysis requires iterative procedure to investigate the influences of some parameters to the dynamics of the system, and the results obtained are usually valid only for limited combination of parameter values. The analytical solutions obtained have been demonstrated to be in excellent agreement with the numerical solutions in the region of validity of the analysis.
- The application of the dynamic analysis technique in this case leads to a unified analytical form for the three classes of problem considered. The unified form is shown to be very advantageous for synthesizing an appropriate control strategy.

7.2 Recommendations

Some recommendations for future research based on the work in this dissertation are as follows.

- In current work, a nonlinear multiple degree-of-freedom mathematical model of an aircraft has been developed and has been demonstrated to be useful for the study of wing rock. As the model developed is quite general, it would be advantageous to investigate its potential use for the study of other nonlinear flight dynamics phenomena, such as roll coupling, jump phenomena, etc.

- The wing rock analysis in this work involves a rigid aircraft. Lately, interest in the development of aircraft with highly flexible wings has been observed. The flexible wings have been shown to have advantages for control. In this regard, research of wing rock on highly flexible aircraft is very important. Knowledge on the effects of the structural flexibility on wing rock properties is of a great value in understanding the dynamics of the flexible aircraft further.

- The development of a more advanced control law for wing rock alleviation combining conventional and advanced controls, based on the unified result of the dynamic analysis, is also an area that can be further explored. Such control law should be designed to overcome the control power issues. Successful control of wing rock can lead to the expansion of the flight envelope of the aircraft.

- The analysis technique used in this dissertation has been demonstrated to be capable of solving the multiple degrees-of-freedom cases systematically. It is also promising to be used for other type of problems involving multiple degrees-of-freedom. Applications of the current analysis technique for other multiple degrees-of-freedom problems are worth investigating.

Appendix A

Derivation of the Rolling Moment for the Single Degree-of-freedom Problem

The work done by the aerodynamic forces through a displacement $\delta\phi$ is given by (see Equation (3.17))

$$\delta W = -\int_{a/c} (dL\cos\alpha_0 + dD\sin\alpha_0)\, y\, \delta\phi\, dy \tag{A.1}$$

where from Equations (3.6) and (3.7)

$$\begin{aligned} dL(y) &= \bar{q}c(y)(c_{L_0} + c_{L_1}\alpha_e + c_{L_2}\alpha_e^2 + c_{L_3}\alpha_e^3)dy \\ dD(y) &= \bar{q}c(y)(c_{D_0} + c_{D_1}\alpha_e + c_{D_2}\alpha_e^2 + c_{D_3}\alpha_e^3)dy \end{aligned} \tag{A.2}$$

with (from Equation (3.16))

$$\alpha_e(y) = \alpha_1(y) + f_2(y)p + f_3(y)\beta + f_4(y)\dot{\beta} \tag{A.3}$$

We focus now on the part of the work due to the lift force on the wing. The derivation for contribution of the drag force will follow the same way and will not be shown here. The substitution of Equation (A.3) into Equation (A.2) yields

$$dL(y) = \bar{q}c(y)(c_L^e(y) + c_L^o(y))dy \tag{A.4}$$

where $c_L^e(y)$ contains terms of even functions of y and $c_L^o(y)$ contains terms of odd functions of y, as follows

$$\begin{aligned}
c_L^e(y) &= c_{L_0} + c_{L_1}\alpha_1(y) + c_{L_2}\alpha_1^2(y) + c_{L_3}\alpha_1^3(y) + c_{L_2}f_2^2(y)p^2 + c_{L_2}f_3^2(y)\beta^2 + \\
&\quad c_{L_2}f_4^2(y)\dot{\beta}^2 + 2c_{L_2}f_2(y)f_3(y)p\beta + 2c_{L_2}f_2(y)f_4(y)p\dot{\beta} + 2c_{L_2}f_3(y)f_4(y)\beta\dot{\beta} + \\
&\quad 3c_{L_3}f_2^2(y)\alpha_1(y)p^2 + 3c_{L_3}f_3^2(y)\alpha_1(y)\beta^2 + 3c_{L_3}f_4^2(y)\alpha_1(y)\dot{\beta}^2 + \\
&\quad 6c_{L_3}f_2(y)f_3(y)\alpha_1(y)p\beta + 6c_{L_3}f_2(y)f_4(y)\alpha_1(y)p\dot{\beta} + 6c_{L_3}f_3(y)f_4(y)\alpha_1(y)\beta\dot{\beta} \\
c_L^o(y) &= \left[c_{L_1}f_2(y) + 2c_{L_2}f_2(y)\alpha_1(y) + 3c_{L_3}f_2(y)\alpha_1^2(y)\right]p + [c_{L_1}f_3(y) + \\
&\quad 2c_{L_2}f_3(y)\alpha_1(y) + 3c_{L_3}f_3(y)\alpha_1^2(y)\Big]\beta + [c_{L_1}f_4(y) + 2c_{L_2}f_4(y)\alpha_1(y) + \\
&\quad 3c_{L_3}f_4(y)\alpha_1^2(y)\Big]\dot{\beta} + c_{L_3}f_2^3(y)p^3 + c_{L_3}f_3^3(y)\beta^3 + c_{L_3}f_4^3(y)\dot{\beta}^3 + \\
&\quad 3c_{L_3}f_2^2(y)f_3(y)p^2\beta + 3c_{L_3}f_2^2(y)f_4(y)p^2\dot{\beta} + 3c_{L_3}f_4^2(y)f_2(y)p\beta^2 + \\
&\quad 3c_{L_3}f_4^2(y)f_2(y)p\dot{\beta}^2 + 3c_{L_3}f_3^2(y)f_4(y)\beta^2\dot{\beta} + 3c_{L_3}f_4^2(y)f_3(y)\beta\dot{\beta}^2 + \\
&\quad 6c_{L_3}f_2(y)f_3(y)f_4(y)p\beta\dot{\beta} \qquad \text{(A.5)}
\end{aligned}$$

Then the contribution of the lift force of the wing to the total work is given by

$$\delta W_L^w = -\int_{-b/2}^{b/2} \bar{q}Sc(y)y(c_L^e(y) + c_L^o(y))\cos\alpha_0\,\delta\phi\,dy \qquad \text{(A.6)}$$

where the subscript L indicates the work due to the lift force and the superscript w indicates wing. In the above equation, $yc_L^e(y)$ gives rise to odd integrands and $yc_L^o(y)$ gives rise to even integrands. The odd integrands will integrate to zero. Therefore the above integral is determined only by the even integrands, that is

$$\delta W_L^w = -\int_{-b/2}^{b/2} \bar{q}Sc(y)yc_L^o(y)\cos\alpha_0\,\delta\phi\,dy \qquad \text{(A.7)}$$

For the first three terms in $c_L^o(y)$ (see Equation (A.5)), we get

$$-\int_{-b/2}^{b/2} \bar{q}Sc(y)y\left[c_{L_1}f_2(y) + 2c_{L_2}f_2(y)\alpha_1(y) + 3c_{L_3}f_2(y)\alpha_1^2(y)\right]dy\,\delta\phi p = \bar{c}_2^w\,\delta\phi p \qquad \text{(A.8)}$$

where $\bar{c}_2^w$ is a constant. The integration of the other terms in $c_L^o(y)$ is performed in the same manner, and by repeating the steps for the drag force and for the contribution of the horizontal tail, we get

$$\begin{aligned}
\delta W &= \Big(\bar{c}_1\beta + \bar{c}_2 p + \bar{c}_3\dot{\beta} + \bar{c}_4\beta^3 + \bar{c}_5\beta^2 p + \bar{c}_6\beta^2\dot{\beta} + \bar{c}_7\beta p^2 + \bar{c}_8\beta\dot{\beta}^2 + \bar{c}_9\dot{\beta}^3 + \\
&\quad \bar{c}_{10}p^3 + \bar{c}_{11}\beta\dot{\beta}p\Big)\,\delta\phi \qquad \text{(A.9)}
\end{aligned}$$

Then, by using

$$Q = \frac{\delta W}{\delta \phi} \tag{A.10}$$

we get the aerodynamic rolling moment expression (3.18).

Appendix B

Derivation of the Aerodynamic Moments for the Two Degrees-of-freedom Problem

The work done by the aerodynamic forces through a roll displacement $\delta\phi$ and a pitch displacement $\delta\theta$ is given by (see Equation (4.17)

$$\delta W = -\int_{a/c}(dL\cos\alpha_0 + dD\sin\alpha_0)y\delta\phi - \int_{a/c}(dL\cos\alpha_0 + dD\sin\alpha_0)l\,\delta\theta \qquad \text{(B.1)}$$

where from Equations (4.7) and (4.8)

$$\begin{aligned} dL(y) &= \bar{q}c(y)(c_{L_0} + c_{L_1}\alpha_e + c_{L_2}\alpha_e^2 + c_{L_3}\alpha_e^3)dy \\ dD(y) &= \bar{q}c(y)(c_{D_0} + c_{D_1}\alpha_e + c_{D_2}\alpha_e^2 + c_{D_3}\alpha_e^3)dy \end{aligned} \qquad \text{(B.2)}$$

with (from Equation (4.16))

$$\alpha_e(y) = \alpha_1(y) + f_2(y)p + f_3(y)\beta + f_4(y)\dot{\beta} + f_5(y)\alpha + f_6(y)q + f_7(y)\dot{\alpha} \qquad \text{(B.3)}$$

We focus now on the part of the work due to the lift force on the wing. The derivation for part due to the drag force will follow in the same way and will not be presented. The substitution of Equation (B.3) into Equation (B.2) yields

$$dL(y) = \bar{q}c(y)(c_L^e(y) + c_L^o(y))dy \qquad \text{(B.4)}$$

where $c_L^e(y)$ contains terms of even functions of y and $c_L^o(y)$ contains terms of odd functions of y, as follows

$$
\begin{aligned}
c_L^e \;=\;& c_{L_3}\alpha_1{}^3 + 3\,c_{L_3} f_2{}^2 \alpha_1 p^2 + 6\,c_{L_3} f_3 f_2 \alpha_1 p \beta + 6\,c_{L_3} f_4 f_2 \alpha_1 p \dot\beta \\
&+ 3\,c_{L_3} f_3{}^2 \alpha_1 \beta^2 + 6\,c_{L_3} f_4 f_3 \alpha_1 \beta \dot\beta + 3\,c_{L_3} f_4{}^2 \alpha_1 \dot\beta^2 + 3\,c_{L_3} f_5 \alpha \alpha_1{}^2 \\
&+ c_{L_2} \alpha_1{}^2 + 3\,c_{L_3} f_6 q \alpha_1{}^2 + 3\,c_{L_3} f_7 \dot\alpha \alpha_1{}^2 + c_{L_2} f_2{}^2 p^2 + 3\,c_{L_3} f_7 f_2{}^2 \dot\alpha p^2 \\
&+ 3\,c_{L_3} f_6 f_2{}^2 q p^2 + 3\,c_{L_3} f_5 f_2{}^2 \alpha p^2 + 6\,c_{L_3} f_7 f_3 f_2 \dot\alpha p \beta + 6\,c_{L_3} f_6 f_3 f_2 q p \beta \\
&+ 2\,c_{L_2} f_3 f_2 p \beta + 6\,c_{L_3} f_5 f_4 f_2 \alpha p \dot\beta + 6\,c_{L_3} f_7 f_4 f_2 \dot\alpha p \dot\beta + 6\,c_{L_3} f_6 f_4 f_2 q p \dot\beta \\
&+ 2\,c_{L_2} f_4 f_2 p \dot\beta + c_{L_2} f_3{}^2 \beta^2 + 3\,c_{L_3} f_6 f_3{}^2 q \beta^2 + 3\,c_{L_3} f_5 f_3{}^2 \alpha \beta^2 \\
&+ 3\,c_{L_3} f_7 f_3{}^2 \dot\alpha \beta^2 + 6\,c_{L_3} f_7 f_4 f_3 \dot\alpha \beta \dot\beta + 6\,c_{L_3} f_6 f_4 f_3 q \beta \dot\beta + 2\,c_{L_2} f_4 f_3 \beta \dot\beta \\
&+ 6\,c_{L_3} f_5 f_4 f_3 \alpha \beta \dot\beta + 3\,c_{L_3} f_5 f_4{}^2 \alpha \dot\beta^2 + c_{L_2} f_4{}^2 \dot\beta^2 + 3\,c_{L_3} f_7 f_4{}^2 \dot\alpha \dot\beta^2 \\
&+ 3\,c_{L_3} f_6 f_4{}^2 q \dot\beta^2 + 2\,c_{L_2} f_6 q \alpha_1 + 6\,c_{L_3} f_7 f_5 \dot\alpha \alpha \alpha_1 + 3\,c_{L_3} f_7{}^2 \dot\alpha^2 \alpha_1 \\
&+ 3\,c_{L_3} f_6{}^2 q^2 \alpha_1 + 2\,c_{L_2} f_5 \alpha \alpha_1 + 6\,c_{L_3} f_7 f_6 \dot\alpha q \alpha_1 + 2\,c_{L_2} f_7 \dot\alpha \alpha_1 \\
&+ 6\,c_{L_3} f_6 f_5 \alpha q \alpha_1 + c_{L_1} \alpha_1 + 3\,c_{L_3} f_5{}^2 \alpha^2 \alpha_1 + c_{L_3} f_7{}^3 \dot\alpha^3 + c_{L_3} f_5{}^3 \alpha^3 \\
&+ c_{L_1} f_7 \dot\alpha + c_{L_3} f_6{}^3 q^3 + 3\,c_{L_3} f_6 f_5{}^2 \alpha^2 q + c_{L_2} f_5{}^2 \alpha^2 + 3\,c_{L_3} f_7 f_5{}^2 \dot\alpha \alpha^2 \\
&+ 3\,c_{L_3} f_6{}^2 f_5 \alpha q^2 + 2\,c_{L_2} f_6 f_5 \alpha q + 6\,c_{L_3} f_7 f_6 f_5 \dot\alpha \alpha q + c_{L_1} f_5 \alpha \\
&+ 3\,c_{L_3} f_7{}^2 f_5 \dot\alpha^2 \alpha + 2\,c_{L_2} f_7 f_5 \dot\alpha \alpha + c_{L_2} f_7{}^2 \dot\alpha^2 + c_{L_2} f_6{}^2 q^2 \\
&+ 3\,c_{L_3} f_7 f_6{}^2 \dot\alpha q^2 + c_{L_1} f_6 q + 3\,c_{L_3} f_7{}^2 f_6 \dot\alpha^2 q + 2\,c_{L_2} f_7 f_6 \dot\alpha q + c_{L_0}
\end{aligned}
$$

$$
\begin{aligned}
c_L^o \;=\;& 3\,c_{L_3} f_2 \alpha_1{}^2 p + 3\,c_{L_3} f_3 \alpha 1^2 \beta + 3\,c_{L_3} f_4 \alpha_1{}^2 \dot\beta + c_{L_3} f_2{}^3 p^3 + 3\,c_{L_3} f_3 f_2{}^2 p^2 \beta \\
&+ 3\,c_{L_3} f_4 f_2{}^2 p^2 \dot\beta + 3\,c_{L_3} f_3{}^2 f_2 p \beta^2 + 6\,c_{L_3} f_4 f_3 f_2 p \beta \dot\beta + 3\,c_{L_3} f_4{}^2 f_2 p \dot\beta^2 \\
&+ c_{L_3} f_3{}^3 \beta^3 + 3\,c_{L_3} f_4 f_3{}^2 \beta^2 \dot\beta + 3\,c_{L_3} f_4{}^2 f_3 \beta \dot\beta^2 + c_{L_3} f_4{}^3 \dot\beta^3 \\
&+ 6\,c_{L_3} f_5 f_2 \alpha \alpha_1 p + 6\,c_{L_3} f_7 f_2 \dot\alpha \alpha_1 p + 6\,c_{L_3} f_6 f_2 q \alpha 1 p + 2\,c_{L_2} f_2 \alpha_1 p \\
&+ 6\,c_{L_3} f_5 f_3 \alpha \alpha_1 \beta + 2\,c_{L_2} f_3 \alpha_1 \beta + 6\,c_{L_3} f_7 f_3 \dot\alpha \alpha 1 \beta + 6\,c_{L_3} f_6 f_3 q \alpha_1 \beta \\
&+ 6\,c_{L_3} f_5 f_4 \alpha \alpha_1 \dot\beta + 6\,c_{L_3} f_7 f_4 \dot\alpha \alpha_1 \dot\beta + 6\,c_{L_3} f_6 f_4 q \alpha_1 \dot\beta + 2\,c_{L_2} f_4 \alpha_1 \dot\beta \\
&+ 2\,c_{L_2} f_7 f_2 \dot\alpha p + 3\,c_{L_3} f_7{}^2 f_2 \dot\alpha^2 p + c_{L_1} f_2 p + 3\,c_{L_3} f_6{}^2 f_2 q^2 p \\
&+ 3\,c_{L_3} f_5{}^2 f_2 \alpha^2 p + 6\,c_{L_3} f_6 f_5 f_2 \alpha q p + 2\,c_{L_2} f_5 f_2 \alpha p + 6\,c_{L_3} f_7 f_5 f_2 \dot\alpha \alpha p \\
&+ 6\,c_{L_3} f_7 f_6 f_2 \dot\alpha q p + 2\,c_{L_2} f_6 f_2 q p + 6\,c_{L_3} f_7 f_6 f_3 \dot\alpha q \beta + 2\,c_{L_2} f_6 f_3 q \beta \\
&+ 6\,c_{L_3} f_6 f_5 f_3 \alpha q \beta + 6\,c_{L_3} f_7 f_5 f_3 \dot\alpha \alpha \beta + c_{L_1} f_3 \beta + 2\,c_{L_2} f_7 f_3 \dot\alpha \beta \\
&+ 2\,c_{L_2} f_5 f_3 \alpha \beta + 3\,c_{L_3} f_6{}^2 f_3 q^2 \beta + 3\,c_{L_3} f_5{}^2 f_3 \alpha^2 \beta + 3\,c_{L_3} f_7{}^2 f_3 \dot\alpha^2 \beta \\
&+ 2\,c_{L_2} f_5 f_4 \alpha \dot\beta + 2\,c_{L_2} f_6 f_4 q \dot\beta + 6\,c_{L_3} f_6 f_5 f_4 \alpha q \dot\beta + 3\,c_{L_3} f_6{}^2 f_4 q^2 \dot\beta \\
&+ 3\,c_{L_3} f_5{}^2 f_4 \alpha^2 \dot\beta + 2\,c_{L_2} f_7 f_4 \dot\alpha \dot\beta + 6\,c_{L_3} f_7 f_6 f_4 \dot\alpha q \dot\beta \\
&+ 6\,c_{L_3} f_7 f_5 f_4 \dot\alpha \alpha \dot\beta + 3\,c_{L_3} f_7{}^2 f_4 \dot\alpha^2 \dot\beta + c_{L_1} f_4 \dot\beta
\end{aligned}
$$

Then the contribution of the lift force on the wing to the total work is given by

$$\begin{aligned}\delta W_L^w &= -\int_{-b/2}^{b/2} \bar{q}Sc(y)y(c_L^e(y)+c_L^o(y))\cos\alpha_0\,\delta\phi\,dy - \\ &\quad -\int_{-b/2}^{b/2} \bar{q}Sc(y)l_w(c_L^e(y)+c_L^o(y))\cos\alpha_0\,\delta\theta\,dy \end{aligned} \tag{B.5}$$

where the subscript L indicates the work due to the lift force and the superscript w indicates the contribution of the wings. In the first integral, $yc_L^e(y)$ gives rise to odd integrands and $yc_L^o(y)$ gives rise to even integrands. The odd integrands will integrate to zero. Therefore the first integral is determined only by $yc_L^o(y)$. In the second integral, $c_L^e(y)$ gives rise to even integrands and $c_L^o(y)$ gives rise to odd integrands. Since the odd integrands integrate to zero, the second integral is then determined only by $c_L^e(y)$. Thus,

$$\delta W_L^w = -\int_{-b/2}^{b/2} \bar{q}Sc(y)yc_L^o(y)\cos\alpha_0\,\delta\phi\,dy - \int_{-b/2}^{b/2} \bar{q}Sc(y)l_wc_L^e(y)\cos\alpha_0\,\delta\theta\,dy \tag{B.6}$$

For example, for the first term in c_L^o,

$$-\int_{-b/2}^{b/2} \bar{q}Sc(y)y[3c_{L_3}f_2(y)\alpha_1^2 p]\cos\alpha_0\,\delta\phi\,dy = \bar{c}_2^w p\delta\phi \tag{B.7}$$

and for the second term in c_L^e, we get

$$-\int_{-b/2}^{b/2} \bar{q}Sc(y)l_w[3c_{L_3}f_2^2(y)\alpha_1 p^2]\cos\alpha_0\,\delta\theta\,dy = \bar{d}_{40}^w p^2\delta\theta \tag{B.8}$$

By integrating the other terms in the similar manner, and repeating the steps for the drag components and for the horizontal tail contribution, and then using the relations

$$\begin{aligned} Q_1 &= \frac{\delta W}{\delta\phi} \\ Q_2 &= \frac{\delta W}{\delta\theta} \end{aligned} \tag{B.9}$$

we obtain Equation (4.18).

Appendix C

Derivation of the Aerodynamic Moments for the Three Degrees-of-freedom Problem

As in the single and two degrees-of-freedom cases, only the part of work due to wings is derived in detail. The work done by the aerodynamic forces on the wings through the angular displacements $\delta\phi$, $\delta\theta$, and $\delta\psi$ is given by (see Equation (5.19)

$$\begin{aligned}\delta W^w &= -\int_w (dL\cos\alpha_0 + dD\sin\alpha_0)y\delta\phi - \int_w (dL\cos\alpha_0 + dD\sin\alpha_0)l_w\delta\theta + \\ &\int_w (dL\sin\alpha_0 - dD\cos\alpha_0)y\delta\psi \qquad \text{(C.1)}\end{aligned}$$

where from Equations (5.15) and (5.16)

$$\begin{aligned}dL(y) &= \bar{q}c(y)(c_{L_0} + c_{L_1}\alpha_e + c_{L_2}\alpha_e^2 + c_{L_3}\alpha_e^3)dy \\ dD(y) &= \bar{q}c(y)(c_{D_0} + c_{D_1}\alpha_e + c_{D_2}\alpha_e^2 + c_{D_3}\alpha_e^3)dy \qquad \text{(C.2)}\end{aligned}$$

with (from Equation (5.18))

$$\alpha_e(y) = \alpha_1(y) + f_2(y)p + f_3(y)\beta + f_4(y)\dot{\beta} + f_5(y)\alpha + f_6(y)q + f_7(y)\dot{\alpha} + f_8(y)r \quad \text{(C.3)}$$

Again, we focus now on the part of the work integral due to the lift force. The derivation for part due to the drag force will follow the same way and will not be shown. The substitution of Equation (C.3) into Equation (C.2) yields

$$dL(y) = \bar{q}c(y)(c_L^e(y) + c_L^o(y))dy \qquad \text{(C.4)}$$

where $c_L^e(y)$ contains terms of even functions of y and $c_L^o(y)$ contains terms of odd functions of y, as follows

$$
\begin{aligned}
c_L^e \;=\;& c_{L_3}\,{\alpha_1}^3 + 3\,c_{L_3}\,{f_2}^2\,\alpha_1\,p^2 + 6\,c_{L_3}\,f_3\,f_2\,\alpha_1\,p\,\beta + 6\,c_{L_3}\,f_4\,f_2\,\alpha_1\,p\,\beta 1 \\
&+ 3\,c_{L_3}\,{f_3}^2\,\alpha_1\,\beta^2 + 6\,c_{L_3}\,f_4\,f_3\,\alpha_1\,\beta\,\beta 1 + 3\,c_{L_3}\,{f_4}^2\,\alpha_1\,\beta 1^2 + c_{L_2}\,{\alpha_1}^2 \\
&+ 3\,c_{L_3}\,f_5\,\alpha\,{\alpha_1}^2 + 3\,c_{L_3}\,f_7\,\dot{\alpha}\,{\alpha_1}^2 + 3\,c_{L_3}\,f_6\,q\,{\alpha_1}^2 + 6\,c_{L_3}\,f_8\,f_2\,r\,\alpha_1\,p \\
&+ 6\,c_{L_3}\,f_8\,f_4\,r\,\alpha_1\,\beta 1 + 3\,c_{L_3}\,f_7\,{f_2}^2\,\dot{\alpha}\,p^2 + 3\,c_{L_3}\,f_5\,{f_2}^2\,\alpha\,p^2 + c_{L_2}\,{f_2}^2\,p^2 \\
&+ 3\,c_{L_3}\,f_6\,{f_2}^2\,q\,p^2 + 6\,c_{L_3}\,f_7\,f_3\,f_2\,\dot{\alpha}\,p\,\beta + 6\,c_{L_3}\,f_6\,f_3\,f_2\,q\,p\,\beta + 2\,c_{L_2}\,f_3\,f_2\,p\,\beta \\
&+ 6\,c_{L_3}\,f_5\,f_3\,f_2\,\alpha\,p\,\beta + 6\,c_{L_3}\,f_6\,f_4\,f_2\,q\,p\,\beta 1 + 6\,c_{L_3}\,f_5\,f_4\,f_2\,\alpha\,p\,\beta 1 \\
&+ 6\,c_{L_3}\,f_7\,f_4\,f_2\,\dot{\alpha}\,p\,\beta 1 + 2\,c_{L_2}\,f_4\,f_2\,p\,\beta 1 + 3\,c_{L_3}\,f_5\,{f_3}^2\,\alpha\,\beta^2 + 3\,c_{L_3}\,f_7\,{f_3}^2\,\dot{\alpha}\,\beta^2 \\
&+ 3\,c_{L_3}\,f_6\,{f_3}^2\,q\,\beta^2 + c_{L_2}\,{f_3}^2\,\beta^2 + 6\,c_{L_3}\,f_5\,f_4\,f_3\,\alpha\,\beta\,\beta 1 + 6\,c_{L_3}\,f_7\,f_4\,f_3\,\dot{\alpha}\,\beta\,\beta 1 \\
&+ 6\,c_{L_3}\,f_6\,f_4\,f_3\,q\,\beta\,\beta 1 + 2\,c_{L_2}\,f_4\,f_3\,\beta\,\beta 1 + 3\,c_{L_3}\,f_5\,{f_4}^2\,\alpha\,\beta 1^2 + c_{L_2}\,{f_4}^2\,\beta 1^2 \\
&+ 3\,c_{L_3}\,f_7\,{f_4}^2\,\dot{\alpha}\,\beta 1^2 + 3\,c_{L_3}\,f_6\,{f_4}^2\,q\,\beta 1^2 + 3\,c_{L_3}\,{f_6}^2\,q^2\,\alpha_1 + 2\,c_{L_2}\,f_6\,q\,\alpha_1 \\
&+ 6\,c_{L_3}\,f_8\,f_6\,r\,q\,\alpha_1 + c_{L_1}\,\alpha_1 + 3\,c_{L_3}\,{f_5}^2\,\alpha^2\,\alpha_1 + 6\,c_{L_3}\,f_6\,f_5\,\alpha\,q\,\alpha_1 \\
&+ 6\,c_{L_3}\,f_7\,f_5\,\dot{\alpha}\,\alpha\,\alpha_1 + 3\,c_{L_3}\,{f_7}^2\,\dot{\alpha}^2\,\alpha_1 + 6\,c_{L_3}\,f_8\,f_7\,r\,\dot{\alpha}\,\alpha_1 + 2\,c_{L_2}\,f_7\,\dot{\alpha}\,\alpha_1 \\
&+ 6\,c_{L_3}\,f_7\,f_6\,\dot{\alpha}\,q\,\alpha_1 + 3\,c_{L_3}\,{f_8}^2\,r^2\,\alpha_1 + 2\,c_{L_2}\,f_5\,\alpha\,\alpha_1 + 6\,c_{L_3}\,f_8\,f_6\,f_2\,r\,q\,p \\
&+ 2\,c_{L_2}\,f_8\,f_2\,r\,p + 6\,c_{L_3}\,f_8\,f_5\,f_2\,r\,\alpha\,p + 6\,c_{L_3}\,f_8\,f_7\,f_2\,r\,\dot{\alpha}\,p + 6\,c_{L_3}\,f_8\,f_7\,f_3\,r\,\dot{\alpha}\,\beta \\
&+ 6\,c_{L_3}\,f_6\,f_5\,f_3\,\alpha\,q\,\beta + 2\,c_{L_2}\,f_6\,f_3\,q\,\beta + 2\,c_{L_2}\,f_8\,f_3\,r\,\beta + 6\,c_{L_3}\,f_8\,f_5\,f_3\,r\,\alpha\,\beta \\
&+ 6\,c_{L_3}\,f_8\,f_6\,f_3\,r\,q\,\beta + 6\,c_{L_3}\,f_8\,f_5\,f_4\,r\,\alpha\,\beta 1 + 6\,c_{L_3}\,f_8\,f_6\,f_4\,r\,q\,\beta 1 \\
&+ 6\,c_{L_3}\,f_8\,f_7\,f_4\,r\,\dot{\alpha}\,\beta 1 + 2\,c_{L_2}\,f_8\,f_4\,r\,\beta 1 + c_{L_3}\,{f_7}^3\,\dot{\alpha}^3 + c_{L_3}\,{f_6}^3\,q^3 \\
&+ c_{L_3}\,{f_5}^3\,\alpha^3 + 3\,c_{L_3}\,{f_8}^2\,f_6\,r^2\,q + c_{L_2}\,{f_5}^2\,\alpha^2 + 3\,c_{L_3}\,f_7\,{f_5}^2\,\dot{\alpha}\,\alpha^2 + c_{L_2}\,{f_8}^2\,r^2 \\
&+ 3\,c_{L_3}\,f_6\,{f_5}^2\,\alpha^2\,q + 6\,c_{L_3}\,f_7\,f_6\,f_5\,\dot{\alpha}\,\alpha\,q + c_{L_1}\,f_5\,\alpha + 3\,c_{L_3}\,{f_6}^2\,f_5\,\alpha\,q^2 \\
&+ 2\,c_{L_2}\,f_6\,f_5\,\alpha\,q + c_{L_2}\,{f_7}^2\,\dot{\alpha}^2 + 3\,c_{L_3}\,{f_8}^2\,f_5\,r^2\,\alpha + c_{L_2}\,{f_6}^2\,q^2 + 3\,c_{L_3}\,f_7\,{f_6}^2\,\dot{\alpha}\,q^2 \\
&+ c_{L_1}\,f_6\,q + 3\,c_{L_3}\,{f_7}^2\,f_6\,\dot{\alpha}^2\,q + 2\,c_{L_2}\,f_7\,f_6\,\dot{\alpha}\,q + 3\,c_{L_3}\,{f_8}^2\,f_7\,r^2\,\dot{\alpha} \\
&+ 3\,c_{L_3}\,{f_7}^2\,f_5\,\dot{\alpha}^2\,\alpha + 2\,c_{L_2}\,f_7\,f_5\,\dot{\alpha}\,\alpha + c_{L_0}
\end{aligned}
$$

$$
\begin{aligned}
c_L^o \;=\;& 3\,c_{L_3}\,f_2\,{\alpha_1}^2\,p + 3\,c_{L_3}\,f_3\,\alpha 1^2\,\beta + 3\,c_{L_3}\,f_4\,{\alpha_1}^2\,\beta 1 + c_{L_3}\,{f_2}^3\,p^3 + 3\,c_{L_3}\,f_3\,{f_2}^2\,p^2\,\beta \\
&+ 3\,c_{L_3}\,f_4\,{f_2}^2\,p^2\,\beta 1 + 3\,c_{L_3}\,{f_3}^2\,f_2\,p\,\beta^2 + 6\,c_{L_3}\,f_4\,f_3\,f_2\,p\,\beta\,\beta 1 + 3\,c_{L_3}\,{f_4}^2\,f_2\,p\,\beta 1^2 \\
&+ c_{L_3}\,{f_3}^3\,\beta^3 + 3\,c_{L_3}\,f_4\,{f_3}^2\,\beta^2\,\beta 1 + 3\,c_{L_3}\,{f_4}^2\,f_3\,\beta\,\beta 1^2 + c_{L_3}\,{f_4}^3\,\beta 1^3 \\
&+ 3\,c_{L_3}\,f_8\,r\,{\alpha_1}^2 + 2\,c_{L_2}\,f_2\,\alpha_1\,p + 6\,c_{L_3}\,f_6\,f_2\,q\,\alpha_1\,p + 6\,c_{L_3}\,f_7\,f_2\,\dot{\alpha}\,\alpha_1\,p \\
&+ 6\,c_{L_3}\,f_5\,f_2\,\alpha\,\alpha_1\,p + 6\,c_{L_3}\,f_6\,f_3\,q\,\alpha 1\,\beta + 6\,c_{L_3}\,f_5\,f_3\,\alpha\,\alpha_1\,\beta + 2\,c_{L_2}\,f_3\,\alpha_1\,\beta \\
&+ 6\,c_{L_3}\,f_7\,f_3\,\dot{\alpha}\,\alpha_1\,\beta + 2\,c_{L_2}\,f_4\,\alpha_1\,\beta 1 + 6\,c_{L_3}\,f_6\,f_4\,q\,\alpha_1\,\beta 1 + 6\,c_{L_3}\,f_5\,f_4\,\alpha\,\alpha_1\,\beta 1 \\
&+ 6\,c_{L_3}\,f_7\,f_4\,\dot{\alpha}\,\alpha_1\,\beta 1 + 3\,c_{L_3}\,f_8\,{f_2}^2\,r\,p^2 + 6\,c_{L_3}\,f_8\,f_3\,f_2\,r\,p\,\beta + 6\,c_{L_3}\,f_8\,f_4\,f_2\,r\,p\,\beta 1 \\
&+ 3\,c_{L_3}\,f_8\,{f_3}^2\,r\,\beta^2 + 6\,c_{L_3}\,f_5\,f_4\,f_3\,\alpha\,\beta\,\beta 1 + 6\,c_{L_3}\,f_8\,f_4\,f_3\,r\,\beta\,\beta 1 \\
&+ 3\,c_{L_3}\,f_8\,{f_4}^2\,r\,\beta 1^2 + 6\,c_{L_3}\,f_8\,f_5\,r\,\alpha\,\alpha_1 + 2\,c_{L_2}\,f_8\,r\,\alpha_1 + 6\,c_{L_3}\,f_8\,f_6\,r\,q\,\alpha_1 \\
&+ 6\,c_{L_3}\,f_8\,f_7\,r\,\dot{\alpha}\,\alpha_1 + 6\,c_{L_3}\,f_7\,f_6\,f_2\,\dot{\alpha}\,q\,p + 3\,c_{L_3}\,{f_7}^2\,f_2\,\dot{\alpha}^2\,p + 2\,c_{L_2}\,f_7\,f_2\,\dot{\alpha}\,p \\
&+ 3\,c_{L_3}\,{f_5}^2\,f_2\,\alpha^2\,p + 6\,c_{L_3}\,f_7\,f_5\,f_2\,\dot{\alpha}\,\alpha\,p + 2\,c_{L_2}\,f_6\,f_2\,q\,p + 3\,c_{L_3}\,{f_6}^2\,f_2\,q^2\,p
\end{aligned}
$$

$$
\begin{aligned}
&+ 6\,c_{L_3}\,f_6\,f_5\,f_2\,\alpha\,q\,p + 2\,c_{L_2}\,f_5\,f_2\,\alpha\,p + c_{L_1}\,f_2\,p + 3\,c_{L_3}\,{f_8}^2\,f_2\,r^2\,p + 2\,c_{L_2}\,f_7\,f_3\,\dot{\alpha}\,\beta \\
&+ 6\,c_{L_3}\,f_7\,f_5\,f_3\,\dot{\alpha}\,\alpha\,\beta + 2\,c_{L_2}\,f_6\,f_3\,q\,\beta + 3\,c_{L_3}\,{f_6}^2\,f_3\,q^2\,\beta + 3\,c_{L_3}\,{f_5}^2\,f_3\,\alpha^2\,\beta \\
&+ 3\,c_{L_3}\,{f_8}^2\,f_3\,r^2\,\beta + 6\,c_{L_3}\,f_7\,f_6\,f_3\,\dot{\alpha}\,q\,\beta + 2\,c_{L_2}\,f_5\,f_3\,\alpha\,\beta + c_{L_1}\,f_3\,\beta \\
&+ 3\,c_{L_3}\,{f_7}^2\,f_3\,\dot{\alpha}^2\,\beta + 6\,c_{L_3}\,f_7\,f_5\,f_4\,\dot{\alpha}\,\alpha\,\beta 1 + 2\,c_{L_2}\,f_5\,f_4\,\alpha\,\beta 1 + 3\,c_{L_3}\,{f_8}^2\,f_4\,r^2\,\beta 1 \\
&+ 2\,c_{L_2}\,f_7\,f_4\,\dot{\alpha}\,\beta 1 + 3\,c_{L_3}\,{f_5}^2\,f_4\,\alpha^2\,\beta 1 + 6\,c_{L_3}\,f_6\,f_5\,f_4\,\alpha\,q\,\beta 1 + c_{L_1}\,f_4\,\beta 1 \\
&+ 3\,c_{L_3}\,{f_6}^2\,f_4\,q^2\,\beta 1 + 3\,c_{L_3}\,{f_7}^2\,f_4\,\dot{\alpha}^2\,\beta 1 + 6\,c_{L_3}\,f_7\,f_6\,f_4\,\dot{\alpha}\,q\,\beta 1 + 2\,c_{L_2}\,f_6\,f_4\,q\,\beta 1 \\
&+ 3\,c_{L_3}\,f_8\,{f_5}^2\,r\,\alpha^2 + 3\,c_{L_3}\,f_8\,{f_6}^2\,r\,q^2 + 6\,c_{L_3}\,f_8\,f_6\,f_5\,r\,\alpha\,q + 2\,c_{L_2}\,f_8\,f_6\,r\,q \\
&+ c_{L_1}\,f_8\,r + 6\,c_{L_3}\,f_8\,f_7\,f_5\,r\,\alpha\,\dot{\alpha} + c_{L_3}\,{f_8}^3\,r^3 + 6\,c_{L_3}\,f_8\,f_7\,f_6\,r\,q\,\dot{\alpha} + 2\,c_{L_2}\,f_8\,f_5\,r\,\alpha \\
&+ 3\,c_{L_3}\,f_8\,{f_7}^2\,r\,\dot{\alpha}^2 + 2\,c_{L_2}\,f_8\,f_7\,r\,\dot{\alpha}
\end{aligned}
$$

Then the contribution of the lift force of the wing to the total work is given by

$$
\begin{aligned}
\delta W_L^w \;=\; & -\int_{-b/2}^{b/2} \bar{q}Sc(y)y(c_L^e(y) + c_L^o(y))\cos\alpha_0\,\delta\phi\,dy - \\
& -\int_{-b/2}^{b/2} \bar{q}Sc(y)l_w(c_L^e(y) + c_L^o(y))\cos\alpha_0\,\delta\theta\,dy + \\
& \int_{-b/2}^{b/2} \bar{q}Sc(y)y(c_L^e(y) + c_L^o(y))\sin\alpha_0\,\delta\psi\,dy
\end{aligned}
\tag{C.5}
$$

where the subscript L indicates the work due to the lift force. In the first and third integrals, $yc_L^e(y)$ gives rise to odd integrands and $yc_L^o(y)$ gives rise to even integrands. The odd integrands will integrate to zero. Therefore the first and third integrals are determined only by $yc_L^o(y)$. In the second integral, $c_L^e(y)$ gives rise to even integrands and $c_L^o(y)$ gives rise to odd integrands. Since the odd integrands integrate to zero, the second integral is then determined only by $c_L^e(y)$. Thus,

$$
\begin{aligned}
\delta W_L^w \;=\; & -\int_{-b/2}^{b/2} \bar{q}Sc(y)yc_L^o(y)\cos\alpha_0\,\delta\phi\,dy - \int_{-b/2}^{b/2} \bar{q}Sc(y)l_w c_L^e(y)\cos\alpha_0\,\delta\theta\,dy + \\
& \int_{-b/2}^{b/2} \bar{q}Sc(y)yc_L^o(y)\sin\alpha_0\,\delta\psi\,dy
\end{aligned}
\tag{C.6}
$$

The contribution of the horizontal tail is obtained in the similar manner. Integrating term by term in the same manner as in Appendix A and B for both lift and drag coefficients, and by using

$$
\begin{aligned}
Q_1 &= \frac{\delta W}{\delta\phi} \\
Q_2 &= \frac{\delta W}{\delta\theta}
\end{aligned}
$$

$$Q_3 = \frac{\delta W}{\delta \psi} \tag{C.7}$$

we obtain Equation (5.20).

Appendix D

Relations Between Coefficients of Equations (4.30) and (4.18)

ϕ-equation :

$$
\begin{aligned}
\omega^2 &= -\bar{c}_1 \sin\alpha_0 \\
\tilde{\mu} &= \bar{c}_2 + c_3 \sin\alpha_0 \\
\tilde{c}_1 &= \left(\frac{n_2}{n_3} - n_1 n_2\right)\bar{c}_1 \sin\alpha_0 + \bar{c}_4 \sin^3\alpha_0 - n_1 \bar{d}_{38} \sin^2\alpha_0 \\
\tilde{c}_2 &= \left(\frac{n_2}{n_3} - n_1 n_2\right)(\bar{c}_2 + \bar{c}_3 \sin\alpha_0) + \bar{c}_5 \sin^2\alpha_0 + \bar{c}_6 \sin^3\alpha_0 - n_1(\bar{d}_{39} + \bar{d}_{41} \sin\alpha_0)\sin\alpha_0 \\
\tilde{c}_3 &= \bar{c}_7 \sin\alpha_0 + \bar{c}_{38} \sin^2\alpha_0 + \bar{c}_8 \sin^3\alpha_0 - n_1(-n_2 + \bar{d}_{40} + \bar{d}_{42} \sin^2\alpha_0) \\
\tilde{c}_4 &= \bar{c}_9 \sin^3\alpha_0 + \bar{c}_{10} \\
\tilde{c}_5 &= \bar{c}_{11} \sin\alpha_0 - n_1 \bar{d}_1 \\
\tilde{c}_6 &= (\bar{c}_{12} + \bar{c}_{13}) \sin\alpha_0 - n_1(\bar{d}_2 + \bar{d}_3) \\
\tilde{c}_7 &= \bar{c}_{14} \sin\alpha_0 + \bar{c}_{17} \\
\tilde{c}_8 &= -n_1 + (\bar{c}_{15} + \bar{c}_{16}) \sin\alpha_0 + \bar{c}_{18} + \bar{c}_{18} \\
\tilde{c}_9 &= \bar{c}_{20} - n_1 \bar{d}_4 \\
\tilde{c}_{10} &= \frac{n_1}{n_3} + (\bar{c}_{21} + \bar{c}_{22} + \bar{c}_{35}) \sin\alpha_0 - n_1(\bar{d}_7 + \bar{d}_8 + \bar{d}_9) \\
\tilde{c}_{11} &= \bar{c}_{23} \sin\alpha_0 + \bar{c}_{26} \\
\tilde{c}_{12} &= (\bar{c}_{24} + \bar{c}_{25} + \bar{c}_{37}) \sin\alpha_0 + \bar{c}_{27} + \bar{c}_{28} + \bar{c}_{36} \\
\tilde{c}_{13} &= (\bar{c}_{29} + \bar{c}_{32}) \sin\alpha_0 - n_1(\bar{d}_5 + \bar{d}_6) \\
\tilde{c}_{14} &= \bar{c}_{30} + \bar{c}_{33} + (\bar{c}_{31} + \bar{c}_{34}) \sin\alpha_0
\end{aligned}
$$

θ-equation :

$$
\begin{aligned}
\Omega^2 &= -\bar{d}_1 \\
\tilde{\nu} &= (\bar{d}_2 + \bar{d}_3) \\
\tilde{d}_1 &= \bar{d}_4 \\
\tilde{d}_2 &= \bar{d}_5 + \bar{d}_6 \\
\tilde{d}_3 &= \bar{d}_7 + \bar{d}_8 + \bar{d}_9 \\
\tilde{d}_4 &= \bar{d}_{10} \\
\tilde{d}_5 &= \bar{d}_{11} + \bar{d}_{12} \\
\tilde{d}_6 &= \bar{d}_{14} + \bar{d}_{15} + \bar{d}_{19} \\
\tilde{d}_7 &= \bar{d}_{13} + \bar{d}_{16} + \bar{d}_{17} + \bar{d}_{18} \\
\tilde{d}_8 &= \left(-\frac{n_2}{n_3} + n_1 n_3\right) \bar{d}_1 + \bar{d}_{20} \sin^2 \alpha_0 - n_2 \bar{c}_{11} \sin \alpha_0 \\
\tilde{d}_9 &= (\bar{d}_{21} + \bar{d}_{22}) \sin \alpha_0 - n_2 (\bar{c}_{14} \sin \alpha_0 + \bar{c}_{17}) \\
\tilde{d}_{10} &= \bar{d}_{23} + (\bar{d}_{24} + \bar{d}_{25} \sin \alpha_0) \sin \alpha_0 \\
\tilde{d}_{11} &= \left(-\frac{n_2}{n_3} + n_1 n_2\right) (\bar{d}_2 + \bar{d}_3) + (\bar{d}_{26} + \bar{d}_{32}) \sin \alpha_0 - n_2 (\bar{c}_{12} + \bar{c}_{13}) \sin \alpha_0 \\
\tilde{d}_{12} &= -2\frac{n_2}{n_3} + n_1 n_2 + (\bar{d}_{27} + \bar{d}_{33}) \sin \alpha_0 + (\bar{d}_{28} + \bar{d}_{34}) \sin^2 \alpha_0 - n_2 ((\bar{c}_{15} + \bar{c}_{16}) \sin \alpha_0 + \\
&\quad \bar{c}_{18} + \bar{c}_{19}) \\
\tilde{d}_{13} &= \bar{d}_{29} + \bar{d}_{35} + (\bar{d}_{30} + \bar{d}_{36}) \sin \alpha_0 + (\bar{d}_{31} + \bar{d}_{37}) \sin^2 \alpha_0 \\
\tilde{d}_{14} &= \bar{d}_{38} \sin^2 \alpha_0 - n_2 \bar{c}_1 \sin \alpha_0 \\
\tilde{d}_{15} &= (\bar{d}_{39} + \bar{d}_{41} \sin \alpha_0) \sin \alpha_0 - n_2 (\bar{c}_2 + \bar{c}_3 \sin \alpha_0) \\
\tilde{d}_{16} &= -n_2 + \bar{d}_{40} + \bar{d}_{42} \sin^2 \alpha_0
\end{aligned}
$$

Appendix E

Relations Between Coefficients of Equations (5.29) and (5.20)

To shorten the notation, we define the following :

$$\begin{aligned} c\alpha &= \cos\alpha_0 \\ s\alpha &= \sin\alpha_0 \\ t\alpha &= \tan\alpha_0 \\ \bar{g} &= \frac{g}{V}\cos\alpha_0 \end{aligned}$$

β-equation :

$$\begin{aligned} \omega_1 &= \frac{1}{1-n_1n_3}\left[(\bar{c}_1+n_1\bar{e}_1)s\alpha-(\bar{e}_1+n_3\bar{c}_1)c\alpha\right] \\ \tilde{\eta}_1 &= \frac{1}{1-n_1n_3}\left[c\alpha\left(\bar{c}_3-\frac{\bar{c}_4}{c\alpha}+n_1(\bar{e}_3-\frac{\bar{e}_4}{c\alpha})\right)-c\alpha\left(\bar{e}_3-\frac{\bar{e}_4}{c\alpha}+\right.\right. \\ &\quad \left.\left. n_3(\bar{c}_3-\frac{\bar{c}_4}{c\alpha_0})\right)\right] \\ \tilde{\kappa}_2 &= \frac{\bar{g}}{1-n_1n_3}\left[-(\bar{e}_4+n_3\bar{c}_4)+t\alpha(\bar{c}_4+n_1\bar{e}_4)\right] \\ \tilde{\eta}_2 &= \bar{g}+\frac{1}{1-n_1n_3}\left[s\alpha(\bar{c}_2+\bar{c}_4t\alpha+n_1(\bar{e}_2+\bar{e}_4t\alpha))-\right. \\ &\quad \left. c\alpha(\bar{e}_2+\bar{e}_4t\alpha+n_3(\bar{c}_2+\bar{c}_4t\alpha))\right] \\ \tilde{e}_1 &= \left(\frac{\left(-\frac{n_1n_3\bar{d}_2}{(1-n_1n_3)n_2}-\frac{n_1\bar{e}_4}{1-n_1n_3}\right)\bar{g}}{c\alpha}+\right. \end{aligned}$$

$$
\left(\frac{n_1\bar{e}_{28}}{1-n_1n_3}-\frac{n_1n_3}{1-n_1n_3}-\frac{n_1n_3\bar{d}_{50}}{(1-n_1n_3)n_2}+\frac{n_1}{(1-n_1n_3)n_2}+\frac{\bar{c}_{28}}{1-n_1n_3}\right)\bar{g}^2
$$

$$
\Big/c\alpha^2+\frac{\left(\frac{n_1\bar{e}_{14}}{1-n_1n_3}+\frac{\bar{c}_{14}}{1-n_1n_3}\right)\bar{g}^3}{c\alpha^3}\Bigg)(s\alpha)+
$$

$$
\left(\frac{n_3}{1-n_1n_3}-\frac{\bar{e}_{28}}{1-n_1n_3}+\frac{n_3\bar{d}_{50}}{(1-n_1n_3)n_2}-\frac{n_3\bar{c}_{28}}{1-n_1n_3}-\frac{n_1n_3}{(1-n_1n_3)n_2}\right)\bar{g}^2\Big/
$$

$$
(c\alpha)+\frac{\left(-\frac{\bar{e}_{14}}{1-n_1n_3}-\frac{n_3\bar{c}_{14}}{1-n_1n_3}\right)\bar{g}^3}{(c\alpha)^2}
$$

$$
+\left(\frac{\bar{e}_4}{1-n_1n_3}+\frac{\bar{d}_2n_3}{(1-n_1n_3)n_2}\right)\bar{g}
$$

$$
\tilde{e}_2 \;=\; \Bigg(\Bigg(\frac{n_1\bar{e}_{24}}{1-n_1n_3}+\frac{n_1n_3\bar{d}_{47}}{(1-n_1n_3)n_2}-3\,\frac{n_1n_3}{(1-n_1n_3)n_2}-2\,\frac{\bar{e}_{28}}{1-n_1n_3}-\frac{n_1}{1-n_1n_3}
$$

$$
+2\,\frac{n_3}{1-n_1n_3}+2\,\frac{n_3\bar{d}_{50}}{(1-n_1n_3)n_2}+\frac{{n_1}^2n_3}{(1-n_1n_3){n_2}^2}-2\,\frac{n_3\bar{c}_{28}}{1-n_1n_3}
$$

$$
+\frac{\bar{c}_{24}}{1-n_1n_3}\Bigg)\bar{g}\Big/(c\alpha)
$$

$$
+\frac{\left(-3\,\frac{\bar{e}_{14}}{1-n_1n_3}+\frac{n_1\bar{e}_{16}}{1-n_1n_3}+\frac{\bar{c}_{16}}{1-n_1n_3}-3\,\frac{n_3\bar{c}_{14}}{1-n_1n_3}\right)\bar{g}^2}{c\alpha^2}-\frac{n_1\bar{e}_2}{1-n_1n_3}
$$

$$
+\frac{\bar{d}_2n_3}{(1-n_1n_3)n_2}+\frac{\bar{e}_4}{1-n_1n_3}\Bigg)(s\alpha)+\frac{\bar{e}_2(c\alpha)}{1-n_1n_3}+\Bigg(
$$

$$
\left(-\frac{\bar{e}_{16}}{1-n_1n_3}-\frac{n_3\bar{c}_{16}}{1-n_1n_3}\right)\bar{g}^2+\frac{1}{2}\frac{n_1n_3\bar{d}_2c(2\alpha)}{(1-n_1n_3)n_2}+\frac{1}{2}\frac{n_1\bar{e}_4c(2\alpha)}{1-n_1n_3}
$$

$$
-\frac{1}{2}\frac{n_1\bar{e}_4}{1-n_1n_3}-\frac{1}{2}\frac{n_1n_3\bar{d}_2}{(1-n_1n_3)n_2}\Bigg)\Big/(c\alpha)+\Bigg(\frac{\bar{c}_{28}}{1-n_1n_3}
$$

$$
-\frac{n_1n_3\bar{d}_{50}}{(1-n_1n_3)n_2}+\frac{n_1n_3\bar{d}_{50}c(2\alpha)}{(1-n_1n_3)n_2}+\frac{n_1n_3c(2\alpha)}{1-n_1n_3}+\frac{n_1\bar{e}_{28}}{1-n_1n_3}
$$

$$
+\frac{n_1}{(1-n_1n_3)n_2}-\frac{n_1c(2\alpha)}{(1-n_1n_3)n_2}-\frac{\bar{c}_{28}c(2\alpha)}{1-n_1n_3}-\frac{n_1n_3}{1-n_1n_3}
$$

$$
-\frac{n_1\bar{e}_{28}c(2\alpha)}{1-n_1n_3}\Bigg)\bar{g}\Big/c\alpha^2+
$$

$$
\left(-\frac{3}{2}\frac{n_1\bar{e}_{14}c(2\alpha)}{1-n_1n_3}+\frac{3}{2}\frac{\bar{c}_{14}}{1-n_1n_3}+\frac{3}{2}\frac{n_1\bar{e}_{14}}{1-n_1n_3}-\frac{3}{2}\frac{\bar{c}_{14}c(2\alpha)}{1-n_1n_3}\right)\bar{g}^2\Big/
$$

$$
c\alpha^3+\Bigg(\frac{1}{1-n_1n_3}-\frac{n_3\bar{d}_{47}}{(1-n_1n_3)n_2}+\frac{n_3}{(1-n_1n_3)n_2}-\frac{n_3n_1}{(1-n_1n_3){n_2}^2}
$$

$$
\begin{aligned}
&- \frac{\bar{e}_{24}}{1-n_1n_3} - \frac{n_3\bar{c}_{24}}{1-n_1n_3}\Big)\,\bar{g} \\
\tilde{e}_3 \;=\; &\Bigg(\frac{\Big(\frac{\bar{c}_{15}}{1-n_1n_3} + \frac{n_1\bar{e}_{15}}{1-n_1n_3}\Big)\,\bar{g}}{(c\alpha)} + \Big(\frac{3}{4}\frac{n_1}{(1-n_1n_3)n_2} + \frac{3}{4}\frac{\bar{c}_{28}}{1-n_1n_3} \\
&- \frac{3}{4}\frac{n_1n_3\bar{d}_{50}}{(1-n_1n_3)n_2} - \frac{3}{4}\frac{n_1n_3}{1-n_1n_3} + \frac{3}{4}\frac{n_1\bar{e}_{28}}{1-n_1n_3}\Big)\Big/(c\alpha)^2 \\
&+ \frac{\Big(\frac{9}{4}\frac{n_1\bar{e}_{14}}{1-n_1n_3} + \frac{9}{4}\frac{\bar{c}_{14}}{1-n_1n_3}\Big)\,\bar{g}}{c\alpha^3} + \frac{n_1n_3}{1-n_1n_3} - \frac{n_1n_3\bar{d}_{45}}{(1-n_1n_3)n_2} - 1 + \frac{n_2}{n_3} \\
&+ \bar{d}_{47} - \frac{n_1}{n_2}\Bigg)\,s\alpha + (-n_2 + \bar{d}_{45} - N62)c\alpha + \Big(\frac{1}{2}\frac{n_1c(2\alpha)}{1-n_1n_3} \\
&- \frac{1}{2}\frac{n_1}{1-n_1n_3} + \frac{1}{2}\frac{n_1n_3c(2\alpha)}{(1-n_1n_3)n_2} - \frac{1}{2}\frac{n_1n_3\bar{d}_{47}}{(1-n_1n_3)n_2} - \frac{1}{2}n_2c(2\alpha) \\
&- \frac{1}{2}\frac{n_1n_3}{(1-n_1n_3)n_2} + \frac{1}{2}\frac{\bar{c}_{24}}{1-n_1n_3} + \frac{1}{2}\frac{n_1n_3\bar{d}_{47}c(2\,\alpha)}{(1-n_1n_3)n_2} \\
&+ \frac{1}{2}\frac{{n_1}^2n_3}{(1-n_1n_3){n_2}^2} - \frac{1}{2}\frac{{n_1}^2n_3c(2\alpha)}{(1-n_1n_3){n_2}^2} + \frac{1}{2}\bar{d}_{50} + \frac{1}{2}n_2 + \frac{1}{2}\frac{n_1\bar{e}_{24}}{1-n_1n_3} \\
&- \frac{1}{2}\frac{n_1\bar{e}_{24}c(2\alpha)}{1-n_1n_3} - \frac{1}{2}\frac{\bar{c}_{24}c(2\alpha)}{1-n_1n_3} - \frac{1}{2}\bar{d}_{50}c(2\alpha)\Big)\Big/((c\alpha)) + \Big(\\
&\Big(-\frac{n_1\bar{e}_{16}c(2\alpha)}{1-n_1n_3} + \frac{\bar{c}_{16}}{1-n_1n_3} - \frac{\bar{c}_{16}c(2\alpha)}{1-n_1n_3} + \frac{n_1\bar{e}_{16}}{1-n_1n_3}\Big)\,\bar{g} \\
&- \frac{1}{4}\frac{n_1\bar{e}_{28}s(3\alpha)}{1-n_1n_3} - \frac{1}{4}\frac{n_1s(3\alpha)}{(1-n_1n_3)n_2} + \frac{1}{4}\frac{n_1n_3s(3\alpha)}{1-n_1n_3} \\
&- \frac{1}{4}\frac{\bar{c}_{28}s(3\alpha)}{1-n_1n_3} + \frac{1}{4}\frac{n_1n_3\bar{d}_{50}s(3\alpha)}{(1-n_1n_3)n_2}\Big)\Big/(c\alpha)^2 \\
&+ \frac{\Big(-\frac{3}{4}\frac{n_1\bar{e}_{14}s(3\alpha)}{1-n_1n_3} - \frac{3}{4}\frac{\bar{c}_{14}s(3\alpha)}{1-n_1n_3}\Big)\,\bar{g}}{c\alpha^3} \\
\tilde{e}_4 \;=\; &\Bigg(\frac{\frac{3}{4}\frac{\bar{c}_{16}}{1-n_1n_3} + \frac{3}{4}\frac{n_1\bar{e}_{16}}{1-n_1n_3} - \frac{3}{4}\frac{n_3\bar{c}_{14}}{1-n_1n_3} - \frac{3}{4}\frac{\bar{e}_{14}}{1-n_1n_3}}{c\alpha^2} + \frac{n_1\bar{e}_{12}}{1-n_1n_3} \\
&+ \frac{\bar{c}_{12}}{1-n_1n_3} - \frac{n_3\bar{c}_{15}}{1-n_1n_3} - \frac{\bar{e}_{15}}{1-n_1n_3}\Bigg)\,s\alpha \\
&+ \Big(-\frac{n_3\bar{c}_{12}}{1-n_1n_3} - \frac{\bar{e}_{12}}{1-n_1n_3}\Big)\,(c\alpha) + \Big(-\frac{1}{2}\frac{\bar{e}_{16}}{1-n_1n_3} + \frac{1}{2}\frac{n_1\bar{e}_{15}}{1-n_1n_3} \\
&- \frac{1}{2}\frac{n_1\bar{e}_{15}c(2\alpha)}{1-n_1n_3} + \frac{1}{2}\frac{\bar{c}_{15}}{1-n_1n_3} + \frac{1}{2}\frac{\bar{e}_{16}c(2\alpha)}{1-n_1n_3} - \frac{1}{2}\frac{\bar{c}_{15}c(2\alpha)}{1-n_1n_3}
\end{aligned}
$$

$$
\begin{aligned}
&\left.-\frac{1}{2}\frac{n_3\bar{c}_{16}}{1-n_1n_3}+\frac{1}{2}\frac{n_3\bar{c}_{16}c(2\alpha)}{1-n_1n_3}\right)\Big/(c\alpha)+\Big(\\
&\frac{1}{4}\frac{\bar{e}_{14}s(3\alpha)}{1-n_1n_3}-\frac{1}{4}\frac{\bar{c}_{16}s(3\alpha)}{1-n_1n_3}+\frac{1}{4}\frac{n_3\bar{c}_{14}s(3\alpha)}{1-n_1n_3}-\frac{1}{4}\frac{n_1\bar{e}_{16}s(3\alpha)}{1-n_1n_3}\\
&\Big)\Big/c\alpha^2+\Big(-\frac{1}{2}\frac{\bar{c}_{14}c(2\alpha)}{1-n_1n_3}+\frac{1}{8}\frac{n_1\bar{e}_{14}c(4\alpha)}{1-n_1n_3}+\frac{3}{8}\frac{\bar{c}_{14}}{1-n_1n_3}\\
&+\frac{1}{8}\frac{\bar{c}_{14}c(4\alpha)}{1-n_1n_3}+\frac{3}{8}\frac{n_1\bar{e}_{14}}{1-n_1n_3}-\frac{1}{2}\frac{n_1\bar{e}_{14}c(2\alpha)}{1-n_1n_3}\Big)\Big/c\alpha^3
\end{aligned}
$$

$$
\tilde{e}_5 = \left(\frac{\bar{c}_5}{1-n_1n_3}+\frac{n_1\bar{e}_5}{1-n_1n_3}\right)s\alpha+\left(-\frac{n_3\bar{c}_5}{1-n_1n_3}-\frac{\bar{e}_5}{1-n_1n_3}\right)c\alpha
$$

$$
\begin{aligned}
\tilde{e}_6 = &\left(\frac{-\dfrac{\bar{c}_7}{1-n_1n_3}-\dfrac{n_1\bar{e}_7}{1-n_1n_3}}{c\alpha}+\frac{\bar{c}_8}{1-n_1n_3}+\frac{n_1\bar{e}_8}{1-n_1n_3}\right)(s\alpha)\\
&+\left(-\frac{n_3\bar{c}_8}{1-n_1n_3}-\frac{\bar{e}_8}{1-n_1n_3}\right)(c\alpha)+\frac{n_3\bar{c}_7}{1-n_1n_3}+\frac{\bar{e}_7}{1-n_1n_3}
\end{aligned}
$$

$$
\begin{aligned}
\tilde{e}_7 = &\left(\frac{-\bar{c}_{38}-n_1\bar{e}_{38}}{(1-n_1n_3)c\alpha}+\frac{\bar{c}_{10}+n_1\bar{e}_{10}}{(1-n_1n_3)(c\alpha)^2}+\frac{\bar{c}_{11}+n_1\bar{e}_{11}}{1-n_1n_3}\right)(s\alpha)\\
&-\frac{(\bar{e}_{11}+n_3\bar{c}_{11})c\alpha}{1-n_1n_3}-\frac{\bar{e}_{10}+n_3\bar{c}_{10}}{(1-n_1n_3)c\alpha}-\frac{-n_3\bar{c}_{38}-\bar{e}_{38}}{1-n_1n_3}
\end{aligned}
$$

$$
\begin{aligned}
\tilde{e}_8 = &\left(\frac{-\dfrac{n_1\bar{e}_{17}}{1-n_1n_3}-\dfrac{\bar{c}_{17}}{1-n_1n_3}}{c\alpha}+\frac{\dfrac{\bar{c}_{18}}{1-n_1n_3}+\dfrac{n_1\bar{e}_{18}}{1-n_1n_3}}{c\alpha^2}+\frac{-\dfrac{n_1\bar{e}_{14}}{1-n_1n_3}-\dfrac{\bar{c}_{14}}{1-n_1n_3}}{c\alpha^3}\right.\\
&\left.+\frac{\bar{c}_{13}}{1-n_1n_3}+\frac{n_1\bar{e}_{13}}{1-n_1n_3}\right)(s\alpha)+\left(-\frac{n_3\bar{c}_{13}}{1-n_1n_3}-\frac{\bar{e}_{13}}{1-n_1n_3}\right)(c\alpha)\\
&+\frac{-\dfrac{\bar{e}_{18}}{1-n_1n_3}-\dfrac{n_3\bar{c}_{18}}{1-n_1n_3}}{(c\alpha)}+\frac{\dfrac{\bar{e}_{14}}{1-n_1n_3}+\dfrac{n_3\bar{c}_{14}}{1-n_1n_3}}{c\alpha^2}+\frac{\bar{e}_{17}}{1-n_1n_3}\\
&+\frac{n_3\bar{c}_{17}}{1-n_1n_3}
\end{aligned}
$$

$$
\begin{aligned}
\tilde{e}_9 = &\left(\frac{\left(\dfrac{n_1\bar{e}_{22}}{1-n_1n_3}+\dfrac{\bar{c}_{22}}{1-n_1n_3}-\dfrac{n_1n_3\bar{d}_{44}}{(1-n_1n_3)n_2}\right)\bar{g}}{c\alpha}+\frac{\left(\dfrac{n_1\bar{e}_{10}}{1-n_1n_3}+\dfrac{\bar{c}_{10}}{1-n_1n_3}\right)\bar{g}^2}{(c\alpha)^2}\right.\\
&\left.-\frac{n_1\bar{e}_1}{1-n_1n_3}\right)(s\alpha)+\\
&\left(-\frac{\bar{e}_1n_1n_3}{1-n_1n_3}+3\frac{\bar{e}_1}{1-n_1n_3}-\frac{\bar{e}_1n_2}{(1-n_1n_3)n_3}+\frac{\bar{e}_1n_1n_2}{1-n_1n_3}-\frac{\bar{e}_1n_3}{(1-n_1n_3)n_2}\right)\\
&c\alpha+\frac{\left(-\dfrac{\bar{e}_{10}}{1-n_1n_3}-\dfrac{n_3\bar{c}_{10}}{1-n_1n_3}\right)\bar{g}^2}{c\alpha}
\end{aligned}
$$

$$
\begin{aligned}
&+\left(-\frac{\bar{e}_{22}}{1-n_1n_3}-\frac{n_3\bar{c}_{22}}{1-n_1n_3}+\frac{\bar{d}_{44}n_3}{(1-n_1n_3)n_2}\right)\bar{g}\\
\tilde{e}_{10} \;=\; &\left(\left(\right.\right.\\
&\left(\frac{n_1\bar{e}_{26}}{1-n_1n_3}+\frac{\bar{c}_{26}}{1-n_1n_3}-\frac{n_1n_3\bar{d}_{49}}{(1-n_1n_3)n_2}\right)\bar{g}+\frac{n_1\bar{e}_4}{1-n_1n_3}+\frac{n_1n_3\bar{d}_2}{(1-n_1n_3)n_2}\Big)\\
&\Big/(c\alpha)+\left(\left(\frac{\bar{c}_{18}}{1-n_1n_3}+\frac{n_1\bar{e}_{18}}{1-n_1n_3}\right)\bar{g}^2+\left(2\,\frac{n_1n_3\bar{d}_{50}}{(1-n_1n_3)n_2}\right.\right.\\
&\left.-2\,\frac{n_1\bar{e}_{28}}{1-n_1n_3}-2\,\frac{n_1}{(1-n_1n_3)n_2}+2\,\frac{n_1n_3}{1-n_1n_3}-2\,\frac{\bar{c}_{28}}{1-n_1n_3}\right)\bar{g}\Big)\Big/c\alpha^2\\
&+\frac{\left(-3\,\frac{\bar{c}_{14}}{1-n_1n_3}-3\,\frac{n_1\bar{e}_{14}}{1-n_1n_3}\right)\bar{g}^2}{c\alpha^3}-\frac{n_1\bar{e}_3}{1-n_1n_3}\Bigg)s\alpha\\
&+\left(-N90+\frac{n_3\bar{c}_3}{1-n_1n_3}-\frac{n_1n_3\bar{e}_3}{1-n_1n_3}-\frac{n_3\bar{e}_3}{(1-n_1n_3)n_2}+3\,\frac{\bar{e}_3}{1-n_1n_3}\right)c\alpha\\
&+\frac{\left(2\frac{n_1n_3\bar{d}_{50}}{1-n_1n_3}-2\,\frac{\bar{d}_{50}}{1-n_1n_3}-2\,\frac{n_2}{1-n_1n_3}+2\,\frac{n_1n_3n_2}{1-n_1n_3}\right)\bar{g}}{(c\alpha)}\\
&+\left(\frac{\bar{d}_{49}}{1-n_1n_3}-\frac{n_1n_3\bar{d}_{49}}{1-n_1n_3}\right)\bar{g}-\frac{\bar{d}_2}{1-n_1n_3}+\frac{n_1n_3\bar{e}_4}{1-n_1n_3}+\frac{n_1n_3\bar{d}_2}{1-n_1n_3}\\
&+\frac{n_3\bar{e}_4}{(1-n_1n_3)n_2}-3\,\frac{\bar{e}_4}{1-n_1n_3}-\frac{n_3\bar{c}_4}{1-n_1n_3}\\
\tilde{e}_{11} \;=\; &\left(\right.\\
&\left.\frac{\frac{3}{4}\frac{\bar{c}_{10}}{1-n_1n_3}+\frac{3}{4}\frac{n_1\bar{e}_{10}}{1-n_1n_3}}{c\alpha^2}-\frac{n_3\bar{c}_{37}}{1-n_1n_3}+\frac{n_1\bar{e}_9}{1-n_1n_3}-\frac{\bar{e}_{37}}{1-n_1n_3}+\frac{\bar{c}_9}{1-n_1n_3}\right)s\alpha+\left(-\frac{n_3\bar{c}_9}{1-n_1n_3}-\frac{\bar{e}_9}{1-n_1n_3}\right)c\alpha+\left(\frac{1}{2}\frac{\bar{e}_{10}c(2\alpha)}{1-n_1n_3}\right.\\
&+\frac{1}{2}\frac{n_1\bar{e}_{37}}{1-n_1n_3}-\frac{1}{2}\frac{n_1\bar{e}_{37}c(2\alpha)}{1-n_1n_3}-\frac{1}{2}\frac{\bar{e}_{10}}{1-n_1n_3}-\frac{1}{2}\frac{n_3\bar{c}_{10}}{1-n_1n_3}\\
&\left.+\frac{1}{2}\frac{n_3\bar{c}_{10}c(2\alpha)}{1-n_1n_3}+\frac{1}{2}\frac{\bar{c}_{37}}{1-n_1n_3}-\frac{1}{2}\frac{\bar{c}_{37}c(2\alpha)}{1-n_1n_3}\right)\Big/(c\alpha)\\
&+\frac{-\frac{1}{4}\frac{n_1\bar{e}_{10}s(3\alpha)}{1-n_1n_3}-\frac{1}{4}\frac{\bar{c}_{10}s(3\alpha)}{1-n_1n_3}}{c\alpha^2}
\end{aligned}
$$

$$
\begin{aligned}
\tilde{e}_{12} \;=\; & \left(\frac{-\dfrac{\bar{c}_{15}}{1-n_1n_3} + 2\dfrac{n_3\bar{c}_{16}}{1-n_1n_3} - \dfrac{n_1\bar{e}_{15}}{1-n_1n_3} + 2\dfrac{\bar{e}_{16}}{1-n_1n_3}}{c\alpha} \right. \\
& + \frac{\dfrac{3}{4}\dfrac{n_1\bar{e}_{18}}{1-n_1n_3} + \dfrac{3}{4}\dfrac{\bar{c}_{18}}{1-n_1n_3}}{c\alpha^2} + \frac{-\dfrac{9}{4}\dfrac{n_1\bar{e}_{14}}{1-n_1n_3} - \dfrac{9}{4}\dfrac{\bar{c}_{14}}{1-n_1n_3}}{c\alpha^3} + \frac{\bar{c}_{19}}{1-n_1n_3} \\
& \left. + \frac{n_1\bar{e}_{19}}{1-n_1n_3} - \frac{\bar{e}_{40}}{1-n_1n_3} - \frac{n_3\bar{c}_{40}}{1-n_1n_3} \right)(s\alpha) \\
& + \left(-\frac{\bar{e}_{19}}{1-n_1n_3} - \frac{n_3\bar{c}_{19}}{1-n_1n_3} \right)(c\alpha) + \left(\frac{1}{2}\frac{n_1\bar{e}_{40}}{1-n_1n_3} + \frac{1}{2}\frac{\bar{e}_{18}c(2\alpha)}{1-n_1n_3} \right. \\
& + \frac{1}{2}\frac{\bar{c}_{40}}{1-n_1n_3} + \frac{1}{2}\frac{n_3\bar{c}_{18}c(2\alpha)}{1-n_1n_3} - \frac{1}{2}\frac{\bar{c}_{40}c(2\alpha)}{1-n_1n_3} - \frac{1}{2}\frac{\bar{e}_{18}}{1-n_1n_3} \\
& \left. - \frac{1}{2}\frac{n_1\bar{e}_{40}c(2\alpha)}{1-n_1n_3} - \frac{1}{2}\frac{n_3\bar{c}_{18}}{1-n_1n_3} \right) \Big/ (c\alpha) + \left(-\frac{1}{4}\frac{\bar{c}_{18}s(3\alpha)}{1-n_1n_3} \right. \\
& + \frac{3}{2}\frac{n_3\bar{c}_{14}}{1-n_1n_3} - \frac{1}{4}\frac{n_1\bar{e}_{18}s(3\alpha)}{1-n_1n_3} + \frac{\bar{c}_{16}c(2\alpha)}{1-n_1n_3} + \frac{3}{2}\frac{\bar{e}_{14}}{1-n_1n_3} \\
& + \frac{n_1\bar{e}_{16}c(2\alpha)}{1-n_1n_3} - \frac{3}{2}\frac{\bar{e}_{14}c(2\alpha)}{1-n_1n_3} - \frac{3}{2}\frac{n_3\bar{c}_{14}c(2\alpha)}{1-n_1n_3} - \frac{\bar{c}_{16}}{1-n_1n_3} \\
& \left. - \frac{n_1\bar{e}_{16}}{1-n_1n_3} \right) \Big/ (c\alpha)^2 + \frac{\dfrac{3}{4}\dfrac{\bar{c}_{14}s(3\alpha)}{1-n_1n_3} + \dfrac{3}{4}\dfrac{n_1\bar{e}_{14}s(3\alpha)}{1-n_1n_3}}{c\alpha^3} + \frac{\bar{e}_{15}}{1-n_1n_3} \\
& + \frac{n_3\bar{c}_{15}}{1-n_1n_3} \\
\tilde{e}_{13} \;=\; & \left(\frac{\left(\dfrac{n_1\bar{e}_7}{1-n_1n_3} + \dfrac{\bar{c}_7}{1-n_1n_3} \right)\bar{g}}{c\alpha} - \frac{n_1n_3\bar{d}_{41}}{(1-n_1n_3)n_2} \right)(s\alpha) \\
& + \left(\frac{\bar{d}_{41}n_1n_3}{1-n_1n_3} - \frac{\bar{d}_{41}}{1-n_1n_3} + \bar{d}_{41} + \frac{\bar{d}_{41}n_3}{(1-n_1n_3)n_2} \right)c\alpha \\
& + \left(-\frac{\bar{e}_7}{1-n_1n_3} - \frac{n_3\bar{c}_7}{1-n_1n_3} \right)\bar{g} \\
\tilde{e}_{14} \;=\; & \left(\left(\left(\frac{n_1\bar{e}_{17}}{1-n_1n_3} + \frac{\bar{c}_{17}}{1-n_1n_3} \right)\bar{g} - \frac{\bar{c}_{26}}{1-n_1n_3} + \frac{n_1n_3\bar{d}_{49}}{(1-n_1n_3)n_2} - \frac{n_1\bar{e}_{26}}{1-n_1n_3} \right) \Big/ (\right. \\
& \left. c\alpha) + \left(\left(-2\frac{\bar{c}_{18}}{1-n_1n_3} - 2\frac{n_1\bar{e}_{18}}{1-n_1n_3} \right)\bar{g} - \frac{n_1n_3}{1-n_1n_3} + \frac{\bar{c}_{28}}{1-n_1n_3} \right. \\
& \left. - \frac{n_1n_3\bar{d}_{50}}{(1-n_1n_3)n_2} + \frac{n_1}{(1-n_1n_3)n_2} + \frac{n_1\bar{e}_{28}}{1-n_1n_3} \right) \Big/ c\alpha^2 \\
& + \left(\frac{\left(3\dfrac{n_1\bar{e}_{14}}{1-n_1n_3} + 3\dfrac{\bar{c}_{14}}{1-n_1n_3} \right)\bar{g}}{c\alpha^3} - \frac{n_1n_3\bar{d}_{48}}{(1-n_1n_3)n_2} \right)(s\alpha)
\end{aligned}
$$

$$
\begin{aligned}
&+\left(-\frac{\bar{d}_{48}}{1-n_1n_3}+\bar{d}_{48}+\frac{n_1n_3\bar{d}_{48}}{1-n_1n_3}+\frac{n_3\bar{d}_{48}}{(1-n_1n_3)n_2}\right)c\alpha+\Big(\\
&\left(2\frac{n_3\bar{c}_{18}}{1-n_1n_3}+2\,\frac{\bar{e}_{18}}{1-n_1n_3}\right)\bar{g}-\frac{\bar{e}_{28}}{1-n_1n_3}-\frac{n_2}{1-n_1n_3}-\frac{n_3\bar{c}_{28}}{1-n_1n_3}+n_2\\
&+\frac{n_3}{1-n_1n_3}+\frac{n_3\bar{d}_{50}}{(1-n_1n_3)n_2}+\bar{d}_{50}+\frac{n_1n_3\bar{d}_{50}}{1-n_1n_3}+\frac{n_2n_1n_3}{1-n_1n_3}\\
&-\frac{n_3n_1}{(1-n_1n_3)n_2}-\frac{\bar{d}_{50}}{1-n_1n_3}\Big)\Big/((c\alpha))+\frac{\left(-3\,\frac{\bar{e}_{14}}{1-n_1n_3}-3\,\frac{n_3\bar{c}_{14}}{1-n_1n_3}\right)\bar{g}}{c\alpha^2}\\
&-\bar{d}_{49}-\frac{n_3\bar{d}_{49}}{(1-n_1n_3)n_2}+\left(-\frac{n_3\bar{c}_{17}}{1-n_1n_3}-\frac{\bar{e}_{17}}{1-n_1n_3}\right)\bar{g}-\frac{n_1n_3\bar{d}_{49}}{1-n_1n_3}\\
&+\frac{n_3\bar{c}_{26}}{1-n_1n_3}+\frac{\bar{e}_{26}}{1-n_1n_3}+\frac{\bar{d}_{49}}{1-n_1n_3}\\
\tilde{e}_{15} \;=\;&\left(\frac{\bar{c}_6}{1-n_1n_3}-\frac{n_3\bar{c}_7}{1-n_1n_3}-\frac{\bar{e}_7}{1-n_1n_3}+\frac{n_1\bar{e}_6}{1-n_1n_3}\right)(s\alpha)\\
&+\left(-\frac{\bar{e}_6}{1-n_1n_3}-\frac{n_3\bar{c}_6}{1-n_1n_3}\right)(c\alpha)\\
&+\frac{\frac{1}{2}\frac{\bar{c}_7}{1-n_1n_3}-\frac{1}{2}\frac{\bar{c}_7c(2\alpha)}{1-n_1n_3}+\frac{1}{2}\frac{n_1\bar{e}_7}{1-n_1n_3}-\frac{1}{2}\frac{n_1\bar{e}_7c(2\alpha)}{1-n_1n_3}}{c\alpha}\\
\tilde{e}_{16} \;=\;&\Bigg(\frac{2\,\frac{\bar{e}_{18}}{1-n_1n_3}+2\,\frac{n_3\bar{c}_{18}}{1-n_1n_3}-\frac{\bar{c}_{40}}{1-n_1n_3}-\frac{n_1\bar{e}_{40}}{1-n_1n_3}}{c\alpha}\\
&+\frac{\frac{\bar{c}_{16}}{1-n_1n_3}-3\,\frac{n_3\bar{c}_{14}}{1-n_1n_3}-3\,\frac{\bar{e}_{14}}{1-n_1n_3}+\frac{n_1\bar{e}_{16}}{1-n_1n_3}}{c(\alpha)^2}-\frac{\bar{e}_{17}}{1-n_1n_3}\\
&+\frac{\bar{c}_{20}}{1-n_1n_3}+\frac{n_1\bar{e}_{20}}{1-n_1n_3}-\frac{n_3\bar{c}_{17}}{1-n_1n_3}\Bigg)(s\alpha)\\
&+\left(-\frac{\bar{e}_{20}}{1-n_1n_3}-\frac{n_3\bar{c}_{20}}{1-n_1n_3}\right)(c\alpha)+\Big(-\frac{1}{2}\frac{\bar{c}_{17}c(2\alpha)}{1-n_1n_3}\\
&-\frac{1}{2}\frac{n_1\bar{e}_{17}c(2\alpha)}{1-n_1n_3}+\frac{1}{2}\frac{\bar{c}_{17}}{1-n_1n_3}+\frac{1}{2}\frac{n_1\bar{e}_{17}}{1-n_1n_3}-\frac{\bar{e}_{16}}{1-n_1n_3}-\frac{n_3\bar{c}_{16}}{1-n_1n_3}\Big)\\
&\Big/(c\alpha)+\frac{-\frac{\bar{c}_{18}}{1-n_1n_3}+\frac{\bar{c}_{18}c(2\alpha)}{1-n_1n_3}+\frac{n_1\bar{e}_{18}c(2\alpha)}{1-n_1n_3}-\frac{n_1\bar{e}_{18}}{1-n_1n_3}}{c\alpha^2}\\
&+\frac{-\frac{3}{2}\frac{n_1\bar{e}_{14}c(2\alpha)}{1-n_1n_3}-\frac{3}{2}\frac{\bar{c}_{14}c(2\alpha)}{1-n_1n_3}+\frac{3}{2}\frac{\bar{c}_{14}}{1-n_1n_3}+\frac{3}{2}\frac{n_1\bar{e}_{14}}{1-n_1n_3}}{c\alpha^3}\\
&+\frac{\bar{e}_{40}}{1-n_1n_3}+\frac{n_3\bar{c}_{40}}{1-n_1n_3}
\end{aligned}
$$

$$
\begin{aligned}
\tilde{e}_{17} &= \left(\frac{\left(\frac{\bar{e}_4}{1-n_1n_3}-\frac{\bar{c}_2}{1-n_1n_3}+\frac{\bar{c}_{27}}{1-n_1n_3}+2\frac{n_3\bar{c}_4}{1-n_1n_3}\right)\bar{g}}{c\alpha}-\frac{n_1n_3\bar{d}_1}{(1-n_1n_3)n_2}\right)\\
&\quad s\alpha+\left(\frac{\bar{d}_1n_1n_3}{1-n_1n_3}+\bar{d}_1+\frac{\bar{d}_1n_3}{(1-n_1n_3)n_2}-\frac{\bar{d}_1}{1-n_1n_3}\right)c\alpha\\
&\quad+\frac{\left(\frac{1}{2}\frac{\bar{c}_4c(2\alpha)}{1-n_1n_3}-\frac{1}{2}\frac{\bar{c}_4}{1-n_1n_3}\right)\bar{g}}{c\alpha^2}\\
&\quad+\left(\frac{n_3\bar{c}_2}{1-n_1n_3}+\frac{\bar{e}_2}{1-n_1n_3}-\frac{\bar{e}_{27}}{1-n_1n_3}-\frac{n_3\bar{c}_{27}}{1-n_1n_3}-\frac{n_3\bar{c}_4}{(1-n_1n_3)n_1}\right)\bar{g}\\
\tilde{e}_{18} &= \left(\left(\frac{1}{1-n_1n_3}+\frac{n_1}{(1-n_1n_3)n_2}-\frac{n_1}{(1-n_1n_3)n_3}+\frac{\bar{c}_{28}}{1-n_1n_3}+\frac{n_1\bar{e}_{28}}{1-n_1n_3}\right.\right.\\
&\quad\left.-2\frac{n_3n_1}{1-n_1n_3}-1\right)\bar{g}\Big/((c\alpha))-\frac{n_1n_3\bar{d}_2}{(1-n_1n_3)n_2}-\frac{n_1n_3\bar{d}_3}{(1-n_1n_3)n_2}\Big)(s\alpha)\\
&\quad+\left(\frac{n_1n_3\bar{d}_2}{1-n_1n_3}+\frac{n_1n_3\bar{d}_3}{1-n_1n_3}+\frac{n_3\bar{d}_3}{(1-n_1n_3)n_2}-\frac{\bar{d}_2}{1-n_1n_3}-\frac{\bar{d}_3}{1-n_1n_3}\right.\\
&\quad\left.+\frac{n_3\bar{d}_2}{(1-n_1n_3)n_2}+\bar{d}_2+\bar{d}_3\right)c\alpha\\
&\quad+\left(\frac{n_3}{1-n_1n_3}-\frac{n_3n_1}{(1-n_1n_3)n_2}+\frac{n_1}{1-n_1n_3}-\frac{n_3\bar{c}_{28}}{1-n_1n_3}-\frac{\bar{e}_{28}}{1-n_1n_3}\right)\bar{g}\\
\tilde{e}_{19} &= \left(\frac{-\frac{3}{4}\frac{\bar{c}_4}{1-n_1n_3}-\frac{3}{4}\frac{n_1\bar{e}_4}{1-n_1n_3}}{c\alpha^2}-\frac{\bar{e}_{27}}{1-n_1n_3}+\frac{\bar{e}_2}{1-n_1n_3}+\frac{n_1\bar{e}_{23}}{1-n_1n_3}\right.\\
&\quad\left.+2\frac{n_3\bar{c}_2}{1-n_1n_3}-\frac{n_3\bar{c}_{27}}{1-n_1n_3}+\frac{\bar{c}_{23}}{1-n_1n_3}-\frac{n_3\bar{c}_4}{(1-n_1n_3)n_1}\right)(s\alpha)\\
&\quad+\left(-\frac{n_3\bar{c}_{23}}{1-n_1n_3}-\frac{\bar{e}_{23}}{1-n_1n_3}-\frac{n_3\bar{c}_2}{(1-n_1n_3)n_1}\right)c\alpha+\Big(\\
&\quad-\frac{1}{2}\frac{n_1\bar{e}_{27}c(2\alpha)}{1-n_1n_3}-\frac{1}{2}\frac{\bar{e}_4c(2\alpha)}{1-n_1n_3}+\frac{1}{2}\frac{n_1\bar{e}_{27}}{1-n_1n_3}-\frac{1}{2}\frac{n_1\bar{e}_2}{1-n_1n_3}\\
&\quad+\frac{1}{2}\frac{n_1\bar{e}_2c(2\alpha)}{1-n_1n_3}+\frac{n_3\bar{c}_4}{1-n_1n_3}+\frac{1}{2}\frac{\bar{e}_4}{1-n_1n_3}-\frac{1}{2}\frac{\bar{c}_2}{1-n_1n_3}\\
&\quad-\frac{1}{2}\frac{\bar{c}_{27}c(2\alpha)}{1-n_1n_3}+\frac{1}{2}\frac{\bar{c}_2c(2\alpha)}{1-n_1n_3}+\frac{1}{2}\frac{\bar{c}_{27}}{1-n_1n_3}-\frac{n_3\bar{c}_4c(2\alpha)}{1-n_1n_3}\Big)\Big/(\\
&\quad c\alpha)+\frac{\frac{1}{4}\frac{\bar{c}_4s(3\alpha)}{1-n_1n_3}+\frac{1}{4}\frac{n_1\bar{e}_4s(3\alpha)}{1-n_1n_3}}{c\alpha^2}
\end{aligned}
$$

$$
\begin{aligned}
\tilde{e}_{20} &= \left(\frac{-\frac{\bar{c}_{28}}{1-n_1n_3} - \frac{1}{1-n_1n_3} - \frac{n_1}{(1-n_1n_3)n_2} + \frac{n_1}{(1-n_1n_3)n_3} + 1}{c\alpha} \right. \\
&\quad \left. + \frac{\bar{c}_{26}}{1-n_1n_3} + \frac{N9}{1-n_1n_3} \right) s\alpha + \left(-\frac{\bar{e}_{26}}{1-n_1n_3} - \frac{n_3\bar{c}_{26}}{1-n_1n_3} \right) c\alpha \\
&\quad - \frac{n_1}{1-n_1n_3} + \frac{n_3\bar{c}_{28}}{1-n_1n_3} - \frac{n_3}{1-n_1n_3} + \frac{\bar{e}_{28}}{1-n_1n_3} + \frac{n_3n_1}{(1-n_1n_3)n_2} \\
\tilde{e}_{21} &= \left(\frac{n_3\bar{c}_1}{1-n_1n_3} + \frac{n_1\bar{e}_{21}}{1-n_1n_3} + \frac{\bar{c}_{21}}{1-n_1n_3} \right) s\alpha \\
&\quad + \left(-\frac{\bar{e}_{21}}{1-n_1n_3} - \frac{n_3\bar{c}_1}{(1-n_1n_3)n_1} - \frac{n_3\bar{c}_{21}}{1-n_1n_3} \right) c\alpha \\
\tilde{e}_{22} &= \left(\left(\right. \right. \\
&\quad \left. -\frac{\bar{c}_{27}}{1-n_1n_3} + \frac{\bar{c}_2}{1-n_1n_3} + \frac{n_1\bar{e}_2}{1-n_1n_3} - \frac{\bar{e}_4}{1-n_1n_3} - 2\frac{n_3\bar{c}_4}{1-n_1n_3} - \frac{n_1\bar{e}_{27}}{1-n_1n_3} \right) \\
&\quad \left. /(c\alpha) + \frac{n_3\bar{c}_3}{1-n_1n_3} + \frac{\bar{c}_{25}}{1-n_1n_3} + \frac{n_1\bar{e}_{25}}{1-n_1n_3} \right) s\alpha \\
&\quad + \left(-\frac{\bar{e}_{25}}{1-n_1n_3} - \frac{n_3\bar{c}_{25}}{1-n_1n_3} - \frac{n_3\bar{c}_3}{(1-n_1n_3)n_1} \right) c\alpha \\
&\quad + \frac{\frac{1}{2}\frac{\bar{c}_4}{1-n_1n_3} - \frac{1}{2}\frac{n_1\bar{e}_4c(2\alpha)}{1-n_1n_3} - \frac{1}{2}\frac{\bar{c}_4c(2\alpha)}{1-n_1n_3} + \frac{1}{2}\frac{n_1\bar{e}_4}{1-n_1n_3}}{c\alpha^2} \\
&\quad + \frac{\bar{e}_{27}}{1-n_1n_3} - \frac{\bar{e}_2}{1-n_1n_3} + \frac{n_3\bar{c}_4}{(1-n_1n_3)n_1} - \frac{n_3\bar{c}_2}{1-n_1n_3} + \frac{n_3\bar{c}_{27}}{1-n_1n_3} \\
\tilde{e}_{23} &= \left(\frac{\bar{c}_{22}}{1-n_1n_3} + \frac{n_1\bar{e}_{22}}{1-n_1n_3} \right) (s\alpha) + \left(-\frac{\bar{e}_{22}}{1-n_1n_3} - \frac{n_3\bar{c}_{22}}{1-n_1n_3} \right) (c\alpha) \\
\tilde{e}_{24} &= \left(\left(-\frac{\bar{c}_{28}}{1-n_1n_3} + 2\frac{n_3n_1}{1-n_1n_3} - \frac{1}{1-n_1n_3} - \frac{n_1}{(1-n_1n_3)n_2} + \frac{n_1}{(1-n_1n_3)n_3} \right. \right. \\
&\quad \left. \left. - \frac{n_1\bar{e}_{28}}{1-n_1n_3} + 1 \right) /((c\alpha)) + \frac{\bar{c}_{26}}{1-n_1n_3} + \frac{n_1\bar{e}_{26}}{1-n_1n_3} \right) (s\alpha) \\
&\quad + \left(-\frac{\bar{e}_{26}}{1-n_1n_3} - \frac{n_3\bar{c}_{26}}{1-n_1n_3} \right) (c\alpha) + \frac{n_3\bar{c}_{28}}{1-n_1n_3} + \frac{n_3n_1}{(1-n_1n_3)n_2} \\
&\quad - \frac{n_1}{1-n_1n_3} - \frac{n_3}{1-n_1n_3} + \frac{\bar{e}_{28}}{1-n_1n_3} \\
\tilde{e}_{25} &= \left(\left(-\frac{-\bar{e}_{27} - \frac{n_3\bar{c}_4}{n_1} + n_3(\bar{c}_2 - \bar{c}_{27}) + \bar{e}_2}{1-n_1n_3} \right. \right. \\
&\quad \left. \left. + \frac{-\bar{c}_{23} + 2\,n_3(\bar{c}_{27} - \bar{c}_2) + n_1(\bar{e}_{35} - \bar{e}_{23}) - \bar{e}_2 + \frac{n_3\bar{c}_4}{n_1} + \bar{c}_{35} + \bar{e}_{27}}{1-n_1n_3} \right.
\end{aligned}
$$

$$
\begin{aligned}
&- \frac{\bar{e}_{27} - \bar{e}_2 + n_3(\bar{c}_{27} - \bar{c}_2) + \dfrac{n_3\bar{c}_4}{n_1}}{1 - n_1 n_3}\Bigg)\, \bar{g}\,/(c\alpha) \\
&+ \frac{-\dfrac{(n_1 n_2 n_3 + n_3 - n_2)\bar{d}_1}{n_2} - \dfrac{n_1 n_3 \bar{d}_4}{n_2}}{1 - n_1 n_3} + \frac{(n_1 n_2 n_3 + n_3 - n_2)\bar{d}_1}{n_2(1 - n_1 n_3)}\Bigg) \\
&s\alpha + \left(\bar{d}_4 + \frac{(n_1 n_2 n_3 + n_3 - n_2)\bar{d}_4}{n_2(1 - n_1 n_3)}\right) c\alpha \\
&+ \frac{\left(\dfrac{-2\, n_3\bar{c}_4 - \bar{e}_4 + \bar{c}_2 + n_1(\bar{e}_2 - \bar{e}_{27}) - \bar{c}_{27}}{1 - n_1 n_3} - \dfrac{-n_3\bar{c}_4 - \bar{e}_4}{1 - n_1 n_3}\right) \bar{g}(s\alpha)^2}{c\alpha^2} \\
&- \frac{\left(\bar{e}_{35} + n_3(\bar{c}_{35} - \bar{c}_{23}) - \bar{e}_{23} + \dfrac{n_3(\bar{c}_{27} - \bar{c}_2)}{n_1}\right) \bar{g}}{1 - n_1 n_3}
\end{aligned}
$$

$$
\begin{aligned}
\tilde{e}_{26} \;=\; &\left(\frac{\left(\dfrac{n_1\bar{e}_{36}}{1 - n_1 n_3} + \dfrac{\bar{c}_{36}}{1 - n_1 n_3}\right)\bar{g}}{(c\alpha)} + \frac{1}{1 - n_1 n_3} + \frac{n_1}{(1 - n_1 n_3)n_2} - 1\right. \\
&\left. - \frac{n_3 n_1 \bar{d}_7}{(1 - n_1 n_3)n_2} - \frac{n_3 n_1 \bar{d}_8}{(1 - n_1 n_3)n_2} - \frac{n_3 n_1 \bar{d}_9}{(1 - n_1 n_3)n_2} - \frac{n_1 n_3}{1 - n_1 n_3}\right)(s\alpha) + \\
&\left(- \frac{n_3 n_1}{(1 - n_1 n_3)n_2} + \frac{n_1 n_3 \bar{d}_7}{1 - n_1 n_3} + \frac{n_1 n_3 \bar{d}_9}{1 - n_1 n_3} + \frac{n_3 \bar{d}_7}{(1 - n_1 n_3)n_2}\right. \\
&+ \frac{n_3 \bar{d}_8}{(1 - n_1 n_3)n_2} + \frac{n_1 n_3 \bar{d}_8}{1 - n_1 n_3} - \frac{\bar{d}_7}{1 - n_1 n_3} - \frac{\bar{d}_8}{1 - n_1 n_3} - \frac{\bar{d}_9}{1 - n_1 n_3} \\
&\left. + \frac{n_3 \bar{d}_9}{(1 - n_1 n_3)n_2} + \bar{d}_7 + \bar{d}_8 + \bar{d}_9\right) c\alpha + \left(-\frac{n_3\bar{c}_{36}}{1 - n_1 n_3} - \frac{\bar{e}_{36}}{1 - n_1 n_3}\right)\bar{g}
\end{aligned}
$$

$$
\begin{aligned}
\tilde{e}_{27} \;=\; &\left(\frac{\dfrac{3}{4}\dfrac{\bar{e}_4}{1 - n_1 n_3} + \dfrac{3}{4}\dfrac{\bar{c}_2}{n_1} - \dfrac{3}{4}\bar{e}_{27} - \dfrac{3}{4}\dfrac{\bar{e}_4}{n_1} - \dfrac{3}{4}\dfrac{\bar{c}_{27}}{n_1} - \dfrac{3}{2}\dfrac{n_3\bar{c}_4}{n_1} + \dfrac{3}{4}\bar{e}_2}{c\alpha^2} + \frac{\bar{e}_{23}}{n_1}\right. \\
&- \frac{\bar{e}_{35}}{1 - n_1 n_3} + \frac{n_3\bar{c}_{23}}{1 - n_1 n_3} + \bar{e}_{31} + \frac{n_3\bar{c}_2}{(1 - n_1 n_3)n_1} + 2\,\frac{n_3\bar{c}_{23}}{n_1} + \frac{\bar{c}_{31}}{n_1} \\
&\left. - \frac{n_3\bar{c}_{27}}{(1 - n_1 n_3)n_1} - \frac{n_3\bar{c}_{35}}{1 - n_1 n_3} + \frac{n_3\bar{c}_2}{n_1}\right)(s\alpha) \\
&+ \left(-\frac{n_3\bar{c}_{23}}{(1 - n_1 n_3)n_1} - \frac{n_3\bar{c}_{31}}{1 - n_1 n_3} - \frac{\bar{e}_{31}}{1 - n_1 n_3}\right) c\alpha + \left(-\frac{1}{2}\frac{n_3\bar{c}_2}{1 - n_1 n_3}\right. \\
&- \frac{1}{2}\frac{\bar{c}_{23}}{n_1} + \frac{1}{2}\frac{n_3\bar{c}_2 c(2\alpha)}{1 - n_1 n_3} + \frac{1}{2}\bar{e}_{35} + \frac{1}{2}\frac{\bar{c}_{35}}{n_1} - \frac{1}{2}\frac{\bar{c}_{35}c(2\alpha)}{n_1} \\
&\left. - \frac{1}{2}\bar{e}_{35}c(2\alpha) + \frac{1}{2}\frac{\bar{e}_2 c(2\alpha)}{n_1} - \frac{n_3\bar{c}_2}{n_1} + \frac{1}{2}\frac{\bar{c}_{23}c(2\alpha)}{n_1}\right.
\end{aligned}
$$

$$
\begin{aligned}
&+\frac{1}{2}\frac{n_3\bar{c}_{27}}{1-n_1n_3}-\frac{1}{2}\frac{n_3\bar{c}_{27}c(2\alpha)}{1-n_1n_3}+\frac{1}{2}\frac{\bar{e}_{27}}{n_1}-\frac{1}{2}\frac{\bar{e}_{27}c(2\alpha)}{n_1}\\
&+\frac{1}{2}\bar{e}_{23}c(2\alpha)-\frac{1}{2}\bar{e}_{23}+\frac{1}{2}\frac{n_3\bar{c}_4}{n_1}-\frac{1}{2}\frac{n_3\bar{c}_4c(2\alpha)}{n_1}+\frac{n_3\bar{c}_2c(2\alpha)}{n_1}\\
&-\frac{1}{2}\frac{\bar{e}_2}{n_1}-\frac{n_3\bar{c}_{27}c(2\alpha)}{n_1}+\frac{n_3\bar{c}_{27}}{n_1}+\frac{1}{2}\frac{n_3\bar{c}_4}{(1-n_1n_3)n_1}\\
&-\frac{1}{2}\frac{n_3\bar{c}_4c(2\alpha)}{(1-n_1n_3)n_1}\Big)\Big/((c\alpha))+\Big(\frac{1}{4}\frac{\bar{e}_4s(3\alpha)}{n_1}-\frac{1}{4}\frac{\bar{c}_2s(3\alpha)}{n_1}\\
&+\frac{1}{2}\frac{n_3\bar{c}_4s(3\alpha)}{n_1}-\frac{1}{4}\frac{\bar{e}_4s(3\alpha)}{1-n_1n_3}+\frac{1}{4}\bar{e}_{27}s(3\alpha)+\frac{1}{4}\frac{\bar{c}_{27}s(3\alpha)}{n_1}\\
&-\frac{1}{4}\bar{e}_2s(3\alpha)\Big)\Big/(c\alpha)^2
\end{aligned}
$$

$$
\begin{aligned}
\tilde{e}_{28} &= \Big(-\frac{\bar{e}_{36}}{1-n_1n_3}+\frac{\bar{c}_{32}}{1-n_1n_3}+\frac{n_1\bar{e}_{32}}{1-n_1n_3}-\frac{n_3\bar{c}_{36}}{1-n_1n_3}\Big)s\alpha\\
&+\Big(-\frac{\bar{e}_{32}}{1-n_1n_3}-\frac{n_3\bar{c}_{32}}{1-n_1n_3}\Big)(c\alpha)\\
&+\frac{-\frac{1}{2}\frac{\bar{c}_{36}c(2\alpha)}{1-n_1n_3}+\frac{1}{2}\frac{n_1\bar{e}_{36}}{1-n_1n_3}+\frac{1}{2}\frac{\bar{c}_{36}}{1-n_1n_3}-\frac{1}{2}\frac{n_1\bar{e}_{36}c(2\alpha)}{1-n_1n_3}}{c\alpha}\\
\tilde{e}_{29} &= \Big(\frac{n_3\bar{c}_{21}}{1-n_1n_3}+\frac{n_1\bar{e}_{29}}{1-n_1n_3}+\frac{\bar{c}_{29}}{1-n_1n_3}\Big)s\alpha\\
&+\Big(-\frac{n_3\bar{c}_{29}}{1-n_1n_3}-\frac{\bar{e}_{29}}{1-n_1n_3}-\frac{n_3\bar{c}_{21}}{(1-n_1n_3)n_1}\Big)c\alpha\\
\tilde{e}_{30} &= \Big(\Big(\frac{n_1\bar{e}_{23}}{1-n_1n_3}+\frac{\bar{c}_{23}}{1-n_1n_3}-\frac{n_3\bar{c}_4}{(1-n_1n_3)n_1}-3\frac{n_3\bar{c}_{27}}{1-n_1n_3}-\frac{\bar{c}_{35}}{1-n_1n_3}\\
&+3\frac{n_3\bar{c}_2}{1-n_1n_3}-\frac{n_1\bar{e}_{35}}{1-n_1n_3}+\frac{\bar{e}_2}{1-n_1n_3}-\frac{\bar{e}_{27}}{1-n_1n_3}\Big)\Big/((c\alpha))+\frac{\bar{c}_{33}}{1-n_1n_3}\\
&+\frac{n_1\bar{e}_{33}}{1-n_1n_3}+2\frac{n_3\bar{c}_{25}}{1-n_1n_3}\Big)(s\alpha)\\
&+\Big(-\frac{n_3\bar{c}_{33}}{1-n_1n_3}-\frac{\bar{e}_{33}}{1-n_1n_3}-\frac{n_3\bar{c}_{25}}{(1-n_1n_3)n_1}\Big)c\alpha+\Big(\frac{n_3\bar{c}_4}{1-n_1n_3}\\
&-\frac{1}{2}\frac{\bar{c}_2}{1-n_1n_3}-\frac{1}{2}\frac{\bar{c}_{27}c(2\alpha)}{1-n_1n_3}-\frac{n_3\bar{c}_4c(2\alpha)}{1-n_1n_3}+\frac{1}{2}\frac{n_1\bar{e}_2c(2\alpha)}{1-n_1n_3}\\
&-\frac{1}{2}\frac{n_1\bar{e}_{27}c(2\alpha)}{1-n_1n_3}+\frac{1}{2}\frac{n_1\bar{e}_{27}}{1-n_1n_3}-\frac{1}{2}\frac{n_1\bar{e}_2}{1-n_1n_3}+\frac{1}{2}\frac{\bar{c}_{27}}{1-n_1n_3}\\
&+\frac{1}{2}\frac{\bar{c}_2c(2\alpha)}{1-n_1n_3}\Big)\Big/c\alpha^2-\frac{n_3\bar{c}_{23}}{1-n_1n_3}-\frac{n_3\bar{c}_2}{(1-n_1n_3)n_1}-\frac{\bar{e}_{23}}{1-n_1n_3}\\
&+\frac{\bar{e}_{35}}{1-n_1n_3}+\frac{n_3\bar{c}_{35}}{1-n_1n_3}+\frac{n_3\bar{c}_{27}}{(1-n_1n_3)n_1}\\
\tilde{e}_{31} &= \Big(\frac{n_1\bar{e}_{30}}{1-n_1n_3}+\frac{\bar{c}_{30}}{1-n_1n_3}\Big)(s\alpha)+\Big(-\frac{\bar{e}_{30}}{1-n_1n_3}-\frac{n_3\bar{c}_{30}}{1-n_1n_3}\Big)(c\alpha)
\end{aligned}
$$

$$
\begin{aligned}
\tilde{e}_{32} &= \left(\frac{-\bar{c}_{36} - n_1\bar{e}_{36}}{c\alpha} + \bar{c}_{34} + n_1\bar{e}_{34}\right)(s\alpha) \\
&\quad + \left(-\frac{n_3\bar{c}_{34}}{1-n_1n_3} - \frac{\bar{e}_{34}}{1-n_1n_3}\right)(c\alpha) + \frac{n_3\bar{c}_{36}}{1-n_1n_3} + \frac{\bar{e}_{36}}{1-n_1n_3} \\
\tilde{e}_{33} &= \left(\frac{\left(-2\,\frac{\bar{e}_{10}}{1-n_1n_3} + \frac{\bar{c}_{37}}{1-n_1n_3} + \frac{n_1\bar{e}_{37}}{1-n_1n_3} - 2\,\frac{n_3\bar{c}_{10}}{1-n_1n_3}\right)\bar{g}}{(c\alpha)} - \frac{n_1n_3\bar{d}_{42}}{(1-n_1n_3)n_2}\right. \\
&\quad \left. - \frac{n_3\bar{c}_{22}}{1-n_1n_3} + \bar{d}_{44} - \frac{\bar{d}_{44}}{1-n_1n_3} - \frac{\bar{e}_{22}}{1-n_1n_3} + \frac{n_1n_3\bar{d}_{44}}{1-n_1n_3} + \frac{n_3\bar{d}_{44}}{(1-n_1n_3)n_2}\right) \\
&\quad s\alpha + \left(\frac{n_3\bar{d}_{42}}{(1-n_1n_3)n_2} + \frac{n_1n_3\bar{d}_{42}}{1-n_1n_3} - \frac{\bar{d}_{42}}{1-n_1n_3} + \bar{d}_{42}\right)c\alpha + \Bigg(\\
&\quad -\frac{1}{2}\frac{n_1\bar{e}_{22}c(2\alpha)}{1-n_1n_3} + \frac{1}{2}\frac{n_1n_3\bar{d}_{44}c(2\alpha)}{(1-n_1n_3)n_2} + \frac{1}{2}\frac{\bar{c}_{22}}{1-n_1n_3} \\
&\quad -\frac{1}{2}\frac{\bar{c}_{22}c(2\alpha)}{1-n_1n_3} - \frac{1}{2}\frac{n_1n_3\bar{d}_{44}}{(1-n_1n_3)n_2} + \frac{1}{2}\frac{n_1\bar{e}_{22}}{1-n_1n_3}\Bigg)\Big/(c\alpha) \\
&\quad + \frac{\left(\frac{\bar{c}_{10}}{1-n_1n_3} - \frac{n_1\bar{e}_{10}c(2\alpha)}{1-n_1n_3} - \frac{\bar{c}_{10}c(2\alpha)}{1-n_1n_3} + \frac{n_1\bar{e}_{10}}{1-n_1n_3}\right)\bar{g}}{c\alpha^2} \\
&\quad + \left(-\frac{n_3\bar{c}_{37}}{1-n_1n_3} - \frac{\bar{e}_{37}}{1-n_1n_3}\right)\bar{g} \\
\tilde{e}_{34} &= \left(\left(\left(\frac{\bar{c}_{40}}{1-n_1n_3} - 2\,\frac{n_3\bar{c}_{18}}{1-n_1n_3} - 2\,\frac{\bar{e}_{18}}{1-n_1n_3} + \frac{n_1\bar{e}_{40}}{1-n_1n_3}\right)\bar{g} - 2\,n_2 + \frac{n_1}{1-n_1n_3}\right.\right. \\
&\quad + 2\,\frac{\bar{e}_{28}}{1-n_1n_3} - 2\,\frac{n_1n_3\bar{d}_{50}}{1-n_1n_3} - 2\,\frac{n_2n_1n_3}{1-n_1n_3} - 2\,\frac{n_3}{1-n_1n_3} - 2\,\bar{d}_{50} \\
&\quad - \frac{\bar{c}_{24}}{1-n_1n_3} + 2\,\frac{\bar{d}_{50}}{1-n_1n_3} + 2\,\frac{n_2}{1-n_1n_3} + 3\,\frac{n_3n_1}{(1-n_1n_3)n_2} + 2\,\frac{n_3\bar{c}_{28}}{1-n_1n_3} \\
&\quad \left.\left. - \frac{{n_1}^2n_3}{(1-n_1n_3){n_2}^2} + \frac{n_1n_3\bar{d}_{47}}{(1-n_1n_3)n_2} - 2\,\frac{n_3\bar{d}_{50}}{(1-n_1n_3)n_2} - \frac{n_1\bar{e}_{24}}{1-n_1n_3}\right)\Big/(\right. \\
&\quad c\alpha) + \frac{\left(-2\,\frac{\bar{c}_{16}}{1-n_1n_3} + 6\,\frac{\bar{e}_{14}}{1-n_1n_3} + 6\,\frac{n_3\bar{c}_{14}}{1-n_1n_3} - 2\,\frac{n_1\bar{e}_{16}}{1-n_1n_3}\right)\bar{g}}{(c\alpha)^2} \\
&\quad + \frac{n_1n_3\bar{d}_{49}}{1-n_1n_3} - \frac{\bar{e}_{26}}{1-n_1n_3} - \frac{n_3\bar{c}_{26}}{1-n_1n_3} + \frac{n_3\bar{d}_{49}}{(1-n_1n_3)n_2} - \frac{n_1n_3\bar{d}_{46}}{(1-n_1n_3)n_2} \\
&\quad \left. - \frac{\bar{d}_{49}}{1-n_1n_3} + \bar{d}_{49}\right)(s\alpha) \\
&\quad + \left(\frac{n_1n_3\bar{d}_{46}}{1-n_1n_3} + \bar{d}_{46} - \frac{\bar{d}_{46}}{1-n_1n_3} + \frac{n_3\bar{d}_{46}}{(1-n_1n_3)n_2}\right)c\alpha + \Bigg(
\end{aligned}
$$

$$
\begin{aligned}
&\left(2\frac{\bar{e}_{16}}{1-n_1n_3}+2\,\frac{n_3\bar{c}_{16}}{1-n_1n_3}\right)\bar{g}+\frac{1}{2}\frac{\bar{c}_{26}}{1-n_1n_3}+\frac{1}{2}\frac{n_1\bar{e}_{26}}{1-n_1n_3}\\
&-\frac{1}{2}\frac{n_1n_3\bar{d}_{49}}{(1-n_1n_3)n_2}+\frac{1}{2}\frac{n_1n_3\bar{d}_{49}c(2\alpha)}{(1-n_1n_3)n_2}-\frac{1}{2}\frac{n_1\bar{e}_{26}c(2\alpha)}{1-n_1n_3}\\
&-\frac{1}{2}\frac{\bar{c}_{26}c(2\alpha)}{1-n_1n_3}\Big)/(c\alpha)+\Big(\\
&\left(\frac{\bar{c}_{18}}{1-n_1n_3}-\frac{\bar{c}_{18}c(2\alpha)}{1-n_1n_3}+\frac{n_1\bar{e}_{18}}{1-n_1n_3}-\frac{n_1\bar{e}_{18}c(2\alpha)}{1-n_1n_3}\right)\bar{g}\\
&-\frac{n_1n_3c(2\alpha)}{1-n_1n_3}+\frac{n_1\bar{e}_{28}c(2\alpha)}{1-n_1n_3}+\frac{n_1n_3}{1-n_1n_3}-\frac{n_1n_3\bar{d}_{50}c(2\alpha)}{(1-n_1n_3)n_2}\\
&-\frac{n_1\bar{e}_{28}}{1-n_1n_3}+\frac{n_1c(2\alpha)}{(1-n_1n_3)n_2}+\frac{n_1n_3\bar{d}_{50}}{(1-n_1n_3)n_2}+\frac{\bar{c}_{28}c(2\alpha)}{1-n_1n_3}\\
&-\frac{n_1}{(1-n_1n_3)n_2}-\frac{\bar{c}_{28}}{1-n_1n_3}\Big)/(c\alpha)^2+\\
&\left(3\frac{n_1\bar{e}_{14}c(2\alpha)}{1-n_1n_3}-3\,\frac{\bar{c}_{14}}{1-n_1n_3}+3\,\frac{\bar{c}_{14}c(2\alpha)}{1-n_1n_3}-3\,\frac{n_1\bar{e}_{14}}{1-n_1n_3}\right)\bar{g}\,/\\
&c\alpha^3+\left(-\frac{n_3\bar{c}_{40}}{1-n_1n_3}-\frac{\bar{e}_{40}}{1-n_1n_3}\right)\bar{g}-\frac{n_1}{(1-n_1n_3)n_2}+1\\
&-\frac{n_3\bar{d}_{47}}{(1-n_1n_3)n_2}+\frac{{n_1}^2n_3}{(1-n_1n_3)n_2}-\frac{n_3}{(1-n_1n_3)n_2}-2\,\frac{1}{1-n_1n_3}\\
&-\frac{n_2n_1}{1-n_1n_3}+\frac{\bar{e}_{24}}{1-n_1n_3}-\bar{d}_{47}+\frac{n_1n_3}{1-n_1n_3}+\frac{n_2}{(1-n_1n_3)n_3}\\
&+\frac{n_3n_1}{(1-n_1n_3){n_2}^2}-\frac{n_2}{n_3}+\frac{n_1}{n_2}+\frac{n_3\bar{c}_{24}}{1-n_1n_3}-\frac{n_1n_3\bar{d}_{47}}{1-n_1n_3}+\frac{\bar{d}_{47}}{1-n_1n_3}\\
\tilde{e}_{35}\;=\;&\left(\left(\left(\frac{\bar{c}_{38}}{1-n_1n_3}+\frac{n_1\bar{e}_{38}}{1-n_1n_3}\right)\bar{g}-\frac{n_1\bar{e}_{22}}{1-n_1n_3}-\frac{\bar{c}_{22}}{1-n_1n_3}+\frac{n_1n_3\bar{d}_{44}}{(1-n_1n_3)n_2}\right)/(\right.\\
&c\alpha)+\left.\frac{\left(-2\,\frac{\bar{c}_{10}}{1-n_1n_3}-2\,\frac{n_1\bar{e}_{10}}{1-n_1n_3}\right)\bar{g}}{(c\alpha)^2}-\frac{n_1n_3\bar{d}_{43}}{(1-n_1n_3)n_2}\right)(s\alpha)\\
&+\left(\frac{n_1n_3\bar{d}_{43}}{1-n_1n_3}+\frac{n_3\bar{d}_{43}}{(1-n_1n_3)n_2}-\frac{\bar{d}_{43}}{1-n_1n_3}+\bar{d}_{43}\right)c\alpha\\
&+\frac{\left(2\frac{\bar{e}_{10}}{1-n_1n_3}+2\,\frac{n_3\bar{c}_{10}}{1-n_1n_3}\right)\bar{g}}{c\alpha}+\left(-\frac{\bar{e}_{38}}{1-n_1n_3}-\frac{n_3\bar{c}_{38}}{1-n_1n_3}\right)\bar{g}-\bar{d}_{44}\\
&+\frac{\bar{e}_{22}}{1-n_1n_3}-\frac{n_3\bar{d}_{44}}{(1-n_1n_3)n_2}+\frac{n_3\bar{c}_{22}}{1-n_1n_3}-\frac{n_1n_3\bar{d}_{44}}{1-n_1n_3}+\frac{\bar{d}_{44}}{1-n_1n_3}\\
\tilde{e}_{36}\;=\;&\left(\frac{2\,\frac{n_3\bar{c}_{10}}{1-n_1n_3}-\frac{n_1\bar{e}_{37}}{1-n_1n_3}+2\,\frac{\bar{e}_{10}}{1-n_1n_3}-\frac{\bar{c}_{37}}{1-n_1n_3}}{c\alpha}+\frac{\bar{c}_{39}}{1-n_1n_3}\right.
\end{aligned}
$$

$$
\begin{aligned}
&+\frac{n_1\bar{e}_{39}}{1-n_1n_3}-\frac{n_3\bar{c}_{38}}{1-n_1n_3}-\frac{\bar{e}_{38}}{1-n_1n_3}\Big)(s\alpha)\\
&+\Big(-\frac{\bar{e}_{39}}{1-n_1n_3}-\frac{n_3\bar{c}_{39}}{1-n_1n_3}\Big)(c\alpha)+\Big(\frac{\bar{c}_{10}}{1-n_1n_3}-\frac{\bar{c}_{10}c(2\alpha)}{1-n_1n_3}\\
&+\frac{1}{2}\frac{n_1\bar{e}_{38}}{1-n_1n_3}-\frac{1}{2}\frac{n_1\bar{e}_{38}c(2\alpha)}{1-n_1n_3}+\frac{1}{2}\frac{\bar{c}_{38}}{1-n_1n_3}-\frac{1}{2}\frac{\bar{c}_{38}c(2\alpha)}{1-n_1n_3}\Big)/(\\
&c\alpha)+\frac{-\frac{n_1\bar{e}_{10}}{1-n_1n_3}+\frac{n_1\bar{e}_{10}c(2\alpha)}{1-n_1n_3}}{(c\alpha)^2}+\frac{\bar{e}_{37}}{1-n_1n_3}+\frac{n_3\bar{c}_{37}}{1-n_1n_3}\\
\tilde{e}_{37} \;=\; &\Big(\Big(-3\frac{n_1}{1-n_1n_3}+2\frac{n_3\bar{c}_{28}}{1-n_1n_3}+\frac{\bar{e}_{28}}{1-n_1n_3}+2\frac{n_3n_1}{(1-n_1n_3)n_2}-2\frac{n_3}{1-n_1n_3}\\
&-\frac{n_1\bar{e}_{24}}{1-n_1n_3}+\frac{n_1\bar{e}_{44}}{1-n_1n_3}+\frac{\bar{c}_{44}}{1-n_1n_3}-\frac{\bar{c}_{24}}{1-n_1n_3}\Big)\bar{g}\,/((c\alpha))-\frac{n_1\bar{e}_2}{1-n_1n_3}\\
&-\frac{n_1n_3\bar{d}_5}{(1-n_1n_3)n_2}-\frac{n_1n_3\bar{d}_6}{(1-n_1n_3)n_2}-\frac{\bar{c}_2}{1-n_1n_3}\Big)s\alpha+\Big(\bar{d}_6+\frac{\bar{e}_2}{1-n_1n_3}\\
&-\frac{\bar{d}_5}{1-n_1n_3}-\frac{\bar{d}_6}{1-n_1n_3}+\bar{d}_5+\frac{n_1n_3\bar{d}_5}{1-n_1n_3}+\frac{n_1n_3\bar{d}_6}{1-n_1n_3}+\frac{n_3\bar{d}_5}{(1-n_1n_3)n_2}\\
&+\frac{n_3\bar{d}_6}{(1-n_1n_3)n_2}+\frac{n_3\bar{c}_2}{1-n_1n_3}\Big)(c\alpha)+\Big(\frac{1}{2}+\frac{1}{2}\frac{n_1}{(1-n_1n_3)n_3}\\
&-\frac{1}{2}\frac{n_1c(2\alpha)}{(1-n_1n_3)n_3}+\frac{n_3n_1}{1-n_1n_3}-\frac{n_1n_3c(2\alpha)}{1-n_1n_3}-\frac{1}{2}\frac{n_1\bar{e}_{28}}{1-n_1n_3}\\
&+\frac{1}{2}\frac{n_1\bar{e}_{28}c(2\alpha)}{1-n_1n_3}-\frac{1}{2}c(2\,\alpha)-\frac{1}{2}\frac{1}{1-n_1n_3}+\frac{1}{2}\frac{c(2\alpha)}{1-n_1n_3}\\
&-\frac{1}{2}\frac{\bar{c}_{28}}{1-n_1n_3}+\frac{1}{2}\frac{\bar{c}_{28}c(2\alpha)}{1-n_1n_3}-\frac{1}{2}\frac{n_1}{(1-n_1n_3)n_2}+\frac{1}{2}\frac{n_1c(2\alpha)}{(1-n_1n_3)n_2}\Big)\bar{g}\\
&/c\alpha^2+\Big(-\frac{n_3\bar{c}_{44}}{1-n_1n_3}+\frac{\bar{e}_{24}}{1-n_1n_3}+\frac{1}{1-n_1n_3}-\frac{n_3}{(1-n_1n_3)n_2}\\
&-\frac{n_3\bar{c}_{28}}{(1-n_1n_3)n_1}+\frac{n_3}{(1-n_1n_3)n_1}+\frac{n_3n_1}{1-n_1n_3}+\frac{n_3\bar{c}_{24}}{1-n_1n_3}-\frac{\bar{e}_{44}}{1-n_1n_3}\Big)\bar{g}\\
\tilde{e}_{38} \;=\; &\Big(\Big(\frac{3}{4}-\frac{3}{4}\frac{n_1\bar{e}_{28}}{1-n_1n_3}+\frac{3}{4}\frac{n_1}{(1-n_1n_3)n_3}+\frac{3}{2}\frac{n_3n_1}{1-n_1n_3}-\frac{3}{4}\frac{\bar{c}_{28}}{1-n_1n_3}\\
&-\frac{3}{4}\frac{n_1}{(1-n_1n_3)n_2}-\frac{3}{4}\frac{1}{1-n_1n_3}\Big)/(c\alpha)^2-2\frac{n_3}{(1-n_1n_3)n_2}+\frac{\bar{e}_{24}}{1-n_1n_3}\\
&+\frac{n_1}{(1-n_1n_3)n_3}+2\frac{n_3}{(1-n_1n_3)n_1}+\frac{\bar{c}_{42}}{1-n_1n_3}-\frac{\bar{e}_{44}}{1-n_1n_3}\\
&+2\frac{n_3\bar{c}_{24}}{1-n_1n_3}-\frac{n_1}{(1-n_1n_3)n_2}+2\frac{n_3n_1}{1-n_1n_3}+\frac{n_1\bar{e}_{42}}{1-n_1n_3}-\frac{n_3\bar{c}_{44}}{1-n_1n_3}\\
&+\frac{1}{1-n_1n_3}-\frac{n_3\bar{c}_{28}}{(1-n_1n_3)n_1}\Big)(s\alpha)
\end{aligned}
$$

$$
\begin{aligned}
&+\left(-\frac{n_3\bar{c}_{24}}{(1-n_1n_3)n_1}-\frac{n_3}{1-n_1n_3}-\frac{\bar{e}_{42}}{1-n_1n_3}-\frac{n_3\bar{c}_{42}}{1-n_1n_3}\right)c\alpha+\Big(\\
&-\frac{3}{2}\frac{n_1}{1-n_1n_3}+\frac{1}{2}\frac{\bar{c}_{24}c(2\alpha)}{1-n_1n_3}+\frac{1}{2}\frac{n_1\bar{e}_{24}c(2\alpha)}{1-n_1n_3}+\frac{1}{2}\frac{\bar{e}_{28}}{1-n_1n_3}\\
&-\frac{1}{2}\frac{\bar{c}_{24}}{1-n_1n_3}-\frac{n_3}{1-n_1n_3}+\frac{n_3c(2\alpha)}{1-n_1n_3}+\frac{3}{2}\frac{n_1c(2\alpha)}{1-n_1n_3}-\frac{1}{2}\frac{n_1\bar{e}_{24}}{1-n_1n_3}\\
&+\frac{n_3n_1}{(1-n_1n_3)n_2}-\frac{n_3n_1c(2\alpha)}{(1-n_1n_3)n_2}+\frac{n_3\bar{c}_{28}}{1-n_1n_3}-\frac{1}{2}\frac{\bar{e}_{28}c(2\alpha)}{1-n_1n_3}\\
&+\frac{1}{2}\frac{\bar{c}_{44}}{1-n_1n_3}-\frac{1}{2}\frac{\bar{c}_{44}c(2\alpha)}{1-n_1n_3}+\frac{1}{2}\frac{n_1\bar{e}_{44}}{1-n_1n_3}-\frac{n_3\bar{c}_{28}c(2\alpha)}{1-n_1n_3}\\
&-\frac{1}{2}\frac{n_1\bar{e}_{44}c(2\alpha)}{1-n_1n_3}\Big)\Big/((c\alpha))+\Big(-\frac{1}{2}\frac{n_1n_3s(3\alpha)}{1-n_1n_3}\\
&+\frac{1}{4}\frac{n_1\bar{e}_{28}s(3\alpha)}{1-n_1n_3}+\frac{1}{4}\frac{n_1s(3\alpha)}{(1-n_1n_3)n_2}+\frac{1}{4}\frac{\bar{c}_{28}s(3\alpha)}{1-n_1n_3}\\
&-\frac{1}{4}\frac{n_1s(3\alpha)}{(1-n_1n_3)n_3}+\frac{1}{4}\frac{s(3\alpha)}{1-n_1n_3}-\frac{1}{4}s(3\alpha)\Big)\Big/c\alpha^2
\end{aligned}
$$

$$
\begin{aligned}
\tilde{e}_{39} \;=\;& \left(\frac{n_3\bar{c}_{22}}{1-n_1n_3}+\frac{n_1\bar{e}_{41}}{1-n_1n_3}+\frac{\bar{c}_{41}}{1-n_1n_3}\right)s\alpha\\
&+\left(-\frac{\bar{e}_{41}}{1-n_1n_3}-\frac{n_3\bar{c}_{22}}{(1-n_1n_3)n_1}-\frac{n_3\bar{c}_{41}}{1-n_1n_3}\right)c\alpha
\end{aligned}
$$

$$
\begin{aligned}
\tilde{e}_{40} \;=\;& \Big(\Big(-\frac{n_1\bar{e}_{44}}{1-n_1n_3}-2\frac{n_3n_1}{(1-n_1n_3)n_2}-2\frac{n_3\bar{c}_{28}}{1-n_1n_3}-\frac{\bar{e}_{28}}{1-n_1n_3}-\frac{\bar{c}_{44}}{1-n_1n_3}\\
&+3\frac{n_1}{1-n_1n_3}+\frac{\bar{c}_{24}}{1-n_1n_3}+2\frac{n_3}{1-n_1n_3}+\frac{n_1\bar{e}_{24}}{1-n_1n_3}\Big)\Big/(c\alpha)\\
&+\frac{\bar{c}_{43}}{1-n_1n_3}+\frac{n_3\bar{c}_{26}}{1-n_1n_3}+\frac{n_1\bar{e}_{43}}{1-n_1n_3}\Big)(s\alpha)\\
&+\left(-\frac{n_3\bar{c}_{26}}{(1-n_1n_3)n_1}-\frac{n_3\bar{c}_{43}}{1-n_1n_3}-\frac{\bar{e}_{43}}{1-n_1n_3}\right)c\alpha+\Big(\frac{1}{2}\frac{n_1\bar{e}_{28}}{1-n_1n_3}\\
&+\frac{1}{2}\frac{\bar{c}_{28}}{1-n_1n_3}-\frac{1}{2}\frac{n_1}{(1-n_1n_3)n_3}-\frac{n_3n_1}{1-n_1n_3}+\frac{1}{2}\frac{1}{1-n_1n_3}\\
&-\frac{1}{2}\frac{n_1\bar{e}_{28}c(2\alpha)}{1-n_1n_3}-\frac{1}{2}-\frac{1}{2}\frac{\bar{c}_{28}c(2\alpha)}{1-n_1n_3}+\frac{1}{2}\frac{n_1c(2\alpha)}{(1-n_1n_3)n_3}\\
&-\frac{1}{2}\frac{c(2\alpha)}{1-n_1n_3}+\frac{1}{2}\frac{n_1}{(1-n_1n_3)n_2}-\frac{1}{2}\frac{n_1c(2\alpha)}{(1-n_1n_3)n_2}+\frac{n_1n_3c(2\alpha)}{1-n_1n_3}\\
&+\frac{1}{2}c(2\alpha)\Big)\Big/c\alpha^2+\frac{n_3}{(1-n_1n_3)n_2}-\frac{\bar{e}_{24}}{1-n_1n_3}-\frac{n_3}{(1-n_1n_3)n_1}\\
&+\frac{n_3\bar{c}_{28}}{(1-n_1n_3)n_1}-\frac{n_3\bar{c}_{24}}{1-n_1n_3}+\frac{\bar{e}_{44}}{1-n_1n_3}-\frac{n_3n_1}{1-n_1n_3}+\frac{n_3\bar{c}_{44}}{1-n_1n_3}\\
&-\frac{1}{1-n_1n_3}
\end{aligned}
$$

ϕ-equation :

$$\tilde{\kappa}_1 = \frac{\bar{c}_1 + n_1\bar{e}_1}{1 - n_1 n_3}$$

$$\tilde{\kappa}_3 = \frac{(\bar{c}_4 + n_1\bar{e}_4)\dfrac{\bar{g}}{c\alpha}}{1 - n_1 n_3}$$

$$\tilde{\xi}_1 = \frac{\bar{c}_2 + n_1\bar{e}_2 + (\bar{c}_4 + n_1\bar{e}_4)\dfrac{s\alpha}{c\alpha}}{1 - n_1 n_3}$$

$$\tilde{\xi}_2 = \frac{\bar{c}_3 + n_1\bar{e}_3 - (\bar{c}_4 + n_1\bar{e}_4)\dfrac{1}{c\alpha}}{1 - n_1 n_3}$$

$$\begin{aligned}\tilde{c}_1 = {} & \frac{\left(-\dfrac{n_1 n_3 \bar{d}_2}{(1 - n_1 n_3)n_2} - \dfrac{n_1\bar{e}_4}{1 - n_1 n_3}\right)\bar{g}}{c\alpha} \\ & + \frac{\left(-\dfrac{n_1 n_3 \bar{d}_{50}}{(1 - n_1 n_3)n_2} + \dfrac{\bar{c}_{28}}{1 - n_1 n_3} - \dfrac{n_1 n_3}{1 - n_1 n_3} + \dfrac{n_1}{(1 - n_1 n_3)n_2}\right)\bar{g}^2}{c\alpha^2} \\ & + \frac{\bar{c}_{14}\bar{g}^3}{(1 - n_1 n_3)c\alpha^3} + \frac{\bar{c}_5}{1 - n_1 n_3}\end{aligned}$$

$$\begin{aligned}\tilde{c}_2 = {} & \left(\frac{-\dfrac{n_1 n_3 \bar{d}_2}{(1 - n_1 n_3)n_2} - \dfrac{n_1\bar{e}_4}{1 - n_1 n_3}}{(c\alpha)} + \left(2\frac{n_1\bar{e}_{28}}{1 - n_1 n_3} + 2\frac{n_1}{(1 - n_1 n_3)n_2}\right.\right. \\ & \left. - 2\frac{n_1 n_3 \bar{d}_{50}}{(1 - n_1 n_3)n_2} + 2\frac{\bar{c}_{28}}{1 - n_1 n_3} - 2\frac{n_1 n_3}{1 - n_1 n_3}\right)\bar{g}\Big/c\alpha^2 \\ & \left. + \frac{\left(3\dfrac{\bar{c}_{14}}{1 - n_1 n_3} + 3\dfrac{n_1\bar{e}_{14}}{1 - n_1 n_3}\right)\bar{g}^2}{c\alpha^3}\right)s\alpha + \left(\frac{\bar{c}_{24}}{1 - n_1 n_3} - \frac{n_1}{1 - n_1 n_3}\right. \\ & \left. - \frac{n_1 n_3 \bar{d}_{47}}{(1 - n_1 n_3)n_2} - \frac{n_1 n_3}{(1 - n_1 n_3)n_2} + \frac{n_1\bar{e}_{24}}{1 - n_1 n_3} + \frac{{n_1}^2 n_3}{(1 - n_1 n_3){n_2}^2}\right)\bar{g}\Big/(\\ & c\alpha) + \frac{\left(\dfrac{n_1\bar{e}_{16}}{1 - n_1 n_3} + \dfrac{\bar{c}_{16}}{1 - n_1 n_3}\right)\bar{g}^2}{c\alpha^2} - \frac{n_1\bar{e}_2}{1 - n_1 n_3}\end{aligned}$$

$$\begin{aligned}\tilde{c}_3 = {} & \left(\left(\frac{\bar{c}_{24}}{1 - n_1 n_3} - \frac{n_1}{1 - n_1 n_3} - \frac{n_1 n_3 \bar{d}_{47}}{(1 - n_1 n_3)n_2} - \frac{n_1 n_3}{(1 - n_1 n_3)n_2} + \frac{n_1\bar{e}_{24}}{1 - n_1 n_3}\right.\right.\end{aligned}$$

$$
\begin{aligned}
&+\frac{{n_1}^2 n_3}{(1-n_1n_3){n_2}^2}\Big)\Big/((c\alpha))+\frac{\left(2\dfrac{n_1\bar{e}_{16}}{1-n_1n_3}+2\dfrac{\bar{c}_{16}}{1-n_1n_3}\right)\bar{g}}{c\alpha^2}\Bigg)s\alpha\\
&+\frac{\left(\dfrac{n_1\bar{e}_{15}}{1-n_1n_3}+\dfrac{\bar{c}_{15}}{1-n_1n_3}\right)\bar{g}}{c\alpha}+\Big(\frac{1}{2}\frac{n_1\bar{e}_{28}}{1-n_1n_3}-\frac{1}{2}\frac{n_1\bar{e}_{28}c(2\alpha)}{1-n_1n_3}\\
&+\frac{1}{2}\frac{\bar{c}_{28}}{1-n_1n_3}+\frac{1}{2}\frac{n_1n_3\bar{d}_{50}c(2\alpha)}{(1-n_1n_3)n_2}+\frac{1}{2}\frac{n_1}{(1-n_1n_3)n_2}\\
&+\frac{1}{2}\frac{n_1n_3c(2\alpha)}{1-n_1n_3}-\frac{1}{2}\frac{n_1c(2\alpha)}{(1-n_1n_3)n_2}-\frac{1}{2}\frac{n_1n_3}{1-n_1n_3}-\frac{1}{2}\frac{\bar{c}_{28}c(2\alpha)}{1-n_1n_3}\\
&-\frac{1}{2}\frac{n_1n_3\bar{d}_{50}}{(1-n_1n_3)n_2}\Big)\Big/(c\alpha)^2+\\
&\left(-\frac{3}{2}\frac{n_1\bar{e}_{14}c(2\alpha)}{1-n_1n_3}+\frac{3}{2}\frac{\bar{c}_{14}}{1-n_1n_3}+\frac{3}{2}\frac{n_1\bar{e}_{14}}{1-n_1n_3}-\frac{3}{2}\frac{\bar{c}_{14}c(2\alpha)}{1-n_1n_3}\right)\bar{g}\Big/\\
&c\alpha^3-\frac{n_1n_3\bar{d}_{45}}{(1-n_1n_3)n_2}+\frac{n_1n_3}{1-n_1n_3}
\end{aligned}
$$

$$
\begin{aligned}
\tilde{c}_4 &= \left(\frac{\dfrac{n_1\bar{e}_{15}}{1-n_1n_3}+\dfrac{\bar{c}_{15}}{1-n_1n_3}}{c\alpha}+\frac{\dfrac{3}{4}\dfrac{n_1\bar{e}_{14}}{1-n_1n_3}+\dfrac{3}{4}\dfrac{\bar{c}_{14}}{1-n_1n_3}}{c\alpha^3}\right)(s\alpha)\\
&+\frac{\dfrac{1}{2}\dfrac{n_1\bar{e}_{16}}{1-n_1n_3}+\dfrac{1}{2}\dfrac{\bar{c}_{16}}{1-n_1n_3}-\dfrac{1}{2}\dfrac{n_1\bar{e}_{16}c(2\alpha)}{1-n_1n_3}-\dfrac{1}{2}\dfrac{\bar{c}_{16}c(2\alpha)}{1-n_1n_3}}{c\alpha^2}\\
&+\frac{-\dfrac{1}{4}\dfrac{\bar{c}_{14}s(3\alpha)}{1-n_1n_3}-\dfrac{1}{4}\dfrac{n_1\bar{e}_{14}s(3\alpha)}{1-n_1n_3}}{c\alpha^3}+\frac{\bar{c}_{12}}{1-n_1n_3}+\frac{n_1\bar{e}_{12}}{1-n_1n_3}\\
\tilde{c}_5 &= \frac{\bar{c}_5+n_1\bar{e}_5}{1-n_1n_3}\\
\tilde{c}_6 &= \frac{-\bar{c}_7-n_1\bar{e}_7}{(1-n_1n_3)c\alpha}+\frac{\bar{c}_8+n_1\bar{e}_8}{1-n_1n_3}\\
\tilde{c}_7 &= \frac{-\bar{c}_{38}-n_1\bar{e}_{38}}{(1-n_1n_3)c\alpha}+\frac{\bar{c}_{10}+n_1\bar{e}_{10}}{(1-n_1n_3)c\alpha^2}+\frac{\bar{c}_{11}+n_1\bar{e}_{11}}{1-n_1n_3}\\
\tilde{c}_8 &= \frac{-\bar{c}_{17}-n_1\bar{e}_{17}}{(1-n_1n_3)(c\alpha)}+\frac{\bar{c}_{18}+n_1\bar{e}_{18}}{(1-n_1n_3)c\alpha^2}+\frac{-\bar{c}_{14}-n_1\bar{e}_{14}}{(1-n_1n_3)c\alpha^3}\\
&+\frac{\bar{c}_{13}+n_1\bar{e}_{13}}{1-n_1n_3}\\
\tilde{c}_9 &= \frac{\left(\dfrac{n_1\bar{e}_{22}}{1-n_1n_3}+\dfrac{\bar{c}_{22}}{1-n_1n_3}-\dfrac{n_1n_3\bar{d}_{44}}{(1-n_1n_3)n_2}\right)\bar{g}}{(c\alpha)}+\frac{\left(\dfrac{n_1\bar{e}_{10}}{1-n_1n_3}+\dfrac{\bar{c}_{10}}{1-n_1n_3}\right)\bar{g}^2}{c\alpha^2}\\
&-\frac{n_1\bar{e}_1}{1-n_1n_3}
\end{aligned}
$$

$$\tilde{c}_{10} = \left(\left(\frac{n_1\bar{e}_{26}}{1-n_1n_3}+\frac{\bar{c}_{26}}{1-n_1n_3}-\frac{n_1n_3\bar{d}_{49}}{(1-n_1n_3)n_2}\right)\bar{g}+\frac{n_1\bar{e}_4}{1-n_1n_3}+\frac{n_1n_3\bar{d}_2}{(1-n_1n_3)n_2}\right)/(c\alpha)+\left(\left(\frac{n_1\bar{e}_{18}}{1-n_1n_3}+\frac{\bar{c}_{18}}{1-n_1n_3}\right)\bar{g}^2+\left(2\frac{n_1n_3\bar{d}_{50}}{(1-n_1n_3)n_2}-2\frac{n_1\bar{e}_{28}}{1-n_1n_3}-2\frac{n_1}{(1-n_1n_3)n_2}+2\frac{n_1n_3}{1-n_1n_3}-2\frac{\bar{c}_{28}}{1-n_1n_3}\right)\bar{g}\right)/c\alpha^2+\frac{\left(-3\frac{\bar{c}_{14}}{1-n_1n_3}-3\frac{n_1\bar{e}_{14}}{1-n_1n_3}\right)\bar{g}^2}{c\alpha^3}-\frac{n_1\bar{e}_3}{1-n_1n_3}$$

$$\tilde{c}_{11} = \frac{\left(\frac{n_1\bar{e}_{37}}{1-n_1n_3}+\frac{\bar{c}_{37}}{1-n_1n_3}\right)s\alpha}{c\alpha}+\frac{\frac{1}{2}\frac{n_1\bar{e}_{10}}{1-n_1n_3}-\frac{1}{2}\frac{n_1\bar{e}_{10}c(2\alpha)}{1-n_1n_3}+\frac{1}{2}\frac{\bar{c}_{10}}{1-n_1n_3}-\frac{1}{2}\frac{\bar{c}_{10}c(2\alpha)}{1-n_1n_3}}{c\alpha^2}+\frac{n_1\bar{e}_9}{1-n_1n_3}+\frac{\bar{c}_9}{1-n_1n_3}$$

$$\tilde{c}_{12} = \left(\frac{\frac{\bar{c}_{40}}{1-n_1n_3}+\frac{n_1\bar{e}_{40}}{1-n_1n_3}}{c\alpha}+\frac{-2\frac{\bar{c}_{16}}{1-n_1n_3}-2\frac{n_1\bar{e}_{16}}{1-n_1n_3}}{c\alpha^2}\right)(s\alpha)+\frac{-\frac{\bar{c}_{15}}{1-n_1n_3}-\frac{n_1\bar{e}_{15}}{1-n_1n_3}}{(c\alpha)}+\frac{-\frac{1}{2}\frac{n_1\bar{e}_{18}c(2\alpha)}{1-n_1n_3}+\frac{1}{2}\frac{\bar{c}_{18}}{1-n_1n_3}+\frac{1}{2}\frac{n_1\bar{e}_{18}}{1-n_1n_3}-\frac{1}{2}\frac{\bar{c}_{18}c(2\alpha)}{1-n_1n_3}}{c\alpha^2}+\frac{-\frac{3}{2}\frac{\bar{c}_{14}}{1-n_1n_3}+\frac{3}{2}\frac{\bar{c}_{14}c(2\alpha)}{1-n_1n_3}-\frac{3}{2}\frac{n_1\bar{e}_{14}}{1-n_1n_3}+\frac{3}{2}\frac{n_1\bar{e}_{14}c(2\alpha)}{1-n_1n_3}}{c\alpha^3}+\frac{n_1\bar{e}_{19}}{1-n_1n_3}+\frac{\bar{c}_{19}}{1-n_1n_3}$$

$$\tilde{c}_{13} = \frac{(\bar{c}_7+n_1\bar{e}_7)\bar{g}}{(1-n_1n_3)(c\alpha)}-\frac{n_1n_3\bar{d}_{41}}{n_2(1-n_1n_3)}$$

$$\tilde{c}_{14} = \left(\left(\frac{n_1\bar{e}_{17}}{1-n_1n_3}+\frac{\bar{c}_{17}}{1-n_1n_3}\right)\bar{g}-\frac{n_1\bar{e}_{26}}{1-n_1n_3}+\frac{n_1n_3\bar{d}_{49}}{(1-n_1n_3)n_2}-\frac{\bar{c}_{26}}{1-n_1n_3}\right)/(c\alpha)+\left(\left(-2\frac{n_1\bar{e}_{18}}{1-n_1n_3}-2\frac{\bar{c}_{18}}{1-n_1n_3}\right)\bar{g}-\frac{n_1n_3}{1-n_1n_3}-\frac{n_1n_3\bar{d}_{50}}{(1-n_1n_3)n_2}+\frac{n_1\bar{e}_{28}}{1-n_1n_3}+\frac{\bar{c}_{28}}{1-n_1n_3}\right)/(c\alpha)^2+\frac{\left(3\frac{\bar{c}_{14}}{1-n_1n_3}+3\frac{n_1\bar{e}_{14}}{1-n_1n_3}\right)\bar{g}}{c\alpha^3}$$

$$
\begin{aligned}
& -\frac{n_1 n_3 \bar{d}_{48}}{(1-n_1 n_3) n_2} \\
\tilde{c}_{15} &= \frac{\left(\frac{\bar{c}_7}{1-n_1 n_3}+\frac{n_1 \bar{e}_7}{1-n_1 n_3}\right) s\alpha}{c\alpha}+\frac{\bar{c}_6}{1-n_1 n_3}+\frac{n_1 \bar{e}_6}{1-n_1 n_3} \\
\tilde{c}_{16} &= \left(\frac{\frac{n_1 \bar{e}_{17}}{1-n_1 n_3}+\frac{\bar{c}_{17}}{1-n_1 n_3}}{c\alpha}+\frac{-2\frac{n_1 \bar{e}_{18}}{1-n_1 n_3}-2\frac{\bar{c}_{18}}{1-n_1 n_3}}{c\alpha^2}\right. \\
& \left.+\frac{3\frac{\bar{c}_{14}}{1-n_1 n_3}+3\frac{n_1 \bar{e}_{14}}{1-n_1 n_3}}{(c\alpha)^3}\right)(s\alpha)+\frac{-\frac{\bar{c}_{40}}{1-n_1 n_3}-\frac{n_1 \bar{e}_{40}}{1-n_1 n_3}}{(c\alpha)} \\
& +\frac{\frac{\bar{c}_{16}}{1-n_1 n_3}+\frac{n_1 \bar{e}_{16}}{1-n_1 n_3}}{c\alpha^2}+\frac{\bar{c}_{20}}{1-n_1 n_3}+\frac{n_1 \bar{e}_{20}}{1-n_1 n_3} \\
\tilde{c}_{17} &= \frac{\left(-\frac{n_1 \bar{e}_4}{1-n_1 n_3}-\frac{\bar{c}_4}{1-n_1 n_3}\right)\bar{g} s\alpha}{(c\alpha)^2}+ \\
& \left(\frac{\bar{c}_{27}}{1-n_1 n_3}-\frac{n_1 \bar{e}_2}{1-n_1 n_3}+\frac{n_1 \bar{e}_{27}}{1-n_1 n_3}-\frac{\bar{c}_2}{1-n_1 n_3}+2\frac{n_3 \bar{c}_4}{1-n_1 n_3}+\frac{\bar{e}_4}{1-n_1 n_3}\right) \\
& \bar{g}\,/(c\alpha)-\frac{n_1 n_3 \bar{d}_1}{(1-n_1 n_3) n_2} \\
\tilde{c}_{18} &= \left(\frac{1}{1-n_1 n_3}+\frac{n_1}{(1-n_1 n_3) n_2}-\frac{n_1}{(1-n_1 n_3) n_3}+\frac{\bar{c}_{28}}{1-n_1 n_3}+\frac{n_1 \bar{e}_{28}}{1-n_1 n_3}\right. \\
& \left.-2\frac{n_1 n_3}{1-n_1 n_3}\right)\bar{g}\,/((c\alpha))-\frac{n_1 n_3 \bar{d}_2}{(1-n_1 n_3) n_2}-\frac{n_1 n_3 \bar{d}_3}{(1-n_1 n_3) n_2} \\
\tilde{c}_{19} &= \frac{(-n_1 \bar{e}_4-\bar{c}_4) s\alpha^2}{(1-n_1 n_3) c\alpha^2}+\frac{(2 n_3 \bar{c}_4+n_1(\bar{e}_{27}-\bar{e}_2)+\bar{e}_4+\bar{c}_{27}-\bar{c}_2) s\alpha}{(1-n_1 n_3) c\alpha} \\
& +\frac{n_1 \bar{e}_{23}+2\, n_3 \bar{c}_2+\bar{c}_{23}+\bar{e}_2}{1-n_1 n_3} \\
\tilde{c}_{20} &= \left(\frac{1}{1-n_1 n_3}+\frac{n_1}{(1-n_1 n_3) n_2}-\frac{n_1}{(1-n_1 n_3) n_3}+\frac{\bar{c}_{28}}{1-n_1 n_3}+\frac{n_1 \bar{e}_{28}}{1-n_1 n_3}\right. \\
& \left.-2\frac{n_1 n_3}{1-n_1 n_3}\right)(s\alpha)\,/(c\alpha)+\frac{\bar{c}_{24}}{1-n_1 n_3}+\frac{n_1}{1-n_1 n_3}+\frac{n_3}{1-n_1 n_3} \\
& -\frac{n_1 n_3}{(1-n_1 n_3) n_2}+\frac{n_1 \bar{e}_{24}}{1-n_1 n_3} \\
\tilde{c}_{21} &= \frac{n_1 \bar{e}_{21}+2\, n_3 \bar{c}_1+\bar{e}_1+\bar{c}_{21}}{1-n_1 n_3} \\
\tilde{c}_{22} &= \frac{\left(\frac{n_1 \bar{e}_4}{1-n_1 n_3}+\frac{\bar{c}_4}{1-n_1 n_3}\right) s\alpha}{c\alpha^2}+\Big(
\end{aligned}
$$

$$\frac{n_1\bar{e}_2}{1-n_1n_3}-\frac{\bar{c}_{27}}{1-n_1n_3}+\frac{\bar{c}_2}{1-n_1n_3}-\frac{n_1\bar{e}_{27}}{1-n_1n_3}-2\frac{n_3\bar{c}_4}{1-n_1n_3}-\frac{\bar{e}_4}{1-n_1n_3}\Big)\Big/($$
$$c\alpha)+\frac{n_1\bar{e}_{25}}{1-n_1n_3}+2\frac{n_3\bar{c}_3}{1-n_1n_3}+\frac{\bar{e}_3}{1-n_1n_3}+\frac{\bar{c}_{25}}{1-n_1n_3}$$

$$\tilde{c}_{23} = \frac{\bar{c}_{22}+n_1\bar{e}_{22}}{1-n_1n_3}$$

$$\tilde{c}_{24} = \frac{-\bar{c}_{28}-1-\frac{n_1}{n_2}+\frac{n_1}{n_3}+n_1(2n_3-\bar{e}_{28})}{(1-n_1n_3)c\alpha}+\frac{\bar{c}_{26}+n_1\bar{e}_{26}}{1-n_1n_3}$$

$$\tilde{c}_{25} = \Big(\frac{n_1\bar{e}_2}{1-n_1n_3}-\frac{\bar{e}_4}{1-n_1n_3}+\frac{\bar{c}_2}{1-n_1n_3}-\frac{n_1\bar{e}_{27}}{1-n_1n_3}-\frac{\bar{c}_{27}}{1-n_1n_3}-2\frac{n_3\bar{c}_4}{1-n_1n_3}\Big)\bar{g}$$
$$s\alpha\Big/(c\alpha)^2+\Big(-\frac{\bar{c}_{23}}{1-n_1n_3}+\frac{n_1\bar{e}_{35}}{1-n_1n_3}+2\frac{n_3\bar{c}_{27}}{1-n_1n_3}-2\frac{n_3\bar{c}_2}{1-n_1n_3}$$
$$-\frac{\bar{e}_2}{1-n_1n_3}+\frac{\bar{c}_{35}}{1-n_1n_3}+\frac{\bar{e}_{27}}{1-n_1n_3}+\frac{n_3\bar{c}_4}{(1-n_1n_3)n_1}-\frac{n_1\bar{e}_{23}}{1-n_1n_3}\Big)\bar{g}\Big/($$
$$c\alpha)-\frac{n_1n_3\bar{d}_4}{(1-n_1n_3)n_2}-\frac{\bar{d}_1n_3}{(1-n_1n_3)n_2}-\frac{\bar{d}_1n_1n_3}{1-n_1n_3}+\frac{\bar{d}_1}{1-n_1n_3}$$

$$\tilde{c}_{26} = \frac{\Big(\frac{n_1\bar{e}_{36}}{1-n_1n_3}+\frac{\bar{c}_{36}}{1-n_1n_3}\Big)\bar{g}}{c\alpha}+\frac{n_1}{(1-n_1n_3)n_2}-\frac{n_1n_3}{1-n_1n_3}-\frac{n_1n_3\bar{d}_7}{(1-n_1n_3)n_2}$$
$$-\frac{n_1n_3\bar{d}_8}{(1-n_1n_3)n_2}-\frac{n_1n_3\bar{d}_9}{(1-n_1n_3)n_2}+\frac{1}{1-n_1n_3}$$

$$\tilde{c}_{27} = \Big(-\frac{\bar{c}_{23}}{1-n_1n_3}+\frac{n_1\bar{e}_{35}}{1-n_1n_3}+2\frac{n_3\bar{c}_{27}}{1-n_1n_3}-2\frac{n_3\bar{c}_2}{1-n_1n_3}-\frac{\bar{e}_2}{1-n_1n_3}$$
$$+\frac{\bar{c}_{35}}{1-n_1n_3}+\frac{\bar{e}_{27}}{1-n_1n_3}+\frac{n_3\bar{c}_4}{(1-n_1n_3)n_1}-\frac{n_1\bar{e}_{23}}{1-n_1n_3}\Big)(s\alpha)\Big/(c\alpha)$$
$$+\Big(\frac{1}{2}\frac{n_1\bar{e}_{27}c(2\alpha)}{1-n_1n_3}+\frac{1}{2}\frac{\bar{c}_2}{1-n_1n_3}-\frac{1}{2}\frac{\bar{c}_2c(2\alpha)}{1-n_1n_3}-\frac{1}{2}\frac{\bar{c}_{27}}{1-n_1n_3}$$
$$+\frac{1}{2}\frac{\bar{c}_{27}c(2\alpha)}{1-n_1n_3}-\frac{n_3\bar{c}_4}{1-n_1n_3}+\frac{n_3\bar{c}_4c(2\alpha)}{1-n_1n_3}-\frac{1}{2}\frac{n_1\bar{e}_2c(2\alpha)}{1-n_1n_3}$$
$$+\frac{1}{2}\frac{n_1\bar{e}_2}{1-n_1n_3}-\frac{1}{2}\frac{\bar{e}_4}{1-n_1n_3}-\frac{1}{2}\frac{n_1\bar{e}_{27}}{1-n_1n_3}+\frac{1}{2}\frac{\bar{e}_4c(2\alpha)}{1-n_1n_3}\Big)\Big/c\alpha^2$$
$$+\frac{\bar{c}_{31}}{1-n_1n_3}+\frac{n_3\bar{c}_2}{(1-n_1n_3)n_1}+\frac{n_1\bar{e}_{31}}{1-n_1n_3}+\frac{\bar{e}_{23}}{1-n_1n_3}+2\frac{n_3\bar{c}_{23}}{1-n_1n_3}$$

$$\tilde{c}_{28} = \frac{(n_1\bar{e}_{36}+\bar{c}_{36})s\alpha}{(1-n_1n_3)c\alpha}+\frac{n_1\bar{e}_{32}+\bar{c}_{32}}{1-n_1n_3}$$

$$\tilde{c}_{29} = \frac{n_1\bar{e}_{29}+\frac{n_3\bar{c}_1}{n_1}+2\,n_3\bar{c}_{21}+\bar{c}_{29}+\bar{e}_{21}}{1-n_1n_3}$$

$$\tilde{c}_{30} = \Big(\frac{\bar{e}_4}{1-n_1n_3}-\frac{n_1\bar{e}_2}{1-n_1n_3}-\frac{\bar{c}_2}{1-n_1n_3}+2\frac{n_3\bar{c}_4}{1-n_1n_3}+\frac{n_1\bar{e}_{27}}{1-n_1n_3}+\frac{\bar{c}_{27}}{1-n_1n_3}\Big)$$

$$
\begin{aligned}
& s\alpha \Big/ (c\alpha)^2 + \left(\frac{n_1 \bar{e}_{23}}{1 - n_1 n_3} - \frac{\bar{c}_{35}}{1 - n_1 n_3} - \frac{\bar{e}_{27}}{1 - n_1 n_3} - 2 \frac{n_3 \bar{c}_{27}}{1 - n_1 n_3} \right. \\
& \left. - \frac{n_1 \bar{e}_{35}}{1 - n_1 n_3} - \frac{n_3 \bar{c}_4}{(1 - n_1 n_3) n_1} + \frac{\bar{e}_2}{1 - n_1 n_3} + 2 \frac{n_3 \bar{c}_2}{1 - n_1 n_3} + \frac{\bar{c}_{23}}{1 - n_1 n_3} \right) \Big/ (\\
& c\alpha) + \frac{n_1 \bar{e}_{33}}{1 - n_1 n_3} + 2 \frac{n_3 \bar{c}_{25}}{1 - n_1 n_3} + \frac{n_3 \bar{c}_3}{(1 - n_1 n_3) n_1} + \frac{\bar{e}_{25}}{1 - n_1 n_3} \\
& + \frac{\bar{c}_{33}}{1 - n_1 n_3}
\end{aligned}
$$

$$
\tilde{c}_{31} = \frac{n_1 \bar{e}_{30} + \bar{c}_{30}}{1 - n_1 n_3}
$$

$$
\tilde{c}_{32} = \bar{c}_{34} + n_1 \bar{e}_{34} + \frac{-\bar{c}_{36} - n_1 \bar{e}_{36}}{(c\alpha)}
$$

$$
\begin{aligned}
\tilde{c}_{33} = & \left(\frac{n_1 \bar{e}_{22}}{1 - n_1 n_3} - \frac{n_1 n_3 \bar{d}_{44}}{(1 - n_1 n_3) n_2} + \frac{\bar{c}_{22}}{1 - n_1 n_3} + \frac{\left(2 \frac{n_1 \bar{e}_{10}}{1 - n_1 n_3} + 2 \frac{\bar{c}_{10}}{1 - n_1 n_3} \right) \bar{g}}{c\alpha} \right. \\
& \left. \frac{}{c\alpha^2} \right) s\alpha + \frac{\left(\frac{n_1 \bar{e}_{37}}{1 - n_1 n_3} + \frac{\bar{c}_{37}}{1 - n_1 n_3} \right) \bar{g}}{c\alpha} - \frac{n_1 n_3 \bar{d}_{42}}{(1 - n_1 n_3) n_2}
\end{aligned}
$$

$$
\begin{aligned}
\tilde{c}_{34} = & \left(\frac{- \frac{n_1 n_3 \bar{d}_{49}}{(1 - n_1 n_3) n_2} + \frac{n_1 \bar{e}_{26}}{1 - n_1 n_3} + \frac{\bar{c}_{26}}{1 - n_1 n_3}}{(c\alpha)} + \right. \\
& \left(2 \frac{\bar{c}_{18}}{1 - n_1 n_3} + 2 \frac{n_1 \bar{e}_{18}}{1 - n_1 n_3} \right) \bar{g} - 2 \frac{\bar{c}_{28}}{1 - n_1 n_3} - 2 \frac{n_1}{(1 - n_1 n_3) n_2} \\
& + 2 \frac{n_1 n_3 \bar{d}_{50}}{(1 - n_1 n_3) n_2} + 2 \frac{n_1 n_3}{1 - n_1 n_3} - 2 \frac{n_1 \bar{e}_{28}}{1 - n_1 n_3} \Big) \Big/ c\alpha^2 \\
& \left. + \frac{\left(-6 \frac{\bar{c}_{14}}{1 - n_1 n_3} - 6 \frac{n_1 \bar{e}_{14}}{1 - n_1 n_3} \right) \bar{g}}{c\alpha^3} \right) s\alpha + \left(\left(\frac{\bar{c}_{40}}{1 - n_1 n_3} + \frac{n_1 \bar{e}_{40}}{1 - n_1 n_3} \right) \bar{g} \right. \\
& + \frac{n_1}{1 - n_1 n_3} + \frac{n_1 n_3}{(1 - n_1 n_3) n_2} - \frac{\bar{c}_{24}}{1 - n_1 n_3} - \frac{{n_1}^2 n_3}{(1 - n_1 n_3) {n_2}^2} - \frac{n_1 \bar{e}_{24}}{1 - n_1 n_3} \\
& \left. + \frac{n_1 n_3 \bar{d}_{47}}{(1 - n_1 n_3) n_2} \right) \Big/ ((c\alpha)) + \frac{\left(-2 \frac{\bar{c}_{16}}{1 - n_1 n_3} - 2 \frac{n_1 \bar{e}_{16}}{1 - n_1 n_3} \right) \bar{g}}{c\alpha^2} \\
& - \frac{n_1 n_3 \bar{d}_{46}}{(1 - n_1 n_3) n_2}
\end{aligned}
$$

$$
\begin{aligned}
\tilde{c}_{35} = & \left(\left(\frac{\bar{c}_{38}}{1 - n_1 n_3} + \frac{n_1 \bar{e}_{38}}{1 - n_1 n_3} \right) \bar{g} + \frac{n_1 n_3 \bar{d}_{44}}{(1 - n_1 n_3) n_2} - \frac{n_1 \bar{e}_{22}}{1 - n_1 n_3} - \frac{\bar{c}_{22}}{1 - n_1 n_3} \right) \Big/ (\\
& c\alpha) + \frac{\left(-2 \frac{\bar{c}_{10}}{1 - n_1 n_3} - 2 \frac{n_1 \bar{e}_{10}}{1 - n_1 n_3} \right) \bar{g}}{(c\alpha)^2} - \frac{n_1 n_3 \bar{d}_{43}}{(1 - n_1 n_3) n_2}
\end{aligned}
$$

$$
\begin{aligned}
\tilde{c}_{36} &= \left(\frac{\bar{c}_{38}+n_1\bar{e}_{38}}{(1-n_1n_3)c\alpha}+\frac{-2\,\bar{c}_{10}-2n_1\bar{e}_{10}}{(1-n_1n_3)c(\alpha)^2}\right)s\alpha \\
&\quad +\frac{-n_1\bar{e}_{37}-\bar{c}_{37}}{(1-n_1n_3)c\alpha}+\frac{n_1\bar{e}_{39}+\bar{c}_{39}}{1-n_1n_3} \\
\tilde{c}_{37} &= \Big(-\frac{1}{1-n_1n_3}+\frac{n_1}{(1-n_1n_3)n_3}-\frac{\bar{c}_{28}}{1-n_1n_3}-\frac{n_1}{(1-n_1n_3)n_2}+2\,\frac{n_1n_3}{1-n_1n_3} \\
&\quad -\frac{n_1\bar{e}_{28}}{1-n_1n_3}\Big)\,\bar{g}(s\alpha)\,\big/c\alpha^2+\Big(-\frac{\bar{c}_{24}}{1-n_1n_3}-6\,\frac{n_3}{1-n_1n_3}-\frac{n_1\bar{e}_{24}}{1-n_1n_3} \\
&\quad +2\,\frac{n_3\bar{c}_{28}}{1-n_1n_3}+\frac{n_1}{1-n_1n_3}+\frac{\bar{c}_{44}}{1-n_1n_3}+\frac{n_1\bar{e}_{44}}{1-n_1n_3}+\frac{\bar{e}_{28}}{1-n_1n_3} \\
&\quad -2\,\frac{n_1n_3}{(1-n_1n_3)n_2}\Big)\,\bar{g}\,\big/((c\alpha))+\frac{\bar{d}_3}{1-n_1n_3}-\frac{n_1\bar{e}_2}{1-n_1n_3}-\frac{n_1n_3\bar{d}_2}{1-n_1n_3} \\
&\quad -\frac{n_3\bar{d}_2}{(1-n_1n_3)n_2}-\frac{n_1n_3\bar{d}_5}{(1-n_1n_3)n_2}-\frac{n_3\bar{d}_3}{(1-n_1n_3)n_2}-\frac{n_1n_3\bar{d}_3}{1-n_1n_3}-\frac{\bar{c}_2}{1-n_1n_3} \\
&\quad +\frac{\bar{d}_2}{1-n_1n_3}-\frac{n_1n_3\bar{d}_6}{(1-n_1n_3)n_2} \\
\tilde{c}_{38} &= \Big(-3\,\frac{n_1}{1-n_1n_3}-\frac{\bar{c}_{24}}{1-n_1n_3}-2\,\frac{n_3}{1-n_1n_3}-\frac{n_1\bar{e}_{24}}{1-n_1n_3}+\frac{n_1\bar{e}_{44}}{1-n_1n_3} \\
&\quad +2\,\frac{n_1n_3}{(1-n_1n_3)n_2}+2\,\frac{n_3\bar{c}_{28}}{1-n_1n_3}+\frac{\bar{c}_{44}}{1-n_1n_3}+\frac{\bar{e}_{28}}{1-n_1n_3}\Big)\,(s\alpha)\,\big/(\\
&\quad c\alpha)+\Big(-\frac{1}{2}\frac{\bar{c}_{28}}{1-n_1n_3}-\frac{1}{2}\frac{n_1c(2\alpha)}{(1-n_1n_3)n_3}-\frac{1}{2}\frac{n_1\bar{e}_{28}}{1-n_1n_3} \\
&\quad +\frac{1}{2}\frac{n_1\bar{e}_{28}c(2\alpha)}{1-n_1n_3}+\frac{1}{2}\frac{\bar{c}_{28}c(2\alpha)}{1-n_1n_3}+\frac{n_1n_3}{1-n_1n_3}-\frac{n_1n_3c(2\alpha)}{1-n_1n_3} \\
&\quad -\frac{1}{2}\frac{n_1}{(1-n_1n_3)n_2}-\frac{1}{2}\frac{1}{1-n_1n_3}+\frac{1}{2}\frac{c(2\alpha)}{1-n_1n_3}+\frac{1}{2}\frac{n_1c(2\alpha)}{(1-n_1n_3)n_2} \\
&\quad +\frac{1}{2}\frac{n_1}{(1-n_1n_3)n_3}\Big)\,\big/c\alpha^2+2\,\frac{n_3\bar{c}_{24}}{1-n_1n_3}+\frac{\bar{c}_{42}}{1-n_1n_3}+\frac{1}{1-n_1n_3} \\
&\quad +\frac{\bar{e}_{24}}{1-n_1n_3}+\frac{n_1\bar{e}_{42}}{1-n_1n_3}+\frac{n_3}{(1-n_1n_3)n_1}-\frac{n_3}{(1-n_1n_3)n_2}+\frac{n_1n_3}{1-n_1n_3} \\
\tilde{c}_{39} &= \frac{n_1\bar{e}_{41}+2\,n_3\bar{c}_{22}+\bar{c}_{41}+\bar{e}_{22}}{1-n_1n_3} \\
\tilde{c}_{40} &= \Big(\frac{1}{1-n_1n_3}+\frac{\bar{c}_{28}}{1-n_1n_3}+\frac{n_1\bar{e}_{28}}{1-n_1n_3}+\frac{n_1}{(1-n_1n_3)n_2}-\frac{n_1}{(1-n_1n_3)n_3} \\
&\quad -2\,\frac{n_1n_3}{1-n_1n_3}\Big)\,(s\alpha)\,\big/c\alpha^2+\Big(2\,\frac{n_3}{1-n_1n_3}-\frac{\bar{e}_{28}}{1-n_1n_3}-\frac{n_1\bar{e}_{44}}{1-n_1n_3} \\
&\quad +\frac{n_1\bar{e}_{24}}{1-n_1n_3}+3\,\frac{n_1}{1-n_1n_3}-2\,\frac{n_1n_3}{(1-n_1n_3)n_2}-\frac{\bar{c}_{44}}{1-n_1n_3}+\frac{\bar{c}_{24}}{1-n_1n_3} \\
&\quad -2\,\frac{n_3\bar{c}_{28}}{1-n_1n_3}\Big)\,\big/((c\alpha))+\frac{\bar{e}_{26}}{1-n_1n_3}+\frac{\bar{c}_{43}}{1-n_1n_3}+2\,\frac{n_3\bar{c}_{26}}{1-n_1n_3}
\end{aligned}
$$

$$+\frac{n_1\bar{e}_{43}}{1-n_1n_3}$$

θ-equation :

$$\begin{aligned}
\tilde{\nu} &= \bar{d}_2+\bar{d}_3\\
\tilde{d}_1 &= \bar{d}_4\\
\tilde{d}_2 &= \bar{d}_5+\bar{d}_6\\
\tilde{d}_3 &= \bar{d}_7+\bar{d}_8+\bar{d}_9\\
\tilde{d}_4 &= \frac{\left(-n_3\bar{c}_4+(1-n_1n_3)\bar{d}_2-\frac{(n_1n_2n_3+n_3-n_2)\bar{e}_4}{n_3}\right)\bar{g}}{(1-n_1n_3)c\alpha}+\frac{(n_2+\bar{d}_{50})\bar{g}^2}{c\alpha^2}\\
\tilde{d}_5 &= \left(\frac{-n_3\bar{c}_4+(1-n_1n_3)\bar{d}_2-\frac{(n_1n_2n_3+n_3-n_2)\bar{e}_4}{n_3}}{(1-n_1n_3)c\alpha}+\frac{(2\bar{d}_{50}+2n_2)\bar{g}}{c\alpha^2}\right)\\
&\quad s\alpha+\frac{\left(\bar{d}_{47}-1-\frac{n_1}{n_2}+\frac{n_2}{n_3}\right)\bar{g}}{c\alpha}+\frac{-n_3\bar{c}_2-\frac{(n_1n_2n_3+n_3-n_2)\bar{e}_2}{n_3}}{1-n_1n_3}\\
\tilde{d}_6 &= \frac{(n_2+\bar{d}_{50})s\alpha^2}{c\alpha^2}+\frac{\left(\bar{d}_{47}-1-\frac{n_1}{n_2}+\frac{n_2}{n_3}\right)(s\alpha)}{c\alpha}-n_2+\bar{d}_{45}\\
\tilde{d}_7 &= \bar{d}_{41}\\
\tilde{d}_8 &= \bar{d}_{43}-\frac{\bar{d}_{44}}{c\alpha}\\
\tilde{d}_9 &= \bar{d}_{48}-\frac{\bar{d}_{49}}{c\alpha}+\frac{n_2\bar{d}_{50}}{(c\alpha)^2}\\
\tilde{d}_{10} &= \frac{\bar{d}_{44}\bar{g}}{(c\alpha)}+\frac{-n_3\bar{c}_1-\frac{(n_1n_2n_3+n_3-n_2)\bar{e}_1}{n_3}}{1-n_1n_3}\\
\tilde{d}_{11} &= \left((1-n_1n_3)\bar{d}_{49}\bar{g}+n_3\bar{c}_4-(1-n_1n_3)\bar{d}_2+\frac{(n_1n_2n_3+n_3-n_2)\bar{e}_4}{n_3}\right)/(\\
&\quad c\alpha)+\frac{(1-n_1n_3)(-2\bar{d}_{50}-2n_2)\bar{g}}{c\alpha^2}-n_3\bar{c}_3-\frac{(n_1n_2n_3+n_3-n_2)\bar{e}_3}{n_3}\\
\tilde{d}_{12} &= \bar{d}_{42}\\
\tilde{d}_{13} &= \left(\frac{\bar{d}_{49}}{c\alpha}+\frac{-2\bar{d}_{50}-2n_2}{c\alpha^2}\right)s\alpha+\frac{-\bar{d}_{47}+1+\frac{n_1}{n_2}-\frac{n_2}{n_3}}{c\alpha}+\bar{d}_{46}\\
\tilde{d}_{14} &= \bar{d}_{10}
\end{aligned}$$

$$
\begin{aligned}
\tilde{d}_{15} &= \bar{d}_{11} + \bar{d}_{12} \\
\tilde{d}_{16} &= \bar{d}_{14} + \bar{d}_{16} + \bar{d}_{19} \\
\tilde{d}_{17} &= \bar{d}_{13} + \bar{d}_{15} + \bar{d}_{17} + \bar{d}_{18} \\
\tilde{d}_{18} &= \left(\left(-\frac{\bar{d}_2}{1-n_1n_3} + \frac{\bar{e}_4}{1-n_1n_3} + \frac{n_1n_2\bar{e}_4}{1-n_1n_3} + \frac{n_1n_3\bar{d}_2}{1-n_1n_3} - \frac{n_2\bar{e}_4}{(1-n_1n_3)n_3} \right.\right. \\
&\quad \left.\left. + \frac{n_3\bar{c}_4}{1-n_1n_3} \right) \bar{g} \,/(c\alpha)^2 \right. \\
&\quad \left. + \frac{\left(2\frac{n_1n_3\bar{d}_{50}}{1-n_1n_3} - 2\frac{n_2}{1-n_1n_3} - 2\frac{\bar{d}_{50}}{1-n_1n_3} + 2\frac{n_1n_3n_2}{1-n_1n_3} \right)\bar{g}^2}{c(\alpha)^3} \right) (s\alpha) + \Big(\\
&\quad -\frac{n_1n_3\bar{d}_5}{1-n_1n_3} - \frac{n_1n_2\bar{e}_{27}}{1-n_1n_3} + \frac{\bar{e}_2}{1-n_1n_3} + \frac{n_1n_2\bar{e}_2}{1-n_1n_3} - \frac{\bar{e}_{27}}{1-n_1n_3} \\
&\quad - \frac{n_2\bar{e}_2}{(1-n_1n_3)n_3} + \frac{n_2\bar{e}_{27}}{(1-n_1n_3)n_3} + \frac{\bar{d}_5}{1-n_1n_3} - \frac{n_3\bar{c}_{27}}{1-n_1n_3} + \frac{n_3\bar{c}_2}{1-n_1n_3} \Big) \bar{g} \\
&\quad /(c\alpha) + \left(-\frac{n_3n_2}{1-n_1n_3} + \frac{n_1n_3\bar{d}_{47}}{1-n_1n_3} - \frac{\bar{d}_{47}}{1-n_1n_3} + \frac{n_2}{(1-n_1n_3)n_1} \right. \\
&\quad \left. + \frac{\bar{d}_{23}}{1-n_1n_3} - \frac{n_1n_3\bar{d}_{23}}{1-n_1n_3} \right) \bar{g}^2 \,/c\alpha^2 + \frac{n_3\bar{d}_1}{(1-n_1n_3)n_2} - 2\,\bar{d}_2 \\
&\quad + \left(-\frac{\bar{c}_4n_2}{(1-n_1n_3)n_1} + \frac{\bar{c}_4n_2n_3}{1-n_1n_3} + \frac{\bar{c}_4n_3}{(1-n_1n_3)n_1} \right) \bar{g} \\
\tilde{d}_{19} &= \left(\frac{n_1}{1-n_1n_3} - \frac{n_3\bar{c}_{28}}{1-n_1n_3} + \frac{\bar{d}_8}{1-n_1n_3} - \frac{n_3n_1}{(1-n_1n_3)n_2} + 2\frac{\bar{d}_7}{1-n_1n_3} \right. \\
&\quad - \frac{\bar{e}_{28}}{1-n_1n_3} - \frac{n_1n_3\bar{d}_8}{1-n_1n_3} + \frac{n_3}{1-n_1n_3} - 2\frac{n_1n_3\bar{d}_7}{1-n_1n_3} + \frac{n_2\bar{e}_{28}}{(1-n_1n_3)n_3} \\
&\quad \left. - \frac{n_1n_2\bar{e}_{28}}{1-n_1n_3} \right) \bar{g} \,/((c\alpha)) + \frac{\left(-\frac{n_1n_3\bar{d}_{27}}{1-n_1n_3} + \frac{\bar{d}_{27}}{1-n_1n_3} \right)\bar{g}^2}{c\alpha^2} + \frac{\bar{d}_2}{1-n_1n_3} \\
&\quad + \frac{n_3\bar{d}_3}{(1-n_1n_3)n_2} - 2\,\bar{d}_2 - 2\,\bar{d}_3 - \frac{n_1n_3\bar{d}_2}{1-n_1n_3} + \frac{n_3\bar{d}_2}{(1-n_1n_3)n_2} \\
\tilde{d}_{20} &= \left(\frac{\bar{d}_{34} - 2\,\bar{d}_{45} + n_2}{c\alpha} + \frac{-\frac{3}{2}\bar{d}_{50} - \frac{3}{2}n_2}{(c\alpha)^3} \right) s\alpha + \left(-\frac{1}{2}\frac{n_2c(2\alpha)}{n_1} - \bar{d}_{47} \right. \\
&\quad + \bar{d}_{47}c(2\alpha) - \frac{1}{2}\bar{d}_{23}c(2\alpha) - \frac{1}{2}\frac{n_1c(2\alpha)}{n_2} - \frac{1}{2}c(2\alpha) + \frac{1}{2}\frac{n_2}{n_1} \\
&\quad \left. + \frac{1}{2}\frac{n_1}{n_2} + \frac{1}{2} + \frac{1}{2}\bar{d}_{23} - \frac{1}{2}\frac{n_2}{n_3} + \frac{1}{2}\frac{n_2c(2\alpha)}{n_3} \right) /(c\alpha)^2
\end{aligned}
$$

$$
\begin{aligned}
&+\frac{\frac{1}{2}\bar{d}_{50}s(3\alpha)+\frac{1}{2}n_2 s(3\alpha)}{(c\alpha)^3}+\bar{d}_{21}\\
\tilde{d}_{21} &= \frac{\bar{d}_{27}(s\alpha)^2}{c\alpha^2}+\frac{\bar{d}_{40}s\alpha}{(c\alpha)}+\bar{d}_{25}+\bar{d}_{28}\\
\tilde{d}_{22} &= \bar{d}_{20}\\
\tilde{d}_{23} &= \left(\frac{\bar{d}_{49}}{c\alpha^2}+\frac{-2\,\bar{d}_{50}-2\,n_2}{c\alpha^3}\right)s\alpha+\frac{-\bar{d}_{33}+\bar{d}_{46}}{c\alpha}+\frac{\bar{d}_{23}+\frac{n_2}{n_1}-\bar{d}_{47}}{c\alpha^2}+\bar{d}_{22}\\
\tilde{d}_{24} &= \bar{d}_{24}\\
\tilde{d}_{25} &= \bar{d}_{26}-\frac{\bar{d}_{39}}{c\alpha}+\frac{\bar{d}_{27}}{(c\alpha)^2}\\
\tilde{d}_{26} &= \left(\frac{(n_1n_2n_3+n_3-n_2)\bar{e}_4}{n_3}+n_3\bar{c}_4-(1-n_1n_3)\bar{d}_2}{(1-n_1n_3)c\alpha^2}+\frac{(-4n_2-4\,\bar{d}_{50})\bar{g}}{c\alpha^3}\right)\\
&\quad s\alpha^2+\left(\left(-n_3(\bar{c}_{27}-\bar{c}_2)-\frac{(n_1n_2n_3+n_3-n_2)(\bar{e}_{27}-\bar{e}_2)}{n_3}\right.\right.\\
&\quad \left.-\frac{(n_1n_2n_3+n_3-n_2)\bar{c}_4}{n_1}+(1-n_1n_3)\bar{d}_5\right)\Big/((1-n_1n_3)c\alpha)\\
&\quad \left.+\frac{\left(2\frac{n_2}{n_1}+1+\frac{n_1}{n_2}-\frac{n_2}{n_3}+2\,\bar{d}_{23}-3\,\bar{d}_{47}\right)\bar{g}}{c\alpha^2}\right)(s\alpha)\\
&\quad +\frac{(\bar{d}_{34}-2\,\bar{d}_{45}+n_2)\bar{g}}{c\alpha}\\
&\quad +\frac{-\frac{(n_1n_2n_3+n_3-n_2)\bar{e}_{23}}{n_3}-n_3\bar{c}_{23}-\frac{(n_1n_2n_3+n_3-n_2)\bar{c}_2}{n_1}}{1-n_1n_3}\\
\tilde{d}_{27} &= \left(\left(-n_3\left(1+\frac{n_1}{n_2}-\frac{n_1}{n_3}+\bar{c}_{28}\right)-\frac{(n_1n_2n_3+n_3-n_2)(-2\,n_3+\bar{e}_{28})}{n_3}\right.\right.\\
&\quad \left.+(1-n_1n_3)(2\bar{d}_7+\bar{d}_8+2\,n_2)\right)\Big/((1-n_1n_3)c\alpha)+2\,\frac{\bar{d}_{27}\bar{g}}{c\alpha^2}\Big)\\
&\quad s\alpha+\frac{\bar{d}_{40}\bar{g}}{c\alpha}+\left(-n_3\bar{c}_{24}-\frac{(n_1n_2n_3+n_3-n_2)\left(1+\frac{n_3}{n_1}-\frac{n_3}{n_2}+\bar{e}_{24}\right)}{n_3}\right.\\
&\quad \left.+(1-n_1n_3)\left(-\frac{n_1}{n_2}-1-\frac{n_2}{n_3}\right)\right)\Big/(1-n_1n_3)\\
\tilde{d}_{28} &= -\frac{\bar{d}_{44}(s\alpha)}{c\alpha}+\frac{-\bar{d}_{31}+\bar{d}_{42}}{c\alpha}+\bar{d}_{30}
\end{aligned}
$$

$$\tilde{d}_{29} = -\frac{\bar{d}_{38}}{(c\alpha)} + \bar{d}_{36}$$

$$\tilde{d}_{30} = -\frac{\bar{d}_{44}\bar{g}s\alpha}{c\alpha^2} + \frac{(\bar{d}_{31} - \bar{d}_{42})\bar{g}}{c\alpha} + \frac{-\frac{(n_1n_2n_3 + n_3 - n_2)\bar{e}_{21}}{n_3} - n_3\bar{c}_{21} - \frac{(n_1n_2n_3 + n_3 - n_2)\bar{c}_1}{n_1}}{1 - n_1n_3}$$

$$\tilde{d}_{31} = \left(\frac{-\bar{d}_{49}\bar{g} + \frac{-n_3\bar{c}_4 - \frac{(n_1n_2n_3 + n_3 - n_2)\bar{e}_4}{n_3} + (1 - n_1n_3)\bar{d}_2}{1 - n_1n_3}}{(c\alpha)^2} + \frac{(4\,\bar{d}_{50} + 4\,n_2)\bar{g}}{c\alpha^3}\right)(s\alpha) + \Big((-\bar{d}_{46} + \bar{d}_{33})\bar{g} + \Big(- \frac{(n_1n_2n_3 + n_3 - n_2)(-\bar{e}_{27} + \bar{e}_2)}{n_3} - (1 - n_1n_3)\bar{d}_5 + \frac{(n_1n_2n_3 + n_3 - n_2)\bar{c}_4}{n_1} - n_3(-\bar{c}_{27} + \bar{c}_2)\Big)/(1 - n_1n_3)\Big)/((c\alpha)) + \frac{\left(-2\,\frac{n_2}{n_1} - 2\,\bar{d}_{23} + 2\,\bar{d}_{47}\right)\bar{g}}{c\alpha^2} + \frac{-\frac{(n_1n_2n_3 + n_3 - n_2)\bar{e}_{25}}{n_3} - \frac{(n_1n_2n_3 + n_3 - n_2)\bar{c}_3}{n_1} - n_3\bar{c}_{25}}{1 - n_1n_3}$$

$$\tilde{d}_{32} = \frac{\bar{d}_{38}\bar{g}}{(c\alpha)} + \frac{-n_3\bar{c}_{22} - \frac{(n_1n_2n_3 + n_3 - n_2)\bar{e}_{22}}{n_3}}{1 - n_1n_3}$$

$$\tilde{d}_{33} = \Big(\bar{d}_{39}\bar{g} + \Big((1 - n_1n_3)(-2\,\bar{d}_7 - \bar{d}_8 - 2n_2) - \frac{(n_1n_2n_3 + n_3 - n_2)(2n_3 - \bar{e}_{28})}{n_3} - n_3\left(-\bar{c}_{28} - 1 - \frac{n_1}{n_2} + \frac{n_1}{n_3}\right)\Big)/(1 - n_1n_3)\Big)/((c\alpha)) - 2\,\frac{\bar{d}_{27}\bar{g}}{c\alpha^2} + \frac{-\frac{(n_1n_2n_3 + n_3 - n_2)\bar{e}_{26}}{n_3} - n_3\bar{c}_{26}}{1 - n_1n_3}$$

$$\tilde{d}_{34} = \frac{(\bar{d}_{31} - \bar{d}_{42})s\alpha}{c\alpha} + \frac{-\frac{1}{2}\bar{d}_{44} + \frac{1}{2}\bar{d}_{44}c(2\alpha)}{c\alpha^2} + \bar{d}_{29}$$

$$\tilde{d}_{35} = \left(\frac{-\bar{d}_{46} + \bar{d}_{33}}{c\alpha} + \frac{\frac{n_2}{n_3} - \frac{n_1}{n_2} - 2\,\frac{n_2}{n_1} - 2\,\bar{d}_{23} - 1 + 3\bar{d}_{47}}{c\alpha^2}\right)s\alpha$$

$$+\frac{-n_2+2\,\bar{d}_{45}-\bar{d}_{34}}{c\alpha}+\frac{-\frac{1}{2}\bar{d}_{49}+\frac{1}{2}\bar{d}_{49}c(2\alpha)}{c(\alpha)^2}$$
$$+\frac{2\,n_2-2\,n_2c(2\alpha)+2\,\bar{d}_{50}-2\,\bar{d}_{50}c(2\alpha)}{c\alpha^3}+\bar{d}_{32}$$

$$\tilde{d}_{36} = \bar{d}_{35}$$

$$\tilde{d}_{37} = \left(\frac{\bar{d}_{39}}{c\alpha}-2\,\frac{\bar{d}_{27}}{c\alpha^2}\right)(s\alpha)-\frac{\bar{d}_{40}}{c\alpha}+\bar{d}_{37}$$

Bibliography

[1] Orlik-Ruckemann, *Aerodynamic Aspects of Aircraft Dynamics at High Angles-of-Attack*, AIAA Paper 82-1363, 1982.

[2] Tobak, M. and Schiff, L.B., *The Role of Time-History Effects in the Formulation of the Aerodynamics of Aircraft Dynamics*, AGARD CP-235, 1980.

[3] Schiff, L.B., Tobak, M. and Malcolm, G.N., *Mathematical Modeling of the Aerodynamics of High Angle-of-Attack Maneuvers*, Proceedings of Atmospheric Flight Mechanics Conference, 1980.

[4] Johnston, D.E., *Identification of Key Maneuver-Limiting Factors in High Angle-of-Attack Flight*, AGARD CP-235, 1980.

[5] Padfield, G.D., *Nonlinear Oscillations at High Incidence*, AGARD CP-235, 1978.

[6] Young, J.W., Schy, A.A. and Johnson, K.G., *Prediction of Jump Phenomena in Aircraft Maneuvers, including Nonlinear Aerodynamic Effects*, Journal of Guidance and Control, Vol. 1, No. 1, 1978.

[7] Carroll, J.V. and Mehra, R.K., *Bifurcation Analysis of Nonlinear Aircraft Dynamics*, Journal of Guidance and Control, Vol. 5, No.5, 1982.

[8] Hui, W.H. and Tobak, M., *Bifurcation Analysis of Aircraft Pitching Motions About Large Mean Angles of Attack*, Journal of Guidance and Control, Vol. 7, No. 1, 1984.

[9] Planeaux, J.B. and Barth, T.J., *High-Angle-of-Attack Dynamic Behavior of a Model High-Performance Fighter Aircraft*, AIAA Paper 88-4368, 1988.

[10] Planeaux, J.B., Beck, J.A. and Baumann, D.D., *Bifurcation Analysis of a Model Fighter Aircraft with Control Augmentation*, AIAA Paper 90-2836, 1990.

[11] Jahnke, C.J., *Application of Dynamical Systems Theory to Nonlinear Aircraft Dynamics*, Ph.D. thesis, California Institute of Technology, 1990.

[12] Ericsson, L.E., *The Fluid Mechanics of Slender Wing Rock*, Journal of Aircraft, Vol. 21, No.5, 1984.

[13] Ericsson, L.E., *The Various Sources of Wing Rock*, AIAA Paper 88-4370, 1988.

[14] Ericsson, L.E., *Analytic Prediction of the Maximum Amplitude of Slender Wing Rock*, Journal of Aircraft, Vol. 26, No. 1, 1989.

[15] Nguyen, L.T., Yip, L. and Chambers,J.R., *Self-Induced Wing Rock of Slender Delta Wings*, AIAA Paper 81-1883, 1981.

[16] Hsu, C. and Lan, C.E., *Theory of Wing Rock*, Journal of Aircraft, Vol. 22, No. 10, 1985.

[17] Konstadinopoulos, P., Mook, D.T. and Nayfeh, A.H., *Subsonic Wing Rock of Slender Delta Wings*, Journal of Aircraft, Vol. 22, No.3, 1985.

[18] Elzebda, J.M., Nayfeh, A.H. and Mook, D.T., *Development of an Analytical Model of Wing Rock for Slender Delta Wings*, Journal of Aircraft, Vol. 26, No. 8, 1989.

[19] Nayfeh, A.H., Elzebda, J.M. and Mook, D.T., *Analytical Study of the Subsonic Wing-Rock Phenomenon for Slender Delta Wings*, Journal of Aircraft, Vol. 26, No. 9, 1989.

[20] Elzebda, J.M., Mook, D.T. and Nayfeh, A.H., *Influence of Pitching Motion on Subsonic Wing Rock of Slender Delta Wings*, Journal of Aircraft, Vol. 26, No. 6, 1989.

[21] Ross, A.J., *Lateral Stability at High Angles-of-Attack, Particularly Wing Rock*, AGARD CP-260, 1978.

[22] Luo, J. and Lan, C.E., *Control of Wing Rock Motion of Slender Delta Wings*, Journal of Guidance, Control, and Dynamics, Vol. 16, No. 2, 1993.

[23] Wong, G.S. et.al., *Active Control of Wing Rock Using Tangential Leading-Edge Blowing*, Journal of Aircraft, Vol. 31, No. 3, 1994.

[24] Singh, S.N., Yim, W., and Wells, W.R., *Direct Adaptive and Neural Control of Wing Rock Motion of Slender Delta Wings*, Journal of Guidance, Control, and Dynamics, Vol. 18, No. 1, 1995.

[25] Araujo, A.D. and Singh, S.N., *Variable Structure Adaptive Control of Wing Rock Motion of Slender Delta Wings*, Journal of Guidance, Control, and Dynamics, Vol. 21, No. 2, 1998.

[26] Liebst, B.S. and DeWitt, B.R., *Wing Rock Suppression in the F-15 Aircraft*, AIAA Paper 97-3719, 1997.

[27] Ramnath, R. V., *A Multiple Scales Approach to the Analysis of Linear Systems*, USAFFDL-TR-68-60, Wright-Patterson AFB, OH, 1968.

[28] Ramnath, R. V. and Sandri, G., *A Generalized Multiple Scales Approach to a Class of Linear Differential Equations*, Journal of Mathematical Analysis and Applications, Vol. 28, 1969.

[29] Ramnath, R. V., et. al. (ed.), *Nonlinear System Analysis and Synthesis : vol. 2 - Techniques and Applications*, chapter 3, The American Society of Mechanical Engineers, New York, 1980.

[30] Ramnath, R.V., *Transition Dynamics of VTOL Aircraft*, AIAA Paper 69-130, 1969.

[31] Tao, Y. C. and Ramnath, R. V., *On the Attitude Motion of an Orbiting Rigid Body Under the Influence of Gravity Gradient Torque*, AIAA Paper 78-1397.

[32] Ramnath, R. V., *Minimal and Subminimal Simplification*, Journal of Guidance and Control, Vol. 3, No. 1, 1980.

[33] Ramnath, R. V., *Gravitational Perturbations of Equatorial Orbits*, Celestial Mechanics, vol. 8, 1973.

[34] Ramnath, R. V. and Sinha, P., *Dynamics of the Space Shuttle During Entry into Earth's Atmosphere*, AIAA Journal, Vol. 13, No. 3, 1975.

[35] Go, T.H. and Ramnath, R.V., *Geomagnetic Attitude Control of Satellites Using Generalized Multiple Scales*, Journal of Guidance, Control, and Dynamics, Vol. 20, No. 4, 1997.

[36] Troger, H. and Steindl, A., *Nonlinear Stability and Bifurcation Theory*, Springer-Verlag, New York, 1991.

[37] Hale, J.K. and Kocak, H., *Dynamics and Bifurcations*, Springer-Verlag, New York, 1991.

[38] Guckenheimer, J. and Holmes, P., *Nonlinear Oscillations, Dynamical Systems, and Bifurcations of Vector Fields*, Springer-Verlag, New York, 1983.

[39] Carr, J., *Applications of Centre Manifold Theory*, Springer-Verlag, New York, 1981.

[40] Ioos, G. and Joseph, D.D., *Elementary Stability and Bifurcation Theory*, Springer-Verlag, New York, 1980.

[41] Klimas, A., Ramnath, R.V., and Sandri, G., *On the Compatibility Problem for the Uniformization of Asymptotic Expansions*, Journal of Mathematical Analysis and Applications, Vol. 32, No. 3, 1970.

[42] Byrd, P.F. and Friedman, M.D., *Handbook of Elliptic Integrals for Engineers and Physicists*, Springer-Verlag, New York, 1971.

[43] Lawden, D.F., *Elliptic Functions and Applications*, Springer-Verlag, New York, 1989.

[44] Grafton, S.B. and Anglin, E.L., *Dynamic Stability Derivatives at Angles of Attack from -5 to 90 Degrees For a Variable-Sweep Fighter Configuration with Twin Vertical Tails*, NASA TN-D-6909, 1972.

[45] Malcolm, G.N., *Rotary and Magnus Balances*, AGARD LS-114, 1981.

[46] Chambers, J.R., Grafton, S.B., and Lutze, F.H., *Curved Flow, Rolling Flow, and Oscillatory Pure-Yawing Wind-Tunnel Test Methods For Determination of Dynamic Stability Derivatives*, AGARD LS-114, 1981.

[47] Iliff, K.W. and Wang, K.C., *X29A Lateral Directional Stability and Control Derivatives Extracted From High Angle-of-Attack Flight Data*, NASA TP-3664, 1996.

[48] Nguyen, L.T., *Control-System Techniques for Improved Departure/Spin Resistance for Fighter Aircraft*, NASA TP-1689, 1980.

[49] Lallman, F.J., *Preliminary Design Study of Lateral-Directional Control System Using Thrust Vectoring*, NASA TM-86425, 1985.

[50] Bowers, A.H. and Pahle, J.W., *Thrust Vectoring on the NASA F-18 High Alpha Research Vehicle*, NASA TM-4771, 1996.

[51] Regenie, V., *Thrust Vectoring Control System Description*, High Alpha Technology Program Workshop, 1989.

[52] Pahle, J.W. et al., *TVCS Control Laws and Systems*, High Alpha Technology Program Workshop, 1989.

[53] Murri, D.G. et al., *Advanced Aerodynamic Controls Research*, High Alpha Technology Program Workshop, 1989.

[54] Brandon, J.M. et al., *Free-Flight Investigation of Forebody Blowing For Stability and Control*, AIAA Paper 96-3444, 1996.

[55] Lallman, F.J., Davidson, J.B., and Murphy, P.C., *A Method for Integrating Thrust-Vectoring and Actuated Forebody Strakes With Conventional Aerodynamic Controls on a High-Performance Fighter Airplane*, NASA TP-208464, 1998.